THE
PHYSICAL REVIEW
A Journal of Experimental and Theoretical Physics Established by E. L. Nichols in 1893

VOL. 49, NO. 11 JUNE 1, 1936 SECOND SERIES

The Disintegration of Li^7 Bombarded by Slow Protons

H. D. DOOLITTLE, *Ryerson Physical Laboratory, University of Chicago*
(Received April 2, 1936)

The number of Li^7 atoms disintegrated by protons of energies from 23.6 to 72.5 electron kilovolts has been determined. Oppenheimer's integration of Gamow's equation giving the probability of the lithium-proton disintegration as $n=bVe^{-a/V^{\frac{1}{2}}}$ has been compared with the experimental data by plotting $\log n-\log V$ against $1/V^{\frac{1}{2}}$. The agreement is within the experimental error. The results of the present experiment have been compared with other observer's data taken at higher voltages; the slopes of the lines have been found to vary somewhat. No indications of resonance nor of a minimum voltage required for disintegration were observed. Considerable difficulty was encountered as regards surface contamination of the target and also the formation of a highly insulating layer of lithium oxide. The latter effect made necessary the frequent use of a Faraday chamber for recording the proton current. An FP-54 pliotron in a modified form of the DuBridge-Brown balanced circuit was used in photographic recording of the alpha-particles.

SEVERAL studies have already been made of the disintegration of lithium bombarded by slow protons.[1] Much of this work was done without magnetic analysis of the proton beam, and often scintillation screens were used for counting the alpha-particles. Very few observations have been made of the absolute yield of the long range particles below 60 kilovolts. Diebner and Hoffman[1] working in this region have reported some indication of resonance. The minimum voltage required for disintegration has been given at anywhere from 10 to 30 kilovolts. Considerable discussion also has arisen concerning the yield as a function of the surface of the target. It is the purpose of this paper to attempt to answer these questions, in part at least, and to continue the yield curve to as low proton energies as possible.

[1] F. Kirchner, Physik. Zeits. **34**, 777 (1933); Naturwiss. **21**, 473 (1933); Traubenberg, Eckardt and Gebauer, Naturwiss. **21**, 26 (1933); Zeits. f. Physik **80**, 557 (1933); Rutherford, Nature **131**, 388 (1933); Oliphant and Rutherford, Proc. Roy. Soc. **A141**, 259 (1933); Döpel, Zeits. f. Physik **81**, 821 (1933); Diebner and Hoffman, Naturwiss. **22**, 119 (1934); Jakowlew, Zeits. f. Physik **93**, 644 (1935).

APPARATUS AND METHOD

A. Discharge tube and high voltage

At first an ordinary Wien type discharge tube was tried with a mechanically rectified high voltage. Although this discharge current could be run as high as 50 milliamperes, it was not possible to get a sufficiently intense beam of protons of a narrow energy range. This tube was then set up at high potential and an additional accelerating field over a distance of 5/16 of an inch was applied to the protons emerging from the canal of the Wien tube, Fig. 1. With this arrangement up to 2.5 microamperes could be recorded in a Faraday chamber after bending the beam through 90° and selecting the desired energy with a $\frac{1}{8}$-inch slit, where the separation of the pole faces was $\frac{1}{4}$ inch. The total ion current without magnetic bending was about 25 micro-

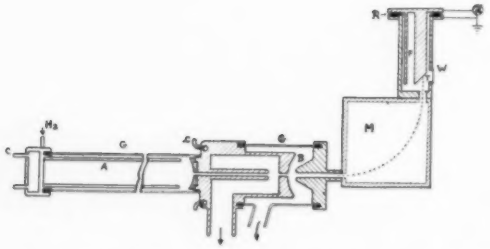

FIG. 1. The discharge tube and the target. *A*, steel tube; *B*, accelerating chamber; *CC*, oil cooling; *GG*, glass tubes; *M*, magnetic field; *W*, mica window; *F*, Faraday chamber; *A'*, microammeter; *T*, target; *R*, rubber gasket.

amperes. In order to keep the pressure sufficiently low in the accelerating chamber a system of double differential pumping was used as shown in Fig. 1. This made possible a pressure of from 2 to 4×10^{-5} mm of Hg in the accelerating chamber, *B*. The hydrogen was admitted to the discharge tube through a palladium valve; this intake as well as the pump connections were protected from sparking back by the use of wire grid electrodes. The metal tube, *A*, which was about 2 feet long served to prevent local heating of the glass due to electron bombardment. When the discharge tube was properly outgassed, it could be run very steadily at anything from 10 to 30 milliamperes discharge current. The voltage supplied to this tube came from a 25-kilovolt transformer whose 110-volt primary was fed by the generator of a motor generator set. The motor and generator were connected by a 3-foot Bakelite shaft and were mounted on kiln-dried and paraffined oak planking. A kenetron rectified the voltage for the discharge tube, but no condensor was used here. The accelerating potential was supplied by another transformer with full wave rectification and condensors. With this arrangement it was possible to get from 10 to 72 kilovolt protons. At 72 kilovolts the tube broke down by sparking in the chamber *B*.

B. Counter, target and measurement of proton current

An FP-54 pliotron in a slight modification of the DuBridge-Brown[2] balanced circuit together with a camera was used to record the alpha-particles. The circuit as given by DuBridge and Brown gave too great a drift at the maximum sensitivity used (2×10^{-16} amp./mm with an input resistance of 8.6×10^{10} ohms). It was found that the plate currents of three different pliotrons changed very rapidly during the first three weeks of continuous operation. It was then necessary to make the resistance, R_a,[2] about 10,000 ohms to secure a balance with proper voltages on the elements. The circuit kept balancing at higher and higher filament current, necessitating frequent changes of R_1 and R_2. After nearly a month of continuous running one tube settled down to steady conditions with 97 milliamperes through the filament and within five percent of the rated voltages elsewhere. It was necessary, however, to put an Edison cell in series with the lead batteries as described by Hafstad.[3] With this arrangement the drift was made as low as 1.5 cm in 36 hours with a galvanometer of 5×10^{-10} amp./mm sensitivity. Since the drift depends upon the change in plate current with the time and since the over-all sensitivity depends upon the input resistance together with the galvanometer sensitivity, the best arrangement for minimum of drift is to use as low a sensitivity galvanometer and as high an input resistance as is possible without making the product of *R* times *C* too great.

The protons after emerging from the accelerating field were bent through 90° in the arc of a circle of 9.2 cm radius. The $\frac{1}{8}$-inch slit selected the beam which fell on the lithium target, *T*, at an angle of 45°. The target was insulated by the rubber gasket, *R*, and by rotating the whole through 180° could be replaced by the Faraday chamber, *F*. The alpha-particles emitted passed through a mica window, *W*, of about 3.5 cm stopping power into the ionization chamber connected to the pliotron. The mica window was waxed over a round hole of 9/16 inch diameter. The aperture of the ionization chamber determined the solid angle over which the particles were counted. This solid angle was 0.276 for most of the counting, although a solid angle of half this value was used as a check and for the higher voltages, where the counting rate would have been too great for sufficient resolution.

The ionization chamber was of the conical type 15 mm deep. An alpha-particle entering the

[2] DuBridge and Brown, Rev. Sci. Inst. **4**, 532 (1933).

[3] Hafstad, Phys. Rev. **44**, 201 (1933).

chamber gave a deflection of the galvanometer of about 16 mm at maximum sensitivity. The fluctuations were cut down to ± 2 mm by taking the usual precautions and evacuating the case containing the pliotron. In general the circuit was used at one-half the maximum sensitivity. The ionization chamber was of steel which gave about one-half the residual count given by a similar chamber of copper. No attempt was made to pass "dead" gas through the chamber or to clean it other than by polishing it with steel wool. The residual count was 7.3 alpha-particles per hour. The circuit was sufficiently shielded so that no amount of sparking or other electrical disturbances due to the high voltage altered the background count.

The Li^7 target was made by hammering a piece of pure lithium into a depression in a brass holder. Since the surface was soon covered by a layer of hydroxide the bombarded target was lithium hydroxide. The proton current falling on this target was measured by a sensitive microammeter, A'. The stray magnetic field was sufficiently great to hold back secondary electrons. This was verified for every target used by rotating the target holder through 180°; this replaced the target with the Faraday chamber, F. Occasionally a disagreement was observed; this was found to be due to a layer of oxide forming between the brass and the metallic lithium, and such targets were discarded since a more accurate control of the proton current could be kept with a new target. A target of Li_2O formed by burning pure lithium in air and condensing the smoke on a brass plate gave yields identical with the lithium hydroxide target, provided the proton current was measured by the Faraday chamber. The current to the Li_2O seemed to be a function of the thickness of the film, and in the case of the thicker films (about 0.1 mm) no current could be detected at all. A study of this discrepancy showed that the protons collected on the surface of the highly insulating Li_2O, building up a charge. As the gas surrounding the target was sufficiently ionized partly to neutralize this charge, an equilibrium was probably set up so that little current reached the target holder. That there was enough gas present to provide sufficient ions to neutralize such a charge was shown by the fact that the current to a brass target depended very markedly upon the potential to which the target was raised.

Unfortunately the area of the target intercepted by the proton beam gradually collected a brown deposit such as has been discussed by Stewart.[4] In most cases no appreciable difference in the counting rate could be detected between the first two fifteen-minute intervals. The third fifteen-minute interval showed a slight decrease at the lowest voltages. At 28 kilovolts the sixth interval showed the count had dropped to nearly half that of the first interval. At higher voltages the effect was not so serious. The yield may thus be slightly higher than the values given, but every effort was made to avoid this source of error and in no case was the count included after a consistent decrease in yield appeared. The uniformity of the results for many targets at a given voltage indicates strongly that little error arises from their method of preparation.

TABLE I. *The number of Li^7-proton disintegrations at low voltage.*

$n\times10^{12}$	$1/V^{\frac{1}{2}}\times10^{3}$	V
0.032	650	23,600
.080	598	28,000
.42	527	36,000
1.08	487	42,000
2.30	452	49,000
5.80	423	56,000
9.60	400	62,500
14.6	383	68,000
22.4	371	72,500

RESULTS AND DISCUSSION

The number, n, of Li^7 atoms disintegrated per proton from a thick target of pure lithium at the bombarding energies used is given in Table I. n is equal to one-half the total yield of alpha-particles, since each disintegration gives rise to two long range particles. The numbers deduced from the experiments have been multiplied by a factor of 4 owing to the fact that pure lithium would give four times the yield of the lithium hydroxide target used. V is expressed in volts.

From 900 to 1500 particles were counted for each proton energy used. The errors due to measuring the energy of the protons from the value of their $H\rho$, and the uncertainty in the solid angle were slightly larger than the proba-

[4] R. L. Stewart, Phys. Rev. **45**, 488 (1934).

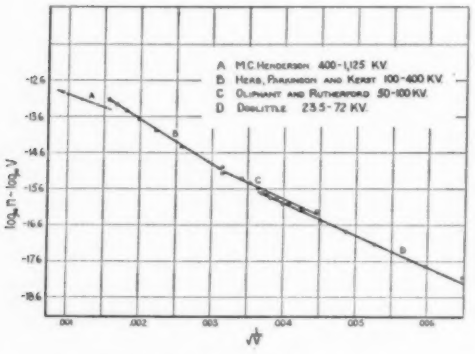

FIG. 2. A comparison of the results of several observers on the disintegration function of Li^7.

bility errors in counting. Taking the relative error for probability fluctuations as $A^{\frac{1}{2}}/A$, where A is the number of atoms breaking up in a given time interval, the error from this source is a little less than $\pm$ three percent. In all cases allowance was made for the residual count. For the lowest point, corresponding to 23.6 kilovolt protons, only about 150 particles above the background were counted; consequently the error in this reading may be quite large. Nevertheless the certainty of disintegrations at this voltage is established. A brass target gave no increase over the usual background count. These data further verified the fact that the pliotron was sufficiently shielded.

The probability of disintegration has been derived by Gamow[5] and the value for thick targets has been derived by Oppenheimer[6] by integrating Gamow's formula assuming the range to be proportional to $V^{1.5}$. The number of disintegrations is found to be proportional to $Ve^{-a/\sqrt{V}}$. Henderson compared this value with his observations at high potentials and found very good agreement. Bearing in mind the analogy with Richardson's thermionic equation, $\log n - \log V$ is plotted against $1/V^{\frac{1}{2}}$. The author's results are shown in Fig. 2 together with those of several other observers which were taken at higher voltages. The curve A represents Henderson's[6] data for very high energy protons. Curve B gives the observations of Herb, Parkinson and Kerst[7] for the range from 100 to 400 kilovolts. Curve C is a portion of the curve taken from the graph of Oliphant and Rutherford.[8] The results of the present paper are given in curve D. The slope of curve A is slightly less than C or D, whereas curve B has a distinctly greater slope than C or D. Curve C has the same slope as D but the values of n are slightly higher. This would indicate a constant factor such as might arise in the measurement of the proton currents, the velocity or the solid angle used. In all cases the data of the various observers have been altered where necessary to agree with the definition of n given at the beginning of this section. From the general form of the disintegration curve (Fig. 2) no signs of resonance are evident, nor does there appear any discontinuity in the lower end of the curve such as would suggest a low voltage limit. By using a more intense proton beam or increasing the efficiency of the detecting apparatus this curve might well be continued to lower voltages.

The yield from a thin film of lithium was calculated from the thick film data after the manner described by Herb, Parkinson and Kerst.[7] However, the theoretical data of Mano[9] indicate that the range of the protons is more nearly given by $R=kV^{1.2}$ rather than $kV^{1.5}$ in the range from 80 to 300 kilovolts. From 80 kilovolts down the departure from the $V^{1.2}$ relation is greater, and it is doubtful if such a curve would have much additional significance. Assuming $R=kV^{1.2}$ a curve similar to the one given by Herb, Parkinson and Kerst[7] is obtained. The assumption of the relation $R=kV^{1.2}$ would alter the theory of the curves of Fig. 2 slightly.

The author wishes to express his appreciation to Professor A. J. Dempster, who suggested the problem, for his valuable advice and discussions throughout the course of the work. It is also a pleasure to acknowledge the benefit derived from several preliminary experiments which were carried out in conjunction with Dr. F. L. Verwiebe.

[5] G. Gamow, *Nuclear Structure and Radioactivity*, pp. 49, 97.
[6] M. C. Henderson, Phys. Rev. **43**, 98 (1933).
[7] Herb, Parkinson and Kerst, Phys. Rev. **48**, 118 (1935).
[8] J. D. Cockcroft, "Noyaux Atomique," Institute de Physique Solvay, 7e Conseil de Physique, p. 35.
[9] G. Mano, J. de phys. rad. **5**, 628 (1934).

Variation of Range with Angle of the Disintegration Alpha-Particles of Li^7

A. ROBERTS, T. ZANDSTRA, R. CORTELL AND F. E. MYERS, *New York University, University Heights*

(Received April 1, 1936)

The range of the alpha-particles emitted from Li^7 under 200 and 240 kv proton bombardment was measured at various angles with respect to the incident beam of protons. The results are fully in accord with the predictions of the principles of conservation of energy and momentum when the straggling due to the penetration of the target by the proton beam is taken into account. The results show, furthermore, that if $_4Be^8$ is formed in this reaction, and subsequently disintegrates into two alpha-particles without the emission of a gamma-ray, it must have a mean life of not more than $3 \cdot 10^{-14}$ second.

INTRODUCTION

IN nuclear disintegration experiments, when the amplifier-counter method is used, usually only those particles emitted in one particular direction are observed. When observations are made with a cloud chamber, particles given off at different angles can be observed, but the number of such observations is generally relatively small.

It was thought desirable to obtain some data by the amplifier-counter method concerning the ranges of alpha-particles given off at several different angles to the direction of the incident proton beam in the disintegration of Li^7 by protons. Such measurements offer a direct check on the conservation of momentum and energy in this nuclear reaction and also provide some information concerning the mean life of $_4Be^8$ if formed. $_4Be^8$ has been observed as a disintegration product in the bombardment of beryllium and boron[1] by protons; it is thus of interest to consider the possibility of its formation in this reaction, and to discuss its mean life if it is assumed to be unstable because of the very high energy release (17 MEV) of the reaction. Finally, information concerning the amount of straggling due to target penetration can be obtained from data of this type.

Some indirect evidence for the conservation of momentum in this reaction has been obtained by Cockcroft and Walton,[2] who found some of the alpha-particles to be emitted simultaneously in pairs in opposite directions, and by Kirchner,[3] who found the maximum angle between pairs of tracks in a cloud chamber to be consistent with the conservation of momentum. Dee and Gilbert[4] obtained consistent results in investigating the disintegration of deuterium by deuterons by assuming the conservation of momentum. Bothe[5] measured the ranges of the protons emitted by boron under alpha-particle bombardment at various angles to the incident beam by interposing absorption screens, and found agreement, within the relatively large error of this method, with the predictions of conservation of momentum.

APPARATUS

The high voltage supply circuit, proton source, and accelerating tube used in this experiment were the same as those used by Giarratana and Brennecke,[6] and were described in detail in their article. The protons, after being accelerated, were separated magnetically and the beam was further defined by two 4 mm circular slits A, B, placed 17 cm apart (see Fig. 1). These served as an additional check on the voltage, since any appreciable change in the energy of the protons would cause the beam to be cut off.

The protons then struck a target T, consisting of a thick film of lithium fluoride, and the disintegration alpha-particles could issue from the chamber through the windows W, making various angles with the proton beam. The target was mounted on a stopcock and was always turned so that it made equal angles with the incident proton beam and the emerging alpha-

[1] Oliphant, Kempton, and Rutherford, Proc. Roy. Soc. **A150**, 241 (1935).
[2] Cockcroft and Walton, Proc. Roy. Soc. **A137**, 229 (1932).
[3] Kirchner, Physik. Zeits. **23**, 777 (1933).
[4] Dee and Gilbert, Proc. Roy. Soc. **A149**, 200 (1935).
[5] Bothe, Zeits. f. Physik **63**, 381 (1930).
[6] Giarratana and Brennecke, Phys. Rev. **49**, 35 (1936).

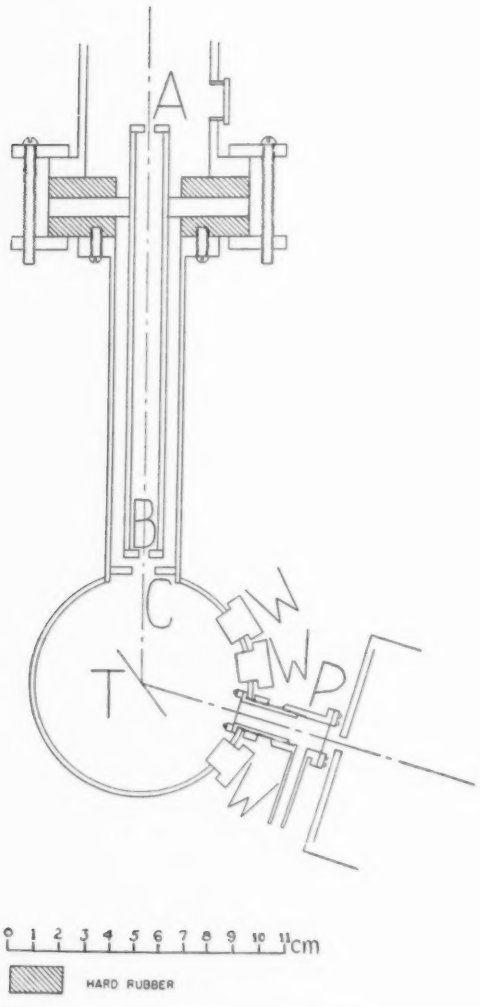

FIG. 1. Target chamber assembly.

particles. The auxiliary slit *C* served to reduce the escape of secondary electrons from the target chamber to a minimum.

The observed alpha-particles passed through a pressure chamber *P*, 3.8 cm long, sealed into one of the four windows *W*. A mercury manometer measured the air pressure in the chamber, which was sealed by mica windows, of which the inner had a stopping power of 3.5 cm air equivalent, the outer 1.5 cm. In addition the last 1.5 cm or more of the path of the alpha-particles was always in air; these precautions were necessary to secure equal stopping power of the mica for all ranges encountered.

The counting method formerly used was changed by replacing the recording oscillograph by a thyratron scale-of-four counter using RCA 885's. Visual observation of the pulses was provided by an RCA cathode-ray oscillograph in parallel with the counter.

The ranges of the alpha-particles were determined from the calibrated stopping power of the mica windows, the distance between the windows, the distance from the outer window to the ionization chamber, and the temperature and pressure of the air through which the alpha-particles travelled. A thermometer placed close to the pressure chamber was read at short intervals. The air pressure within the calibrated chamber was read to within one millimeter of mercury. The distance between the outer window and the ionization chamber was measured at the beginning and end of each run. In addition, the alpha-particles of thorium C′ were used to check the range measurements directly.

While counts were being recorded the proton current entering the insulated target chamber was permitted to charge a 1-mfd mica condenser. The total charge collected in a convenient interval of time was then determined by means of a ballistic galvanometer. Since the ranges were determined by plotting the counts per unit deflection of the galvanometer against the corresponding range, variations in the amount of the proton current did not affect the accuracy of the data and there was no necessity for maintaining a constant proton current. It was sufficient to adjust the hydrogen leak from time to time as the pressure in the supply tank decreased, in order to keep the proton current at a point where a convenient number of counts could be obtained. The actual currents used varied from 0.2 to 2.0 microamperes, averaging about 0.75 microampere.

The voltage across the accelerating tube was maintained constant by working just under sparking voltage of a 25-cm sphere gap adjusted to the correct distance.

Calculations

1. Conservation of momentum

From the equations expressing conservation of momentum and energy for the lithium-proton reaction, the following relationship can easily be derived between the momentum p of an emitted alpha-particle and the angle θ which its path makes with the direction of the incident proton beam:

$$p=\frac{p_0\cos\theta}{2}+\frac{1}{2}\left\{p_0^2\cos^2\theta+2\left[p_0^2\left(\frac{M-m}{m}\right)+2Mk\right]\right\}^{\frac{1}{2}}, \quad (1)$$

where p_0 is the momentum of the proton, M the mass of the alpha-particle, m the mass of the proton, and k the energy released in the disintegration. Using this formula, the momentum, and hence the range of alpha-particles emitted in any direction can be calculated.

2. Mean life of $_4Be^8$

If $_4Be^8$ is formed in this reaction, the above formula will hold provided the $_4Be^8$ nucleus disintegrates into two alpha-particles before losing appreciable energy by gamma-ray emission or by collision. Since the $_4Be^8$ recoil nucleus loses appreciable momentum by collision in about $3\cdot10^{-14}$ second, its mean life must be less than this if the ranges of the alpha-particles are found to agree with formula (1), assuming that there is no gamma-ray emission. This figure is obtained by assuming that if the $_4Be^8$ nucleus lost an appreciable portion of its momentum by any process, this would be easily observable in the range of the alpha-particles, which would then be emitted with different momenta. If the incident proton has an energy of 0.24 MEV, the range of the recoil $_4Be^8$ particle, which has approximately one-eighth the velocity of the proton, can be interpolated from Blackett's data,[7] and turns out to be 0.2 mm in air, or not more than 0.0001 mm in the solid LiF target, whose density is 2.2. If we assume the Geiger range-velocity relation to hold, the average velocity of the particle will be three-fourths the initial velocity, which gives a time of $1.5\cdot10^{-13}$ second to completely stop the recoil. It seems reasonable to suppose that in the first 20 percent of the range enough momentum is lost to be measurable as a change of range of the alpha-particles in the forward and backward directions when the recoiling particle finally does disintegrate. This leads to the value of $3\cdot10^{-14}$ second as an upper limit for the mean life of $_4Be^8$ if this nucleus is formed and subsequently disintegrates into two long-range alpha-particles.

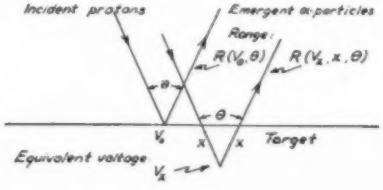

FIG. 2.

3. Thickness of target

Because of target penetration, the proton energy varies from a maximum at the surface of the target to zero at some point within. Since the yield of alpha-particles is a function of the proton energy, a calculation was made to determine the effect of target penetration on the mean range at different angles.

Experimentally, the target was always turned so that the distance traversed in the target was the same for both protons and alpha-particles. From Fig. 2 it appears that a proton whose initial voltage is V_0 and whose total range in the target is X penetrates the target to some distance x where it causes disintegration of a lithium nucleus. The range $R(x, V_x, \theta)$ of the alpha-particles emitted at this point will depend on the depth x, the equivalent voltage V_x at this depth of the proton, and the angle θ at which the alpha-particle is emitted. If we let $Y(V_x)$ represent the yield resulting from bombardment at the voltage V_x of a thin target, the mean range of all the alpha-particles emitted from a thick target will be

$$\bar{R}=\frac{\int_0^X Y(V_x)R(x, V_x, \theta)dx}{\int_0^X Y(V_x)dx}. \quad (2)$$

θ is a constant for any one window and $Y(V_x)$ can be obtained from a yield curve. In these calculations the yield data of Herb, Parkinson, and Kerst[8] were used.

[7] Blackett, Proc. Roy. Soc. **A103**, 62 (1923).
[8] Herb, Parkinson and Kerst, Phys. Rev. **48**, 118 (1935).

TABLE I. *Summary of results.*

Equivalent Angle with Incident Proton Beam I	Voltage (kv) II	Mean Range (cm) at 76 cm, 15°C Observed III	Calculated *Thin Target* IV	Calculated *Thick Target* V	Spread of Range Corresponding to Straight Portion of Range Curve (cm) Observed VI	Calculated VII
46°	240	9.156±0.04	9.31	9.13	0.90±0.1	0.90
71°	240	8.859± .04	8.83	8.79	.85± .1	.68
96°	240	8.347± .04	8.32	8.32	.45± .075	.45
122°	240	7.839± .035	7.91	7.93	.35± .05	.37
46°	200	9.132± .08	9.14	9.09	.95± .15	.82
71°	200	8.624± .06	8.77	8.73	.65± .15	.58
96°	200	8.308± .06	8.29	8.30	.50± .1	.43
122°	200	7.856± .035	7.91	7.94	.30± .05	.37
Thorium C′ [13]		Extrapolated Range 8.623± .025			.35± .05	

The integration is approximated numerically using for x the values given by Mano[9] and calculating $R(x, V_x, \theta)$ from formula (1). The results are shown in Table I.

A simple consideration of formula (1) shows that at the voltages used in this experiment the range of the alpha-particles increases as the proton energy increases when θ is less than a critical angle which is slightly over ninety degrees, while at angles larger than this the opposite is true. Hence the straggling effects due to target penetration should be counteracted to some extent in the backward direction and exaggerated in the forward direction.

RESULTS

The results of the experiment are given in Table I, and are shown graphically in Fig. 4. In the table, for convenience, the calculated mean ranges are listed, as found from formula (1) (listed as thin target) and as calculated from formula (2) (listed as thick target). It is well to note that, to the precision with which the results were obtained, the thick and thin target predictions are experimentally indistinguishable except in the direction closest to that of the incident beam, where the straggling is at a maximum. It is seen that where the results are unambiguously distinguishable (46°, 240 kv) the agreement is with the prediction for the thick target. As an additional check on the straggling calculations, the observed maximum spread in range of the alpha-particles, corresponding to the straight portion of the range curve, is given. The calculated spread shown in the table includes the straggling due to the thick target, the variation in range due to the fact that the particles were observed through an aperture covering a spread of 7.5° in angle with the incident beam, and the ordinary straggling to be expected from a homogeneous source; the last was observed directly, using Th C′. The agreement between observed and calculated quantities in this case is seen to be at least qualitatively correct, the straight portion of a range curve not being an extremely definite quantity.

In Fig. 3 the runs taken at the extreme angles at 240 kv are plotted, with Th C′ as a comparison on the same scale.

In Fig. 4 the results of the range measurements are plotted, the full line here representing the

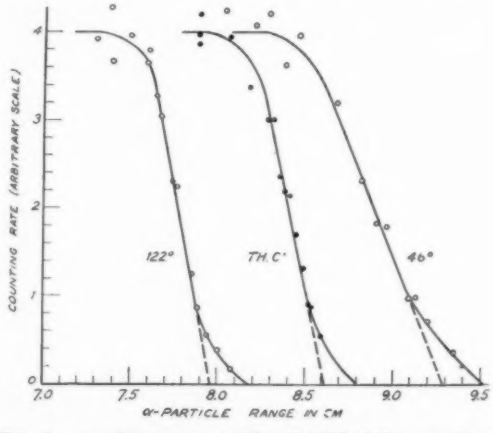

FIG. 3. α-particle range at 46° and 122°; 240 kv protons; Th C′ for comparison.

[9] Mano, J. de phys. et rad. **5**, 628 (1934).

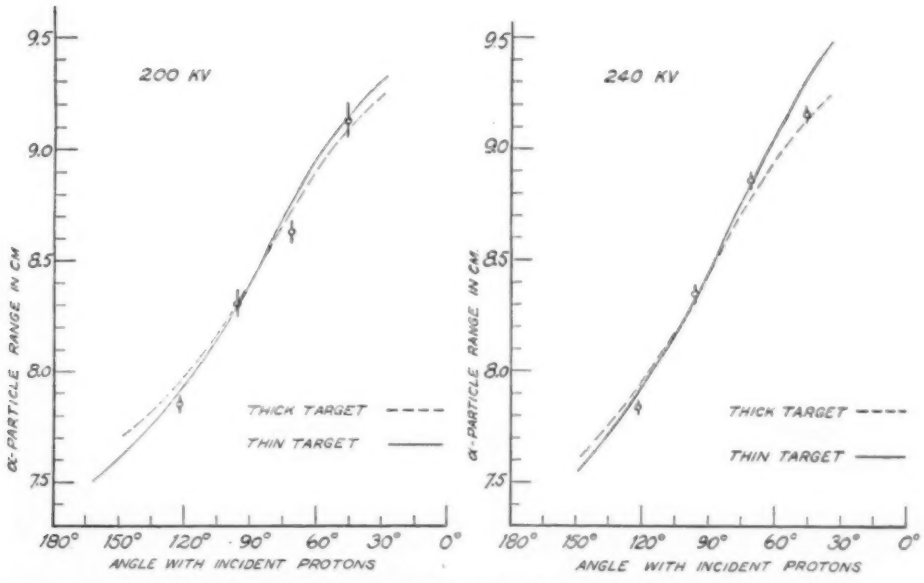

FIG. 4. α-particle range as a function of angle with incident protons.

range calculated for thin targets, the dotted line the range calculated for thick targets, and the circles experimental points. The range calculations are based on an energy release of 17.06 MEV, as found by Oliphant, Kempton and Rutherford,[10] and with which our results agreed.

The data for the range-velocity relations for alpha-particles were taken from the Cavendish laboratory curves.

PRECISION OF RESULTS

The most important uncertainty in determining the ranges arises from the extrapolation of the straight portion of the range curves. Taking into consideration this uncertainty and those mentioned in the discussion of the calibration of the stopping power of the apparatus, we estimate the total probable error to be that given in the table for each run. This includes the uncertainty in stopping power obtained from the thorium C′ measurements.

Since the circular opening of the ionization chamber subtended an angle of 7.5° at the target, a calculation was necessary to determine the angle corresponding to the effective range of the spectrum of particles obtained. An integration taking into account the change of range with angle and the varying area of the opening gives as a result for the equivalent angle the median angle minus three degrees.

The condenser circuit, including the insulated target chamber, was found to have a resistance to ground of more than 10^{10} ohms, which would introduce a negligible error in the galvanometer readings. Condenser polarization was also checked and found to have a negligible effect. The ballistic galvanometer could be read to within less than one millimeter in an average deflection of about 10 cm giving an error of less than one percent. The voltages can be considered as correct within five percent, and the voltage fluctuations were not greater than two percent.

CONCLUSIONS

It may be seen from the results that within the error of measurement and in the voltage range investigated, momentum is conserved in the lithium-proton reaction.

[10] Oliphant, Kempton and Rutherford, Proc. Roy. Soc. **A149**, 406 (1935).

Since it has been shown by Alexopoulos[11] and Oliphant and Westcott[12] that no gamma-rays accompany the disintegration at the voltages used in this experiment, the variation in range with angle makes it appear that at these voltages, if $_4Be^8$ is formed and subsequently disintegrates into two 8.4-cm alpha-particles without the emission of a gamma-ray, it must have a mean life of not more than $3 \cdot 10^{-14}$ second.

The ranges calculated for a thick target at these voltages show no experimentally observable deviation from those for a thin target except in the extreme forward direction where the difference is observable and the observed range agrees with that calculated for the thick target. This agreement gives a separate additional check on the conservation of momentum, and, assuming that the theoretical data of Mano for the proton energy-range relation are correct, gives an approximate verification of the shape of the yield curves obtained by Herb, Parkinson and Kerst.[8] It must be noted, however, that the predicted mean range is not very sensitive to the shape of the yield curve, and a factor of 1.5 would not affect the calculations enough for the difference to exceed the experimental error.

We wish to acknowledge the valuable assistance of Drs. Giarratana and Brennecke in the construction of the apparatus used in this experiment.

[11] Alexopoulos, Zeits. f. Physik **98**, 336 (1935).
[12] Oliphant and Westcott, London Conf. Rep. I, p. 152.
[13] Rutherford, Wynn-Williams, Lewis and Bowden, Proc. Roy. Soc. **A139**, 617 (1933).

JUNE 1, 1936 PHYSICAL REVIEW VOLUME 49

The Transmutation of Platinum by Deuterons

J. M. CORK AND E. O. LAWRENCE, *Radiation Laboratory, Department of Physics, University of California*
(Received April 7, 1936)

The radioactivity induced in platinum by 5 MV deuterons is composite in character. Chemical separations of the active elements together with an analysis of the decay curves establish that at least two radioactive isotopes each of iridium and platinum are formed. The decay periods of the former are about 28 min. and 8.5 hrs. while the latter have periods in the neighborhood of 49 min. and 14.5 hrs. Inasmuch as the platinum activity emits both positrons and electrons it seems reasonable to ascribe the activities to the isotopes Pt^{193} and Pt^{197} resulting from neutron capture. The active iridium isotopes are probably formed in reactions involving deuteron capture and alpha-particle emission, and the likely radioactive isotopes are Ir^{191} and Ir^{196}. The transmutation functions for the reactions leading to iridium isotopes exhibit maxima indicative of resonance penetration of the platinum nucleus by the deuteron; the nature of the transmutation functions for the reactions giving platinum isotopes is not made certain by these experiments, because of the relative weakness of the platinum activities.

INTRODUCTION

ONE of the noteworthy results of investigations of artificial radioactivity induced by deuterons is that these nuclear reactions can be observed much farther up the periodic table than was expected on the basis of penetration of charged particles through nuclear barriers according to the theories of Gurney and Condon and Gamow. The theory of Oppenheimer and Phillips adequately accounts for the observations of reactions in which only the neutron of the deuteron enters the nucleus, but in the cases of some heavy elements investigated in our laboratory recently, the observations were not even in accord with this theory. Almost every heavy element that was bombarded with 5 MV deuterons exhibited evidences of induced radioactivity characteristic of the element. The yields of radioactivity, however, were small in comparison to those of lighter elements and accordingly the observations were suspected as being due possibly to contaminations.

Platinum, which was one of the heavy elements showing relatively strong radioactivity under deuteron bombardment, was selected for careful study as its chemical and physical proper-

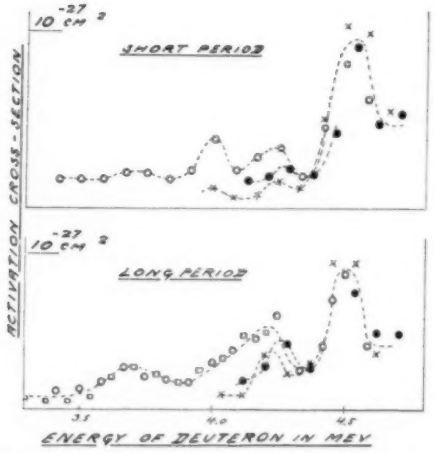

FIG. 1. Transmutation functions (energy-activation curves). Platinum.

ties are favorable to the reduction of contaminants to a minimum. The results of the investigation here reported show definitely that platinum is disintegrated by deuterons of less than 5 MV energy and that the nuclear reactions are understandable in part as an example of resonance penetration of the deuteron into the platinum nucleus.

THE TRANSMUTATION FUNCTION

Preliminary chemical tests[1] indicated that the radioactive substance induced in platinum by deuterons was a noble metal and therefore that in all probability the observed effects were not ascribable to contaminations. It was of immediate interest therefore to determine the transmutation function (the variation with energy of bombarding particle of the probability of the nuclear reaction) for the reaction involved, as it was not clear that platinum should be penetrated to an appreciable extent by such low energy deuterons. The transmutation function was accordingly determined in the same way as in earlier investigations of lighter elements. Stacks of thin platinum foils (thickness 0.000035 inch, stopping power equivalent to 0.45 cm of air) were placed in the beam of deuterons emerging from the magnetic resonance accelerator through a platinum window. The foils were known to be more than 99.9 percent pure platinum and much care was exercised in cleaning them individually. They were rinsed in various solvents including dilute aquaregia and heated to incandescence in a hydrogen flame. That the foils were practically clean was indicated by the consistency of the several sets of observations.

Preliminary experiments indicated that the induced radioactivity was of a complex character with at least two periods, a long period of about 10 hours and a short period of less than an hour. Accordingly the stacks of foils were bombarded with 5μA of deuterons having energies of about 5 MV after which the radioactivity in each foil was observed as a function of the time. From the decay curves of the individual foils it was possible to separate the long and short period activities and evaluate the transmutation function for each activity.[2] The stopping power of the individual foils was determined for alpha-particles from polonium, and a correction which according to Mano[3] is suitable to the faster deuterons was included in evaluating the data.

Three sets of observations are shown in Fig. 1 which is a plot of the activity in arbitrary units in the successive foils through which the deuteron beam passed with an energy indicated by the abscissa. It is seen that the yield of activity is not a monotonic function of deuteron energy as in all previously studied cases, but is a function having several maxima and minima. The observations have a natural interpretation as evidence of the resonance penetration of the platinum nucleus by the deuterons. For the short period activity there are in the range investigated resonance levels in the neighborhood of 4.5, 4.2, 4.0 and 3.7 MV while for the long period activity the 4 MV resonance level seems to be absent. In the region between 3 and 3.5 MV the transmutation function was not examined carefully although it was established that deuterons of energy as low as 3 MV produced an appreciable activity in platinum.

[1] J. M. Cork and E. O. Lawrence, Phys. Rev. **49**, 205 (1936).

[2] Since, as we shall see, both the long and short period activities are complex, these transmutation functions refer to a composite activity and cannot be uniquely interpreted in terms of the elementary reactions involved.

[3] G. Mano, J. de phys. et rad. **5**, 628 (1934).

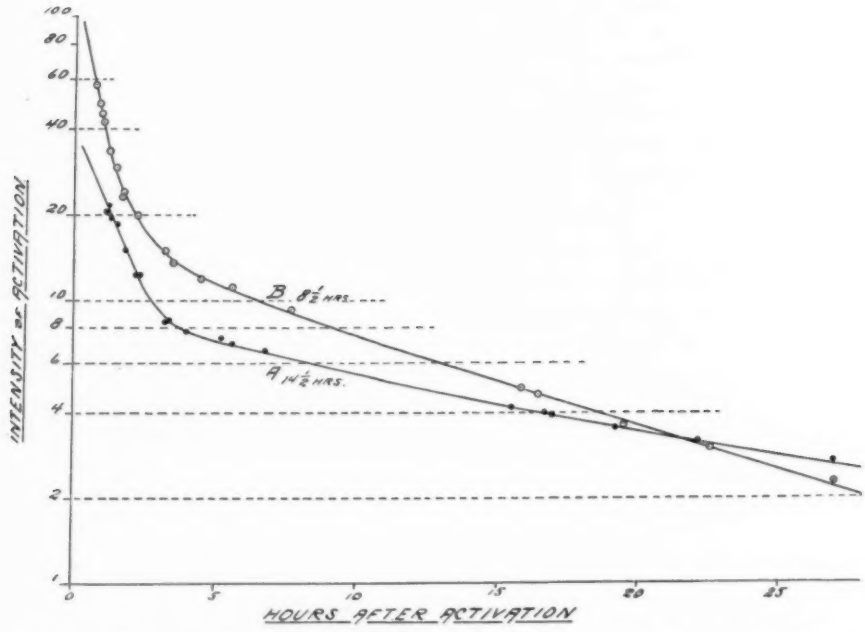

FIG. 2. Decay curves for platinum bombarded by deuterons. Chemical separations. Curve *A*, radio-platinum (49 min.) (14.5 hrs.); curve *B*, radio-platinum (28 min.) (8.5 hrs.).

The order of magnitude of the nuclear activation cross section was obtained from the observation that a platinum foil 3.5×10^{-5} inch thick exposed to 2μA of 4.7 MV deuterons yielded a short period saturation activity of about 10^4 β-particles per sec. This gives for the activation cross section the not unreasonable order of magnitude 10^{-27} cm^2.

Fermi[4] has observed that platinum is rendered weakly radioactive by neutrons. Since we wished to find out whether they played an appreciable role in these experiments, a thick target of platinum was activated by neutrons from a beryllium target bombarded by the deuterons. The neutron intensity from the Be target was about 20 times as great as the neutron radiation from the rest of the accelerator chamber while the activity produced in the thick Pt was less than that produced by the deuteron beam in the individual foils. It was thus clear that the deuterons were reacting directly with the platinum and not through the intermediary of neutrons.

CHEMICAL IDENTIFICATION OF THE RADIOACTIVE SUBSTANCES

It was clearly important to identify by chemical means the radioactive substances as this would throw essential light on the character of the nuclear reactions involved. Accordingly a careful chemical separation of the substances was made, an account of which follows.[5]

In the chemical analysis of the activated platinum tests were made to make sure that the effects observed were not due to traces of lighter elements. In particular the possibility of traces of the platinum-like elements, rhodium and palladium, was examined carefully since these substances would probably be activated about one hundred times as strongly as platinum. It will be seen that the analysis was carried out in a variety of ways in order to eliminate other possible contaminants. In addition, the operations of the analysis eliminated the possibility that the effect was due to the common surface

[4] E. Fermi, E. Amaldi, O. d'Agostino, F. Rasetti and E. Segrè, Proc. Roy. Soc. **A146**, 483 (1934).

[5] We are greatly indebted to Dr. H. W. Newson who very kindly carried through these chemical separations for us.

contaminations, sodium, chlorine, carbon, and oxygen.

In a preliminary experiment an activated platinum foil was dissolved in aquaregia and the platinum was precipitated by reduction with formic acid. Since the precipitated metal carried the radioactivity with it, there was a strong presumption that the active atoms were isotopic with the platinum metals, gold or mercury. An analysis was carried out for all these elements, with the exception of osmium and ruthenium which would distill away as volatile oxides during the solution of the sample in aquaregia. Several active platinum foils were dissolved in aquaregia and small amounts of test solutions of gold, iridium, rhodium, and palladium were added. The analysis was carried out by the method of Noyes and Bray;[6] gold and any mercury present were separated by extraction, platinum and iridium were precipitated together, and finally palladium and rhodium were precipitated separately in the order given. Only the platinum and iridium precipitate showed an appreciable activity so that it is quite definite that the long periods at least are due to isotopes of these elements. The reactions in this case are very nearly unique; the precipitates were $(NH_4)_2PtCl_6$ and $(NH_4)_2IrCl_6$ and because of the rarity of insoluble ammonium salts almost no other elements could be precipitated at this point which would also be precipitated by formic acid. Because of the time required in the analysis, the possibility that the shorter periods were due to rhodium was not eliminated since these periods would have disappeared before the separation was complete. The conditions in the case of palladium which was precipitated next to last were much more favorable, and it is probable that either of the short periods would have been detected if it had been precipitated at this point.

For the final separation a free sample was activated and dissolved, and a small amount of iridium test solution was added. Iridium was precipitated as IrO_2 by the addition of $NaBrO_3$, and platinum was precipitated from the filtrate as $(NH_4)_2PtCl_6$. Both precipitates were found to be active and the activities were observed to decay as shown in Fig. 2. Palladium and rhodium, if present, would precipitate with iridium so that there is a possibility that the short period which precipitated with iridium was due to rhodium. No rhodium period, however, is known to correspond to this half-life so that there is no reason to attribute this period to rhodium.

In order to be sure that the separations were clean, the precipitates were examined after the decay curves had been measured. From the color of the platinum precipitate it was estimated that not more than 0.1 mg of iridium had precipitated with 10 mg of platinum. An analysis of the IrO_2 precipitate showed the presence of about the same percentage of platinum. The separations were, therefore, as complete as could be expected.

In order to be certain that the iridium activity was not due to an iridium impurity in the platinum target, a piece of platinum was covered with a layer of iridium and bombarded. If this activity were due to iridium in the platinum, the contaminated target should give at least one hundred times the activity of the clean platinum target since the platinum did not contain more than 0.2 percent iridium. However, the contaminated target was found to be no more active than the clean target.

Discussion

Thus the evidence is conclusive that the bombardment of platinum by deuterons yields radioactive isotopes of platinum and iridium. Both the platinum and iridium activities are complex, and each element gives a contribution to both long and short period activities. We have thus to account for the formation of at least four radioactive nuclei.

The stable isotopes for this region of the periodic table, as found by Dempster,[7] are shown in the following table where the abundant isotopes are italicized.

76 Os	190		*192*							
97 Ir		*191*		*193*						
78 Pt			192		*194*	*195*	*196*		198	
79 Au								*197*		

[6] A. A. Noyes and W. C. Bray, *Analysis for the Rare Elements* (Macmillan, 1927), p. 110. We are indebted to Professor Bray for his suggestions.

[7] A. J. Dempster, Nature **136**, 65, 909 (1935); also **135**, 993 (1935).

Platinum activity

There are clearly three likely radioactive platinum isotopes formed by addition of neutrons, namely, 193, 197 and 199. The first of these would be expected to emit positrons and go over to the iridium isotope of the same mass number, whereas 197 and 199 would be expected to be electron active.

The β-particles emitted from the activated platinum target (containing both radio-iridium and radio-platinum) were observed in the Wilson chamber soon after bombardment, and it was indeed found that about one-fourth of the particles were positrons. The upper energy limit of the positron spectrum is in the neighborhood of 2.1 MV, while that of the electrons is somewhat lower (about 1.7 MV).[8]

Since very soon after bombardment when the short period activities predominate, the platinum activity was about one-fourth that of the iridium, i.e., the same as the ratio of positrons to electrons, it seems probable that the 49 min. platinum activity is to be identified with Pt^{193}, i.e.,

$$_{78}Pt^{192}+{}_{1}H^{2}\rightarrow{}_{78}Pt^{193}+{}_{1}H^{1}$$

$$_{78}Pt^{193}\rightarrow{}_{77}Ir^{193}+{}_{+1}e.$$

Because of the greater abundance of Pt^{196} the 14.5-hr. electron activity of platinum can reasonably be ascribed to Pt^{197}, which decays to gold, i.e.,

$$_{78}Pt^{196}+{}_{1}H^{2}\rightarrow{}_{78}Pt^{197}+{}_{1}H^{1}$$

$$_{78}Pt^{197}\rightarrow{}_{79}Au^{197}+{}_{-1}e.$$

Iridium activity

It is rather more difficult to make tentative identifications of the iridium isotopes because the nuclear reactions in the formation of the radioactive nuclei here involve a decrease by unity of nuclear charge. It is most attractive to assume that these isotopes result from the capture of the deuteron and emission of an alpha-particle. Now Wilson cloud-chamber observations showed that the β-particles from radio-iridium are negatively charged. Since the isotopes of iridium that would be expected to be radioactive with emission of electrons are 194, 195 and 196, which can go to stable platinum isotopes, it seems probable that the stable platinum isotopes Pt^{196} and Pt^{198} are involved in the iridium reaction. Thus for example

$$_{78}Pt^{196}+{}_{1}H^{2}\rightarrow{}_{97}Ir^{194}+{}_{2}He^{4}$$

$$_{97}Ir^{194}\rightarrow{}_{98}Pt^{194}+{}_{-1}e.$$

It is of course not possible to decide which of the two iridium activities is to be ascribed to the above reaction. This kind of a reaction of deuterons with Pt^{194} should yield Ir^{192}, which would presumably decay with the emission of a positron to form Os^{192}. These positrons have as yet not been observed.

The fact that the iridium activities were larger than the platinum activities leads to the definite conclusion that the maxima observed in the composite transmutation function are at least in large part (and probably entirely), due to the iridium activation. The interpretation of these maxima as an indication of resonance penetration of the deuteron as a whole into the platinum nucleus is consistent with the type of reaction here concerned. The platinum activity involving necessarily only the penetration of the neutron into the nucleus probably follows the Oppenheimer-Phillips transmutation function. Whether this is true cannot be decided from the present experiments, but remains for future investigation.

We acknowledge with thanks grants in support of this investigation from the Research Corporation, the Chemical Foundation and the Josiah Macy, Jr. Foundation. In addition, one of us (J. M. C.) is indebted to the Horace A. and Mary A. Rackham Trust Fund for valuable aid.

[8] These observed upper limits for the β-ray spectra are not precise. Probably the actual upper limits are somewhat higher, particularly in view of the theory of Uhlenbeck and Konopinski. (F. N. D. Kurie, J. R. Richardson and H. C. Paxton, Phys. Rev. **49**, 368 (1936).)

The Beta-Ray Spectra of Several Slow Neutron-Activated Substances

E. R. GAERTTNER, J. J. TURIN AND H. R. CRANE, *University of Michigan*

(Received April 3, 1936)

Indium, silver, rhodium, manganese and dysprosium have been rendered radioactive by exposure to slow neutrons from a 200 millicurie radon-beryllium source surrounded by paraffin, and their beta-ray spectra obtained by the cloud-chamber method. The plots of the energy distributions were transformed into straight lines according to the Konopinski-Uhlenbeck formula, and extrapolated to find the upper energy limits. The fit with the K-U theory was found to be good. The extrapolated upper energy limits found were: In (54-minute period), 1.3 MEV; In (13-second period), 3.2 MEV; Ag, 2.8 MEV; Rh, 2.8 MEV; Mn, 2.8 MEV; Dy, 1.4 MEV.

INTRODUCTION

BECAUSE of the wide theoretical interest in the energy distribution of electrons emitted from natural and artificially stimulated radioactive substances, and the relation of their decay[1] periods to the upper energy limits of the electrons, it has become desirable to obtain such data on as wide a variety of beta-ray emitters as possible. The Konopinski-Uhlenbeck modification of the Fermi theory of beta-decay gives us a method of transforming the energy distribution curves onto a scale in which they appear approximately as straight lines and makes it possible to obtain an estimate of the upper energy limit by an extrapolation which is reasonably impersonal and consistent when used to compare various spectra. Estimates of the upper limit without the use of such a transformation become largely guess work, because of the "tailing out" of the upper end of the spectrum.

By means of a 200 millicurie radon-beryllium neutron source we have been able to activate a number of substances and have obtained their beta-ray energy spectra by the cloud-chamber method.

EXPERIMENTAL METHOD

The cloud chamber employed was 15 cm in diameter and 3 cm deep, filled with air and ethyl alcohol vapor at 1 atmosphere pressure, and equipped with a pair of Helmholz coils arranged so as to bend the electron tracks in the plane of the chamber. A collimated beam of parallel light limited the visible part of the chamber to a sheet 1.5 cm deep, located centrally between the top and bottom. A well in which to place the active substances was set into the top glass plate of the chamber near one side, as shown in Fig. 1. This was 2.5 cm in diameter and had a copper wall 0.0025 cm thick. A 2 mm lead lining having a window 1.5 cm high and extending around 90 degrees of the well at the height of the light beam was inserted to define the source of the beta-rays. In the measuring process only those tracks were considered which appeared to originate within this defined window. With this arrangement it was easy to drop activated substances into the well so that they faced the window, and they could be interchanged within about two seconds, which was essential with several of the short lived substances. Non-stereoscopic photographs were taken and later reprojected natural size for measuring, which was accomplished in the usual way, namely, by matching the tracks with circles of known radii drawn on a card. In most of the present work the strength of the magnetic field was 850 gauss, which made the radius of curvature of a 1 MEV track about 5.5 cm and that of a 2 MEV track about 9.5 cm. The tracks were measured and recorded in groups differing by 1/2 cm radius of curvature, which amounts to 10 percent accuracy for 1 MEV and 5 percent for 2 MEV tracks.

Several possible sources of error are recognized to be present in this type of experiment and have been discussed at length by other authors[2, 3] who use essentially the same method, with somewhat varying opinions as to the seriousness of their effects. These may be listed mainly as the following:

[1] Konopinski and Uhlenbeck, Phys. Rev. **48**, 7 (1935).

[2] Kurie, Richardson and Paxton, Phys. Rev. **49**, 368 (1936).

[3] Fowler, Delsasso and Lauritsen, Phys. Rev. **49**, 561 (1936).

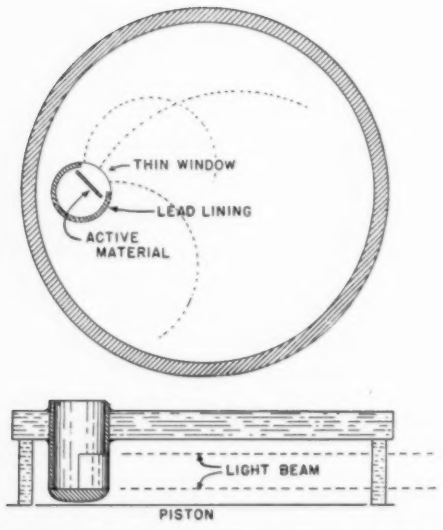

FIG. 1. Horizontal and vertical sections through the cloud chamber, showing the well into which the active substances were introduced.

1. *Scattering:* The probability of scattering is, according to theory, inversely proportional to the square of the energy of the electron and proportional to the square of the atomic number of the gas in the chamber. Also, the probability of small angle scattering is greater than that of large angle scattering. In the present work most of the reprojected tracks were sharp enough so that single scattering of as much as 2° could be recognized, and also appreciable departure of the track from circularity could be recognized; the latter taking care to a large extent of the effect of multiple small angle scattering. In most cases where scattering was recognized in one part of a track, the remaining circular part of the track could be measured with the required accuracy. In a typical run of pictures, only about one otherwise measurable track out of 15 had to be discarded completely on account of scattering. Scattering which is not recognized but large enough to shift the measured radius of curvature of the track by 1/2 cm (the interval used in measuring) is not believed to be frequent and it is estimated that the ordinates of the curves obtained are not influenced to more than a few percent from this cause.

2. *Dependence upon curvature of* (a) the length of track required for accurate measurement of curvature and (b) the chance of a measurable portion of the track lying within the visible part of the chamber. Both these effects are in the direction of favoring the tracks of small curvature.

3. *Effect of thickness of source.* The thicknesses of the substances activated, in terms of stopping power for 1 MEV electrons, were estimated to be as follows: In, 0.2 MEV; Ag, 0.2 MEV; Rh, 0.25 MEV; Mn, 0.35 MEV; Dy, 0.25 MEV. The effect of this is to distort the curve slightly toward the low energy.

4. *Material between the source and the chamber* (copper foils): The stopping power of this material was taken into account in plotting the curves. It varies somewhat with the energy of the electron. For 1 MEV electrons it was estimated to be as follows: In the set-up used for the Ag, In and Rh sources, 0.035 MEV; in that used for the Dy and Mn sources, 0.07 MEV.

5. *Relation between the $H\rho$ interval and the energy interval:* The ratio between the $H\rho$ and the corresponding energy interval is a varying factor in the region of low energies, and consequently in plotting the data on an energy scale as in Figs. 2 to 7, it was necessary to apply a small correction to the ordinates obtained for the 1/2 cm curvature intervals.

6. *Magnetic field strength:* The strength of the magnetic field was calculated from the geometry of the windings and the current, and, as a check, about 1000 recoil electron tracks from the gamma-rays of Th C″ were measured and found to give a cut-off which was in exact agreement with the known energy.

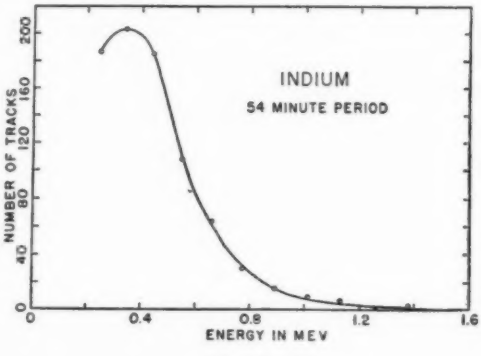

FIG. 2.

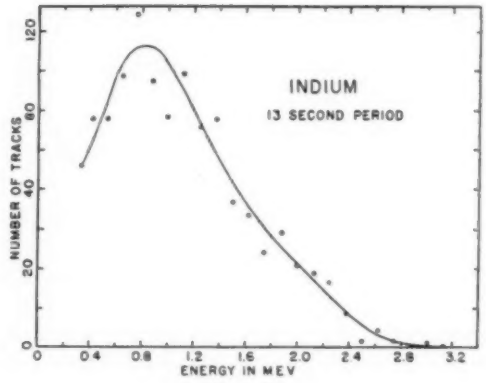

FIG. 3.

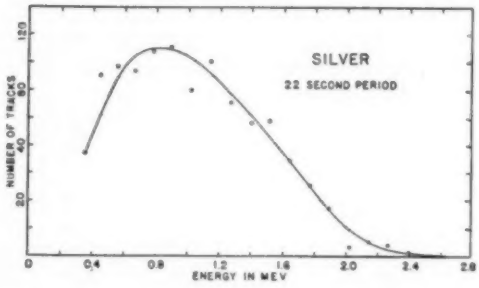

FIG. 4.

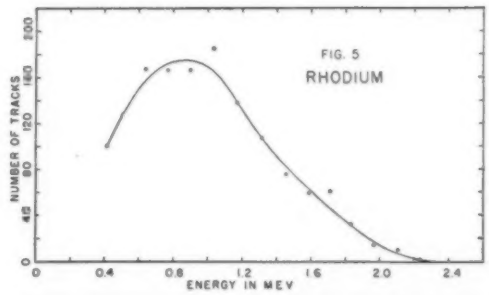

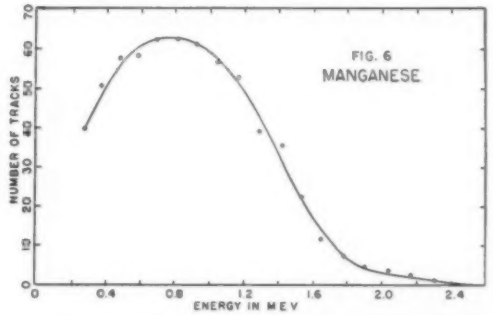

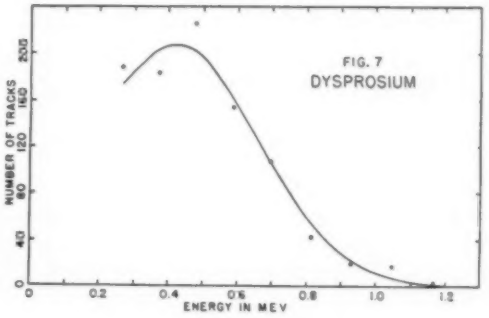

FIGS. 5, 6 and 7.

RESULTS

Indium

Indium emits two groups of negative electrons with half-lives 54 minutes and 13 seconds,[4] respectively. It seems reasonable to assume that these result from two separate isotopes. The spectrum of electrons of the 54-minute period was obtained by exposing the indium for several hours, then waiting about 5 minutes before beginning the measurements, which should have reduced the activity of the 13-second period by a factor of 10^7. In measuring the short period activity, five foils were activated in rotation, each for about 15 seconds before being placed in the cloud chamber. A freshly activated foil was used for each expansion. A consideration of the times involved in this procedure indicated that less than 2 percent of the tracks obtained should have been due to the long period, and these cannot affect the upper end of the 13-second spectrum, as is seen by comparing the energies of the two spectra. Figs. 2 and 3 show the distribution in energy of the tracks for the two periods.

Gamma-rays were detected from the 54-minute period and a few recoil electron tracks were obtained from a thin sheet of glass placed across the center of the chamber. A gamma-ray in the neighborhood of 1 MEV was indicated, with a few tracks also extending to higher energies, indicating the possible presence of an additional weaker and somewhat higher energy line. The small number of tracks makes an estimate of the gamma-ray energy extremely

[4] Amaldi, d'Agostino, Fermi, Pontecorvo, Rasetti and Segrè, Proc. Roy. Soc. **A149**, 522 (1935).

hazardous. No attempt was made to detect gamma-rays from the 13-second period.

Silver

Silver emits negative electrons with half-lives 22 seconds and 2.3 minutes,[4] which have been reported to be of roughly equal intensity and both water sensitive. By placing the silver in the cloud chamber immediately after activation for several minutes, a number of tracks were obtained on the first one or two expansions (the expansion interval was 30 seconds), but tracks on later expansions, which were expected to be present due to the 2.3-minute period were found to be comparatively rare. In obtaining the data in Fig. 4, six silver samples were used; each was activated for only 30 seconds, prior to the expansion, to safeguard further against the possibility of getting any tracks belonging to the 2.3-minute period.

Rhodium

Two periods have been reported for rhodium: 44 seconds and 3.9 minutes.[4] We have measured the energy spectrum of the 44-second period only. A freshly activated foil was used for every two expansions. Fig. 5 shows the energy distribution of negative electrons obtained.

Manganese[4] and dysprosium[5, 6]

These substances emit negative electrons, each with a half-life of approximately 2.5 hours. Photographs were taken over a period of about 2 hours after activation. The results are shown in Figs. 6 and 7. The upper energy limit for dysprosium is in agreement with that reported by Hevesy and Levi.[5]

Comparison with the Konopinski-Uhlenbeck Theory

In Figs. 8, 9 and 10 are plotted the data of the 6 spectra on scales whose ordinates are $[N(\rho)/(H\rho)^2]^{\frac{1}{2}}$ ($N(\rho)$ is the number of tracks in a 1/2 cm interval) and whose abscissa are the total energy of the electrons, including the rest mass, in mc^2 units. Agreement of the experimental data with the K−U theory is indicated if the points fall on straight lines when plotted on this scale. Statistical fluctuations in the ponts near the high energy end of the curves render the last few points untrustworthy, but it is seen that, with the exception of the extreme ends, the points fall reasonably well on straight lines. The upper energy limits of the spectra obtained by extrapolation are: In (54-minute period), 1.3 MEV; In (13-second period), 3.2 MEV; Ag, 2.8 MEV; Rh, 2.8 MEV; Mn, 2.8 MEV; Dy, 1.4 MEV.

According to the Konopinski-Uhlenbeck modification of the Fermi theory the shape of the beta-ray curves depends to some extent upon the nuclear charge especially for elements of high atomic number. In calculating the points for all the K-U plots shown, however, the atomic number was taken equal to zero. As a justifica-

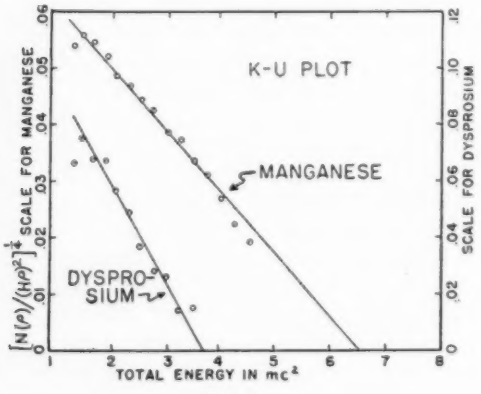

FIG. 8.

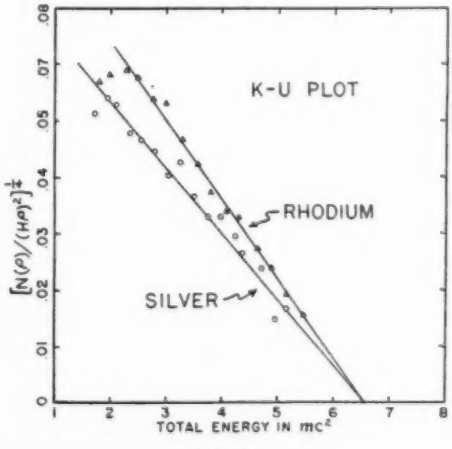

FIG. 9.

[5] Hevesy and Levi, Nature **136**, 102 (1935).
[6] Marsh and Sugden, Nature **136**, 102 (1935).

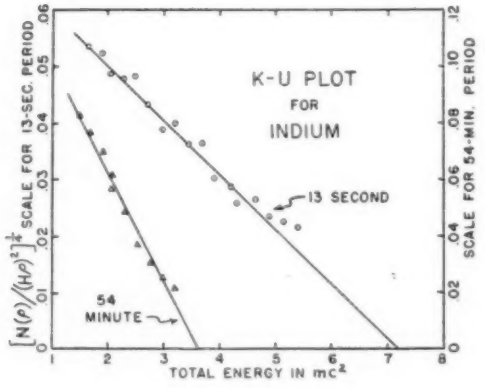

FIG. 10.

tion of this we applied the atomic number correction to the plot of dysprosium (66) and, rhodium (45), and found that it made no significant change either in their form or their end points, insofar as the accuracy of the present data is concerned.

This work was made possible by a grant from the Rackham Foundation. The authors wish to express their appreciation for this support.

Note: Since completing these experiments a paper has appeared by R. Naidu and R. E. Siday (Proc. Phys. Soc. **48**, 332 (1936)) in which they describe measurements of the energy spectra of Ag, Rh, and Dy. Their upper energy limits, obtained by inspection of the energy distribution plots, are 3.8, 3.6, and 1.9 MEV, respectively. These are about 30 percent higher than the values we obtain by inspection. Also, the limits they give for Si and F are very much higher than previous measurements on the same substances by Kurie, Richardson and Paxton (Phys. Rev. **48**, 167 (1935)) and by Crane, Delsasso, Fowler and Lauritsen (Phys. Rev. **47**, 971 (1935)). Alichanow, Alichanian and Dzelepow (Nature **136**, 257 (1935)) have reported energy limits for Rh, Ag and Mn, which are in fair agreement with our values.

JUNE 1, 1936 PHYSICAL REVIEW VOLUME 49

The Emission Spectrum of D_2 in the Extreme Ultraviolet

C. RULON JEPPESEN,* *The Johns Hopkins University*

(Received April 3, 1936)

The emission spectrum of the D_2 molecule has been photographed in the extreme ultraviolet region by use of a grazing incidence vacuum spectrograph with 2-meter grating In the $2p\,^1\Sigma - 1s\,^1\Sigma$ system 37 bands have been analyzed. In the $2p\,^1\Pi - 1s\,^1\Sigma$ system 29 bands were obtained. Constants of the three observed electronic states of the D_2 molecule are given and the data are compared with that of the H_2 molecule. Electronic shifts of 4 cm^{-1} and 23 cm^{-1} are observed for the $2p\,^1\Sigma - 1s\,^1\Sigma$ and $2p\,^1\Pi - 1s\,^1\Sigma$ systems, respectively.

INTRODUCTION

THE following paper is concerned with a description of the $2p\,^1\Sigma - 1s\,^1\Sigma$ $(B-A)$ and $2p\,^1\Pi_{cd} - 1s\,^1\Sigma$ $(C-A)$ band systems in the extreme ultraviolet spectrum of the D_2 molecule. Considerable study has been applied to these systems in the spectra of the H_2[1] and HD[2, 3, 4] molecules and in the present work a comparison is made between the H_2 and D_2 spectra.

EXPERIMENTAL PROCEDURE

For excitation of the D_2 bands in the extreme ultraviolet the methods used previously[1] for the study of H_2 are in general applicable. The chief difficulty in the production of the D_2 spectrum is the problem of outgassing the discharge tube so completely that the remaining amount of H_2 in the electrodes and the glass is negligible. In our case this is somewhat complicated by the fact that no window can be used between the discharge tube and the slit of the spectrograph. It is therefore necessary either to use a stopcock between the source and slit or to admit air into the discharge tube before attaching it to the spectrograph and after each exposure. It is found that by taking suitable precautions the latter method

* Johnston scholar at The Johns Hopkins University.

[1] See C. R. Jeppesen, Phys. Rev. **44**, 165 (1933) and references given there.

[2] C. R. Jeppesen, Phys. Rev. **45**, 480 (1934).

[3] Kurt Mie, Zeits. f. Physik **91**, 475 (1934).

[4] Y. Fujioka and T. Wada, Scientific Papers of the Institute of Physical and Chemical Research, Komagome, Hongo, Tokyo, **27**, 210 (1935).

TABLE IA. $2p\,^1\Sigma - 1s\,^1\Sigma$ *bands of* D_2.

K	I	R BRANCH	I	P BRANCH
		0−3 BAND ν_0 = 82016.4		
0	0d	82036.8		
1	00	021.0	0	81964.5
2			00	874.6
3				
4	0	81776.1*		
5			00d	416.7
6			0d	197.5
7			3	80952.0
		0−5 BAND ν_0 = 76836.0		
0	3	76855.1		
1	1	845.0	1	76786.3
2	3	804.9	3	707.1
3	1	735.3	2	599.6*
4	1	632.2	2	461.9
5	0	504.0	2	295.7*
6	00d	353.8	1	105.2*
7			00	75887.5
8			00	643.3
		0−6 BAND ν_0 = 74421.1		
0	2	74440.2		
1	1	431.3	1	74372.7
2	2	395.9	3	297.5
3	1	332.3	2	195.5
4	1	240.7	3	067.5
5	00	124.6	1	93912.6
6	0	73980.3	2	733.2
7			0	527.8
		0−7 BAND ν_0 = 72121.8		
0	0	72141.3		
1	0	135.0	1	72076.2*
2	2	102.7	2	005.1
3	1	045.1	2	71908.3
4	1	71961.6	2	787.5
5	00d	854.1	0	642.5
6	0	721.1	1	474.0
7			00	282.9
8			00	070.7
		0−8 BAND ν_0 = 69936.2		
0	0	69955.5		
1	0	950.6	0	69892.9
2	1	920.3	2	824.6
3	0	871.4	1	734.5
4	0	796.3	2	621.9
5			1	487.9
6	0d	579.2	0	330.8
7			00	153.4
8			00	68957.4
		1−2 BAND ν_0 = 85704.9		
0	0	85723.5		
1	0d	706.3	0d	85652.0
2	0d	652.0*	3	554.2*
3			0	429.8
4			0d	266.0*
5			1	069.4
6	1	075.0	0d	84832.7
		1−3 BAND ν_0 = 82949.4		
0	1	82968.3		
1	0	951.8		
2	3	902.6*	1	82806.5
3	4	819.6*	1	685.6
4	2	699.3*	2	529.8
5	0d	542.9	2	342.7
6	0	361.9	0	124.7
7			0	81874.6
		1−4 BAND ν_0 = 80304.2		
0	1	80323.2		
1	0	312.3	2d	80252.3
2	1d	264.6	2	171.0
3	00	185.7	3	052.5
4	1	073.7	1	79907.3
5			00d	728.3
6			0	521.9
		1−5 BAND ν_0 = 77778.5		
0	0	77797.1		
1	0	786.8	00	77729.1
2	1	743.9	1	649.1
3	00	670.8	0	540.4
4	0	568.1	1	400.5
5	1	434.1	00	232.5
6	1	277.0*	0	036.8
7			00	76815.5
8			0	566.7

K	I	R BRANCH	I	P BRANCH
		1−7 BAND ν_0 = 73063.8		
0	00	73083.4		
1	0	073.2	00	73018.8
2	1	042.3	1	72948.5
3	00	72978.3	00	848.6
4			0	725.7
		1−8 BAND ν_0 = 70877.8		
0	0	70895.3		
1	00	891.6	00	70833.1
2	1	859.7	2	764.9
3			1	674.4
4	0	727.4	2	559.7
5			0	421.0
6			0	262.2
		1−9 BAND ν_0 = 68806.2		
0	0	68825.0		
1	0	821.7	0	68764.4
2	1	795.7	1	701.1
3	0	747.4	1	615.3
4	0	677.1	2	508.1
5	0	582.4	1	379.8
6			1	233.3
7				
8			0b	67881.3
		2−2 BAND ν_0 = 86629.9		
0	1	86647.6		
1	0	627.5	2	86572.4*
2	2	572.4*	0d	480.5*
3	0d	480.5*	1d	354.3*
4	1d	354.3*	2	185.8
5	2	185.8*	2	85984.5*
6	1	85984.5*	0	750.9
7			2d	483.3*
		2−4 BAND ν_0 = 81229.0		
0	00	81248.0		
1	0	232.1		
2	00	184.8	00	81094.0
3	00	105.0	00	80975.9
4	0	80990.0	3	830.5
5	0	845.3	0dd	644.5
6			2	431.1
7			00	195.0
		2−6 BAND ν_0 = 76286.9		
0	2	76303.8		
1	2	295.7*	00	76239.0
2	0	254.4*	3b	165.0*
3			00	058.1
4	00	087.3	2	75924.9
5			00	764.5
6			00	577.8
		2−7 BAND ν_0 = 73985.8		
0	1	74003.4		
1	0	73995.1	0	73939.9
2	1	959.6	2	867.8
3	00	896.2	1	769.7
4	0d	807.3	2	644.2
5	00	691.4	0	494.3
6	0	547.2	0	319.2
7			0	117.6*
		3−2 BAND ν_0 = 87533.1		
0	1	87551.1		
1	1	528.1	0	87476.8
2	2d	473.0	3	383.6
3	00	376.6	1d	257.6
4			1	087.1
5			0d	86884.7
6	0	873.3	1	647.6
		3−3 BAND ν_0 = 84775.0		
0				
1	0	84775.0	0	84721.3*
2	0	721.3*	1	631.4*
3	1	631.4*	0	507.6*
4	0	507.6*	1	349.2*
5	1	349.2*		
6			00	83931.3
		3−6 BAND ν_0 = 77191.4		
0	0	77209.3		
1	0	197.1	1	77145.6
2	1d	154.9	2	066.5
3	0	084.3	1	960.9
4	1	985.2*	1	825.6
5	2	855.2	2	663.0
6	0	699.2	00	474.2
7			0	254.4

K	I	R BRANCH	I	P BRANCH
		3−9 BAND ν_0 = 70632.3		
0	0	70649.9		
1	0	644.4	0	70591.1
2	1	614.5	2	525.8
3	2	559.7		437.9
4	0	485.1	1	327.4
5			00	196.6
6			0	041.7
		4−1 BAND ν_0 = 91293.1		
0	3	91309.2*		
1	0	290.9		
2	0	220.1	0d	91137.8
3	00	119.5	0	90999.7
4	0	90976.0	0	823.6
5			0	610.9
6	0	578.1	3	354.6
		4−2 BAND ν_0 = 88419.0		
0	0	88435.3		
1	0	415.1	0	88362.6
2	0	355.3	2	269.8
3			0	139.0
4			1	87969.7
5			0	765.3
6			1	528.1
		4−5 BAND ν_0 = 80492.7		
0	3	80510.2		
1	2	493.3		
2	0d	447.4	1	80361.8
3	00	368.5	1d	248.5
4			0	103.4
5			0D	79927.1
6			00d	728.3
		4−7 BAND ν_0 = 75777.4		
0	0	75794.6		
1	00	783.4		
2	00	744.4	2	75659.6
3				
4	00	777.8*	1	428.5
5	0	459.8	1	274.0
6	00	309.4	00	094.8
		4−8 BAND ν_0 = 73590.8		
0	1	73607.9		
1	0	599.2	0	73547.2
2	1	563.5	2	477.6
3	0	502.9	1	382.6*
4	0	415.5	1	262.2
5			0	117.6*
6			1	72948.5
		5−1 BAND ν_0 = 92163.5		
0				
1	00	92155.3		
2	00	091.2	1	92008.2
3	00	91984.9	0d	91868.7
4	00	840.0	0	691.0
5			1	474.4
6	00	430.7	0	220.1
7			0d	90931.4
8			0	610.9
		5−4 BAND ν_0 = 83889.0		
0	0	83906.7		
1	1	886.9	1	83836.0*
2	1	836.0*	1	751.4*
3	0	747.9*	1	632.1*
4	2	632.1	0d	478.7
5	0	473.3	00	290.0
6			0d	074.4
		5−7 BAND ν_0 = 76646.9		
0	2	76663.0		
1	0	651.5	2	76599.6*
2	1	610.4	2	527.8
3	0	542.4	1	425.4
4	0	446.1	2	295.7*
5			0	139.1
6	2b	165.0*	2	75957.2
7			0	744.4
8			00	532.1

K	I	R BRANCH	I	P BRANCH
		5−9 BAND ν_0 = 72387.7		
0	0	72405.0		
1	00d	398.2	0	72345.3
2	0b	361.5	0	280.5
3	0	308.1	0	190.2
4			1	076.2*
5			00	940.4
		6−1 BAND ν_0 = 93017.6		
0	0	93034.1		
1	1d	009.0*	00	92960.6
2			00	861.7
3	2	92834.7	0	722.2
4	00	687.0	1	543.3
5	00	501.8	0	323.3
6			0	067.0
		6−4 BAND ν_0 = 84742.8		
0	0	84759.4		
1	2d	736.4	1	84691.2
2	2b	868.9	1	604.9
3	0d	597.2	0	483.9
4	0	474.8	2	329.2
5	00	152.0	00	140.1
6			00	83921.1
		6−7 BAND ν_0 = 77500.5		
0	0	77517.6		
1	0	503.5	00	77454.5
2	1	462.3	1	380.2
3			1	277.0*
4	0	292.0	1	145.6*
5			1	76985.2*
6			2	804.9*
		6−9 BAND ν_0 = 73241.2		
0	0	73257.4		
1	0	244.0?	0	73199.5
2	2	214.5	2	133.1
3	0	155.6	1	042.3*
4	0	073.2*	2	72927.8
5			0	789.2
6			0	629.0
		7−3 BAND ν_0 = 88220.8		
0	1	88236.4		
1	0	214.9	1	88165.6*
2	3	153.5*	1	076.2*
3	3	060.4*	1	948.4
4	0	87926.6	1	785.1
5			1	585.5
6			1	352.2
7			1	087.1*
		7−4 BAND ν_0 = 85579.3		
0	00	85594.8		
1	1	575.6		
2	0	520.4	0	85440.9
3	0	429.8	00d	319.1
4	00	305.7		
		7−6 BAND ν_0 = 80637.3		
0	0	80653.6		
1	00d	639.3	2	80591.9*
2	2	591.9*	2	510.2*
3	2	510.2*	1	403.0*
4	1	403.0*	1d	260.7*
5	1d	260.7*	00	090.3
6			00	79891.9
		7−8 BAND ν_0 = 76149.3		
0	2b	76165.0		
1	0	154.0	1	76105.2*
2	2	113.6	2	035.5
3	00	047.9	1	75937.3
4	2	75957.2*	2	813.6
5	00d	833.4	0	666.7
6			0	488.8
7			1	291.8
8			0	071.1
		7−9 BAND ν_0 = 74076.8		
0	00	74092.2		
1			00	74035.1
2	0	047.7	0	73968.9
3	0	73988.0	00	877.1
4	00	902.2	0	761.0
5				
6	00	661.0	00	459.7

TABLE IB. $2p\ ^1\Pi_{rd} - 1s\ ^1\Sigma$ *bands of* D_2.

K	I	R BRANCH	I	P BRANCH	I	Q BRANCH
		0−1 BAND ν_0 = 96413.4				
0	00	96431.1*				
1	00	431.1*			0	96371.8
2	00	411.1	0	96255.7	0	318.7*
3	00	363.3	1	146.5	2	235.5
4			1	011.5	0	131.7
5			1d	95851.2	0	95995.7
6			0	667.7		
		0−2 BAND ν_0 = 93539.7				
0	2	93555.9				
1	1	561.1			2	93499.0
2	2	543.0	2	93388.4	3	499.9
3			1	284.9	2	376.2
4	0	433.2	3	157.3	1	278.4
5	0d	344.5	1d	009.0	3	157.3
		0−3 BAND ν_0 = 90779.4				
0	2	90795.2				
1	2	803.6			3	90741.2
2	2	789.8	2	90634.7	4	695.5*
3	3	753.2	4	538.5*	0	627.3
4	4	695.5	3	417.7	4	538.5*
5			1	276.3	0d	425.5
6	0	511.4	3	118.5	00	299.2
		0−4 BAND ν_0 = 88138.0				
0	3	88153.5*				
1	2	165.6*			2	88102.3
2	3	153.5*	3	87999.0*	3	060.4*
3	1	122.8	0	908.2	3	87999.0*
4	1	076.2*	2	797.0	1	916.7
5			0	667.0	00	813.2
6			0	518.0	0	696.8
		1−1 BAND ν_0 = 98075.5				
0	2	98091.3*				
1	2	091.3*			2	98028.6
2	0	067.6	2	97920.2	2	977.5
3	0	013.8	1	805.5	1	893.3
4	1	97932.6	2	667.4	1	783.2
5	00	825.8	1	502.0	2	642.2
6			1	313.5	00	432.7
7					0	298.0
		1−2 BAND ν_0 = 95200.4				
0	1	95216.3				
1	00	220.9			1	95159.4
2	0	197.7	0	95049.1	2	107.7
3	00	150.2	0	94942.4	0d	029.9
4	0	090.5	1	812.8	0	94928.0
5			00	661.1*		
6					00d	661.1*
		1−3 BAND ν_0 = 92442.1				
0	0d	92453.9				
1	0d	464.2			0	92403.5
2	00	446.2	0	92296.5	1	355.5
3			00	198.2	0	284.1
4			1	073.8*	00D	187.1
5			0	91929.0	1	073.8*
		1−4 BAND ν_0 = 89798.1				
0	2	89813.4				
1	0	821.4			2	89761.8
2	0	808.6	1	89657.8	3	717.5
3	1	773.8	4	566.4	1	652.3
5	00	638.7	1	316.3	1	459.0
6	0	544.0	2	163.1	0	332.8
		1−5 BAND ν_0 = 87271.7				
0	4	87287.5*				
1	3	297.4			3	87237.3
2	4	287.5*	3	87138.4	4	197.7
3	1d	257.6	2	050.9	3	138.4
4	1	210.1	3	86944.8	3	060.4
5			1	820.8	1	86963.7
6	2	060.4	3	679.9	0	849.1
7			1	521.3	1b	713.7
		1−6 BAND ν_0 = 84857.1				
0	3	84871.7				
1	3	886.0			2	84824.8
2	2	879.9	1	84730.7	4	789.1
3	1	855.2	1	648.4	2d	736.4*
4	0	815.4	2	550.2	2	666.1*
5	0	759.4	1	434.7	0db	576.2
6	2b	686.9	1	305.8	0	474.8

K	I	R BRANCH	I	P BRANCH	I	Q BRANCH
		2−1 BAND ν_0 = 99666.9				
0	3	99680.7*				
1	3	680.7*			2	99624.6
2	1	649.4	1	99509.6	1	566.4
3	2	593.6	1	395.6	3	478.0
4	1	509.6	2	253.4	0	364.2
5			1	084.2	00	222.1
6	00	253.4	2	98888.8	0d	053.7
		2−2 BAND ν_0 = 96793.4				
0	2	96807.9*				
1	2	807.9*			1	96749.2
2	0	786.7	0	96641.7	1	698.7
3	0dd	735.2	0	534.4	00d	615.1
4	00	665.1?	1	400.6	0	510.7
5	00	554.2	2	235.5?		
6			00	057.8		
7					00	040.2
		2−3 BAND ν_0 = 94035.8				
0	2	94050.4				
1	2	053.9			1	93996.4
2	2	033.6	2	93889.7	4	946.1
3	0d	93988.1	1	787.7	3	871.8
4	1	917.6	3	662.1	3	773.4
5	0	826.7	1d	513.9	0	651.5
6	0	712.8	0d	344.5	00	506.0
7					0d	338.4
		2−4 BAND ν_0 = 91392.2				
0	1	91406.8				
1	00	414.3			1	91355.1
2	1	396.0	0d	91251.7	2	309.2
3			0	157.3	0	240.9
4			1	037.4*	0d	151.0
5			0d	90901.2	1	037.4*
		2−5 BAND ν_0 = 88863.0				
0	1	88877.8				
1	00	885.7			1	88826.7
2	0	874.7	0	88729.5	2	786.3
3	1	838.3	1	640.6	0	724.8
4	2	786.3	1	530.8	1	640.6
5	00	711.4	1	400.5		
6	0	623.0	1b	255.6		
		2−6 BAND ν_0 = 86450.6				
0	4	86466.1*				
1	1d	476.7			3	86417.8
2	4	466.1*	4	86323.8*	4	380.3
3	1	438.6	2	239.8	4	323.8
4	1	392.2	4	137.8	3	249.6
5			2	018.5	1b	154.7
6	3	249.6*	3	85882.6	0d	047.4
7					1	85918.0
		2−7 BAND ν_0 = 84148.9				
0	2	84163.2				
1	2	175.7			3	84118.1
2	2	171.0	2d	84027.6	4	083.9
3	1	149.7	2	83944.7	3	033.6
4	1	110.8	3	855.7	4	83967.1
5			1	751.4	1	886.9
6	00	83989.1	2	622.1	1	786.2
		2−8 BAND ν_0 = 81963.4				
0	2	81978.0*				
1	2	991.8*			1	81934.5
2	2	991.8*	1	81848.0*	1	904.1
3	2	978.0*	0	776.1	0	860.7
4	0	945.4	2	690.2	1	801.6
5	3	904.1*	2	587.3?	00	928.7
6	1	848.0*	0d	479.5	00	642.0
		3−2 BAND ν_0 = 98320.9				
0	3	98335.2*				
1	3	335.2*			2	98278.4
2	2	305.4	2	98168.4	3	222.8
3	00	249.2	0	058.5	1	138.6
4	2	168.4*	2	97920.2	2	028.6
5					1	97893.3*
6			1	571.8	0	726.9
		3−3 BAND ν_0 = 95562.4				
0	3	95576.7*				
1	3	576.7*			0	95522.8
2	1	554.3	1	95416.2	2	470.6
3	1	509.3	1	312.7	1	393.6
4	0	434.4	1	181.2	2	289.8
5	00	329.8	0d	029.9	1	159.4*
6	0	192.8	00	94857.7	00	014.6

K	I	R BRANCH	I	P BRANCH	I	Q BRANCH
		3−4 BAND ν_0 = 92919.7				
0	0d	92937.3*				
1	0d	937.3*				
2	0	916.9	0	92778.8	3	92834.7
3			0	681.5	0	761.8
4			0	559.3	0	667.7
5					00	549.8
6			0d	255.2	00	409.5
		3−5 BAND ν_0 = 90389.7				
0	0	90404.0				
1	0	409.0			3	90351.6*
2	0	392.9	2	90255.1	3	310.3
3	3	354.6*	2	162.6	2	243.7
4			3	049.5	1	156.7
5			0	89911.9	3	049.5*
6			2	761.8	0d	89920.7
7					1	773.8*
8					00	606.5
		3−7 BAND ν_0 = 85675.9				
0	4	85689.8*				
1	0d	699.0			1	85644.0
2	4	689.8*	3	85554.2*	3	608.0
3			0	473.7	3	554.2*
4	0	626.0	3	375.9	1d	483.3
5			0d	266.0	00	394.2
6			0	139.1	1	290.7
7					00	170.8
8					00	035.1
		3−8 BAND ν_0 = 83488.3				
0	3	83501.1				
1	2	513.9			5	83458.8
2	2	509.7	1d	83372.2	5	426.5
3	1	484.8	2	297.2	3	379.2
4	1	448.6	3	208.5	4	316.7
5	00	407.3	1d	100.0	1	237.6
6			00	82980.0	1	146.3
7						
8					0d	921.7
		3−9 BAND ν_0 = 81416.6				
0	2	81430.9*				
1	3b	444.6*			2	81389.0
2	3b	444.6*	1	81306.8	4	361.5
3	2	430.9*	1	237.1	2b	319.7
4	1	408.2	3	157.1	2	264.7
5			0	068.1	0d	197.5
6			0	80964.8	1	117.6
		4−4 BAND ν_0 = 94382.5				
0	0	94392.2				
1	0	398.8			2	94343.4
2	2	375.0	1	94238.3	3	291.6
3	0d	327.2	0	142.5	1	217.4
4	0	255.9	0	016.8*	2	118.5
5			2	93871.8	2	93996.4*
6			1	698.8	0	846.0
		4−7 BAND ν_0 = 87137.5				
0	1	87148.8*				
1	0	160.7			0	87105.0
2	1	148.8*	1	87011.2*	2	066.3
3	00	114.1	0	86933.5*	1	011.2*
4			00	834.2	0	86933.5*
5			1b	713.7*	00	839.8
6					00	730.7
		4−8 BAND ν_0 = 84950.8				
0	0d	84966.1*				
1	1	974.7			0d	84918.5
2	0d	966.1*	0d	84832.7*	2	886.0*
3			0	759.4*	0d	832.7*
4	00	901.0	0d	666.1*	00	767.3
5	00	845.0			2d	686.9*
		4−9 BAND ν_0 = 82879.7				
0	2	82888.7				
1	1	905.3			4	82850.0
2	3	902.6	2	82765.2	4	819.6
3	1	883.7	1	699.3	3	744.8
4	3	850.0*	3	614.8	3	715.7
5	2	806.5	1	517.1	1	642.6
6			1	408.2	0	556.3

may be used, making the objectionable presence of a stopcock unnecessary.

The amount of remaining H_2 which outgasses continuously to dilute the concentration of D_2 may be reduced by continuous operation of the discharge tube and frequent refilling with a high concentration of deuterium. In the present study this process was so successfully carried out that no H_2 lines and less than a score of the strongest HD lines appeared on the spectrograms.

The spectrum was photographed by use of a grazing incidence spectrograph with a two-meter glass grating having 30,000 lines per inch. The dispersion of this instrument in the region of the present study is about 2.4A per mm. The lines of carbon, nitrogen, and oxygen as measured by Boyce and Rieke[5] were used as standards for the reduction of the plates. All the wave numbers given in the tables accompanying this paper are (with the exception of a limited region near 1400A) the results of measurements of two, and in more than half of the range, three spectrograms. Wave-lengths should in general be accurate to within 0.02A and relative values over the range of a single band are somewhat better than this.

Analysis

The previous data on H_2 and HD are of course useful in making the analysis of the D_2 bands. In general the theoretical relations derived for the isotope effect in diatomic molecules furnish preliminary values of the vibrational and rotational constants that can be used to locate the approximate position of any band in the systems under consideration. As usual in this type of spectrum the very great number of closely spaced lines and consequent overlapping of bands forms the chief obstacle to a ready analysis. It may be mentioned that while considerably more than 2000 lines have been measured in the extreme ultraviolet spectrum, less than half of this number has been identified. The same situation exists in the case of the H_2 and HD spectra. It is thought that the data now made available will materially assist in the more difficult analysis of the remaining parts of these spectra.

The wave numbers of all identified lines together with the origins of the bands to which they belong and eye estimates of their intensities are given in Table I. Lines indicated by an asterisk are known blends. The letter "d or b" following the intensity estimate of a line indicates that the line is either diffuse or broad, as the case may be.

Derivation of the Constants

The calculation of the rotational constants for the D_2 molecule has been carried out in detail by the analytical method described by Birge.[6] The method of least squares has been used throughout.

The rotational energy for the $1s\ ^1\Sigma$ and $2p\ ^1\Sigma$ states may be expressed as usual:

$$F=BK(K+1)+DK^2(K+1)^2 + FK^3(K+1)^3\cdots \quad (1)$$

and for the $2p\ ^1\Pi_{cd}$ states:

$$F=B_i^x[K(K+1)-\Lambda^2]+D_i^xK^2(K+1)^2 + F_i^xK^3(K+1)^3\cdots. \quad (2)$$

In the latter case the subscript i indicates the double valued nature of the function, one set of rotational constants being necessary for the c component levels and another for the d components of the Λ-type doubling. The superscript x indicates that these are the so-called "effective" values of the constants, the B^x for example being different from the "true" B. As is indicated previously,[1] however, the true rotational constants for our $2p\ ^1\Pi_{cd}$ level are equal to those given by the c component levels (our B_c^x, D_c^x, etc.). Unfortunately these cannot be directly determined since only Q branches originate on the c component levels. This difficulty is not serious, however, as the rotational term differences (Δ_2F values) can first be determined for the final $1s\ ^1\Sigma$ state and these in combination with the wave numbers of the Q-branch lines yield values of ΔF for the c component levels of the $2p\ ^1\Pi_{cd}$ state.

Unfortunately, no bands were found with $v=0$ in the normal ($1s\ ^1\Sigma$) state as their final level. But the accurate Raman effect measurements of Teal and MacWood[7] happily supply both the

[5] J. C. Boyce and C. A. Rieke, Phys. Rev. **47**, 653 (1935).

[6] R. T. Birge, Bull. Nat. Res. Council No. 57, "Molecular Spectra in Gases."

[7] G. K. Teal and G. E. MacWood, J. Chem. Phys. **3**, 760 (1935).

TABLE IIA. Δ_2F *values for the* $1s\ ^1\Sigma$ *state.*

$v=$	1	2	3	4	5	6	7	8	9
K									
1	171.5(4)	167.1(8)	160.5(7)	154.8(10)	148.5(6)	142.4(5)	135.9(9)	130.0(6)	124.0(7)
2	286.1(4)	275.9(7)	265.9(7)	256.1(10)	245.8(6)	236.7(6)	226.0(7)	216.3(7)	206.6(4)
3	398.5(5)	385.8(8)	372.2(6)	357.6(9)	343.4(6)	329.0(5)	315.4(9)	300.3(7)	287.0(7)
4	510.6(6)	492.3(2)	476.5(6)	457.5(7)	438.8(4)	420.3(5)	401.3(4)	385.5(4)	367.1(4)
5	620.2(5)	596.6(1)	575.8(7)	555.7(5)	529.8(4)	507.7(6)	488.1(5)	467.0(5)	443.2(6)
		702.5(1)	668.9(2)		62.7(2)	598.8(2)	572.5(2)		

TABLE IIB. Δ_2F *values for* $2p\ ^1\Sigma$ *state.*

$v=$	0	1	2	3	4	5	6	7
K								
1	58.5(4)	56.4(4)	55.6(3)	52.5(4)	52.3(2)	51.9(3)	47.0(2)	48.5(2)
2	97.4(9)	94.6(5)	91.0(4)	89.1(4)	84.8(5)	82.8(4)	81.8(3)	79.3(5)
3	136.6(4)	131.9(4)	127.3(3)	122.2(4)	120.0(3)	116.7(4)	113.0(3)	110.3(5)
4	173.3(4)	168.0(4)	161.3(2)	158.6(3)	151.7(3)	149.7(2)	145.3(4)	142.4(4)
5	210.6(2)	201.5(2)	199.7(3)	192.1(1)	185.8(1)	183.3(1)	178.5(1)	172.1(2)
6	247.5(3)	241.3(2)	230.8(1)	225.4(2)		209.2(1)		

required Δ_2F values for $v=0$ and the vibrational term difference between the $v=0$ and $v=1$ levels. The data given by these authors are therefore used in combination with the data on the levels $v=1$ to 9 of the present study for extrapolation to $v=-\frac{1}{2}$ of the normal state.

The values of B_v are given by the following least squares equations:

For the $1s\ ^1\Sigma$ state:

$$B_v=30.4286-1.04917(v+\tfrac{1}{2})+0.0057934(v+\tfrac{1}{2})^2-0.00027486(v+\tfrac{1}{2})^3\cdots. \quad (3)$$

In this equation the extrapolated value of $B_e=30.4286$ agrees sufficiently well with the value 30.430 obtained graphically and the value $B_0=29.905$ may be compared with the 29.906 obtained by the least squares method from the Δ_2F values of Teal and MacWood.

For the $2p\ ^1\Sigma$ state one obtains:

$$B_v=10.0018-0.350924(v+\tfrac{1}{2})+0.00921916(v+\tfrac{1}{2})^2+0.000199495(v+\tfrac{1}{2})^3\cdots. \quad (4)$$

This equation gives the values of B_v from $v=0$ to $v=7$ inclusive but the curvature of the $B_v:v$ function is so pronounced that the least squares cubic does not give a good extrapolated value of B_e. A graphical solution together with difference tables gives the value $B_e=9.994\ \text{cm}^{-1}$.

For the $2p\ ^1\Pi_{cd}$ states we have the equations:

$$(B_d{}^z)_v=15.857-0.5875(v+\tfrac{1}{2})+0.02070(v+\tfrac{1}{2})^2-0.003417(v+\tfrac{1}{2})^3\cdots \quad (5)$$

and

$$(B_c{}^z)_v=15.665-0.5739(v+\tfrac{1}{2})+0.009017(v+\tfrac{1}{2})^2-0.001500(v+\tfrac{1}{2})^3\cdots. \quad (6)$$

In each of the above equations the extrapolated values of $(B_i{}^z)_e$ agree with those obtained graphically. As before mentioned, the $(B_c{}^z)_v$ of the above equation is to be considered the "true" B of the $2p\ ^1\Pi_{cd}$ state. The available data as given by the two equations above extend from $v=0$ to $v=4$ of the $2p\ ^1\Pi$ state.

The vibrational term differences are given by the least squares equations which follow:

For the $1s\ ^1\Sigma$ state:

$$\Delta G_v=3118.77-128.30(v+\tfrac{1}{2})+3.7627(v+\tfrac{1}{2})^2-0.42448(v+\tfrac{1}{2})^3+0.017133(v+\tfrac{1}{2})^4\cdots. \quad (7)$$

This equation fits the data to within the experimental error from $v=\frac{1}{2}$ to $v=8\frac{1}{2}$.

For the $2p\ ^1\Sigma$ state:

$$\Delta G_v=963.52-21.960(v+\tfrac{1}{2})+0.83907(v+\tfrac{1}{2})^2-0.04369(v+\tfrac{1}{2})^3\cdots. \quad (8)$$

In this equation the value of ΔG_v is given from $v=\frac{1}{2}$ to $6\frac{1}{2}$.

For the $2p\ ^1\Pi_{cd}$ state ΔG_v is given from $v=\frac{1}{2}$ to $v=3\frac{1}{2}$ by the equation:

TABLE IIC. Δ_2F *values for* $2p\ ^1\Pi_d$ *state.*

$v=$	0	1	2	3	4
K					
2	154.9(4)	149.0(6)	143.5(8)	137.4(7)	136.3(4)
3	214.7(2)	207.4(5)	200.4(7)	192.2(2)	183.2(3)
4	277.6(3)	266.3(5)	255.3(6)	250.7(4)	235.1(2)
5	335.5(1)	323.6(3)	310.9(1)	299.9(1)	289.4(1)
6	392.9(1)	380.8(3)	366.5(4)		

TABLE III. B_v *values.*

v	$1s\,^1\Sigma$ Obs. B	$1s\,^1\Sigma$ Calc. B	$2p\,^1\Sigma$ Obs. B	$2p\,^1\Sigma$ Calc. B	$2p\,^1\Pi_e$ Obs. B	$2p\,^1\Pi_e$ Calc. B	$2p\,^1\Pi_d$ Obs. B	$2p\,^1\Pi_d$ Calc. B
0	29.906	29.905	9.827	9.828	15.451	15.380	15.560	15.567
1	28.834	28.867	9.495	9.497	14.805	14.820	15.021	15.010
2	27.838	27.837	9.196	9.185	14.283	14.264	14.453	14.464
3	26.817	26.816	8.898	8.895	13.724	13.703	13.960	13.908
4	25.850	25.800	8.582	8.628	13.056	13.130	13.381	13.321
5	24.754	24.788	8.390	8.384				
6	23.761	23.778	8.178	8.165				
7	22.773	22.770	7.966	7.973				
8	21.780	21.760						
9	20.739	20.748						

TABLE IV. ΔG_v *values.*

v	$1s\,^1\Sigma$ Obs. ΔG	$1s\,^1\Sigma$ Calc. ΔG	$2p\,^1\Sigma$ Obs. ΔG	$2p\,^1\Sigma$ Calc. ΔG	$2p\,^1\Pi_{ed}$ Obs. ΔG	$2p\,^1\Pi_{ed}$ Calc. ΔG
$\frac{1}{2}$	2993.5	2993.8	942.4	942.4	1736.2	1736.2
$1\frac{1}{2}$	2874.1	2874.1	922.6	922.6	1661.4	1661.6
$2\frac{1}{2}$	2758.0	2757.7	903.8	904.0	1592.8	1592.7
$3\frac{1}{2}$	2643.0	2643.0	886.3	886.3	1527.0	1527.1
$4\frac{1}{2}$	2527.8	2529.0	869.2	869.2	1462.5	1462.5
$5\frac{1}{2}$	2413.9	2415.0	853.7	852.5		
$6\frac{1}{2}$	2300.6	2300.6	835.8	835.9		
$7\frac{1}{2}$	2186.3	2186.0				
$8\frac{1}{2}$	2071.7	2071.8				

$$\Delta G_v = 1736.18 - 78.215(v+\tfrac{1}{2}) + 4.0143(v+\tfrac{1}{2})^2 - 0.39167(v+\tfrac{1}{2})^3 \cdots ; \quad (9)$$

in each of the above three equations for ΔG_v the extrapolated values of ΔG_e were determined by difference tables and graphs.

In Table II are given values of $\Delta_2 F$ for the three states under consideration. The integer in parentheses following each entry indicates the number of independent values of which the entry is the average. Table III gives the values of B_v as determined by the analytic least squares method[6] together with calculated values from Eqs. (3), (4), (5) and (6). The values of ΔG_v as determined directly from the data and as calculated from Eqs. (7), (8), and (9) are given in Table IV. Values of the band origins for both systems are collected in Table V.

The program of research on the visible spectra of HD and D_2 being carried out in this laboratory by Professor Dieke will give additional data on the $2p\,^1\Sigma$ and $2p\,^1\Pi_{ed}$ states and the accuracy of the results should be increased. Comparison between the data of this paper and the unfinished work in the visible and infrared regions indicate satisfactory agreement.

COMPARISON OF THE H_2 AND D_2 DATA

The well-known theory of the isotope effect in diatomic molecules required the equality of certain ratios between corresponding constants of the two isotopic substances. The constants for H_2 have been previously[1] determined, but in this former work the difference between $(K+\frac{1}{2})^2$ and $K(K+1)$ in the rotational energy function was neglected. Also in the case of the $^1\Pi$-level the Λ in the equation for the rotational energy was not taken into consideration.

In the case of the $1s\,^1\Sigma$-state, in addition to correcting for the above differences, the Raman effect measurements[7] of Teal and MacWood together with a re-examination of the data have slightly changed the extrapolation of the $\Delta G_v : v$ function to $v=-\frac{1}{2}$ giving $\Delta G_e = 4406.4$ cm^{-1}. Teal and MacWood obtain 4405.3 cm^{-1}. Considering the uncertainty of extrapolation together with the error of measurement the two values agree as closely as should be expected. For the

TABLE VA. *Origins of the* $2p\,^1\Sigma - 1s\,^1\Sigma$ *bands.*

v' / v''	0	1	2	3	4	5	6	7
0								
1					91293.1	92163.5	93017.6	
2		85704.9	86629.9	87533.1	88419.0			
3		82949.4		84775.0				
4		80304.2	81229.0			83889.0	84742.8	85579.3
5	76836.0	77778.5			80492.7			
6	74421.1		76286.9	77191.4				80637.3
7	72121.8	73063.8	73985.8		75777.4	76646.9	77500.5	
8	69936.2	70877.8			73590.8			76149.3
9		68806.2		70632.3		72387.7	73241.2	74076.8

TABLE VB. *Origins of the* $2p\,^1\Pi - 1s\,^1\Sigma$ *bands.*

v' / v''	0	1	2	3	4
0	96413.4	98075.5	99666.9		
1	93539.7	95200.4	96793.4	98320.9	
2	90779.4	92442.1	94035.8	95562.4	
3	88138.0	89798.1	91392.2	92919.7	94382.5
4		87271.7	88863.0	90389.7	
5		84857.1	86450.6		
6			84148.9	85675.9	87137.5
7			81963.4	83488.3	84950.8
8				81416.6	8287.79

TABLE VI. *Spectroscopic constant of the deuterium molecule.*

	$1s\,^1\Sigma$	$2p\,^1\Sigma$	$2p\,^1\Pi_{cd}$
B_e(cm^{-1})	30.429	10.186	15.665
B_e^x(cm^{-1})		9.994	15.857
D_e(cm^{-1})	−0.011586		−0.005154
D_e^x(cm^{-1})		−0.004301	−0.005291
F_e(cm^{-1})	6.22×10^{-6}		2.24×10^{-6}
F_e^x(cm^{-1})		2.66×10^{-6}	2.34×10^{-6}
α_e(cm^{-1})	1.0492		0.5739
α_e^x(cm^{-1})		0.35092	0.5875
G_0(cm^{-1})	1543.5	479.0	858.4
ω_e(cm^{-1})	3118.8	963.5	1736.2
$2x_e\omega_e$(cm^{-1})	128.3	21.96	78.215
T_e(cm^{-1})	0	91698.4	100092.1
B_e^i/B_e	0.49989	0.49848	0.50067
calc. ρ^2	0.50035		
ω_e^i/ω_e	0.70777	0.70946	0.70348
calc. ρ	0.70735		

$2p\,^1\Sigma$ and $2p\,^1\Pi_{cd}$ states we have $\Delta G_e = 1358.0$ and 2468.0, respectively. The corrected values of ν_e are 91694.4 cm^{-1} for the $2p\,^1\Sigma - 1s\,^1\Sigma$ system and 100069.3 for the $2p\,^1\Pi - 1s\,^1\Sigma$ system.

Values of the constants for the D_2 molecule are collected in Table VI. In this table the B_e given for the $2p\,^1\Pi_{cd}$ state is the $(B_e^x)e$ of Eq. (6), since this determines the true moment of inertia. The B_e^x of the table is the "effective" $(B_d^x)e$ of Eq. (5).

The presence of a l vector in the $2p\,^1\Sigma$ state gives rise to uncoupling terms because of quantum mechanical interaction with the neighboring $2p\,^1\Pi$ state. The B_v determined from the experimental data for this state is therefore also an "effective" B_v and should be denoted by B_v^x. This is not commonly done, however, since for nearly all practical purposes, such as the calculation of term values, the B_v^x is required. It has thus become customary for the sake of simplicity to call this B_v. In addition the correction that must be applied to B_v^x to obtain B_v is often not known with any degree of accuracy. In our particular case, however, the correction can be made, as indicated in a paper[8] by Professor Dieke. Accordingly for the $2p\,^1\Sigma$ state values of both B_e^x and B_e are given in Table VI. Because of the method that must be used to calculate the correction, the value of B_e^x is more accurate than that of B_e. This is especially true in the case of H_2 where there is a great number of perturbations in the perturbing $2p\,^1\Pi$ state the data of which must be used to obtain the difference between B_e^x and B_e.

When the ratio of the B_e values for the two isotopes are to be compared with the calculated ρ^2 it is of course the true B_e rather than B_e^x that must be used. It is for this reason that both values are given here.

The calculated value of ρ given in the table is obtained from the mass spectrograph measurements of Aston.[9] There are several other corrections as discussed by Dieke[10] that should be applied to some of the constants of Table VI. These are all so small, however, that in view of the very unfavorable ratio of wave number intervals to differences of wave-length in the extreme ultraviolet as well as the comparatively larger error of measurement, these corrections are found to be inappreciable.

A comparison of the electronic term values listed in the table with those given above for H_2 indicates that for the $2p\,^1\Pi - 1s\,^1\Sigma$ system the electronic shift is 23 cm^{-1} and for the $2p\,^1\Sigma - 1s\,^1\Sigma$ system is 4 cm^{-1}. The probable error in these values is perhaps 3 or 4 cm^{-1}.

The value of the shift for the latter system is rather surprising since it is considerably less than the corresponding shift between H_2 and HD. In the case of the $2p\,^1\Pi - 1s\,^1\Sigma$ system the shift is approximately twice that for HD. The value given in a previous paper[2] for this shift in the $2p\,^1\Pi_{cd} - 1s\,^1\Sigma$ system of HD, as has been pointed out several times, is in error. The corrected value is 9 cm^{-1} units.

If the values given by Mie and Fujioka and Wada are corrected to take into account the Λ as well as the difference between $(K+\frac{1}{2})^2$ and $K(K+1)$ in the rotational energy function, one obtains 9 cm^{-1} from the data of each of these investigations also. For the $2p\,^1\Sigma - 1s\,^1\Sigma$ system of HD the data of Mie and of Fujioka and Wada give, when corrected for the difference between $(K+\frac{1}{2})^2$ and $K(K+1)$ a value of the shift equal to 14 cm^{-1}.

[8] G. H. Dieke, Phys. Rev. **44**, 610 (1935).

[9] F. W. Aston, Nature **135**, 541 (1935).

[10] G. H. Dieke, Phys. Rev. **47**, 661 (1935).

New Lines in the Ultraviolet Spectrum of Atomic Iodine

J. H. McLeod, *Harvard University**

(Received April 6, 1936)

A total of 250 lines in the arc and first spark spectrum of atomic iodine have been photographed with a vacuum grating spectrograph. A grating of one meter radius and ruled with 30,000 lines per inch was used. The region covered extended from λ1900A to λ800A. The spectrum was produced in a mixture of argon and iodine. In part of the work, iodine was prevented from entering the spectrograph by a continual flow of pure argon from the spectrograph through the slit to the discharge tube. This permitted the extension of wave-length measurements below the fluorite region to λ800A.

THE arc spectrum of atomic iodine has been observed by Turner[1] and others to wave-lengths as short as 1235A. The range of the work has been limited on the short wave-length side by the necessity of having a fluorite window between the discharge tube and the vacuum grating spectrograph. The object of the present work was twofold: first, to reexamine the spectrum in the fluorite region with higher resolution, and second, to extend the work to shorter wave-lengths.

Apparatus

The vacuum spectrograph had a grating of one meter radius of curvature and was ruled with 30,000 lines per inch. The dispersion was about 8.4A per mm. Schumann plates made by Messrs. Adam Hilger Co. were used throughout.

The plateholder could be dropped to successive positions by means of a magnetic control. An occulter was placed in front of the plateholder and could be moved from the outside by a tapered joint. This arrangement permitted comparison spectra to be placed adjacent to each other without moving the plateholder.

Fig. 1 shows the general arrangement of the vacuum system used for the first part of the investigation. A fluorite window over the slit prevented the iodine from entering the spectrograph. The discharge was excited in a mixture of iodine and argon. The partial pressure of iodine was its vapor pressure at room temperature, about 0.2 mm of Hg. The argon pressure was kept at about 5 to 6 mm of Hg.

A mercury diffusion pump circulated the argon in such a direction as to prevent as far as possible the iodine from coming in contact with the waxed-on fluorite window over the slit. The two refrigerated traps collected iodine and mercury vapor, respectively.

All the stopcocks shown, except the one connecting to the main vacuum pump were of a special "dry" type. They were the right-angled type and were greased only at the end of the barrel next the atmosphere. A circular groove around the plug of the stopcock prevented grease from working down to the vacuum system. They were vacuum tight to the outside atmosphere but were not of course completely tight between different parts of the system. Their purpose, in most cases, was to control the diffusion of iodine throughout the apparatus when it was not in use. Their "dry" feature reduced the chance of the iodine being contaminated with stopcock grease. Apiezon grease was used.

The whole discharge tube could be quickly cleared of iodine by circulating argon through it.

The electrodes were of coiled tungsten wire. A current of 100 ma from a transformer secondary could be run through the tube without overheating it.

Some plates were exposed when a condenser and spark gap were in the circuit. A few spark lines of iodine were recorded in that way.

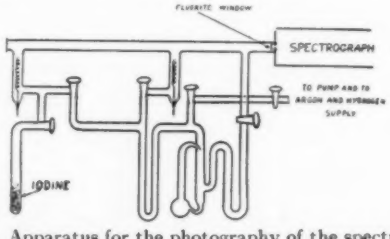

FIG. 1. Apparatus for the photography of the spectrum of iodine to the limit of transmission of fluorite.

* Now at Kodak Research Laboratories.

[1] Turner, Phys. Rev. **27**, 397 (1926); Kalia, Ind. J. Phys. **9**, 179 (1934).

TABLE I. *Iodine ultraviolet lines.*

	λ	Int.	ν		λ	Int.	ν		λ	Int.	ν		λ	Int.	ν		λ	Int.	ν
A	2062.2	10	48491	A	1358.06	5	73634	A	1220.88	6	81908	S	1103.58	6	90614		947.71	1	105518
A	1876.4	7	53292	A	1355.18	3	73791		1216.10	4	82230		1102.09	1	90737		946.99	2	105598
A	1844.4	8	54217	S	1350.31	1	74057		1212.68	2	82462		1101.08	6	90820		942.45	1	106106
A	1839.6	1	54361	S	1349.01	2	74128		1212.17	2d	82497	A	1099.35	3	90963		941.95	0	106163
Abs.	1830.4	10	54634	S	1343.67	2	74423		1210.67	1d	82599		1097.52	1	91114		940.88	2	106283
A	1799.1	9	55583	A	1340.79	3	74583	S	1209.38	2d	82755		1094.64	3	91354		931.52	1	107351
Abs.	1782.8	10	56092	S	1339.96	1	74629		1205.92	6	82924		1090.32	2	91716		931.10	3	107400
A	1702.1	8	58750	A	1336.58	5	74818	S	1204.00	1d	83058		1089.97	1	91746		930.47	2	107473
Abs.	1642.2	6	60893		1336.06	1	74847		1198.86	10	83413		1089.79	2	91761		930.10	2	107515
A	1640.8	9	60945		1331.11	0	75125		1198.25	2d	83455	S	1085.39	6	92133		929.12	3	107629
Abs.	1617.66	5	61818	A	1330.26	3	75173		1194.18	1	83739	S	1082.50	4	92379		925.47	1	108053
A	1593.64	7	62749		1327.63	1	75322		1190.85	9	83974		1076.37	2	92905		922.05	1	108454
Abs.	1582.69	3	63184		1325.09	1	75467		1187.33	9	84222		1075.20	9	93006		921.66	2	108500
A	1561.48	2	64042	A	1317.62	4	75894		1185.75	1	84335		1068.93	2	93552		916.99	3	109054
A	1560.75	1	64072	A	1314.02	1	76102		1185.25	1	84370		1066.34	2	93789		914.92	2	109299
A	1526.52	3	65508	A	1313.51	1	76132		1184.98	1	84390		1065.00	5	93897		910.26	3	109859
A	1518.10	9	65872	S	1306.08	2d	76565	S	1184.15	4	84449	S	1054.64	6	94816		907.98	0	110135
Abs.	1514.76	8	66017	A	1303.06	2	76742		1178.66	9	84842		1042.14	0	95956		905.27	1	110464
A	1514.38	4	66034	S	1302.64	1	76767		1175.83	9	85046		1034.67	6	96649		902.10	1	110852
Abs.	1507.14	5	66351	A	1300.43	4	76898	A	1174.92	1	85112		1033.79	3	96731		900.98	1	110990
A	1492.96	7	66981	S	1296.50	4	77131		1171.01	2	85396	A	1030.04	4	97084		896.65	2	111526
A	1486.01	1	67294	A	1291.12	2	77452		1170.59	0	85427		1026.05	3	97461		896.34	2	111565
	1468.43	0	68100	A	1289.36	2	77558		1168.84	8	85555		1023.53	2	97701		895.89	3	111621
	1465.92	5	68217	S	1286.06	6	77757		1168.54	1	85577		1019.35	5d	98102		893.10	2	111969
A	1459.22	5	68530	S	1285.73	5	77777		1168.21	2	85601		1018.59	6	98175		890.97	1	112237
A	1458.88	6	68546	S	1275.41	10	78406		1167.67	1	85641		1017.97	4	98235		886.49	0	112804
A	1458.07	9	68584		1261.23	1d	79288	S	1167.07	9	85685		1016.39	1d	98387		884.85	0	113013
A	1457.48	9	68612		1259.50	2	79397		1166.47	9	85729		1016.07	1d	98418		877.22	2	113996
	1453.28	5	68810	A	1259.14	4	79419		1165.55	0	85796		1009.91	4	99018		873.47	2	114486
	1446.34	7	69140	A	1251.30	2	79917		1164.83	1	85849	S	1003.44	8	99656		872.37	1	114630
	1443.44	0	69279	S	1250.51	8	79967		1163.36	0	85958	A	1000.61	6	99939		870.30	1	114903
	1440.97	1	69398		1243.16	2	80440		1161.76	0	86076		999.04	1	100096		861.10	2	116130
	1437.64	0	69558		1239.94	1	80649	A?	1160.57	9	86164	S	995.76	5	100427		857.94	1	116558
	1436.25	1	69626		1239.26	3	80693		1159.86	7	86217		994.73	1	100530		855.50	1	116891
	1435.12	0	69681	A	1237.90	2	80782		1159.41	1	86251		992.46	4	100759		847.85	3	117945
A	1425.61	9	70145		1236.37	1d	80882	S	1154.68	10	86604		988.42	4	101173		846.28	4	118164
Abs.	1421.47	7	70350	A	1234.06	10	81033		1139.79	10	87735		978.38	4	102209		845.63	1	118255
	1400.11	2	71423		1233.45	2	81073	S	1132.71	1	88286						843.07	1	118614
	1393.05	2	71785		1233.06	5	81099		1131.50	6	88378		*Measured on one plate only from here on*				841.08	2	118895
A	1390.86	6	71898		1230.19	4	81288		1125.25	7	88869						838.02	1	119329
A	1383.33	6	72289		1228.91	2	81373		1123.89	1	88977		968.65	1	103236		834.09	1	119891
A	1380.60	1	72432		1224.85	2	81643		1117.21	6	89509		967.36	2	103374		831.24	0d	120302
S	1368.28	3	73084		1224.52	1	81665	S	1111.16	6	89996		861.97	0	103953		823.84	1	121383
A	1367.80	4	73110		1224.05	1	81696		1110.51	5	90049		959.60	2	104210		809.13	1	123590
S	1366.56	1	73176		1223.31	1	81745		1104.99	9	90498		953.45	3	104882				
A	1361.03	8	73473						1104.34	1	90552		948.64	0	105414				

Each of the plates exposed for measurement purposes had three overlapping spectra. The two outer ones were of iodine and the third, placed in the middle, was of hydrogen for comparison. One of the iodine spectra was made first, then the hydrogen one, and finally the second iodine one. Between each exposure the discharge tube had to be pumped out and the proper gas or gases admitted. Only such plates as showed no shift between the two iodine spectra were used for measurement. Table I includes the lines measured. Those marked "Abs." were previously reported[2] as absorption lines.

SEPARATION OF ARC AND SPARK LINES

A few plates were exposed for the purpose of distinguishing between arc and spark lines of iodine. They were made by alternately exciting the tube for short periods with a spark discharge and with uncondensed a.c. The occulter was moved between each exposure in such a way that all the "spark" exposures came on one part of the plate and all the "arc" exposures came on an adjacent strip. The total time of exposure for each type of discharge was adjusted so as to give about the same average intensity to the two spectra.

Lines that appeared to be definitely stronger in the spectrum made with the arc discharge are marked A in Table I, and those definitely stronger in the spectrum made with the spark discharge are marked S. A great many lines were too weak in intensity, or for other reasons did not give sufficient indication of their character, to be classified.

LINES OF SHORTER WAVE-LENGTH

In order to photograph the spectrum below the transmission limit of fluorite it was necessary to make some changes in the apparatus. The fluorite window over the slit of the spectrograph had to be removed of course, but, since iodine would corrode the grating if allowed to come in

[2] McLeod, Phys. Rev. **45**, 802 (1934).

contact with it, some other means had to be found to prevent iodine from entering the spectrograph. This was successfully accomplished by extending the circulating system of argon to include the whole spectrograph. As shown in Fig. 2 pure argon filled the spectrograph and was maintained in it at a higher pressure than in the discharge tube. Argon therefore continually flowed outward through the slit and thus prevented the entry of iodine. As an extra precaution the old circulating system shown in Fig. 1 was maintained.

When an exposure was being made the light from the discharge tube passed through the large bore of the stopcock *T*. The stopcock was closed whenever the spectrograph was not in use. After a run the argon in the spectrograph was recovered by adsorbing it on charcoal cooled with liquid air.

The plates were exposed in the same general manner as already described. Lines down to λ809A were recorded. They are listed in Table I. As already mentioned lines that were stronger when a condensed spark discharge was passed through the argon and iodine mixture are marked S. Those stronger when an uncondensed discharge was used are marked A. Intensities are as usual estimated from 0 to 10. Diffuse or broad lines are marked d.

Standard Wave-Lengths

The values for the wave-lengths of the hydrogen lines in the comparison spectrum were those given by Hori[3] from λ1100 to λ1350, and those given by Hyman[4] from λ1350 to λ1600. In addition the impurity lines given in Table II were used as standards. Since the wave-lengths

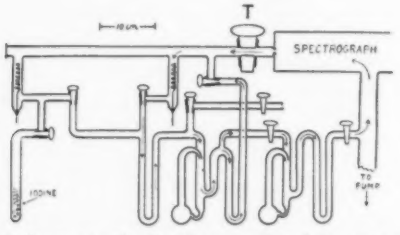

FIG. 2. Apparatus for the photography of the spectrum of iodine to wave-lengths shorter than those transmitted by fluorite.

[3] Hori, Zeits. f. Physik **44**, 834 (1927).
[4] Hyman, Phys. Rev. **36**, 194 (1930).

TABLE II. *Impurity lines used as standards.*

A II	919.78	N I	1199.547
A II	932.05	N I	1200.220
H I	1025.73	N I	1200.706
N I	1134.171	O I	1302.27
N I	1134.419	O I	1304.96
N I	1134.980		

of these lines are known to greater precision than those of hydrogen, considerable weight was given them in determining the correction curves for the plates.

The probable error in the wave-lengths given in Table I is thought to be of the order of ±0.03A between λ800 and λ1600. Because of the lack of standard wave-lengths above λ1600A the accuracy in that region is not very good. The values given above λ1600A were obtained partly by extrapolation and partly by use of the well-known frequency difference of 7601 cm^{-1}.

Analysis

The analysis of the spectrum has not as yet progressed very far. It might be remarked, however, that the well-known frequency difference 7601 cm^{-1} is prominent. The pairs of lines given in Table III show this frequency difference. The pairs marked with an asterisk are believed to be new.

Evans[5] has given an analysis of a number of lines in the visible and infrared. His arrangement

TABLE III. *Pairs of lines showing the frequency difference 7601 cm^{-1}.*

	ν	$\Delta\nu$		ν	$\Delta\nu$		ν	$\Delta\nu$
10 A	48491	7601	4 A	73110		1 S	76767	7603*
10 Abs.	56092		9 A	65872	7601	1	84370	
7 A	53292	7601	8 A	73473		2 A	80782	7596*
6 Abs.	60893		4 A	66034	7600*	6	88378	
8 A	54217	7601	5 A	73634		2	81373	7604*
6 Abs.	61818		7 A	66981	7602	1	88977	
8 A	55583	7601	3 A	74583		6 A	81908	7601*
3 Abs.	63184		5 A	68530	7602	6	89509	
7 A	58750	7601	1 A	76132		9	90498	7604*
4 Abs.	66351		7	69140	7602*	5 b	98102	
9 A	60945	7601	2	76742		6	90820	7598*
6 A	68546		1 S	74629	7601*	1 d	98418	
7 A	62749	7601	4	82230		0	105414	7599*
6 Abs.	70350		1	75322	7602*	0	113013	
3 A	65508	7602*	6	82924				

[5] Evans, Proc. Roy. Soc. **A133**, 417 (1931).

has been supported by work by Tolansky.[6] Turner,[7] it may be recalled, located the two low terms $^2P_{1/2}$ and $^2P_{3/2}$. Their frequency difference is 7601 cm^{-1}. A careful search was made for lines connecting these two low levels with the appropriate levels found by Evans in the visible. No set of lines gave the frequency differences to be expected. It is thought that many of the arc lines in the region investigated must arise from electronic transitions from higher levels built upon the ^1S and ^1D states of the iodine spark spectrum.

Murakawa[8] has made an analysis of the first spark lines in the visible. This work would indicate the presence of a number of prominent spark lines in the ultraviolet having predictable frequency differences. These frequency differences have not been found.

It is with pleasure that I take this opportunity to thank Professor O. Oldenberg for the benefit of many helpful discussions.

[6] Tolansky, Proc. Roy. Soc. **A136**, 585 (1932); **A149**, 269 (1935).
[7] Turner, Phys. Rev. **31**, 983 (1928).
[8] Murakawa, Sci. Pap. Inst. Phys. and Chem. **20**, 285 (1933).

JUNE 1, 1936 PHYSICAL REVIEW VOLUME 49

Magneto-Optical Rotation and Natural Dispersion in Gases

R. T. LAGEMAN AND F. G. SLACK, *Department of Physics, Vanderbilt University*

(Received April 6, 1936)

Formulae for the natural dispersion and for the magnetic rotation are tested together by use of recently determined data for gases. Similar checks have been made by Evans and his co-workers for liquids. Dispersion equations of the Kettelar-Helmholtz type, with a single ultraviolet absorption term, together with Becquerel's equation for the Verdet constant are found to fit the experimental data in the case of the gases, acetylene, ethylene and carbon dioxide. The computed wave-lengths of absorption bands lie within the experimentally determined bands for these gases. Other constants of the two equations are also computed. For several other gases, methyl chloride, chloroform, oxygen, nitrogen and hydrogen, apparently more complicated formulae are required.

OTHER than the early work of Becquerel, Siertsema, and later Sirks, very few data have been available on the Verdet constants of gases at different wave-lengths. Recently however Gabiano[1] measured the Verdet constants of a number of gases under low pressure at three different wave-lengths. He has thus made possible the following investigation. This is an attempt to fit the magnetic rotation and the natural dispersion of gases by expressions involving only one absorption band in the ultraviolet. The method is similar to that used by Evans[2] and his associates in their study of liquids.

According to Becquerel[3] and to Larmor's[4] theory of magneto-optical rotation Verdet's constant δ is given by the relation

$$\delta = \frac{e}{2mC^2}\lambda\frac{dn}{d\lambda} \tag{1}$$

where $dn/d\lambda$ is the dispersion of the refractive index, C is the velocity of light, and e/m is the effective ratio of the charge to the mass of the dispersion electrons.

If it is assumed that there is only one ultraviolet absorption band influencing the dispersion, then an equation of the Kettelar-Helmholtz type giving the variation of the refractive index with wave-length is

$$n^2-1=b_0+b_1/(\lambda^2-\lambda_1^2), \tag{2}$$

where b_0 and b_1 are constants and λ_1 is the wave-length of the absorption band. Differentiation of (2) with respect to λ and combination with (1) gives

$$\delta = \frac{eb_1}{2mC^2n}\cdot\frac{\lambda^2}{(\lambda^2-\lambda_1^2)^2}, \tag{3}$$

[1] P. Gabiano, Ann. de physique **20**, 68 (1933).
[2] E. J. Evans, Phil. Mag. **3**, 546 (1927); **5**, 593 (1928); **8**, 137 (1929); **10**, 749 (1930); **11**, 377 (1931); **11**, 1220 (1931); **13**, 265 (1932); **15**, 905 (1933); **15**, 1065 (1933); **17**, 351 (1934); **18**, 386 (1934).
[3] H. Becquerel, Comptes rendus **125**, 679 (1897).
[4] Sir J. Larmor, *Aether and Matter*, App. F. 352.

TABLE I. *Indices of refraction and Verdet constants of acetylene at various wave-lengths.*

WAVE-LENGTH (A)	$\delta \times 10^6$ (from Gabiano)	$(n-1)\times 10^7$ (observed)	$(n-1)\times 10^7$ (calculated)	DIFFERENCE
6708		5929.6	5930.2	+0.6
6438		5944.8	5945.4	+0.6
6104		5966.7	5967.5	+0.8
5893		5983.0	5983.5	+0.5
5780	3.30	5993.5	5994.4	+0.9
5460	3.73	6022.7	6022.8	+0.1
5086		6065.7	6065.8	+0.1
4800		6106.4	6107.0	+0.6
4602		6139.9	6139.7	−0.2
4360	6.27	6189.0	6187.3	−1.7
4047		6262.3	6263.9	+1.6

and placing $$\frac{eb_1}{2mC^2}=K \qquad (4)$$

Eq. (3) becomes $$n\delta=K\frac{\lambda^2}{(\lambda^2-\lambda_1^2)^2}. \qquad (5)$$

By use of Eq. (5), from any two values of $n\delta$ corresponding to two values of λ it is possible to determine the numerical values of the constants K and λ_1. Substituting the value of λ_1 in Eq. (2) one may evaluate b_0 and b_1 from any two values of n corresponding to two wave-lengths. Eq. (2) may then be used to calculate values of n which may be compared with the directly observed values as a check on the validity of the relations involved. This procedure has been followed for several gases as given below.

ACETYLENE. (C_2H_2)

Values of the Verdet constant of acetylene are secured from the observations of Gabiano[4] and refractive indices are taken from the work of Lowery.[5] Lowery represents his results as showing the refractivity of the respective gases for the same number of molecules per unit volume as hydrogen contains at N.T.P. His refractivity measurements thus expressed in relation to the densities of the substances must be converted to the corresponding values under N.T.P. conditions. This was done by multiplying his values by the factor 1.176/1.159 which is the ratio of the experimental to the standard density.

These experimental data for acetylene are shown in Table I. Pairs of values of $n\delta$ and λ from this table have been used in sets of two simultaneous equations of type (5) to find the values of the constants K and λ_1. The mean value of K is $0.994\pm0.005\times10^{-5}$, and that of λ_1 is $0.1282\pm0.0020\mu$. Likewise the mean values of the constants b_0 and b_1 are obtained from several pairs of n and λ by use of Eq. (2). b_0 and b_1 are $11.520\pm0.007\times10^{-4}$ and $1.491\pm0.020\times10^{-5}$, respectively. Thus all the constants of the natural dispersion Eq. (2) are known. This equation has been used to calculate the values of the refractive index given in the fourth column of Table I. The differences between the observed and calculated values are given in column five.

ETHYLENE (C_2H_4)

Similarly for ethylene the values of the Verdet constant are from Gabiano and the refractive indices from Lowery's observations which have been multiplied by the factor 1.261/1.249 to bring them to N.T.P. conditions. These data are given in Table II.

Use of pairs of values given in Table II in the calculation of λ_1 and K from Eq. (5) gives $0.1287\pm0.0030\mu$ as the mean value of λ_1 and $0.947\pm0.007\times10^{-5}$ as the mean value of K. By substituting 0.1287μ for λ_1 in Eq. (2) the mean values of the constants b_0 and b_1 are found from several pairs of n and λ to be $13.974\pm0.020\times10^{-4}$ and $1.560\pm0.030\times10^{-5}$, respectively. Thus the formula for the natural dispersion of ethylene was written with these constants and used to calculate the values given in the fourth column of Table II.

CARBON DIOXIDE

In the case of carbon dioxide the values of the Verdet constant are from Gabiano and the

TABLE II. *Indices of refraction and Verdet constants of ethylene at various wave-lengths.*

WAVE-LENGTH (A)	$\delta \times 10^6$ (from Gabiano)	$(n-1)\times 10^7$ (observed)	$(n-1)\times 10^7$ (calculated)	DIFFERENCE
6708		7162.9	7163.4	+0.5
6438		7178.9	7180.4	+1.5
5780	31.5	7230.0	7229.9	−0.1
5460	35.6	7261.0	7261.3	+0.3
5086	59.9	7305.9	7306.3	+0.4
4800		7348.7	7348.1	−0.6
4358		7433.8	7430.4	−3.4

[5] H. Lowery, Proc. Roy. Soc. **A133**, 188 (1933).

TABLE III. *Indices of refraction and Verdet constants of carbon dioxide at various wave-lengths.*

WAVE-LENGTH (A)	$\delta \times 10^6$ (from Gabiano)	$(n-1)\times 10^7$ (observed)	$(n-1)\times 10^7$ (calculated)	DIFFERENCE
7281		4462.7	4464.0	+1.3
7065		4465.9	4467.0	+1.1
6678		4473.1	4474.0	+0.9
5875		4493.0	4491.5	−1.5
5780	9.4	4495.5	4495.5	+0.0
5460	10.6	4506.4	4505.9	−0.5
5047		4523.3	4523.0	−0.3
5015		4524.9	4525.0	+0.1
4921		4529.3	4528.9	−0.4
4713		4540.2	4540.4	+0.2
4471		4554.7	4555.9	+1.2
4437		4557.2	4557.9	+0.7
4388		4560.7	4562.4	+1.7
4360	17.6	4562.5	4563.7	+1.2

indices of refraction from Stoll.[6] Calculated in the same manner as for the preceding gases λ_1, is found to be $0.1168\pm0.0040\mu$ and K to be $2.882\pm0.030\times10^{-6}$. For b_0 and b_1 $8.826\pm0.006\times10^{-4}$ and $5.357\pm0.150\times10^{-6}$, respectively were found. From the natural dispersion equation determined by these constants the values in column four of Table III were calculated. The small differences in the fifth column indicate how well the dispersion formula fits the experimental data.

From the close agreement between the calculated and observed values of n for the three gases it is concluded that the natural dispersion may be represented as affected by a single absorption frequency in the ultraviolet. It is of interest that the absorption frequency has been found by utilizing the connection between the Faraday effect and the refractive index. Recent measurements of absorption frequencies in acetylene and ethylene have been made by Price[7] who found strong absorption bands in acetylene from 1520 to 1050A and in ethylene from 1750 to 1200A. The bands calculated above for acetylene (1282A) and for ethylene (1287A) lie within these absorption regions found by Price. Similarly the absorption frequency calculated for carbon dioxide at 1168A is experimentally confirmed by Rathenau[8] who found a region of absorption from 957 to 1174A covering the calculated frequency.

[6] E. Stoll, Ann. d. Physik **69**, 80 (1922).
[7] W. C. Price, Phys. Rev. **47**, 444 (1935).
[8] G. Rathenau, Zeits. f. Physik **87**, 32 (1933).

From Eq. (4) it is seen that an opportunity is presented to calculate e/m for the dispersion electrons, since the constants b_1 and K have already been found. K was found when δ was expressed in min. per gauss cm. For use in relation (4) it must be adjusted to fit when δ is in radians per gauss cm. This is done by dividing the value found by 3437.3. For acetylene e/m is found to be 1.16×10^7 e.m.u. which is 65 percent of the accepted value. For ethylene e/m is found to be 1.059×10^7 e.m.u. and for carbon dioxide 0.939×10^7 e.m.u. These are 60 and 53 percent, respectively, of the accepted value. This discrepancy is in agreement with the work of Darwin and Watson[9] who found that e/m calculated from the Faraday effect for a great variety of substances is usually between 40 and 80 percent of the accepted value.

It is apparent that equations of type (5) may be used to represent the magneto-optical dispersion of the three gases within the range of the spectrum considered. This is shown by the fact that the values of the constants K and λ_1 as found by different pairs of values as described are in close agreement. Also, it is seen that relation (1) holds for the three gases. That is, Verdet's constant is proportional to the natural dispersion. However the constant of proportionality is not that predicted by classical theory but is only a fraction of that value.

Calculations similar to the ones above have been attempted on the gases, methyl chloride, chloroform, oxygen, nitrogen and hydrogen. It was found that dispersion in these gases cannot be represented by expressions of type (2) and (5) which involve only one ultraviolet absorption band.

It is unfortunate that there are no data available for the gas ethane. This would add another member to the acetylene-ethylene series and some interesting conclusions might be drawn from the effect of the successive addition of a hydrogen molecule. Further data on the Verdet constants of gases at atmospheric pressure are much to be desired and would aid in checking the present theories.

[9] C. G. Darwin and W. H. Watson, Proc. Roy. Soc. **A114**, 474 (1927).

Rotational Constants of SnS

E. N. SHAWHAN,* *Mendenhall Laboratory of Physics, Ohio State University*

(Received March 3, 1936)

Rotational constants of SnS in its lowest state and one excited state have been determined from the (0,0) and (1,0) bands of the visible system. Empirical formulae were used to determine the combination differences. The constants determined are $B' = 0.140$ cm^{-1} and $r_e' = 2.18$A for the upper state of the visible system and $B'' = 0.157$ cm^{-1} and $r_e'' = 2.01$A for the lowest state of the molecule.

OUR knowledge of the molecular constants of the metallic sulphides is confined to the vibrational constants of MgS,[1] GeS,[2] PbS[3] and SnS.[4, 5] Recent interest[6, 7, 8] in theoretical relationships between the molecular constants of similar molecules makes additional data on the metallic sulphides desirable, and in particular, data on the heavier sulphide molecules. The relatively simple structures of the (0,0)† and (1,0)† bands in the visible SnS system indicated that rotational constants of this molecule might be determined in spite of the complex isotopic composition of Sn.

EXPERIMENTAL

The spectrograms used for the analysis were taken in the first order of a 21-ft. concave grating in a Paschen-Runge mount. This grating is ruled with 30,000 lines to the inch and gives a dispersion of 1.25A/mm in the first order. The SnS was introduced into an iron tube approximately 80 cm long and 1 cm in internal diameter, which was heated to about 1000°C in two nichrome-wound Hoskins furnaces placed end to end. A five-hundred watt projection lamp provided the continuous radiation that was passed through the iron tube containing the SnS vapor. Fe comparison lines were added to the spectrograms by replacing the lamp with an iron arc.

RESULTS

The lines of the (1,0) band are sharp near the tail of the band because of cancelation of the vibrational and rotational isotope displacements and appear increasingly diffuse toward the head. The lines of the (0,0) band are sharp toward the head, but become increasingly diffuse and finally blend together at a considerable distance from the head because of the combined vibrational and rotational displacements. The other bands of the system are made hopelessly complex by the overlapping of the patterns corresponding to the five abundant and six less abundant tin isotopes.

The lines of the (1,0) band, whose head is at 23,899.3 cm^{-1}, clearly separate into two branches of approximately equal intensity near the tail of the band. Nearer the head the lines of the two branches are practically coincident and, because of their diffuseness, in most cases cannot be separated. In this part of the band the centers of the blended lines were measured. The lines of the P branch are represented within the errors indicated in Fig. 1(a) by the formula:

$$\nu = 23{,}879.70 - 0.998m - 0.0169m^2. \quad (1)$$

The lines of the R branch in this band differ by the amounts shown in Fig. 1(b) from the values calculated from the formula:

$$\nu = 23{,}879.70 - 1.011m - 0.0166m^2. \quad (2)$$

The lines of the two branches are practically coincident over the portion of the (0,0) band

* Now at University of Minnesota.

[1] H. A. Wilhelm, Iowa State Coll. J. Sci. **6**, 475 (1932).

[2] C. V. Shapiro, R. C. Gibbs and A. W. Laubengayer, Phys. Rev. **40**, 354 (1932).

[3] G. D. Rochester and H. G. Howell, Proc. Roy. Soc. **A148**, 157 (1935).

[4] G. D. Rochester, Proc. Roy. Soc. **A150**, 668 (1935).

[5] E. N. Shawhan, Phys. Rev. **48**, 521 (1935).

[6] C. H. Clark, Phil. Mag. **19**, 476 (1935).

[7] M. L. Huggins, J. Chem. Phys. **3**, 473 (1935).

[8] H. S. Allen and A. K. Longair, Phil. Mag. **19**, 1032 (1935).

† Rochester, reference 4, using moderate dispersion, assigned an additional v'' progression to this system which would make these bands (1,0) and (2,0), respectively. Measurements from high dispersion plates show that Rochester's v'' values for bands in this progression should be increased by one. Hence the progression cannot belong to this system. Moreover, the system origin corresponding to his assignment is inconsistent with the isotope structure observed at high dispersion. The first constant of the formula used to calculate heads in this system appears incorrectly in our paper.[5] It should be 23,591.81.

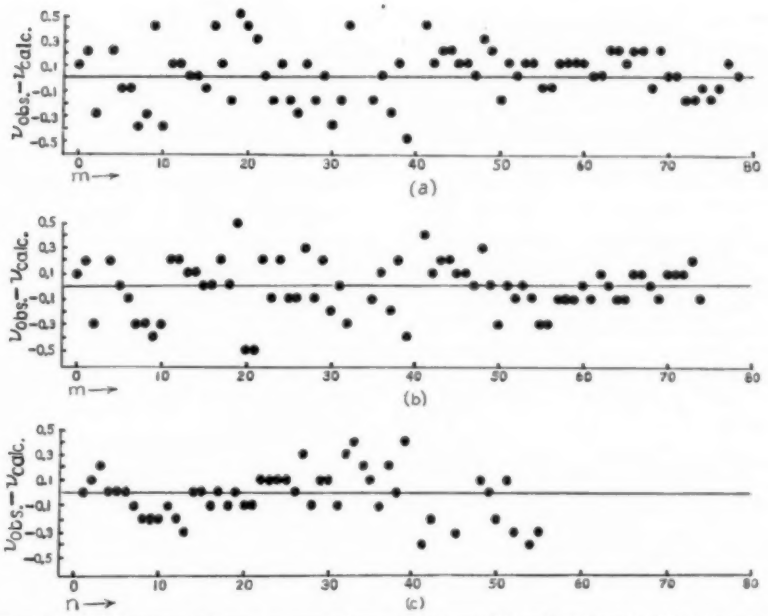

FIG. 1. (a) Differences between measured wave numbers of lines in P branch of (1,0) band and values calculated from (1). (b) Differences between measured wave numbers in R branch of (1,0) band and values calculated from (2). (c) Differences between measured centers of blended lines from P and R branches of (0,0) band and values calculated from (3).

where measurements may be made. Toward the head, which lies at 23,531.9 cm^{-1}, the lines appear quite sharp. The width of the blended lines at a greater distance from the head agrees with the calculated spread of lines arising from the more abundant tin isotopes. Fig. 1(c) gives the difference between the measured wave numbers of the centers of the blended lines and the values calculated from the formula:

$$\nu = 23{,}514.66 - 0.903n - 0.0185n^2. \qquad (3)$$

Since the most accurate measurements are obtained in different portions of the (1,0) and (0,0) bands the empirical series formulae were used to determine the combination differences.

From (1) and (2) the wave number difference

TABLE I. *Observed and calculated values of* Δ_2F'' *from the (1,0) and (0,0) bands.*

n	Δ_2F''calc.(1,0)	Δ_2F''obs.(1,0)	Δ_2F''calc.(0,0)	Δ_2F''obs.(0,0)	n	Δ_2F''calc.(1,0)	Δ_2F''obs.(1,0)	Δ_2F''calc.(0.0)	Δ_2F''obs.(0,0)
1	21.31		21.34	21.4	20	33.26	33.0	33.29	33.0
2	21.94		21.97	22.1	21	33.90	—	33.92	34.0
3	22.57		22.60	22.9	22	34.54	—	34.55	34.7
4	23.19		23.21	23.2	23	35.18	35.3	35.18	—
5	23.82		23.86	23.8	24	35.81	36.0	35.81	36.3
6	24.45		24.49	24.4	25	36.45	36.7	36.44	36.6
7	25.07	24.7	25.12	24.9	26	37.09	37.6	37.07	—
8	25.66	25.5	25.75	25.4	27	37.73	38.0	37.70	—
9	26.28	25.7	26.38	26.1	28	38.38	—	38.33	38.8
10	26.92	—	27.00	26.5	29	39.02	38.8	38.96	—
11	27.55	28.0	27.63	27.6	30	39.66	39.5	39.58	—
12	28.18	28.1	28.26	28.0	31	40.31	40.3	40.21	40.0
13	28.82	28.9	28.89	28.5	32	40.96	40.7	40.84	41.1
14	29.44	29.4	29.52	29.6	33	41.59	41.4	41.47	41.7
15	30.08	29.7	30.15	29.8	34	42.24	42.4	42.10	42.4
16	30.72	30.6	30.78	30.3	35	42.89	42.8	42.73	43.2
17	31.36	31.0	31.41	31.1	36	43.54	43.4	43.36	—
18	31.99	31.6	32.04	31.8	37	44.19	—	43.99	44.6
19	32.60	33.0	32.67	32.8	38	44.84	—	44.62	44.9

between a line in the R branch of the (1,0) band corresponding to $m=n-u$ and a line in the P branch of that band corresponding to $m=n-u+r$ is given by:

$$(0.998r+0.0169r^2+0.013u+0.0003u^2-0.0338ur)(-0.013+0.0338r-0.0006u)n+0.0003n^2. \quad (4)$$

From (3), the wave number of a line in the R branch of the (0,0) band corresponding to n and a line in the P branch of that band corresponding to $n+s$ differ by:

$$(0.903s+0.0185s^2)+(0.0370s)n. \quad (5)$$

With $r=19$, $s=17$, $u=7$ and n as given in the first column of Table I, (4) and (5) represent the calculated combination differences listed in the second and fourth columns, respectively. No other set of integer values of r, s and u gives satisfactory agreement. The third and fifth columns of Table I list the corresponding differences between measured lines in the (1,0) and (0,0) bands, respectively. Observed values of Δ_2F'' have been omitted wherever one of the band lines involved is obscured by an atomic line or where blending makes the measurement too uncertain to have significance.

One-quarter of the difference of successive values of Δ_2F'' gives $B''=0.157$ cm^{-1}. Then $r_e''=2.01$A. The complex isotope structure of the other bands in the system prevents a direct check on the values of Δ_2F' but from the branch formulae of the (1,0) band, $B''-B'=0.017$ so that $B'=0.140$ cm^{-1} and $r_e'=2.18$A.* Allen and Longair[8] have noted that for the lighter molecules the product $\omega_e r_e^3\mu^{\frac{1}{2}}$ is approximately proportional to the number of completed shells in the molecule. For the ground state of SnS this product is 27.4×10^{-33} g$^{\frac{1}{2}}$ cm^2 while for the corresponding state of PBO it is 25.2×10^{-33} g$^{\frac{1}{2}}$ cm^2. This is somewhat better agreement than that obtained from the simpler Morse rule which gives $\omega_e r_e^3\mu^{\frac{1}{2}}=4.25\times10^{-21}$ cm^2 for SnS and 5.10×10^{-21} cm^2 for PbO.

* From these considerations we may estimate very roughly the values of J for the lower levels of the lines measured. In Fig. 1(a), $J=m+21$; in Fig. 1(b), $J=m+38$; in Fig. 1(c), $J=n+16$ for the P branch and $J=n+31$ for the R branch. These numbers are probably in error by several units, but all by the same amount.

JUNE 1, 1936 PHYSICAL REVIEW VOLUME 49

The Diamagnetism of Some Organic Binary Mixtures at Different Temperatures

SAMUEL SEELY, *Department of Physics, Columbia University*

(Received April 3, 1936)

Measurements of the magnetic susceptibilities of mixtures consisting of binary combinations of carbon tetrachloride, benzene and nitrobenzene, made with the improved manometric balance of Wills and Boeker over the range of temperatures from 10°C to 50°C, are described. The results for mixtures of benzene and nitrobenzene, each of which shows no variation of mass susceptibility with temperature, show that the principle of additivity of susceptibilities is valid within the limits of precision of measurement. For mixtures of either benzene or nitrobenzene with carbon tetrachloride, a systematic deviation from additivity is found. The deviations for both groups show a definite dependence upon both concentration and temperature.

INTRODUCTION

IN a recent article, N. N. Pal[1] reported the results of his measurements on the dielectric polarization of mixtures of nitrobenzene and carbon tetrachloride, and also the results of similar measurements on mixtures of nitrobenzene and benzene. The measurements were made with various concentrations over a considerable temperature range. The practically nonpolar liquids, carbon tetrachloride and benzene, were considered as solvents for the highly polar nitrobenzene. The results showed apparently a notable dependence of the polarization of nitrobenzene upon both concentration and temperature, which was accounted for by the author in his theoretical discussion by assuming the association of the nitrobenzene molecules to depend upon both concentration and temperature.

Since changes in association are sometimes accompanied by changes in magnetic suscep-

[1] N. N. Pal, Phil. Mag. **10**, 265 (1930).

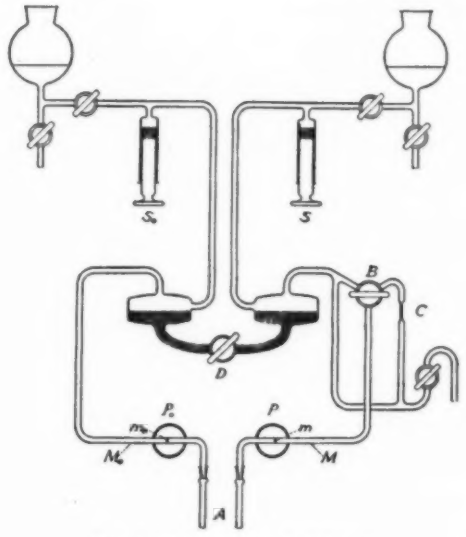

FIG. 1. The manometric balance.

tibility, the investigations described below on mixtures of nitrobenzene and carbon tetrachloride, suggested by Pal's results, were undertaken. Small but measurable deviations from the principle of additivity, dependent upon both concentration and temperature, were found. Later results of experiments on mixtures of nitrobenzene and benzene showed, however, that these deviations could not be ascribed to changes of association in nitrobenzene depending upon concentration and temperature. This conclusion was supported by measurements on mixtures of carbon tetrachloride and benzene, which also showed definite departures from the principle of additivity, depending upon both concentration and temperature.

APPARATUS AND METHOD

The apparatus used in the present investigations was the manometric balance of Wills and Boeker,[2] as modified by Woodbridge.[3] A schematic diagram of the balance is given in Fig. 1. The principle upon which this instrument operates depends upon balancing the force exerted by a magnetic field upon a standard liquid of known susceptibility against the force exerted by a second magnetic field upon the liquid whose susceptibility is to be measured. The liquids terminate in Pyrex tubes of small diameter (M_0, M). The free surface (meniscus), m_0, of one of the liquids is maintained at a fixed position in the field, the meniscus, m, of the other liquid being moved, when a balance is to be obtained, to a determined position in the second field, whose gradient along the tube is known, until the two forces equilibrate.

If the liquids contained in the menisci tubes have volume susceptibilities κ_0 and κ, respectively, the free surfaces being in contact with a medium of volume susceptibility κ_a, then the condition for balance under the action of the magnetic fields, when the field strengths at the menisci are H_0 and H respectively, is

$$\tfrac{1}{2}(\kappa_0-\kappa_a)H_0^2=\tfrac{1}{2}(\kappa-\kappa_a)H^2. \qquad (1)$$

In measuring temperature variations of susceptibility,[4] both menisci are in contact with helium, for which κ_a is negligible in comparison with κ_0 and κ. In this case we obtain from (1) for the mass susceptibility, χ, at any temperature in terms of the mass susceptibility, χ_{T_0}, at the standard temperature

$$\chi=\frac{\rho_{T_0}}{\rho}\frac{H^2}{H_0^2}\chi_{T_0}, \qquad (2)$$

where ρ represents the density.

The susceptibility, χ_{T_0}, of each binary mixture at the standard temperature, T_0, (21.85°C)[5] was determined by means of the balance in terms of a test solution of nickel chloride[6] whose susceptibility is known in terms of the susceptibility of water ($\chi_W=-0.7200\times10^{-6}$ at 20°C) in the manner described by Woodbridge.[3]

The method of calibrating the fields, i.e., the determination of the ratio H^2/H_0^2 for different settings of the variable meniscus has been described in previous papers.[3]

The density values for the various nitrobenzene-carbon tetrachloride mixtures and for the various nitrobenzene-benzene mixtures for all

[2] A. P. Wills and G. F. Boeker, Phys. Rev. **42**, 687 (1932).

[3] D. B. Woodbridge, Phys. Rev. **48**, 672 (1935).

[4] The temperature is regulated by means of water jackets (not shown) surrounding M_0 and M.

[5] The standard temperature 21.85°C was the temperature of neutrality of the nickel chloride neutral solution used in preparing the test solutions.

[6] The volume susceptibility of organic liquids is generally too small to permit balancing directly against water in the manometric balance.

TABLE I. *Nitrobenzene-carbon tetrachloride mixtures.*

					MIXTURE		
c	$-\kappa_{21.85}\times10^6$	$-\frac{1}{\kappa_{20}}\frac{d\kappa}{dT}\times10^6$	T(°C)	ρ_T	$-\chi\times10^6$	$-\chi_{cal.}\times10^6$	$\Delta\chi\times10^{10}$
0.00000	0.6837	13.37	10	1.6135	0.4305	0.4305	0
			20	1.5939	.4300	.4300[1]	0
CCl_4			30	1.5746	.4295	.4295	0
		$\Delta_a=0.0002$	40	1.5547	.4290	.4290	0
			50	1.5352	.4285	.4285	0
.09757[2]	.6750	12.13	10	1.5650	.4375	.4376	− 1
			20	1.5473	.4372	.4372	0
			30	1.5295	.4369	.4367	+ 2
		$\Delta_a=$ .0004	40	1.5116	.4366	.4363	3
			50	1.4936	.4363	.4358	5
.15367	.6698	11.70	10	1.5381	.4416	.4417	− 1
			20	1.5211	.4414	.4413	+ 1
			30	1.5041	.4413	.4409	4
		$\Delta_a=$ .0002	40	1.4871	.4411	.4405	6
			50	1.4700	.4409	.4400	9
.29692	.6589	10.43	10	1.4731	.4526	.4521	+ 5
			20	1.4579	.4526	.4518	8
			30	1.4428	.4526	.4515	11
		$\Delta_a=$ .0003	40	1.4277	.4526	.4511	15
			50	1.4124	.4526	.4508	18
.47424	.6444	9.70	10	1.3967	.4667	.4651	+16
			20	1.3834	.4667	.4648	19
			30	1.3700	.4667	.4646	21
		$\Delta_a=$ .0002	40	1.3566	.4667	.4643	24
			50	1.3434	.4667	.4640	27
.59886	.6349	—	10	1.3479	.4760	.4742	+18
			20	1.3357	.4760	.4740	20
			30	1.3234	.4760	.4738	22
			40	1.3111	.4760	.4736	24
			50	1.2987	.4760	.4734	26
.72128	.6252	—	10	1.3035	.4847	.4831	+16
			20	1.2921	.4847	.4829	18
			30	1.2805	.4847	.4828	19
			40	1.2690	.4847	.4827	20
			50	1.2576	.4847	.4825	22
.85486	.6150	—	10	1.2587	.4936	.4928	+ 8
			20	1.2481	.4936	.4928	8
			30	1.2374	.4936	.4927	9
			40	1.2266	.4936	.4926	10
			50	1.2160	.4936	.4925	11
1.00000	.6048	8.20	10	1.2132	.5034	.5034[3]	0
			20	1.2033	.5034	.5034[3]	0
$C_6H_5NO_2$			30	1.1934	.5034	.5034[3]	0
		$\Delta_a=$ .0003	40	1.1835	.5034	.5034[3]	0
			50	1.1736	.5034	.5034[3]	0
			60	1.1637	.5034	.5034[3]	0

[1] The mean value of χ_{20} for carbon tetrachloride obtained from the results of seven other observers is -0.4308×10^{-6}.
[2] The mean value of χ_{20} for nitrobenzene obtained from the results of five other observers is -0.5026×10^{-6}.
[3] Density values obtained by interpolation with the aid of a large scale graph of experimental measurements.

temperatures were determined by pycnometer measurements. For the benzene-carbon tetrachloride mixtures, the data employed were those given in the *International Critical Tables*. The densities of several solutions of intermediate concentration (the susceptibilities of which were not measured) were measured for comparison. The values obtained are in good quantitative agreement with the *I. C. T.* data.

SUSCEPTIBILITY MEASUREMENTS

Nitrobenzene-carbon tetrachloride

The nitrobenzene and carbon tetrachloride used in these measurements were furnished by

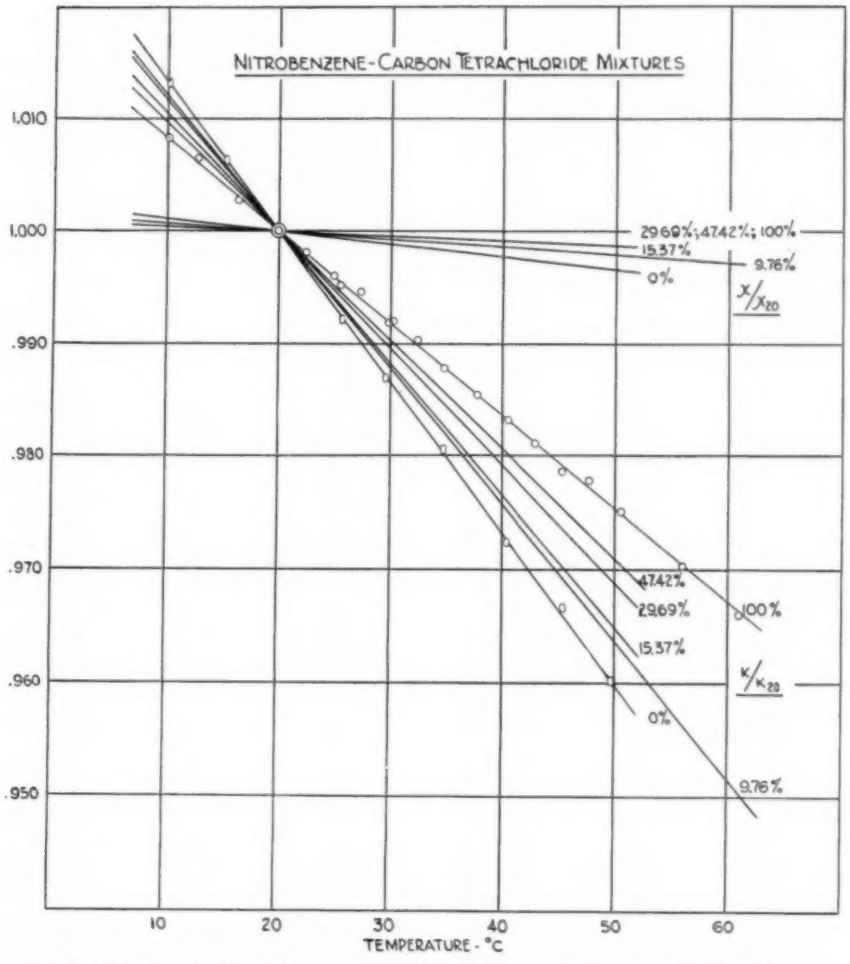

FIG. 2. Variation of χ/χ_{20} with temperature for nitrobenzene-carbon tetrachloride mixtures.

Eimer and Amend. Some Eastman Kodak Company nitrobenzene was measured for comparison with the Eimer and Amend product. The results were the same, within the limits of precision of measurement. All material were carefully distilled.

Measurements were made of the relative volume susceptibility κ/κ_{20} at various temperatures. For all concentrations used, it was found that κ/κ_{20} is a linear function of the temperature within the limits of precision of measurement. The straight lines representing κ/κ_{20} as a function of the temperature are reproduced in Fig. 2. In order to avoid confusion, the experimental points for the pure liquids only are shown; the deviations of the experimental points for the lines appertaining to the mixtures are about the same as the deviations for those of the pure liquids.

The data obtained for the nitrobenzene-carbon tetrachloride mixtures are all contained in Table I. In the first column are found the concentrations of nitrobenzene in carbon tetrachloride considered as the solvent for the several mixtures used. In the second column are found the experimental values obtained for the volume susceptibilities of the various mixtures, assuming the mass susceptibility of water to be

TABLE II. *Benzene-carbon tetrachloride mixtures.*

c	$-\kappa_{21.85}\times10^6$	$-\frac{1}{\kappa_{20}}\frac{d\kappa}{dT}\times10^4$	T (°C)	ρ_T	MIXTURE $-\chi\times10^6$	$-\chi_{cal.}\times10^6$	$\Delta\chi\times10^{10}$
0.00000	0.6837	13.37	10	1.6135	0.4305	0.4305	0
			20	1.5939	.4300	.4300	0
CCl_4			30	1.5746	.4295	.4295	0
		$\Delta_a=0.0002$	40	1.5547	.4290	.4290	0
			50	1.5352	.4285	.4285	0
		12.33					
.01299		$\Delta_a=$ .0002					
		12.13					
.04266		$\Delta_a=$ .0002					
		12.03					
.09811		$\Delta_a=$ .0002					
.10972	.6709	—	10	1.4806	.4597	.4598	−1
			20	1.4626	.4598	.4594	+4
			30	1.4446	.4600	.4589	11
			40	1.4266	.4602	.4585	17
			50	1.4087	.4604	.4581	23
.22166	.6604	—	10	1.3667	.4898	.4897	+1
			20	1.3501	.4900	.4893	7
			30	1.3335	.4902	.4889	13
			40	1.3169	.4904	.4886	18
			50	1.3000	.4906	.4882	24
.33736	.6500	12.07	10	1.2656	.5210	.5206	+4
			20	1.2502	.5212	.5203	9
			30	1.2348	.5214	.5200	14
		$\Delta_a=$ .0002	40	1.2194	.5216	.5196	20
			50	1.2038	.5218	.5193	25
.45969	.6410	—	10	1.1740	.5539	.5533	+6
			20	1.1597	.5541	.5530	11
			30	1.1454	.5543	.5528	15
			40	1.1312	.5545	.5525	20
			50	1.1169	.5547	.5522	25
.55485	.6349	—	10	1.1114	.5794	.5787	+7
			20	1.0979	.5796	.5785	11
			30	1.0844	.5797	.5783	14
			40	1.0709	.5799	.5781	18
			50	1.0574	.5800	.5779	21
.61032	.6313	12.13	10	1.0779	.5942	.5936	+6
			20	1.0648	.5943	.5934	9
			30	1.0517	.5945	.5932	13
		$\Delta_a=$ .0002	40	1.0386	.5946	.5930	16
			50	1.0255	.5947	.5928	19
.69197	.6268	—	10	1.0322	.6159	.6154	+5
			20	1.0197	.6160	.6152	8
			30	1.0072	.6162	.6151	11
			40	.9946	.6163	.6149	14
			50	.9822	.6164	.6148	16
.78741	.6218	—	10	.9836	.6413	.6409	+4
			20	.9717	.6414	.6408	6
			30	.9598	.6414	.6407	7
			40	.9479	.6415	.6406	9
			50	.9360	.6416	.6405	11
1.00000	.6117	—	10	.8894	.6977	.6977[1]	0
			20	.8787	.6977	.6977[1]	0
C_6H_6			30	.8681	.6977	.6977[1]	0
			40	.8573	.6977	.6977[1]	0
			50	.8465	.6977	.6977[1]	0

[1] The mean value of χ_{18} for benzene obtained from the results of ten other observers is -0.7038×10^{-6}.

TABLE III. *Nitrobenzene-benzene mixtures.*

ϵ	$-\kappa_{21.85}\times10^6$	$-\frac{1}{\kappa_{20}}\frac{d\kappa}{dT}\times10^4$	T (°C)	ρ_T	MIXTURE $-\chi\times10^6$	$-\chi_{cal.}\times10^6$	$\Delta\chi\times10^{10}$
0.00000	0.6048	8.20	10	1.2132	0.5034	0.5034	0
			20	1.2033	.5034	.5034	0
$C_6H_5NO_2$			30	1.1934	.5034	.5034	0
			40	1.1835	.5034	.5034	0
		$\Delta_a=0.0003$	50	1.1736	.5034	.5034	0
			60	1.1637	.5034	.5034	0
.10864	.6062	—	10	1.1674	.5245	.5245	0
			20	1.1575	.5245	.5245	0
			30	1.1476	.5245	.5245	0
			40	1.1377	.5245	.5245	0
			50	1.1278	.5245	.5245	0
.22961[1]	.6074	—	10	1.1200	.5481	.5480	+1
			20	1.1105	.5481	.5480	+1
			30	1.1010	.5481	.5480	+1
			40	1.0915	.5481	.5480	+1
			50	1.0820	.5481	.5480	+1
.33555	.6083	9.30	10	1.0819	.5685	.5686	−1
			20	1.0719	.5685	.5686	−1
			30	1.0619	.5685	.5686	−1
		$\Delta_a=$ .0002	40	1.0519	.5685	.5686	−1
			50	1.0420	.5685	.5686	−1
.43490	.6092	—	10	1.0479	.5879	.5879	0
			20	1.0379	.5879	.5879	0
			30	1.0279	.5879	.5879	0
			40	1.0179	.5879	.5879	0
			50	1.0080	.5879	.5879	0
.54844	.6100	10.03	10	1.0125	.6097	.6099	−2
			20	1.0023	.6097	.6099	−2
			30	0.9921	.6097	.6099	−2
		$\Delta_a=$ .0002	40	.9819	.6097	.6099	−2
			50	.9719	.6097	.6099	−2
.65307[1]	.6106	—	10	.9814	.6301	.6302	−1
			20	.9710	.6301	.6302	−1
			30	.9606	.6301	.6302	−1
			40	.9503	.6301	.6302	−1
			50	.9404	.6301	.6302	−1
.76962	.6113	10.67	10	.9485	.6531	.6529	+2
			20	.9379	.6531	.6529	+2
			30	.9273	.6531	.6529	+2
		$\Delta_a=$ .0002	40	.9169	.6531	.6529	+2
			50	.9068	.6531	.6529	+2
.88209[1]	.6115	—	10	.9190	.6747	.6747	0
			20	.9083	.6747	.6747	0
			30	.8976	.6747	.6747	0
			40	.8871	.6747	.6747	0
			50	.8769	.6747	.6747	0
1.0000[2]	.6117	—	10	.8894	.6977	.6977	0
C_6H_6			20	.8787	.6977	.6977	0
			30	.8681	.6977	.6977	0
			40	.8573	.6977	.6977	0
			50	.8465	.6977	.6977	0

[1] Density values obtained by interpolation with the aid of a large scale graph of experimental measurements.
[2] Density values taken from *International Critical Tables*.

-0.7200×10^{-6} at 20°C. These values represent the mean of from three to six independent observations, the maximum deviation from the mean being $\pm0.0003\times10^{-6}$. In the third column are found the temperature coefficients of the relative volume susceptibilities $(-1/\kappa_{20})(d\kappa/dT)$ obtained with the aid of the experimental curves for the volume susceptibilities reproduced in Fig. 2. The average deviations, Δ_a, of the experimental points from the curves are listed. In the fifth column are found the density values for the various concentrations used, at the various temperatures listed in the fourth column. In the sixth column are found the mass susceptibilities for the several mixtures determined from the experimental results. In the seventh column are found the corresponding mass susceptibilities found by calculation from the mass susceptibilities of the pure liquids assuming additivity. The differences between the experimental and the calculated values are found in the last column.

Inspection of the numbers in the sixth column of Table I giving the mass susceptibilities for the several mixtures at different temperatures brings out a number of interesting facts. In the first place, the mass susceptibility of carbon tetrachloride has a definite temperature coefficient, in agreement with the results of Boeker,[7] whereas nitrobenzene, although it is a highly polar liquid, has not. Furthermore, for intermediate concentrations having less than 30 percent nitrobenzene by weight, the mass susceptibilities are dependent upon the temperature; while for intermediate concentrations greater than 30 percent, the mass susceptibilities are independent of the temperature.

The departures from additivity indicated by the numbers in the last column of Table I show dependence upon both concentration and temperature. It does not appear possible to explain these facts on the basis of molecular association in the nitrobenzene. In fact, the anomalous character of the results would seem to depend more upon the behavior of the nonpolar carbon tetrachloride than upon that of the highly polar nitrobenzene. It was thought, therefore, that it would be of interest to investigate the magnetic susceptibilities of mixtures of carbon tetrachloride and nonpolar benzene.

Benzene-carbon tetrachloride

The benzene employed in these measurements was furnished by Mallinckrodt, the carbon tetrachloride by Eimer and Amend. Each of the liquids was carefully distilled.

The data obtained for the benzene-carbon tetrachloride mixtures are tabulated in Table II in quite the same manner as those for nitrobenzene and carbon tetrachloride in Table I, and their estimated precision is the same. In the last column, the deviations $\chi-\chi_{cal.}$ are given. A definite departure from additivity will be noted, which depends upon both concentration and temperature.

With benzene as the solvent, results are found which are notably different from the results obtained with nitrobenzene as the solvent. It is found that for mixtures containing less than 1.3 percent benzene by weight, the mass susceptibilities decrease with increasing temperatures. For mixtures containing more than this percentage of benzene, the mass susceptibilities increase with increasing temperatures, the relative change increasing with concentration for mixtures containing 20 percent benzene by weight or less. For mixtures of higher benzene concentration, the relative change with temperature gradually decreases.

Nitrobenzene-benzene

Mixtures of nitrobenzene and benzene were investigated as regards the effects of varying concentration and temperature. The data obtained for these mixtures are tabulated in Table III, in the same manner as those in Tables I and II.

The numbers in the last column of this table indicate that the principle of additivity of susceptibilities holds with close approximation for mixtures of these two liquids at all temperatures, the departures from additivity being within the limits of precision of measurements.

Discussion of Errors

The sources of error to be considered in connection with the absolute values given for the mass susceptibilities in Tables I, II and III, assuming the mass susceptibility of water to be

[7] G. F. Boeker, Phys. Rev. **43**, 756 (1933).

-0.7200×10^{-6} at 20°C are: (1) errors of observation, (2) the differences in surface tension of the organic liquids and the nickel chloride solutions,[8] (3) slight variations in the neutral solution in the course of time, (4) uncertainties in the density values. The probable error in absolute values, based on an analysis of these factors, supplemented by experimental data to determine the effects owing to (2) and (3), is estimated to be $\pm0.0010\times10^{-6}$. Relative values, however, depend on only (1) and (4), and for such, the maximum error is estimated to be $\pm0.0006\times10^{-6}$.

If we may assume on the basis of the values listed in Table III, that the principle of additivity of susceptibilities applies for mixtures of nitrobenzene and benzene, it then follows that the departures relative to each other are considerably less than the estimated errors.

In connection with the measurements of relative volume susceptibilities at various temperatures, the figures for the average deviations, Δ_a, of the experimental points from the curve, given in the third columns of Tables I, II and III, may be considered as a measure of the precision of these measurements.

The probable error in density values given in Tables I and III is estimated to be ±0.0004. However, the average deviation of the experimental points from the density-temperature curves for the various measurements is ±0.0001.

Discussion

The measurements of the temperature variation of susceptibility of nitrobenzene indicates that the mass susceptibility is independent of the temperature, in agreement with the results of Cabrera and Fahlenbrach[9] and Rao and Varadachari.[10] If association of the molecules in nitrobenzene exists, depending upon concentration and temperature, the present experiments tend to show that changes in molecular association are not accompanied by appreciable changes in magnetic susceptibility

The measurements of the temperature variation of susceptibility of carbon tetrachloride shows that the mass susceptibility of this liquid decreases with increased temperatures. This might be regarded as due to an effective paramagnetic component, increasing with the temperature, but such an explanation would be difficult to justify on theoretical grounds. It is worthy of notice, perhaps, that carbon tetrachloride is anomalous as regards Pascal's law, in that its Pascal constitutive constant is exceptionally large.

The measurements of the temperature variation of susceptibility of the various benzene-carbon tetrachloride mixtures show that the relative mass susceptibilities depend upon the concentration in an irregular, though continuous, manner. Consistency of this variation requires that the relative mass susceptibilities of benzene be independent of the temperature, in agreement with the results of Boeker[7] and Cabrera and Fahlenbrach.[9]

The density values given in Table I for the nitrobenzene-carbon tetrachloride mixtures are in good agreement with the measurements of Pal,[1] provided that the values of Pal are so adjusted that the densities of the end points agree with the values given in the *I. C. T.* for the densities of the pure liquids. The values given for the densities of the pure liquids agree very well with the *I. C. T.* values. The density values at 25°C for mixtures of nitrobenzene and benzene interpolated from the experimental data listed in Table III are in good agreement with the data given in the *I. C. T.*

I wish to express my appreciation of the many helpful suggestions and criticisms given me by Professor A. P. Wills, under whose direction these experiments were performed.

[8] Since the position of the two menisci are determined by setting the telescope cross hairs tangent to the images of the menisci, a slight error is introduced if the two menisci do not have the same shape.

[9] B. Cabrera and H. Fahlenbrach, Zeits. f. Physik **85**, 568 (1933); **89**, 682 (1934).

[10] Rao and Varadachari, Proc. Ind. Acad. Sci. **1-A**, 77 (1934).

The Inverse Piezoelectric Properties of Rochelle Salt at Audiofrequencies

OSCAR NORGORDEN, *University of Minnesota*

(Received March 28, 1936)

Measurements of the inverse piezoelectric dilatation were made as a function of the temperature and of the frequency and intensity of the applied electric field. It was found to be proportional to the intensity of the electric field from 5 to 47 peak volts/cm for temperatures above the upper Curie point (23.8°C) and from 5 to 40 peak volts/cm for temperatures below the Curie point; also it was found to be practically independent of the frequency from 100 to 4000 cycles/sec. and for temperatures from 13.3°C to 35.4°C. For temperatures below the Curie point the inverse piezoelectric dilatation increased as the frequency was decreased from 100 cycles/sec. This increase was explained in terms of Schulwas-Sorokin and Posnov's theory of relaxation time. For temperatures above the Curie point the inverse piezoelectric dilatation decreased as the frequency was decreased from 100 cycles/sec. Mueller's theory explained the experimental results for frequencies from 100 to 4000 cycles/sec. and temperatures above the upper Curie point. This theory was approximately in agreement with experiment for temperatures from 13.3°C to the Curie point and for frequencies from 100 to 4000 cycles/sec. Below 100 cycles/sec. the theory is not in good agreement with the experimental results.

THE similarity of the electrical properties of Rochelle salt to the magnetic properties of ferromagnetic materials was first pointed out by Valasek.[1] In recent years numerous measurements have been made on the electrical properties of Rochelle salt. Cady,[2] however, made the first attempt to develop a theory. Later Kurtschatow[3] developed a theory analogous to the Weiss theory of ferromagnetism. Mueller[4] combined the two theories to explain a number of the electrical and optical properties of Rochelle salt.

In this investigation the inverse piezoelectric dilatation was measured as a function of the frequency and intensity of the applied electric field, the temperature being a parameter. An attempt is made to correlate the results with Mueller's theory, which states that the piezoelectric dilatation is proportional to the susceptibility. Thus the measurements of the inverse piezoelectric dilatation can be compared directly with the measurements of the dielectric constant.

THEORY

If an electric field E is applied parallel to the a axis on a Rochelle salt crystal, then Voigt's general piezoelectric equations[5] reduce to

$$y_z = d_{14}E, \tag{1}$$

where y_z is the piezoelectric strain and d_{14} is the piezoelectric modulus. The piezoelectric dilatation in a direction making an angle of 45° with the b and c axes and 90° with the a axis is a maximum and is a pure translation. The inverse piezoelectric dilatation, the change in length per unit length $\Delta r/r$, in this direction is[6]

$$\Delta r/r = \tfrac{1}{2}d_{14}E. \tag{2}$$

The microscopic field F acting upon an electric charge placed in a polarized dielectric is different from the macroscopic field E. If P is the polarization per unit volume

$$F = E + fP, \tag{3}$$

where f is a constant which depends upon the arrangement of the molecules and was shown by Lorentz to be $4\pi/3$ in special cases.

In a medium containing dipoles which are free to rotate, Langevin showed that when a field was applied the thermal motion at a temperature T brought about an equilibrium condition such that

$$P = Np(\coth pE/kT - kT/pE) = NpL(pE/kT),$$

where p is the moment per dipole, N is the number of dipoles per cc and k is the Boltzmann constant. Expanding the Langevin function $L(pE/kT)$ and taking the first two terms

$$P = (NppE/3kT)[1-(1/15)(pE/kT)^2]$$
$$= \alpha' E - \beta' E^3,$$

[1] Valasek, Phys. Rev. **15**, 537 (1920); **17**, 475 (1921); **19**, 478 (1922); **24**, 560 (1924).
[2] Cady, Phys. Rev. **33**, 278 (1929).
[3] I. B. Kurtschatow, Seignette-Electricity, Monograph, (1933).
[4] Mueller, Phys. Rev. **47**, 175 (1935).
[5] Voigt, *Lehrbuch der Kristallphysik* (1910), pp. 830, 902.
[6] Bloomenthal, Physics **4**, 172 (1933).

in which α' and β' are functions of the temperature.

Guided by the form of this equation Mueller[4] assumed that we may, for the dielectric, write

$$P=\alpha F-\beta F^3, \tag{4}$$

in which F replaces E and the linear term α is the sum of four effects

$$\alpha=\alpha_1+\alpha_2+\alpha_3+\alpha_4,$$

where α_1 is the optical polarizability, α_2 is due to the displacement of the ions in the lattice, $\alpha_3=e_{14}\delta_{14}$ is due to the piezoelectric back-polarization $e_{14}y_z$, and α_4 is the contributions of the dipoles. In a finite crystal, α_3 depends upon the dimensions of the crystal and vanishes if the piezoelectric deformations are prevented. α_3 and α_4 are responsible for the marked temperature dependence of α.

Mueller[4] also assumed the microscopic field F should replace E in Eq. (2)

$$\Delta r/r=\tfrac{1}{2}d_{14}F. \tag{5}$$

If one assumes βF^3 to be small, the susceptibility is given by

$$P/E=\alpha/(1-\alpha f).$$

Here if we set

$$\alpha=\theta/fT \tag{6}$$

and assume for the moment that θ is a constant, the susceptibility is given by

$$P/E=C/(T-\theta) \quad \text{where} \quad C=\theta/f.$$

In this expression θ appears as a "Curie temperature" when comparison is made with the theory for ferromagnetic materials. In the case of dielectrics with which we are dealing, θ may be a function of the temperature. It is to be considered as a quantity entering in the expression for the susceptibility rather than a *fixed* transition temperature.

From Eqs. (3), (4) and (6)

$$E=(1-\theta/T)F+f\beta F^3. \tag{7}$$

On solving Eq. (7) for F to the second approximation

$$F=TE/(T-\theta)-T^4\beta f E^3/(T-\theta)^4. \tag{8}$$

If the cubic term in Eq. (8) is neglected

$$\Delta r/r=d_{14}TE/2(T-\theta). \tag{9}$$

Near T_c, the temperature where the transition from the normal to the "ferro" dielectric state occurs, where $\theta=T_c$ we may write as an approximation

$$r/\Delta r=2(T-T_c)/d_{14}ET_c. \tag{10}$$

This obviously is good only for temperatures near T_c as we have set $T-T_c$ for $T-\theta$ and T_c in place of T in the denominator. The above applies if $T>\theta$.

If $T<\theta$, then there is a real solution to Eq. (7) for $E=0$

$$F_0^2=1/f\beta(\theta/T-1). \tag{11}$$

This gives the part of the microscopic field which is due to the spontaneous polarization.

The total microscopic field existing when the medium is "permanently" polarized and an external field is applied is

$$\begin{aligned} F+F_0&=E+f(P+P_0)\\ &=E+f[\alpha(F+F_0)-\beta(F+F_0)^3]. \end{aligned} \tag{12}$$

The microscopic field produced by spontaneous polarization is

$$F_0=fP_0=f(\alpha F_0-\beta F_0^3). \tag{13}$$

By obtaining a solution for F, to the second approximation, from Eqs. (6), (11), (12) and (13) and substituting this value of F in Eq. (5)

$$\frac{r}{\Delta r}=\frac{4(\theta/T-1)}{d_{14}E[1-(3E/4)(\beta f/(\theta/T-1)^3)^{\frac{1}{2}}]}. \tag{14}$$

For the first approximation on Eq. (14) reduces to

$$r/\Delta r=4(T_c-T)/d_{14}T_cE \tag{15}$$

for temperatures near the Curie point.

Eqs. (10) and (15) can be tested experimentally by variation of E and T. Note that the first order approximation Eqs. (10) and (15) for temperatures above and below the Curie point (23.8°C), respectively, are the same except for a factor 2 in the numerator of Eq. (15).

The Crystals

Three cubes approximately two cm on an edge were cut by a wet string from a large Rochelle salt crystal obtained from the Brush Development Company. The crystals were pol-

ished on a piece of slightly moist plate glass. Two of the surfaces were cut perpendicular to the a axis, and the other four surfaces made an angle of 45° with the b and c axes.

The Rochelle salt crystals were annealed in a manner used by Mueller. The crystals were placed in a temperature-controlled oven and heated slowly to 42°C. They were kept at this temperature for seven hours, then allowed to cool slowly to room temperature. This treatment made it possible to get more reproducible results.

Thin metal foil electrodes were fastened to the two surfaces perpendicular to the a axis with a small amount of Canada balsam dissolved in xylol as described by Bush,[7] Mueller[4] and others. These surfaces were completely covered by the foil. This type of electrode has been found to give good results.

A thin sheet of paper was glued with celluloid dissolved in amyl acetate to the surface of the crystal: then alternate sheets of mica and metal foil were glued on as shown in Fig. 1. The lower grounded metal foil acted as an electrostatic shield from the electric field applied to the crystal. These paper and mica sheets glued to the crystal would offer a resistance to the inverse piezoelectric displacement in the horizontal direction, and thus indirectly, to the displacement in the vertical direction. However, for a large number of mountings of this type on the three different crystals, the inverse piezoelectric amplitude was independent of the mounting within the experimental accuracy of the measurements.

The crystals were next placed in an air-tight chamber containing a saturated solution of Rochelle salt. They would absorb a maximum amount of water of crystallization. At the end of four days the crystals were removed and painted with clear glyptal lacquer. Valasek,[1] Vigness[8] and Korner[9] have pointed out the dependence of the electrical properties of Rochelle salt upon the humidity, and this variation of results could be eliminated by the above precaution.

The crystal was glued to a mica insulator and the insulator glued to the brass plate (Fig. 1). A heavy piece of metal was sweat-soldered to the brass plate. Two small blocks of Bakelite were placed against the crystal on adjacent sides and glued in place but not glued to the crystal. These precautions eliminated a large number of extraneous resonance frequencies.

[7] Bush, Helv. Phys. Acta **6**, 315 (1933).
[8] Vigness, Phys. Rev. **48**, 198 (1935).
[9] Korner, Zeits. f. Physik **94**, 801 (1935).

Theory of the Measurements

A brass plate of area S was mounted above the crystal and at a distance u from the top lead foil; cf. Fig. 1. The distance u could be varied by a calibrated vernier screw. Let the capacitance of the condenser formed by the brass plate and the top foil on the crystal be C; then

$$C = 1.124S/4\pi u \text{ mmf}. \tag{16}$$

The condenser C was connected in series with a high potential V and a high resistance R. The condenser C, the potential V, the resistance R and the connecting wires had to be very carefully shielded from the alternating voltage applied to the crystal and all stages of the amplifier except the input to the first stage. The input to the first stage was connected across the high resistance R, but we shall at first neglect the effect of the input admittance of the amplifier upon this simple series circuit. Let C_1

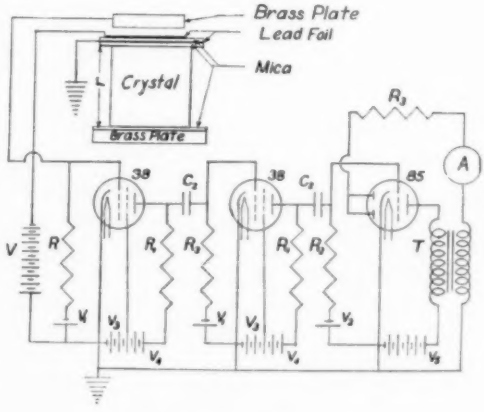

FIG. 1. Circuit diagram.

V—including V_1 —184.2 volts
V_1—1.5 volts
V_2—10.5 volts
V_3—6.0 volts
V_4—28.5 volts
V_5—150 volts
R—5×10^9 ohms
R_1—300,000 ohms
R_2—1,000,000 ohms
R_3—100,000 ohms
C_2—0.04 mf
T—audiofrequency transformer
A—microammeter (0–30 : 0–300 microamperes)

be the stray capacitance in mmf in parallel with the condenser C; let Q be the charge on the condensers C and C_1; then

$$Q=V(C+C_1). \tag{17}$$

When an alternating voltage is applied to the electrodes perpendicular to the a axis, the crystal vibrates in the vertical direction because of the inverse piezoelectric effect. Let the alternating voltage change from zero to a maximum in a time Δt (one-quarter of a cycle). Then the distance u will change by an amount Δu. If the resistance R is so large that no appreciable charge can leak from the condensers C and C_1 in the time Δt; then

$$dQ=VdC+(C+C_1)dV=0. \tag{18}$$

By differentiating Eq. (16) and substituting this value of dC in Eq. (18)

$$du=(u/V)(1+4\pi uC_1/1.124S)dV. \tag{19}$$

Since Δu, the amplitude of vibration, is very small, then du can be replaced by Δu without an appreciable error. For a fixed position of the upper brass plate, $r+u$ must be equal to a constant or $\Delta r+\Delta u=0$; thus

$$\Delta r=(u/V)(1+4\pi uC_1/1.124S)\Delta V. \tag{20}$$

ΔV is the peak alternating voltage across the condenser C and must be equal to the peak alternating voltage drop in R.

The Audiofrequency Amplifier

The values of all the circuit constants are given in Fig. 1. The input and second stages were resistance-coupled and were operated at a low plate voltage using type 38 tubes, as described by Johnson and Neitzert.[10] The input admittance of the input stage to the amplifier was calculated using Chaffee's[11] formula. The input conductance was found to be of the order of 10^{-11} mhos and the input susceptance was equivalent to an input capacitance slightly greater than the given input value. Our previous assumption of neglecting the input impedance of the tube is justified if a slightly smaller equivalent value of R is used. This small change in R does not affect the validity of the assumptions made in deriving Eq. (20). From the calibration curves of the amplifier and the microammeter, A, (Fig. 1) reading, the input voltage to the amplifier ΔV can be calculated.

[10] Johnson and Neitzert, Rev. Sci. Inst. **5**, 196 (1934).
[11] Chaffee, *Theory of Thermionic Vacuum Tubes*, p. 274.

The Determination of the Circuit Constants

The following data are on crystal No. 2. In Eq. (20) the terms u, Δr, V and ΔV are variables while C_1 and S are constants for any particular mounted crystal. The stray capacitance C_1 was measured at radio frequencies by a resonance circuit substitution method. The measured value of C_1 was 9.1 ± 0.2 mmf. The area S of the brass plate was 1.995 cm^2. The value of ΔV could be calculated from the microammeter reading, as explained in a previous paragraph. The distance u could be read directly on a vernier except for a small error in the zero reading. If these numerical values are substituted in Eq. (20), one obtains

$$\Delta r=(u/V)(1+51u)\Delta V. \tag{21}$$

Consider the special case of Eq. (21) in which Δr and V are constant; u is taken as the independent variable and ΔV is the dependent variable. Then Eq. (21) reduces to the form

$$(1+51u)u\Delta V=\Delta rV=k=\text{constant}. \tag{22}$$

Experimentally u was varied, and the values of ΔV were calculated from the microammeter readings. The circles in Fig. 2 represent these experimentally obtained points. The theoretical curve obtained from Eq. (22) was matched to the experimental points at the point $u=0.0457$ cm and is drawn in Fig. 2. The agreement between the theoretical curve and the experimental points is good. Therefore the measured value of the constant C_1 must be reasonably accurate.

Next consider the special case of Eq. (21) in which Δr and u are constant; thus V and ΔV are the independent and dependent variables, respectively. Eq. (21) becomes

$$V=K\Delta V, \tag{23}$$

where K is a constant. In Fig. 3 a straight line is drawn through the experimentally obtained

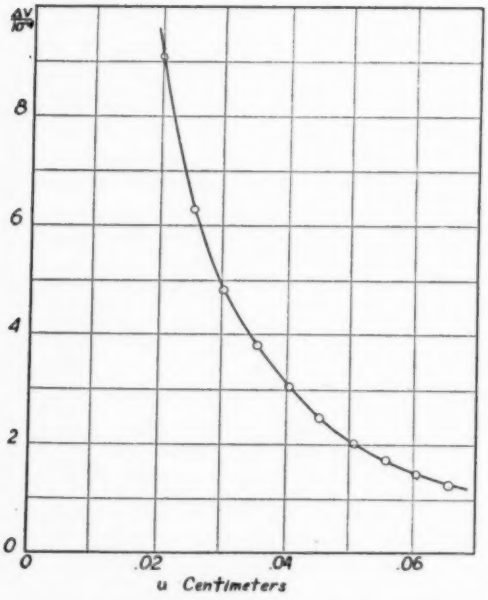

FIG. 2. Comparison of experimental and calculated values of ΔV obtained for different values of u. Circles, experimental values; curve, calculated values.

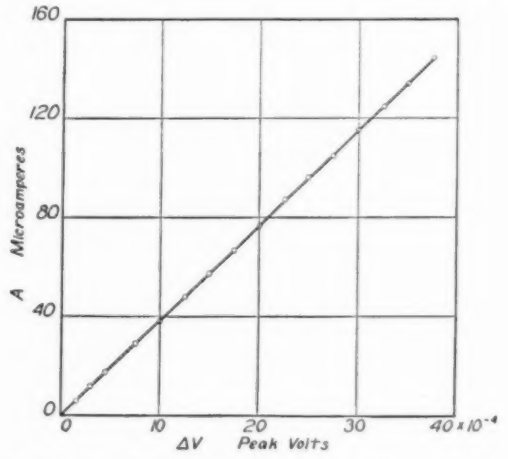

FIG. 3. Check on Eq. (21) and Eq. (23). Values of ΔV (measured by A) when Δr and u are constant and V varied.

points. The theoretical equation, Eq. (23), is satisfied within the experimental error.

Finally, consider the case in which V is made equal to the C bias of the input of the 38 type tube. With V at a very small potential of less than one percent of its original value, the variation of ΔV produced by varying Δr and u should also be less than one percent of their original values. This was found to be experimentally true.

The curves in Figs. 2 and 3 show that the values of ΔV measured must be due to Δr, the amplitude of vibration of the vibrating crystal, and not from spurious effects such as feed back or extraneous pick up in the input stage.

STABILITY OF OPERATION

The temperature was kept constant for six hours previous to taking readings in order to insure temperature equilibrium. At a temperature of 35.4°C, a definite alternating voltage was applied to the crystal for four hours and during that time ΔV remained constant within $\frac{1}{4}$ of one percent. This showed that the apparatus was stable and also that the inverse piezoelectric dilatation showed no fatigue effect under alternating current conditions.

SENSITIVITY OF THE EXPERIMENTAL ARRANGEMENT

In making the inverse piezoelectric measurements on crystal No. 2, u was set at 0.0457 $\pm$0.0009 cm and the potential V at 184.2 volts. Substituting these values in Eq. (21) gives

$$\Delta r = (8.2 \pm 0.4) \times 10^{-4} \Delta V. \qquad (24)$$

From the calibration curves of the amplifier and the sensitivity of the microammeter, the sensitivity or the minimum amplitude of vibration that could be easily detected was about 1.5×10^{-9} cm at 1000 cycles/sec., and 5×10^{-9} cm at 30 cycles/sec.

RESULTS

The curves given in this paper are from data taken on crystal No. 2. Figs. 4 and 5 give curves for $\Delta r/r$ as a function of the electric field E for different frequencies at temperatures above and below the Curie point (23.8°C) respectively; E in peak volts/cm is the alternating electric field applied parallel to the a axis. The curves in

Fig. 4 are linear except for fields below 5 peak volts/cm. In Fig. 5 the curves deviate from linearity for fields below 5 peak volts/cm and above 40 peak volts/cm.

In Fig. 6, $\Delta r/r$ is given as a function of the field E for different temperatures at a constant frequency of 700 cycles/sec. The curves are all approximately linear, and the slope of the curves increases as the upper Curie point, 23.8°C, is approached. Similar curves were found for other frequencies in the audio band. This justifies the assumption, made in the theory, in neglecting the cubic term in E in Eq. (8).

Vigness[8] measured the inverse piezoelectric displacement as a function of the applied electrostatic field. He obtained a linear relation between $\Delta r/r$ and the electrostatic field, for fields up to 40 volts/cm.

David[12] measured the dielectric constant, K_{11}, along the a axis at a frequency of 50 cycles/sec. He observed the dielectric constant K_{11} to be independent of the applied field for fields up to 50 volts/cm. Because of the close relationship between the dielectric constant K_{11} and $\Delta r/r$, one would expect $\Delta r/r$ to be linear with respect to the applied field up to 50 volts/cm. The measurements of Vigness and David are in agreement with the curves in Figs. 4, 5 and 6.

In Figs. 7 and 8, $\Delta r/r$ is given as a function of the frequency for various applied fields at temperatures above and below the Curie point, respectively. The curves in Fig. 9 are for an applied field of 18.9 peak volts/cm and for

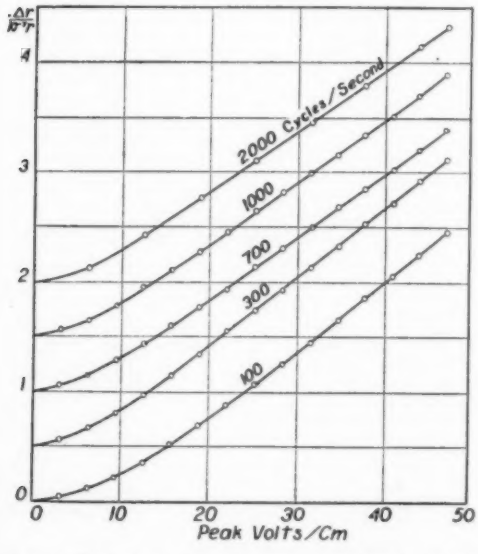

FIG. 4. Variation of the inverse piezoelectric dilation with the electric field applied parallel to the a axis. The temperature is 35.4°C. The zero is shifted for all the curves except the 100 cycles per second curve.

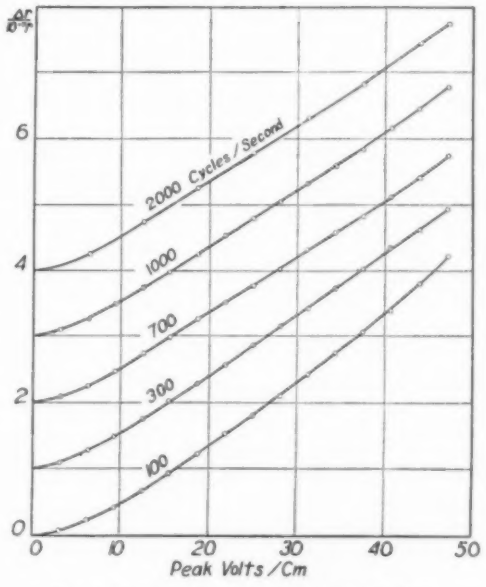

FIG. 5. Same as Fig. 4. Temperature 17.7°C.

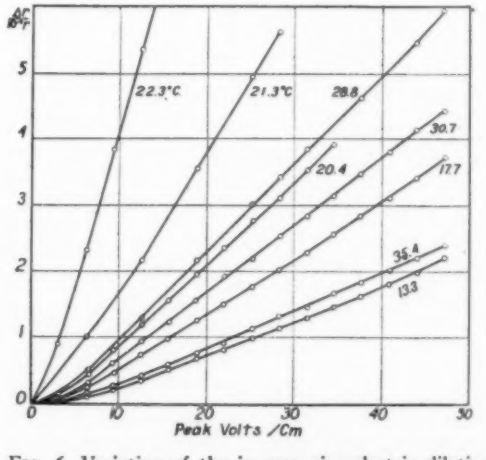

FIG. 6. Variation of the inverse piezoelectric dilation with the electric field applied parallel to the a axis at a frequency of 700 cycles per second.

[12] David, Helv. Phys. Acta **8**, 431 (1935).

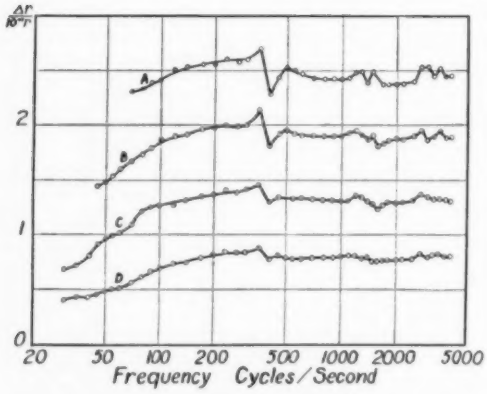

FIG. 7. Variation of the inverse piezoelectric dilation with the frequency. The four curves are for different electric field of *A*—47.2, *B*—37.7, *C*—28.3 and *D*—18.9 peak volts per cm applied parallel to the *a* axis. The temperature is 35.4°C.

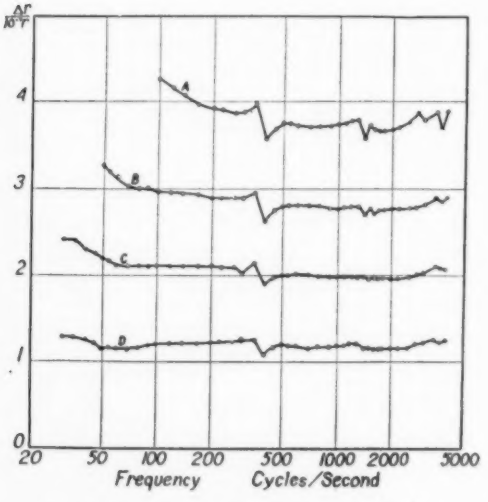

FIG. 8. Same as Fig. 7. Temperature 17.7°C.

temperatures from 13.3°C to 35.4°C. Similar curves were obtained for other applied fields of 28.3, 37.7 and 47.2 peak volts/cm.

A resonance frequency at about 370 cycles/sec. was found for all crystals and for different mountings on the brass plate. By gluing the crystal to the brass plate and by mounting braces to prevent the crystal from vibrating as a rod supported on one end, a large number of resonance frequencies were removed; however that of 370 cycles/sec. remained. Increasing and

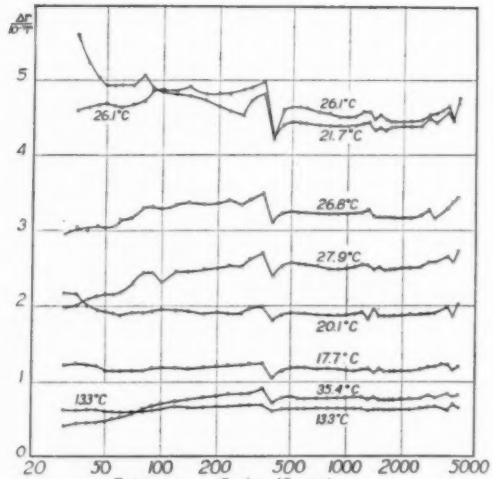

FIG. 9. Variation of the inverse piezoelectric dilation with the frequency for an electric field of 18.9 peak volts per cm applied parallel to the *a* axis.

decreasing the mass and rigidity of the base plate did not effect this resonance frequency.

Certain conclusions can be drawn from Figs. 7, 8 and 9, $\Delta r/r$ is approximately independent of the frequency from 100 to 4000 cycles/sec. For temperatures above the Curie point, $\Delta r/r$ decreases as the frequency is lowered below 100 cycles/sec.; also $\Delta r/r$ decreases more rapidly with the increasing temperature, for frequencies below 100 cycles/sec., than above. Below the Curie point $\Delta r/r$ increases as the frequency is lowered from 100 cycles/sec., and also as the temperature approaches the Curie point. Schulwas-Sorokin and Posnov[13] developed a theory of relaxation time for Rochelle salt that explains the variation of $\Delta r/r$ for temperatures below the Curie point and for frequencies less than 100 cycles/sec. They assumed that the motion of the dipoles relative to the lattice could be represented by the equation

$$E=\rho\dot{y}_z+(1/d_{14})y_z, \tag{25}$$

where ρ is the "viscosity" constant, d_{14} is the piezoelectric modulus and E is the electric field parallel to the *a* axis. This equation assumes that E depends on y_z in a linear manner and therefore

[13] Schulwas-Sorokin and Posnov, Phys. Rev. **47**, 166 (1935).

will hold only for fields up to about 45 volts/cm. The solution of Eq. (25) is

$$y_z = d_{14}E(1-e^{-t/\rho d_{14}}). \tag{26}$$

If a field E is applied to the crystal, the inverse piezoelectric displacement $\Delta r/r$, which is proportional to y_z, does not take place instantaneously; but follows the law given in Eq. (26). The time, $t_0=\rho d_{14}$, is defined as the relaxation time.

Vigness[8] took oscillograms of the inverse piezoelectric displacement, $\Delta r/r$, as a function of the time the electric field was applied. Approximately exponential curves were obtained; these curves appeared to be the sum of three exponential curves. The relaxation times of the three exponential curves were as follows: (1) the order of minutes (2) the order of seconds and (3) too short to be measured. The second relaxation time was a function of the temperature. It had a maximum at 4°C and then decreased to zero at both Curie points.

When the frequency is lowered below 100 cycles/sec. and the temperature is below the upper Curie point, the time for a cycle becomes appreciable compared to the relaxation time ρd_{14}. The lower the frequency, the larger t becomes in this equation; also the closer the temperature approaches the Curie point the smaller the value of the relaxation time ρd_{14}. The larger values of t and the smaller values of ρd_{14} will increase y_z in Eq. (26). This increase in $\Delta r/r$ from the contribution of Eq. (26) explains the rise in $\Delta r/r$ at frequencies below 100 cycles/sec. and temperatures below the Curie point in Figs. 8 and 9.

In Fig. 10, $\Delta r/r$ is given as a function of the temperature for various fields E and at a frequency of 700 cycles/sec. Because $\Delta r/r$ is independent of the frequency from 100 to 4000 cycles/sec., curves practically identical with those in Fig. 10 were obtained for all frequencies in this range. The upper Curie point, as defined by the curve for 6.3 peak volts/cm, is about 23.8°C. The value given by Mueller[4] is 23.7°C.

The data in Fig. 10 are plotted in another way in Figs. 11 and 12; namely, $r/\Delta r$ is given as a function of the temperature. According to Eqs. (10) and (15), for the first approximation in Mueller's theory, $r/\Delta r$ is a linear function of the temperature, the intercept on the abscissa axis is the temperature t_c and d_{14} can be calculated from the slope of the curves.

In Fig. 11, the value of t_c is about 23.0°C, and the values of d_{14} calculated from the four curves for different fields E are shown in Fig. 13 curve A.

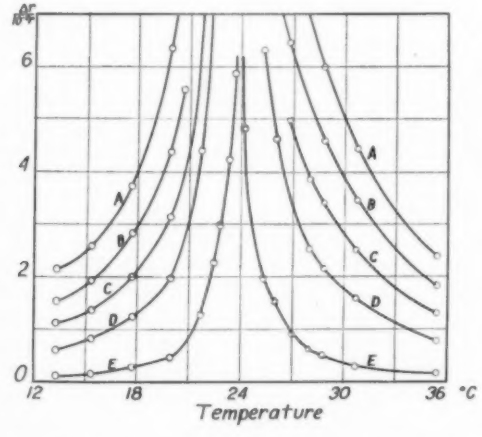

FIG. 10. Variation of the inverse piezoelectric dilation with the temperature at a frequency of 700 cycles per second. The five curves are for different electric fields of *A*—47.2, *B*—37.7, *C*—28.3, *D*—18.9 and *E*—6.3 peak volts per cm applied parallel to the *a* axis.

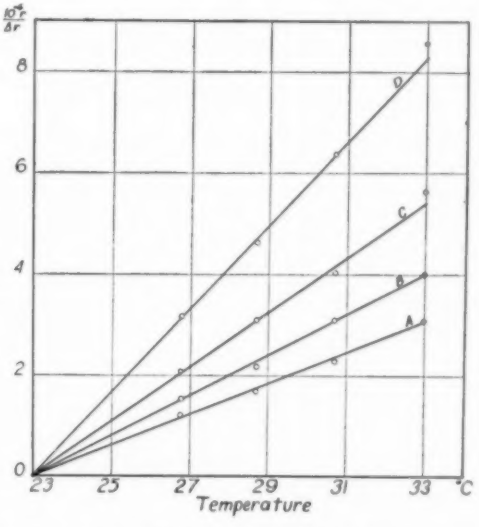

FIG. 11. Variation of the reciprocal of the inverse piezoelectric dilation with the temperature at a frequency of 700 cycles per second. The four curves are for different electric fields of *A*—47.2, *B*—37.7, *C*—28.3 and *D*—18.9 peak volts per cm applied parallel to the *a* axis.

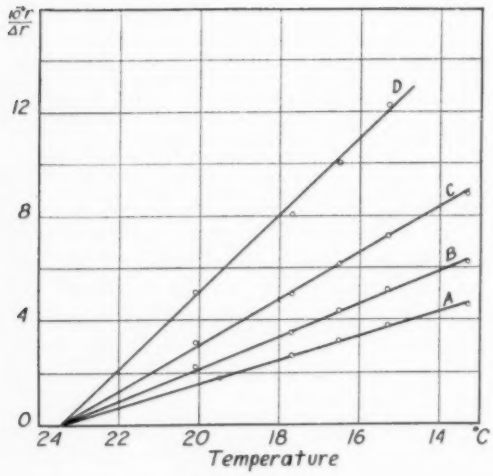

FIG. 12. Same as Fig. 11.

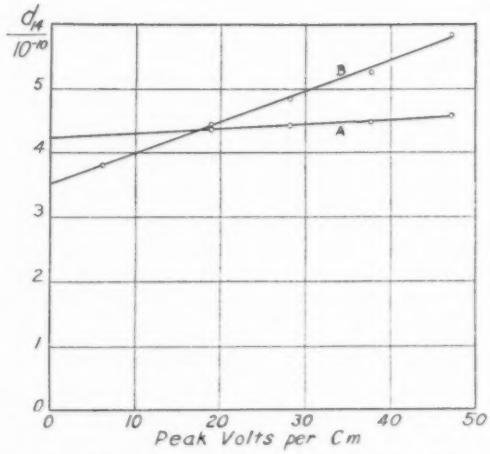

FIG. 13. Variation of d_{14} in Mueller's theory with the electric field. Curves A and B are for temperatures above and below the Curie point, respectively.

From measurements of the susceptibility above the Curie point, Mueller[4] found $t_c=23.0°C$. This small variation of d_{14} from its average value is about equal to the probable error. The fact that d_{14} appears to be a linear function of the applied field could be due to systematic errors.

Next consider the agreement between the experiment and theory for temperatures below the upper Curie point. The value of $t_c=23.5°C$ in Eq. (15) is read from the intercept with the temperature axis of the curves in Fig. 12. d_{14} can be calculated from the slope of the curves. d_{14} is not a constant but increases linearly with the field E as shown in Fig. 13 curve B. Thus the experimental results are not in good agreement with Eq. (15).

The Eq. (14) made accurate to the second approximation in E might be expected to give the increase of d_{14} with E in Eq. (15). Rewriting Eq. (14)

$$\frac{r}{\Delta r}=\frac{4(t_c-t)}{d_{14}ET_cH}, \tag{27}$$

where

$$H=1-\frac{3E}{4}\left(\frac{\beta fT^3}{(t_c-t)^3}\right)^{\frac{1}{2}}. \tag{28}$$

However H decreases with an increase in the field E instead of increasing. Thus Mueller's theory gives approximately the same value of d_{14} below the Curie point as above, but d_{14} is not a constant for temperatures below the Curie point.

At a frequency of 50 cycles/sec., curves similar to those in Figs. 11 and 12 were drawn. The temperature t_c was found to be about 23.0°C. d_{14} was not a constant and increased with the field E for temperatures below and above the upper Curie point. Mueller's theory is not in agreement with experiment for frequencies below 100 cycles/sec.

ACKNOWLEDGMENTS

I wish to express my sincere appreciation to Drs. J. Valasek and A. Zeleny for their helpful advice and constructive criticism in this work.

Energy Transmission by High Energy Electrons

W. F. G. SWANN, *Bartol Research Foundation of the Franklin Institute*

(Received April 11, 1936)

In considering the theory of energy transfer at close collisions between charged particles, one of which is of high energy, J. R. Oppenheimer has postulated the condition that in calculating the effect of the field of the high energy particle, one must omit from its appropriate Fourier analysis all of those harmonic terms whose frequency lies above a certain critical value characteristic of the charged particle acted upon. Some time ago, the writer proposed a modification of the fundamental wave-mechanical equation which was designed so as to lead statistically to the classical equation of motion of an electron including the so-called radiation reaction terms. It is now shown that the Oppenheimer condition is a direct analytical consequence of the modified wave-mechanical equation referred to. The significant feature of the matter is that the terms which in Oppenheimer's postulate are simply omitted are, on the writer's theory, rendered automatically impotent by having associated with them large denominators which kill their effects.

IN a recent publication, J. R. Oppenheimer,[1] in seeking harmonization with the experimental facts concerning the absorption of cosmic-ray energy has been led to make a certain postulate. This postulate is to the effect that in considering the action of a high energy charged particle upon an electron of an atomic system, we must analyze the field of the high energy particle into harmonic waves according to the Fourier principle and then discard those frequencies which lie above a certain value ν_m whose order of magnitude is given by

$$2\pi\nu_m = v/\rho = 3m_0c^2v/2e^2, \tag{1}$$

where ρ is the radius of the electron as given by classical dynamics, and is given in terms of the rest mass m_0 by the expression $\rho = 2e^2/3m_0c^2$. The velocity of the high energy particle is v, and is approximately equal to c, the velocity of light.

The purpose of the present paper is to show that the Oppenheimer postulate or its equivalent, is a direct consequence of the principles embodied in a generalization of wave mechanics which I published in 1933.[2]

The procedure adopted in my former publication is as follows:[3] According to the classical theory, with the neglect of so called radiation terms the acceleration $\ddot{s}$ of a particle of rest mass m_0 and charged e, is related to the electric field E the magnetic field H and the velocity of light c by the equation

$$m_0\ddot{s}/e = E + [\dot{s}H]/c. \tag{2}$$

It was recalled that, according to the theory of P. Ehrenfest and of E. H. Kennard, this equation could be represented wave mechanically in the sense that the centroid of the wave packet representing the moving charged particle moves according to (2), $\ddot{s}$ being of course the acceleration in question. Remembering that the complete classical equation of motion of an electron is of the form

$$m_0(\ddot{s} - a_1\dddot{s} + a_2\ddddot{s}, \text{ etc.})/e = E + [\dot{s}H]/c, \tag{3}$$

the attempt was made to modify the wave-mechanical equation for ψ so as to cause it to lead to an equation of this type by principles analagous to those which through Kennard's theorem caused the ordinary wave-mechanical equation to lead to (2).

Writing (3) in the form

$$m_0P\ddot{s}/e = E + [\dot{s}H]/c, \tag{4}$$

where P is the operator defined by

$$P = 1 - a_1D + a_2D^2, \text{ etc.}, \tag{5}$$

D being written for d/dt, it was shown that the desired end could be secured by *replacing the scalar and vector potentials φ and $\bar{U}$ of the external field in the ordinary wave-mechanical equation by $P^{-1}\varphi$ and $P^{-1}\bar{U}$.*

[1] Oppenheimer, Phys. Rev. **47**, 44 (1935).

[2] W. F. G. Swann, Phys. Rev. **44**, 943 (1933): also W. F. G. Swann, J. Frank. Inst. **217**, 59 (1934).

[3] For the present purpose I omit certain refinements contained in the original papers, and having to do with the magnetic field and with relativistic invariance of the equations. These matters are of only secondary importance in the present discussion.

The particle whose equation of motion is under discussion is of course the electron whose ejection from the atom is being examined. Its velocity is small in contrast to that of the high energy electron responsible for the scalar and vector potentials φ, and $\bar{U}$. Thus, it is possible to replace d/dt by $\partial/\partial t$ in P; and, in what follows, we shall regard D as meaning $\partial/\partial t$.

Now following the foregoing principles and taking, for simplicity, but not of necessity, as illustration, the case where we confine our attention to a classical Eq. (3) which has no more than two terms on the left-hand side, our corresponding operator P is $(1-a_1D)$. The wave-mechanical principle applied according to the Kennard method to produce (2) must now be modified by replacing φ and $\bar{U}$ by φ_1 and $\bar{U}$, where

$$\varphi_1=(1-a_1D)^{-1}\varphi, \quad \bar{U}_1=(1-a_1D)^{-1}.\bar{U} \quad (6)$$

Following Oppenheimer, we expand the field, or the field potentials, in the form of a Fourier integral.[4] Thus, for example,

$$\varphi=\int A_\nu e^{2\pi i\nu t}d\nu,$$

where it is to be understood that the real parts are to be taken. While (6) with a corresponding expression for $\bar{U}$ gives the expansion of the potentials, the effective potentials required by our theory are φ_1 and $\bar{U}_1$.

Thus,
$$\varphi_1=\int \frac{A_\nu e^{2\pi i\nu t}}{1-a_1D}d\nu.$$

Now any function of D operating on $e^{2\pi i\nu t}$ may be replaced by the same function of $2\pi i\nu$ operating on $e^{2\pi i\nu t}$. Hence,

$$\varphi_1=\text{Real part of } \int \frac{A_\nu e^{2\pi i\nu t}}{1-2\pi a_1\nu i}d\nu,$$

i.e.,
$$\varphi_1=\int \frac{A_\nu \cos(2\pi\nu t+\theta_\nu)d\nu}{(1+4\pi^2a_1^2\nu^2)^{\frac{1}{2}}}, \quad (7)$$

where
$$\tan\theta_\nu=2\pi a_1\nu.$$

When $4\pi^2a_1^2\nu^2$ becomes appreciably larger than unity the value given by (7) for the contribution of the corresponding frequency to φ_1 becomes small compared with the contribution of that frequency to φ. In other words, the frequencies which in Oppenheimer's theory are discarded, are here rendered *impotent by the natural consequences of the theory*. The theory thus provides a basis for the Oppenheimer conditions. Without such a basis the most that can be said concerning frequencies greater than the critical value is that the contributions which the ordinary theory would cause them to make to the story are probably wrong. This, alone, does not provide for the actual contributions being negligible, however.

On the classical theory, the quantity a_1 occurring in (3) and in subsequent equations would be equal to ρ/c, where ρ is the classical radius of the electron. Thus, the limiting frequency ν_m is given by

$$2\pi\nu_m=c/\rho=3m_0c^3/2e^2. \quad (8)$$

Thus, since $v=c$ for high energy particles, we see by comparison with (1) that (7) not only reproduces the qualitative significance of the Oppenheimer conditions but provides for them quantitatively. It must be admitted, however, that it would be straining matters too much to hold to the magnitude of a_1 predicted by the classical theory, particularly as there is no direct experimental verification of the magnitude of a_1 as there is for the mass of the electron. The significant thing is that there is *some* value which is appropriate for this coefficient.

In conclusion, I wish to thank Dr. A. Bramley for calling the Oppenheimer conditions to my attention.

[4] We only need expression of the integral in its dependence on the time; for, as the high energy particle passes by the electron to be ejected, the latter experiences, in view of the small velocity to which it is limited, variations in φ which are concerned only with the time variations of that function. The complete expression of the field involves a coefficient A_ν' of the form given by Oppenheimer,

$$A_\nu'=(2\pi^2ie\nu/2\epsilon v^2)H_1^{(1)}(2\pi\nu pi/\epsilon v)e^{-2\pi i\nu z/v}$$

where v is the velocity of the high energy particle, $\epsilon=(1-v^2/c^2)^{-1/2}$, where the high energy particle moves parallel to the axis of z, and the origin is at the electron to be ejected. p is the perpendicular distance from this electron to the path of the high energy particle, and $H_1^{(1)}$ is the Hankel function of the first kind.

Variation of Resistance and Structure of Cobalt with Temperature and a Discussion of Its Photoelectric Emission

LOUIS MARICK, *University of Wisconsin*

(Received April 3, 1936)

X-ray (Hull-Debye-Scherrer) diffraction patterns were obtained for cobalt in a camera designed for high temperature work. No crystallographic change for this metal has been observed in the region about 850°C at which the change in the photoelectric emission has been reported. The α to β transformation is observed at 492°C and no change in this transition temperature is detected by heating at 875°C for a period of 55 hours. The variation of electrical resistance with temperature is extended to 1200°C showing a change in slope occurring at the Curie point which is determined to be 1100°C from these curves. An expansion of approximately 0.6 percent in the lattice edge is observed as cobalt is heated through the Curie temperature. No evidence of a reversion to the hexagonal form at 1015°C has been observed. The temperature coefficient of expansion determined from these lattice measurements is 0.143×10^{-4} per °C and this agrees well with the macroscopic coefficient as determined by the usual methods. An explanation is suggested for the photoelectric emission discontinuity reported at 850°C.

INTRODUCTION

THE photoelectric emission of cobalt as determined by Cardwell[1, 2] showed a very abnormal behavior at a temperature of approximately 850°C. The curve obtained was such a one as could be explained on the basis of a transformation from one crystal type to another[1, 2, 3] and it was suggested that the known transformation from the α hexagonal to the β face-centered cubic form for this metal which has been reported at 477°C,[4] 457°C,[5] 400°C,[6] 490°C and 465°C[7] and 446°C,[8] had in this case occurred at 850°C.

Masumato[4] has shown that impurities, notably iron, caused the transformation temperature to drop and reports that 0.1 percent causes a drop to 422°C and 0.33 percent Fe drops it to 427°C. Schulze[5] shows the transformation beginning at 405°C, with a specimen which analyzed 99.2 percent Co, 0.47 percent Fe, and 0.26 percent Mn. Hendricks, Jefferson and Schultz[6] report 400°C±20° on cobalt containing 0.98 percent Ni and 0.05 percent Fe. Wever and Haschimoto,[7] on the other hand, show by magnetometric measurements on the alloy system cobalt-chromium that the transformation temperature rises from 490°C to 710°C as the amount of chromium present varies from 0 to 7.5 percent. Their dilatometric measurements show the same effect but beginning at 465°C for pure cobalt. The material used by Cardwell was a very pure specimen of Kahlbaum cobalt. Analysis showed that it was more than 99.9 percent pure. Neither iron nor nickel were present to more than 0.01 percent. It was supposed that for this condition of purity the transformation temperature was at 850°C or that it increased to this temperature with outgassing by heat treatment. The statement is made[3] that "the usual 'resistance-hysteresis' characteristic of the crystal change occurred at the same temperature as the photoelectric discontinuity" but no data nor reference is given for this fact.

From the data given above on the depression and the elevation of the transformation temperature it seemed unlikely that the purity of the cobalt used by Cardwell would cause the transformation temperature to rise some 400° or more. It also seems unlikely that outgassing would cause such a great rise.

Since the x-ray analysis of Cardwell's specimen had been performed at room temperature it was believed that diffraction photographs of the metal taken while the latter is at elevated temperatures would readily show where the transformation occurred.

[1] A. B. Cardwell, Proc. Nat. Acad. Sci. **15**, 544 (1929).
[2] A. B. Cardwell, Phys. Rev. **38**, 2033 (1931).
[3] A. L. Hughes and L. A. DuBridge, *Photoelectric Phenomena* (McGraw-Hill Co., 1932), p. 105.
[4] Masumato, Sci. Rep. Tohoku Univ. **15**, 449 (1926).
[5] Schulze, Zeits. f. tech. Physik **9**, 365 (1927).
[6] Hendricks, Jefferson and Schultz, Zeits. f. Krist. **73**, 376 (1930).
[7] Wever and Haschimoto, Mitt. Kaiser Wilhelm Inst. für Eisenforschung **11**, 293 (1929).
[8] W. C. Ellis, Rensselaer Polytechnic Institute Engineering and Science Series No. 16, June, 1917.

The cobalt specimens used in this investigation were cut from the same stock piece of Kahlbaum cobalt used by Cardwell and were rolled and cut to the same size in the same manner as the photoelectric specimens were prepared. In addition to determining the α to β transformation temperature the following were also included in the investigation: variation of resistance and lattice size with temperature, changes at the Curie point, and an explanation of the reported photoelectric emission curve.

Experimental Procedure

The camera used in this work was so designed that diffraction photographs could be taken of electrically heated wires or strips of metal and resistance measurements could be made at the same time.

The resistance of the specimen was obtained by measuring the potential drop across 2 or 3 mm of its length and at the same time measuring the heating current. The potential leads were of platinum and spotwelded to the cobalt in the middle of its length on one face of the specimen. The x-ray beam was incident upon the other face. Temperatures were determined by means of a platinum and platinum plus ten percent rhodium thermocouple, the junction of which was spotwelded to the cobalt between the potential leads. Potential differences, currents, and thermal e.m.f.'s were measured by means of a Wolff potentiometer. At a given temperature all three were measured for direct and reverse current and average values used.

The potential leads as well as the thermocouple wires were small (0.06 mm in diameter) to prevent cooling of the specimen. Heat losses by conduction along these wires were small, in fact tests made over this region by an optical pyrometer through an observing window showed no more variations than are obtained in balancing the pyrometer itself on a single portion of the specimen. Most of the specimens were 8 cm long and gave practically a uniform temperature over a region 1 cm in length.

The thermocouple while attached to the cobalt was calibrated at the melting points of zinc 419°C, aluminum 658°C, and gold 1063°C. The x-ray diffraction analysis was performed by the powder method. The camera had a diameter of 19.741 cm and was water-cooled throughout.

A shield magnetically operated externally allowed two exposures to be taken before it was necessary to reload with fresh film. The camera was evacuated by a separate pumping system from that of the x-ray tube and had a fine capillary to allow gases to be introduced into the chamber at any desired pressure. An exposure time of approximately six hours was required for a photograph. A nickel target was used as the source of radiation with no filter, as the cobalt K absorption edge is between the $K\alpha$ and $K\beta$ lines

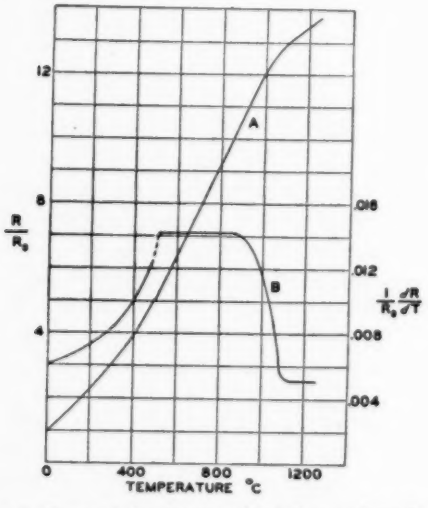

FIG. 1. Curve A. Resistance of cobalt as a function of temperature. Curve B. Temperature coefficient of resistance.

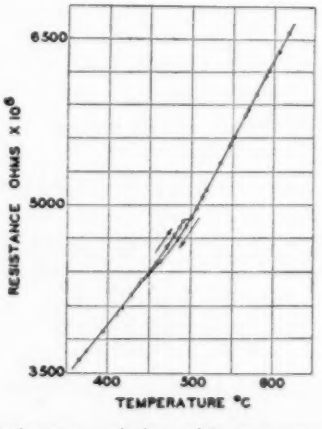

FIG. 2. Resistance variation with temperature in the vicinity of the α to β structure change.

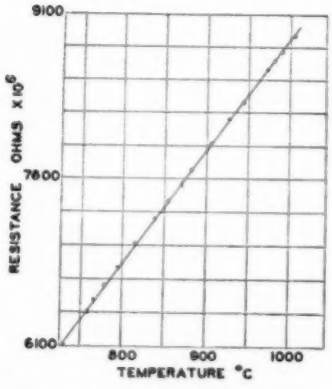

FIG. 3. Resistance variation with temperature in the region of the reported abnormal photoelectric emission.

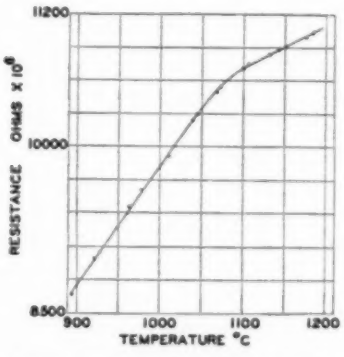

FIG. 4. Resistance variation with temperature in the region of the Curie point.

of nickel thus giving practically a monochromatic beam after absorption by the cobalt specimen itself.

RESULTS

Resistance measurements

In Fig. 1, curve *A* shows the variation of the resistance of cobalt over the complete range of temperature investigated. The variation of the simple temperature coefficient is shown by curve *B*. The particular regions of temperature over which there was special interest were carried out separately very slowly giving the metal about 20 minutes to reach equilibrium at each setting of the heating current. Fig. 2 shows the range 350°C to 600°C in which the α to β change occurs. The break in the curve for increasing temperature was found to occur at the following values for specimens prepared in the same way from the same stock piece:

Specimen	Temperature °C
A	492
B	490
B[1]	490
C	493
C[1]	493
D	492

B[1] After heat treatment of 55 hours at approximately 875°C.

C[1] After heat treatment of 20 hours at approximately 590°C.

As can be seen from the above table, heat treatment of specimens *B* and *C* caused no rise of the transition temperature.

The magnitude of the displacement which occurs in the resistance curve at the transformation temperature depends upon how completely the metal is in the α form when it is below this temperature. X-ray analysis showed that practically all of the specimens contained some of the β or face-centered cubic form at temperatures below the transition. Larger displacements in the curve were always obtained when a new specimen was heated for the first time. The mechanical work it received in its preparation by rolling at room temperature would probably favor the presence of more of the form which is stable at that temperature. The face-centered cubic form is retained to a considerable extent on quick cooling from above the transition temperature and when passing through the transition temperature on reheating only a small displacement is obtained.

The curve of Fig. 3 shows the behavior of the resistance in the temperature range about 850°C. This is the temperature at which the peculiar change in the photoelectric emission was observed by Cardwell.[1, 2] From this curve it can be seen that the region, 725°C to 1005°C, shows no abnormalities in resistance. The curve of Fig. 4 shows the variation of resistance from 900°C to 1220°C. These data were obtained with the specimen in an atmosphere of hydrogen of approximately 0.3 mm of mercury pressure.

The Curie point, the temperature at which the metal ceases to be ferromagnetic, is here taken as 1100°C. The change is not as abrupt as the

displacement which occurs at the structure change and there is no lag in this transformation on cooling. The form of the curve is similar to the resistance curves reported for iron and nickel at their Curie points.

Structure investigation

The structure of cobalt was first reported by Hull[9] showing the existance of two forms, α the hexagonal close-packed and β the face-centered cubic. He showed that cobalt cooled from 600°C was face-centered cubic while the hexagonal close-packed form was characteristic of the metal at room temperatures. Sekito[10] reported face-centered cubic for a specimen cooled from 700°C following Masumato's work.[4] More recent determinations have been made by Wever and Haschimoto.[7] In the present work, diffraction photographs were taken of the metal while it was in the heated condition. At room temperature and up to the α to β transition the photographs always showed the hexagonal close-packed form. Many photographs in this range of temperature showed the presence of the face-centered form in addition to the hexagonal. Above the transition point photographs showed only the face-centered cubic form. Photographs were taken as high as 1187°C. Curve *A* of Fig. 5 shows the variation of the hexagonal unit edge with temperature. The values are given in Table I. Photograph 2 showed no evidence of the β form. The others showed the presence of slight amounts of the β form. The values for the various constants as listed by Neuburger[11] were calculated for room temperature and are given following Table I.

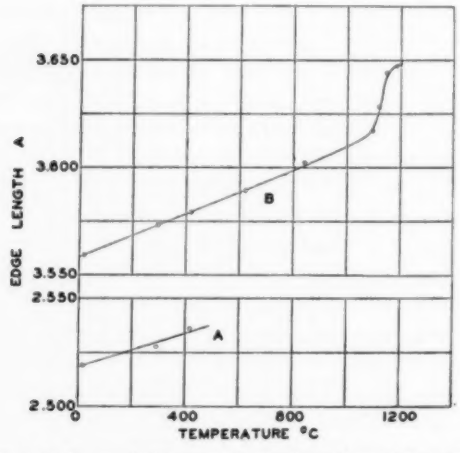

FIG. 5. Curve *A*. Hexagonal edge length variation with temperature. Curve *B*. Face-centered cube edge length variation with temperature.

TABLE I. *Hexagonal close-packed cobalt.*

PHOTOGRAPH	TEMPERATURE	a IN A		r	
1	Room	2.5179	2.519 ±0.002	1.6241	1.624 ±0.002
2	Room	2.5198		1.6238	
3	295°C	2.527 ±0.003		1.630 ±0.003	
4	420°C	2.536		1.631	

Room Temperature Calculations

X-ray density	8.65 g/cc
Density (Standard method)	8.71 g/cc
Atomic radius	1.255A
Volume of elementary rectangular prism	22.48A³
Volume per atom	11.24A³
Atomic volume	6.815 cc
Atom space per elementary volume	16.55A³
Space packing	73.65 percent

For an exact hexagonal close-packed structure the axial ratio is 1.633. The values of the axial ratio here obtained are slightly less than this and there seems to be a tendency to approach this value as the temperature is increased.

The hexagonal edge length for room temperature is slightly larger and the value of the axial ratio is slightly smaller than the respective values previously reported as follows:

a in A	r	
2.514	1.633	Hull[9]
2.514±0.005	1.633	Wever and Haschimoto[7]

The temperature coefficient of linear expansion obtained from the expansion of the unit edge as given by the curve of Fig. 5 is 0.142×10^{-4} per °C for the range 0° to 450°C, which agrees well with the values given by Schulze[5] obtained on cobalt in the usual macroscopic way. His average value for the range 0° to 400° is 0.139×10^{-4} per °C.

Curve *B* of Fig. 5 shows the variation of the face-centered cube edge length with temperature. The experimental values are given in Table II. The value of the edge length for this form at room

[9] A. W. Hull, Phys. Rev. **17**, 571 (1921).
[10] Sekito, Sci. Rep. Tohoku Univ. **16**, 545 (1927).
[11] M. C. Neuburger, Zeits. f. Krist. **80**, 103 (1931).

temperature is 3.559±0.002A which is slightly larger than that reported by Hull[9] who gave 3.554A. Wever and Haschimoto[7] report 3.553A ±0.005. No evidence was found of a reversion to the hexagonal form at 1015°C as reported by Hendricks, Jefferson and Schultz[6] who worked at room temperatures with rapidly cooled specimens. It was found that specimens cooled rapidly to room temperature from any value above the α to β transition always gave evidence of both the α and the β forms. The average coefficient of linear expansion obtained from the curve up to 600°C is 0.143×10^{-4} per °C which agrees with the values given by Schulze very well.

The curve shows a decided expansion of the lattice in the region of the Curie point. It amounts to a change in length of 0.6 percent which means a volume change of 1.8 percent. This appears to be a larger value than that which would be expected on the basis of the extension of Heisenberg's theory of ferromagnetism to magnetostriction and its relation to phenomena occurring at the Curie point made by Fowler and Kapitza[12] and Powell.[13]

TABLE II. *Face-centered cubic cobalt.*

PHOTOGRAPH	TEMPERATURE	a IN A
5	Room	3.5557
6	Room	3.5595
7	Room	3.5583
8	Room	3.5642
	Average Room Temperature	3.559±0.002
9	295°C	3.573±0.003
10	420	3.579
11	625	3.589
12	843	3.602
13	1099	3.617
14	1121	3.628
15	1148	3.644
16	1187	3.647

Room Temperature Calculations

X-ray density	8.62 g/cc
Density (Standard Method)	8.71 g/cc
Atomic radius	1.258A
Volume of elementary cube	45.09A³
Volume per atom	11.27A³
Atomic volume	6.851 cc
Atom space per elementary volume	33.39A³
Space packing	74.05 percent

[12] R. H. Fowler and P. Kapitza, Proc. Roy. Soc. **124**, 1–15 (1929).
[13] F. C. Powell, Proc. Phys. Soc. **42**, 390 (1930).

Discussion of the photoelectric emission reported for cobalt

When the region of temperature between 725°C and 1000°C was first investigated an erratic behavior of resistance and temperature measurements was observed even with pressures as low as 10^{-6} mm of mercury. Careful observations through a window showed that when a temperature of approximately 850°C was reached, a small region of the metal strip would become much hotter than the surrounding part and this would progress along the strip. This occurred with no change in the heating current. Usually the bright region was observed beginning at the center of the strip and increasing in extent towards the ends. When the effect had traveled over the specimen the latter would return to the temperature which was present before the effect began. Observations showed that the surface had become covered with a very thin film and that it no longer had a bright metallic luster. This behavior is explained as an oxidation reaction taking place on the surface of the metal.

When the cobalt specimen is heated in an atmosphere of hydrogen no such effect appears. Hydrogen has no effect upon cobalt other than being occluded by it, especially when the metal is in a powder form and the temperature is below 200°C. Friend[14] states that above this temperature hydrogen is readily driven off and the absorption is negligible. The gas was passed into the camera so that a pressure of 0.2 to 0.3 mm of mercury was maintained with the pumps on this system in action.

The behavior described above shows that metallic strips of cobalt will visibly oxidize when heated to temperatures in the region of 850°C even when the pressure is 10^{-6} mm of mercury, i.e., reduced by approximately 10^9 fold from atmospheric conditions. It is then believed that the specimens used by Cardwell,[1, 2] who attained pressures of 1 to 3×10^{-3} mm of mercury, may not have been entirely free from an oxide layer on the surface. Accordingly, the stability of the cobalto-cobaltic oxide, Co_3O_4, and its change to the cobaltous oxide, CoO, as described by

[14] J. N. Friend, *Inorganic Chemistry*, Vol. 9, Part 1 (Griffin and Company, 1920), p. 28.

Kalmus[15] is here suggested as a possible explanation of the peculiar photoelectric emission observed by Cardwell. Kalmus has shown that the most common oxides of cobalt exist as Co_3O_4 and CoO and that the former is more stable at temperatures below 910°C, above which temperature the reduction reaction

$$2Co_3O_4 \rightarrow 6CoO + O_2$$

takes place very rapidly.

Cardwell's photoelectric emission curve is reproduced in Fig. 6. On the basis of this new hypothesis, curve 2 up to 850°C would represent the emission due to the oxide which is stable at low temperatures. At 850°C the increase in the emission as given by the same curve would be due to the formation of the oxide CoO which is stable at high temperatures. Upon decreasing the heating current from its highest value it is to be noted that the photoelectric emission curve does not follow back on itself but shows higher values of emission characteristic of the monoxide CoO, which is now present on the surface either entirely or very much predominating in amount. The reverse exothermic reaction

$$6CoO + O_2 \rightarrow 2Co_3O_4$$

takes place upon cooling and the sudden increase in the photoelectric emission curve at *a* may be due either to the combined effect of the liberation of this heat of reaction and the unstable conditions accompanying a chemical change or to the presence of a temporary intermediate oxide of greater photoelectric sensitivity. Cardwell states that within a few seconds the point *b* is reached and that with no further change in the heating current, the sensitivity increased during the next six minutes to the value *c*. A further drop in temperature at this point produced by diminishing the heating current by 0.1 ampere caused the photoelectric emission to pass to values *d*, *e*, and *f* as noted by Cardwell in 1½, 15, and 65 minutes, respectively. The fact that the process is spontaneous and uncontrollable after it starts fits very well with the usual characteristics of a chemical reaction. Neither Cardwell nor the author has observed any increase in the temperature while decreasing the

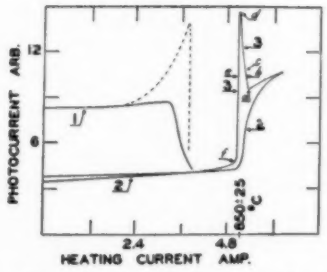

FIG. 6. Photoelectric emission curve (Cardwell).

heating current in this region and this may indicate that the change from CoO to Co_3O_4 is only taking place in the first few molecular layers. Calculations show that the rise in temperature produced by the liberation of heat when a layer 50×10^{-8} cm thick (several molecular layers) changes from CoO to Co_3O_4 is only of the order of one or two degrees. Thus it does not seem possible to attribute the large change from *a* to *d* to an increase in temperature produced by the heat of reaction. However, this large change in photoelectric emission may be due to the unstable conditions which exist in the topmost layer while the chemical change is in progress. Just what the photoelectric characteristics of the surface undergoing such changes are is a matter of conjecture and in the explanation of Cardwell's results it is here assumed that the surface is photoelectrically more sensitive when it is undergoing chemical change.

Assuming no reflection of molecules upon impact, the time required to bring enough molecules into contact with the surface to form a monomolecular layer is of the same order of magnitude as the time effects described by Cardwell and it suggests a possible connection between the formation of a monomolecular layer of Co_3O_4 and the change in the photoelectric emission from point *a* to point *c*. The temporary arrest in the process at point *c* might be due to the protective action of this monomolecular layer in preventing oxygen from directly coming into contact with more of the CoO. The drop in temperature at this point caused by diminishing the heating current may cause a condition of greater instability for the presence of CoO and the oxidation to Co_3O_4 would be accelerated and would probably occur in layers beneath the

[15] H. T. Kalmus, J. Ind. Eng. Chem. **6**, 115 (1914).

surface. The mechanism of supplying oxygen to these under layers of CoO may consist in oxygen being given up to them by the surface layer of Co_3O_4 and then the surface layers obtaining more oxygen from the gas about the specimen. In this way, the Co_3O_4 serves as a carrier of the oxygen molecules, the latter being displaced inwardly to more CoO. This process would disturb the surface layers, and hence probably the emission of photoelectrons, as long as it continued. The photoelectric emission during this further oxidation would be passing through the values *d*, *e*, and *f*. Cardwell suggests that the total observed effect would probably take place without interference to completion thus taking several hours time if he had not accelerated it at the point *c* by decreasing the temperature. This suggests that the point *c* indicates the characteristics of a surface which is active to some extent because it is acting as a carrier of oxygen to layers beneath. Its chemical activity is then momentarily increased when the temperature is reduced because the rate at which the CoO takes oxygen from the upper layers of Co_3O_4 is increased. It is at this stage that the photoelectric emission increases from *c* to *d*. The decrease from *d* to *f* would then be due to the decreased activity on the surface as the reaction goes to completion. The longer periods of time involved here could be ascribed to the fact that the oxygen must be displaced or handed on through progressively thicker layers of Co_3O_4 as the process continues.

Curve 1 of Fig. 6 is explained then as the emission due to cobalt with a thin layer of CoO on its surface which has been retained from higher temperatures by rapid cooling. Kalmus points out specifically that CoO oxidizes to Co_3O_4 when heated in air to any temperature between 385°C and 910°C. This could account for the drop of curve 1 to values along curve 2. Both the large increase in curve 1 just before dropping to curve 2 as shown by the dotted line in Fig. 6 and the small increase in curve 1 shown by the full line would require an explanation similar to that required by the increase marked by the points *a*, *b*, *c*, *d*, *e* and *f* since the same reaction takes place. The magnitude of this rise is no doubt governed by the extent to which the chemical reaction is taking place. The dotted curve was not always observed by Cardwell probably due to the fact that the temperature range, 385°C to 910°C, over which the reaction might occur is large. This would indicate a possible slow conversion to the Co_3O_4 form having no very marked effect on the photoelectric emission.

As has been presented in this paper, no evidence of a crystallographic change has been observed in the region of temperature about 850°C nor has any evidence been found of intermediate structure types occurring at the α to β change. Further, no shift in the temperature at which the α to β change takes place has been observed by continued heating for 55 hours at 875°C. These facts together with the known behavior of the oxides at this temperature seem to indicate that the photoelectric effect observed was due to the action of the oxides of cobalt on the surface of the metal.

The writer wishes to express his appreciation to Dr. H. B. Wahlin and to the late Dr. C. E. Mendenhall for their suggestions and criticisms.

A Determination and Analysis of the Thermionic Constants of Thoriated Tungsten

ALBERT ROSE, *Cornell University**

(Received March 2, 1936)

The slopes and intercepts of Richardson plots are obtained for states of activation from a flashed to a completely thoriated surface, and for applied fields up to 3×10^4 volts/cm. The following observations are described: (1) abnormal decrease of work function with low applied fields, (2) effect of bombardment with positive ions, (3) effect of aging at high temperatures, (4) proportionality of the log of the intercept and the slope at a given state of activation, (5) variation of the low field intercept of the Richardson plot with activation, (6) variation of the high field intercept of the Richardson plot with activation, (7) (8) emission lag effects at high and low applied fields (9) dependence on temperature of the anomalous Schottky effect. The observations are analyzed in terms of an assumed patch distribution of adsorbed atoms such that the concentration difference between patches decreases with increasing temperature. More complete information is presented concerning the temperature coefficients of the work function for thoriated tungsten, and the precautions necessary before comparisons are made with temperature coefficients obtained photoelectrically or by contact potential measurements.

INTRODUCTION

THE reported values of the thermionic constants of thoriated tungsten, namely, the slope and intercept of the Richardson plot, show a divergence larger than the experimental errors of the individual values. Reimann[1] gives the extent of this divergence for the reported values of the intercept as a function of activation. The reported slopes disagree by several tenths of a volt. Experimentally, Brattain and Becker[2] have shown why this lack of agreement is to be expected. For any given state of activation the slope and intercept decrease markedly with applied field, in the range of applied fields generally used. The over-all change of intercept is of the order of a factor 10, and the over-all change of slope of the order of 0.5 volt. For any given state of activation, therefore, depending upon the applied field, the reported values of the slope and intercept might be expected to differ by as much as these amounts.

The rapid decrease of the slope of the Richardson plot with applied field, which, in terms of the current-voltage curve, has been long familiar as the anomalous Schottky effect, has been successfully analyzed in terms of the patch theory.[3, 4] The rapid decrease of intercept with applied field may also be accounted for by the patch theory if it is assumed that the concentration difference between patches decreases with increasing temperature.[5] This analysis is undertaken below. For the purpose of the analysis, it was necessary to make a more thorough study of the dependence of the thermionic constants for thoriated tungsten on activation and applied field than was reported in the paper by Brattain and Becker. These results, also, are summarized below.

EXPERIMENTAL ARRANGEMENT

The tube consisted essentially of a one-mil thoriated tungsten filament, 6 cm long, mounted along the axis of a cylindrical collector, and two guard rings. The filament was a "long" filament down to 1200°K as shown both by the unbroken Richardson lines in this temperature range and by calculations based on the paper by Langmuir, McLane and Blodgett.[6] This allowed the current-temperature scale of the Jones and Langmuir[7] tables to be applied directly. The vacuum was 10^{-7} mm of Hg or better as read by an ionization gauge. Two significant tests of the vacuum conditions were first, that emission values could be repeated over a period of several weeks and second, that no appreciable sputtering of the thorium occurred at 300 volts applied collecting voltage. These tests are an adequate measure of the presence of chemically active and inert gases.

* Now employed by RCA Manufacturing Co., Radiotron Division, Harrison, New Jersey.

[1] A. L. Reimann, *Thermionic Emission*, page 127.
[2] Brattain and Becker, Phys. Rev. **43**, 428 (1933).
[3] J. A. Becker, Rev. Mod. Phys. **7**, 95 (1935).
[4] A. Rose, Phys. Rev. **47**, 806 (1935).
[5] A. Rose, Phys. Rev. **47**, 889 (1935).
[6] Langmuir, McLane and Blodgett, Phys. Rev. **35**, 478 (1935).
[7] Jones and Langmuir, Gen. Elec. Rev., pp. 310–319, 354–361, 408–412 (1927).

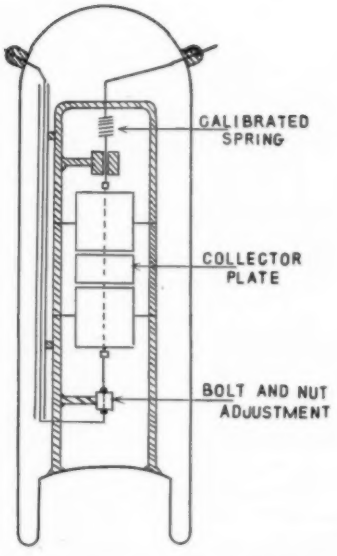

FIG. 1. Experimental tube. The calibrated spring and adjustment at the lower end were necessary to accurately fix the filament tension to prevent sagging and burning out at the higher temperatures.

RESULTS

The emission current was measured as a function of the three variables, temperature, T, applied field, E, and activation, f, in the ranges:

$$1300°\text{K} < T < 1800°\text{K}$$

$$0 < E < 3 \times 10^4 \text{ volts/cm}$$

$$0 < f < 1.$$

The f values were based upon tables given by Brattain and Becker[2] in the paper cited above. Although the f value does not uniquely characterize the surface, because of its patchy nature, it is a convenient index to the concentration of thorium atoms in the more concentrated patches. The results are summarized by the curves in Figs. 2 and 3 showing the observed slopes and intercepts of the Richardson plots ($\ln I - 2 \ln T$ against $1/T$) as a function of applied voltage for various states of activation. The field at the surface of the filament in volts/cm calculated from the geometry of the elements was 117 times the applied voltage. A similar set of data was taken after the filament had been aged several hours at 3000°K. These curves differed from the set shown here in that they flattened out at lower collecting voltages.

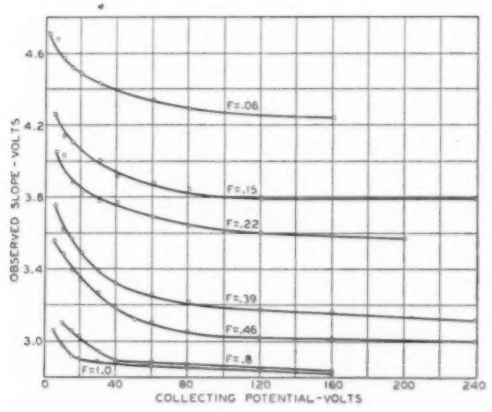

FIG. 2. Slopes of Richardson plots as a function of collecting potential for various states of activation. The field (volts/cm) at the surface of the filament = 117 × collecting potential.

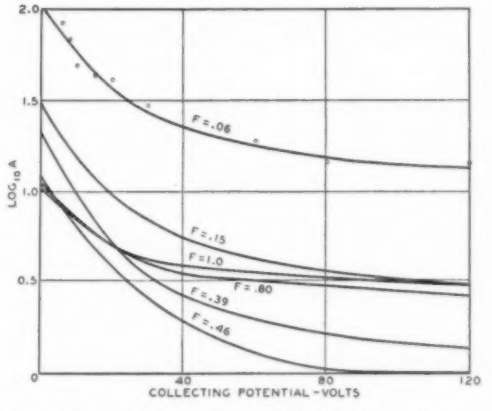

FIG. 3. Log of the intercepts of Richardson plots as a function of collecting voltage for various states of activation.

DISCUSSION OF RESULTS

Because of the patch distribution of adsorbed atoms on the surface, and the consequent dependence of the thermionic constants on the particular surface investigated, the absolute magnitudes of the constants are not to be emphasized. What should be emphasized is the variation of these constants with activation and applied field. This is characteristic of all thoriated tungsten surfaces and, therefore, requires an

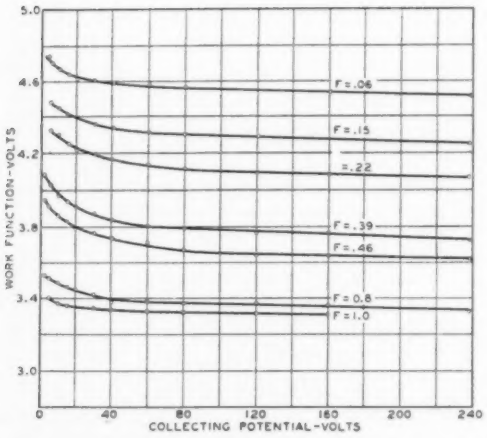

FIG. 4. Work functions (obtained from the slopes and intercepts of Richardson plots) as a function of collecting potential for various states of activation.

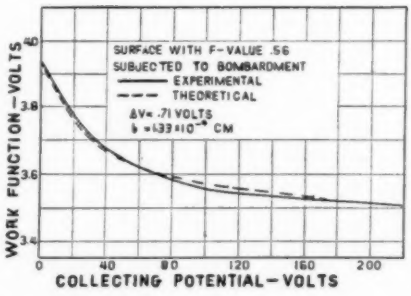

FIG. 5. Effect of positive-ion bombardment on the surface of a partially activated thoriated tungsten filament. The enhanced over-all change in work function with applied potential is the well-known anomalous Schottky effect. (b=length of side of square patch.)

explanation. The major facts concerning this variation are enumerated below.

(1) The most prominent characteristic is the marked decrease of the work function[8] with applied field for low applied fields. The curves (Fig. 4) flatten out at around 10^4 volts/cm. This is the counterpart of the poor saturation observed for all coated surfaces, namely, a more rapid decrease of the work function with applied field than is predicted by the normal Schottky effect.

(2) The rate of decrease of the work function with applied field is accentuated by bombardment of the thoriated surface with positive ions. (See Fig. 5.)

(3) The curves for work function against applied field flatten out at lower applied fields after the filament has been aged at high temperatures.

(4) Within the accuracy of measurement of the intercept of the Richardson plot, and for applied fields below the point where the curves flatten out, the change of the log of the intercept is proportional to the change of the slope at a given state of activation. (See Fig. 6.) It is to be remembered that at a given state of activation the slope and the intercept are both a function of the applied field. (This is not to be confused with the reported proportionality between the slope and intercept for different states of activation and the same applied field.)

(5) The intercept of the Richardson plot for low applied fields decreases steadily with activation to a minimum at complete activation.

(6) The intercept of the Richardson plot at high applied fields (in the neighborhood of the point where the curves in Fig. 4 flatten out) decreases with activation to a minimum around *half* activation. (See Fig. 7.) This is borne out also by the results of Brattain and Becker, which show the intercept against applied field for $f=0.6$ intersecting similar curves for $f=0.86$ and $f=1.0$.

(7) At high applied fields, when the temperature of a partially activated filament is suddenly dropped from about 1600°K to about 1300°K, the emission increases (by as much as a factor of two) with time at this lower temperature approaching asymptotically a reproducible value. If the temperature is now suddenly increased to 1600°K, no time lag in the emission is observed within the 7-second period of the galvanometer.

(8) At low applied fields, when the filament temperature is suddenly dropped to a low value, the emission at this lower temperature decreases only *slightly* with time or may even be constant.[9]

ANALYSIS OF RESULTS

It is the purpose of this part to analyze the facts enumerated above on the basis of a patch distribution of adsorbed atoms such that the concentration difference between patches decreases with increasing temperature. The patch distribution is well established by electron microscope pictures of activated surfaces. The temperature dependence is a natural assumption by Boltzmann's distribution function, if the adsorption energy of neighboring patches is different.

To carry out the analysis, certain simplifying assumptions must be made since an exact treatment is both out of the question and not in keeping with the experimental uncertainties. It is hoped that these assumptions will be within the range of experimental variations due to the patches, or, at least, faithful to the more important elements of the problem. In particular, use

[8] The work function as indicated below in Eq. (5) is obtained from the slope and intercept of the Richardson plot.

[9] I am indebted to Dr. Nottingham for this fact.

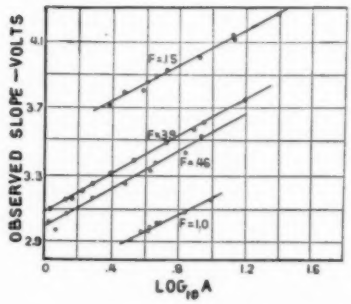

FIG. 6. Linear relation between observed slopes and intercepts of Richardson plots for several states of activation.

will be made of the fact that about ten or twenty times as much emission comes from the low work function patches as from the high work function patches. And since the low work function patches dominate the variation of the observed constants with activation and applied field, the approximation will be made that they are entirely responsible for the observed variation. This is especially true, since, as will appear below, the rapid variation of the constants is due to the local retarding patch field above the low work function patches. The local patch field above the high work function patches is an accelerating field, and changes in it introduce only the relatively small *normal* Schottky correction. Other approximations will be explained as they are introduced.

For the purpose of the analysis, a more explicit form of the Richardson equation, based upon three assumptions, is employed. These assumptions are:

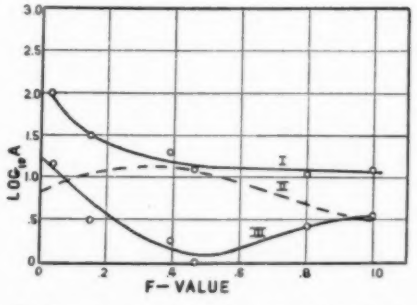

FIG. 7. Curve I: log of the low applied field intercept: $\log U-(\epsilon/2.3k)(\alpha_1+\alpha_2)$. Curve III: log of the high applied field intercept: $\log U-(\epsilon/2.3k)(\alpha_1+\alpha_2+\alpha_3)$. Curve II: Curve I–Curve III: $(\epsilon/2.3k)\alpha_3$.

(1) The validity of the statistical form of the Richardson equation

$$I=UT^2e^{-\epsilon\phi/kT},$$

where U = universal constant 120 amp./cm²/°K²,
T = absolute temperature,
ϕ = work function,
ϵ, k have their usual significance.

(2) The work function ϕ is a function of applied field and temperature

$$\phi=\phi(E, T).$$

(3) $\partial^n\phi/\partial T^n=0$ for $n>1$.

(1) is based upon the Fermi distribution for electrons in metals; (2) is an experimental fact; and (3) merely states that only Richardson plots which are straight lines will be considered. This last is a valid restriction since the Richardson plots even for coated surfaces are indistinguishable from straight lines in the experimental range of temperatures.

If $\phi(E, T)$ is expanded in a Taylor series in the neighborhood of (E_1, T_1) in the experimental range of applied field and temperature and the terms grouped together with due regard to (3), the result will take the form:

$$\phi(E, T)=\phi_0+\alpha T+\beta(E)T+\gamma(E), \qquad (1)$$

where $\beta(E)$ and $\gamma(E)$ may be any functions of the applied field and ϕ_0 and α are constants. The Richardson equation now becomes:

$$I=Ue^{-(\epsilon/k)[\alpha+\beta(E)]}T^2e^{-(\epsilon/k)[\phi_0+\gamma(E)]/T}, \qquad (2)$$

where

$$Ue^{-(\epsilon/k)[\alpha+\beta(E)]} \qquad (3)$$

is the observed intercept.[10]

$$(\epsilon/k)[\phi_0+\gamma(E)] \qquad (4)$$

is the observed slope and

$$\phi_0+\gamma(E)+[\alpha+\beta(E)]T \qquad (5)$$

is the work function at temperature T and applied field E.

The eight experimental observations enumerated in the previous section may now be examined in order.

[10] In the case of patch distributions, the intercept should also contain a surface factor $e^{\delta(E)}$ to take care of the fact that at higher fields more of the emission comes from the low work function patches, that is, the effective emitting area decreases. This effect, however, is small compared with the change of intercept actually observed (see appendix).

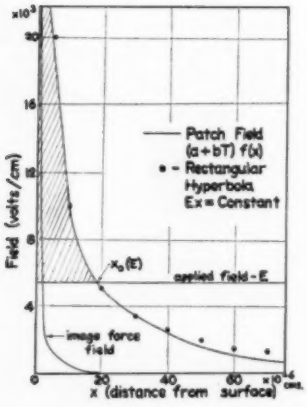

FIG. 8. The above figure shows: (1) The relative unimportance of the image force field as compared with the patch field $(a+bT)f(x)$. (2) The increase in work function (shaded area) of the low work function patch due to the retarding patch field at an applied collecting field E. (3) The approximation of the patch field by a rectangular hyperbola.

1.

The curves in Fig. 2 must be corrected by the intercept, according to (5), to get the actual work function at a given applied field and temperature. Fig. 4 shows the variation of work function, so obtained, with applied field for several states of activation. The temperature chosen was 1600°K. The abnormal decrease of work function for low applied fields is due to the local retarding field above the low work function patch. These local fields were calculated for a checker-board array of patches. The adjustable parameters are ΔV, the contact potential difference (or difference in work function) between the two kinds of patches, and s the length of side of each square patch. (See appendix for mathematical detail.) Knowing the local fields due to the patches and the applied field, the work function may be calculated for each point on the surface and averaged over the whole surface to give the observed value.

A typical comparison of calculated and observed work function against applied field curves is shown in Fig. 9. The agreement is as close as can be expected from the arbitrary assumed distribution of patches. Where the curves flatten out, the applied field becomes equal to the patch field at the surface. Beyond this point the variation of work function with applied field is practically that predicted by the normal Schottky

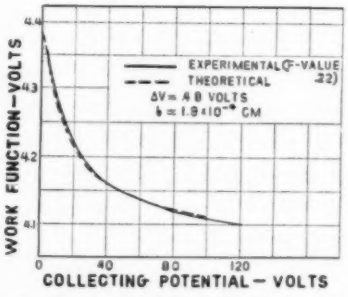

FIG. 9. Agreement between calculated and observed variation of work function with applied field. Calculations were made on the basis of a square array patch theory. (b = length of side of square patch.)

effect, and the calculated curve, which neglects the normal Schottky effect, is not valid.

The parameters s and ΔV were obtained for states of activation from $f=0$ to $f=1$ and recorded in Table I. It is to be noted that the ΔV values are well within the contact potential, about two volts, between clean and completely thoriated tungsten. The values of the average patch size are of the order of the size of crystal observed by an optical microscope for this filament. The quantitative comparison is made below in (2). In Table I are recorded, also, values of s and ΔV estimated from Brattain and Becker's data. The s values in their case are consistently larger than ours. Since, as is noted below in (2), the patch size is of the order of the exposed tungsten crystal faces, this difference is explainable. The patch size remains roughly constant with activation, as would be expected. The average contact potential between patches shows a maximum for states of activation around $f=0.5$ and decreases as $f\rightarrow 1$. The reason for this is that a given concentration difference corresponds to a larger difference in work function for the lower states of activation than for the higher ones. (The work function against activation curve drops rapidly in the range $f=0$ to $f=0.5$ and then flattens out to a broad minimum at $f=1$.)

2.

Also in Table I are recorded the values of s and ΔV obtained from a set of slope and intercept against applied field curves for various states of activation after the filament had been aged several hours at 3000°K. The values of s are

seen to be about twice as large as those recorded before the aging. This is in agreement with the act that crystal growth is known to occur at this temperature.

While the method used here of estimating the average patch size is a reliable means of determining relative values, as in the comparison of the average patch size before and after aging, it is not to be expected that it will give more than the order of magnitude of the absolute values. In particular, the flattening out point of the work function against applied field curves is used to determine the value of the patch field at the surface, and this is likely to be determined by the higher patch fields of the smaller patches rather than by the field corresponding to the average sized patch. With this in mind, the comparison of the following optical observations on the exposed crystal faces of the filament with the s values of average patch size just cited will be significant. The optical microscope showed about 75 percent of the exposed crystal faces to be rectangles with their long side 3 or 4 times their short side, and lying parallel to the length of the filament. The short side, which would determine the patch field at the surface, was of the order of 6×10^{-4} cm. Further work with the electron microscope should show how meaningful the comparison between the 6×10^{-4} cm crystal dimension and the $3-4\times10^{-4}$ cm average patch size is. One further fact is brought out by the s values in the last column of Table I, namely, for low states of activation s is small. Electron microscope pictures at these states of activation show a number of isolated spots smaller than the average patch size at higher activations.

TABLE I. *Parameters s and ΔV for various states of activation.* Values of ΔV (average contact potential difference between patches) and s (average size of patch computed on the basis of the square array patch theory) were computed from work function against applied field curves at various states of activation.

			After Aging 2 Hours at 3000°K			Computed from Bratain and Becker's Data on a 4-Mil Thoriated Tungsten Filament		
f Value	ΔV (volts)	s (cm)	f Value	ΔV (volts)	s (cm)	f Value	ΔV (volts)	s (cm)
0.06	0.46	1.5×10^{-4}	0.08	0.36	1.5×10^{-4}			
.15	.50	1.6	.27	.46	2.8	0.3	0.8	4.6×10^{-4}
.22	.60	1.7	.57	.46	3.8	.6	.70	2.8*
.39	.68	1.9	.76	.48	4.0	.86	.34	4.6
.46	.70	2.0	.87	.38	3.2	1.0	.30	5.4
.8	.36	2.0	1.0	.22	3.7			
1.0	.24	1.2						

* Data incomplete.

3.

Fig. 5 shows the effect on the work function against applied field curve of bombarding the thoriated surface with positive ions. Under the action of the bombardment, thorium is sputtered off in spots, resulting in a larger difference in concentration between patches. This is brought out by the larger value of ΔV necessary to be assumed to match the calculated and observed curves.

4.

The fact that at a given state of activation the change of slope is proportional to the change of the log of the intercept (Fig. 6) (both being functions of the applied field) is a stringent condition to be satisfied by any theory of the thermionic constants for coated surfaces. The difficulty comes in trying to find a mechanism which will cause the intercept to decrease rapidly for low applied fields and yet have no effect at high applied fields. The explanation, several times offered, to account for changes in the intercept, namely, that the transmission coefficient varies with applied field, is immediately seen to be invalid here. The transmission coefficient explanation is most effective at high applied fields. Actually, however, the intercept decreases most rapidly for low applied fields and becomes constant at around 10^4 volts/cm. The temperature-dependent patch theory not only accounts for this rapid decrease at low fields but shows why the change of the log of the intercept is linked up with the change of slope and, in particular, why these changes are *proportional*.

The explanation is qualitatively this: the slope decreases rapidly with low applied fields because the local retarding patch field above the low work function patch is rapidly neutralized by the applied field. The intercept will change, according to Eq. (3), if the temperature coefficient of the work function is also a function of the applied field. This condition is provided by the temperature dependent patch theory in the following way: Since the local patch fields are proportional to the contact potential difference between patches, and since this changes with temperature

due to the decrease of concentration difference with increasing temperature, then the local retarding field above the low work function patch must also change with temperature. Corresponding to this change there will be a temperature coefficient of the work function which will depend upon the applied field in the same way as the slope, since it will be proportional to the amount of retarding field not neutralized by the applied field. In other words, a given change of retarding field with temperature has its maximum effect on the work function when the applied field is zero. When the applied field completely neutralizes the retarding field, changes in the retarding field with temperature have no effect upon the work function. Hence, the intercept at these fields remains constant.

To make the argument more definite: (1) Let the contact potential between patches be

$$\Delta V = a + bT$$[11]

where a and b are constants. (2) Let all of the emission come from the low work function patches. According to Eqs. (3) and (4), this proof must show that:

$$d\beta(E)/dE \sim d\gamma(E)/dE.$$

At any applied field E, the contribution of the patch field to the work function is (see Fig. 8):

$$\beta(E)T+\gamma(E)=\int_0^{X_0(E)}[(a+bT)f(X)-E]dX$$

$$=-EX_0(E)+(a+bT)\int_0^{X_0(E)}f(X)dX, \quad (6)$$

where $(a+bT)f(X)$[12] is the retarding patch field as a function of X, the distance from the surface; $X_0(E)$[13] is the distance from the surface at which the applied field equals the retarding field.

$$\beta(E)=\frac{\partial}{\partial T}\left[-EX_0(E)+(a+bT)\int_0^{X_0(E)}f(X)dX\right]$$

$$=b\int_0^{X_0(E)}f(X)dX,$$

$$\gamma(E)=-EX_0(E)+a\int_0^{X_0(E)}f(X)dX.$$

It is evident by inspection of $\beta(E)$ and $\gamma(E)$ that $d\beta(E)/dE = \text{const.}\ X d\gamma(E)/dE$ if

$$(d/dE)[EX_0(E)]$$

$$=0 \text{ or const. } X(d/dE)\int_0^{X_0(E)}f(X)X.$$

The former possibility is nearly satisfied, since the form of the surface field $f(X)$ is, in the important part of its range, nearly that of a rectangular hyperbola for which $(d/dE)[EX_0(E)] = 0$. This is evident from Fig. 8 in which a rectangular hyperbola is matched with the retarding field $(a+bT)f(X)$ computed along a normal to the center of a low work function patch. *Hence, within the limits of experimental error, the temperature dependent patch theory accounts for the significant straight lines in Fig. 6.*

5 and 6.

Fig. 7 shows that the low field intercept decreases with activation to a minimum near complete activation. The high field intercept, on the other hand, shows a minimum around $f=0.5$. The following is a qualitative analysis to explain the difference by the temperature dependent patch theory.

In general the intercept is

$$Ue^{-(a/k)[\alpha+\beta(E)]}.$$

The $\beta(E)$ has been identified with the change of the local fields with temperature due to the decrease of the concentration difference between patches. The α term may be split into three

[11] The contact potential undoubtedly contains higher powers of T, but these may be neglected, as long as the Richardson plots are indistinguishable from straight lines.

[12] As may be seen from Fig. 8, the image force field may be neglected in comparison with the patch field up to a short distance from the surface about 5×10^{-6} cm. (Although for large values of X, the image field must be larger than the patch field, since the image field decreases as $1/X^2$ and the patch field as $e^{-\text{const. } X}$, the values of E for which this is true are so small that an applied potential of one volt already brings $X_0(E)$ in the range shown in Fig. 8.) However, for applied fields that bring $X_0(E)$ within this distance 5×10^{-6} cm the proportionality between the log of the intercept and the slope no longer holds experimentally so that this analysis may be restricted to the range of $X_0(E)$ for which the patch field is much greater than the image field.

[13] $X_0(E)$ is also a function of T, but its dependence on T is of the order of the dependence of the slopes of the Richardson plots on T, which has been neglected as long as these are indistinguishable from straight lines.

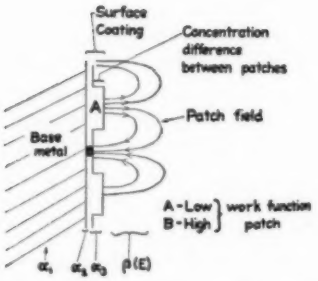

FIG. 10. Schematic representation of the various causes for a temperature coefficient of the work function: α_1—base metal—change of Fermi limit. α_2—uniform adsorbed layer of atoms. e.g. A surface uniformly covered with an adsorbed layer shows a temperature coefficient different from α_1. α_3—concentration difference between the two kinds of patches. This concentration difference decreases with increasing temperature. $B(E)$—retarding patch field above the low work function patches. This retarding field decreases with decreasing concentration difference, i.e., with increasing temperature.

parts: α_1 associated with the base metal, α_2 associated with the temperature change of the dipole moment per adsorbed atom, and α_3 with the temperature change of concentration of the patches (see Fig. 10). The purpose of the separation is to show that as the applied field→zero, $\beta(E)\rightarrow-\alpha_3$, so that at zero applied field the intercept of the Richardson plot is determined by

$$Ue^{-(\epsilon/k)(\alpha_1+\alpha_2)}.$$

To simplify the analysis, the low work function patches are assumed to control the variation of the intercept with activation and applied field. (The approximation is permissible for two reasons: first, that most of the emission comes from the low work function patches, and second, that the work function of these patches is more sensitive to concentration difference and applied field because the patch field above it is a retarding field. The accelerating patch field on the high work function patch introduces only the normal Schottky correction which is small compared with the contribution to the work function of the retarding patch field.)

From Eq. (6), $\gamma(E)+\beta(E)T=$increase of work function due to the retarding patch field. At zero applied field $\gamma(E)+\beta(E)T=\Delta V/2=a/2+bT/2$, from which $\beta(E)=b/2$.

α_3 is the change of work function per degree change of temperature due to the decrease of concentration in the low work function patches. The temperature dependent part of $\Delta V\,(=a+bT)$ is a result both of the increase of work function of the low work function patch and of the decrease of work function of the high work function patch when adsorbed atoms pass from the low to the high work function patch. For small changes of concentration, the changes in work function of the two patches may be considered equal. That means that the temperature coefficients of their work functions due to changes in concentration are equal. Since they add up to give the temperature coefficient of ΔV, namely b, then the temperature coefficient of either patch is $b/2$. In particular, the temperature coefficient of the low work function patch with which we are concerned is $b/2$. It has been shown, therefore, that α_3 and $\beta(E)$ are numerically equal at zero applied field. That they have the opposite sign is evident, since an increase in temperature decreases the local fields and therefore their contribution to the work function, while at the same time it decreases the concentration in the low work function patch increasing its work function.

The intercept at zero applied field is, then,

$$Ue^{-(\epsilon/k)(\alpha_1+\alpha_2)}.$$

Since α_1 is not a function of applied field, the variation of the intercept with activation is determined solely by α_2. From Fig. 7 the low field intercept decreases steadily to a minimum at maximum activity. This requires that α_2 increase steadily with activation to a maximum at maximum activity.

As the applied field is increased from zero, $\beta(E)\rightarrow0$ due to the neutralization of the local retarding field upon which $\beta(E)$ depends. For applied fields greater than the patch field at the surface, that is, when the local retarding field is completely neutralized, $\beta(E)=0$. The high field intercept is therefore

$$Ue^{-(\epsilon/k)(\alpha_1+\alpha_2+\alpha_3)}.$$

It differs from the zero field intercept by the additional factor $e^{-(\epsilon/k)\alpha_3}$. It is this factor which shifts the minimum of the high field intercept against activation curve toward $f=0.5$. The argument is as follows: α_3 is the temperature

coefficient of the work function of the low work function patch due to the temperature change of concentration of atoms in the patch. α_3 is large for states of activation up to $f=0.5$, but decreases for activations >0.5. The reason is the same as that used to explain the variation of ΔV with activation, namely, that a given change of concentration is associated with a larger change of work function at the lower states of activation than at the higher states. α_3 plotted against activation (see Fig. 7) gives a decreasing curve near $f=1$. This added to the curve for $\alpha_1+\alpha_2$ which is increasing slowly to a maximum near $f=1$ shifts the maximum to lower values of f. The maximum of $\alpha_1+\alpha_2+\alpha_3$ corresponds to the minimum in the observed intercept

$$Ue^{-(\epsilon/k)(\alpha_1+\alpha_2+\alpha_3)}.$$

7.

The emission lags described in the previous section are *direct evidences* of the *temperature-dependent patch theory*. When the temperature of the filament is dropped from 1600°K to about 1300°K, migration of the atoms at the lower temperature is sufficiently slow to delay the concentration equilibrium from being reached for several minutes. During this time, atoms from the high work function patch migrate to the low work function patch to establish the higher concentration difference characteristic of the lower temperature. Since the low work function patch contributes most of the emission, its decrease of work function with time causes the corresponding increase in the observed emission current. Accompanying changes in the local retarding field have no effect, since the retarding field is neutralized by the high applied field. If, after coming to equilibrium, at the lower temperature, the temperature is suddenly raised to 1600°K, the concentration equilibrium is rapidly established by the greater rate of migration of the atoms, so that no lag effects are observed.

8.

The above observations are for high collecting fields. For low collecting fields, when the temperature is dropped suddenly, the emission is observed to decrease only slightly, if at all, with time. The reason for this is that at low collecting fields changes in the local retarding field above the low work function patch must be considered as well as changes in the concentration of this patch. The sum of the two effects maintains the emission from the low work function patch constant even though its concentration increases with time. The argument here is the same as that used to show that $\alpha_3=-\beta(E)$ at low fields, namely, the decrease of work function due to the increase in concentration is equal and opposite to the corresponding increase in work function due to the increased local retarding field. Although the emission from the low work function patch remains constant during the time that the concentration equilibrium is arrived at, the emission from the high work function patch decreases because of its decreasing concentration of atoms. Since the high work function patches account for a small part of the observed emission current, a decrease in its emission will cause the observed slight decrease in the measured current.

9.

Compton and Langmuir[14] report a decrease of the anomalous Schottky effect with increasing temperature. Since, according to the temperature dependent patch theory, the concentration difference approaches zero as the temperature is increased, this observed fact is accounted for quite naturally.

Conclusion

The major purpose of this paper will have been satisfied if the temperature dependent patch distribution is established as the most important determinant of the variation of the thermionic constants of thoriated tungsten with applied field and activation. To this end, nine distinct observed facts have been enumerated and analyzed. It is reaffirmed that relatively small effects as surface irregularities and change of effective emitting area with applied field have been neglected to emphasize the more significant aspects of the patch theory. Even with these simplifications the picture is complex. In particular, temperature coefficients of the work function for these surfaces as observed photoelectrically, thermionically and by contact poten-

[14] Compton and Langmuir, Rev. Mod. Phys. **2**, 156 (1930).

tial measurement, may not readily be compared before due account is taken of the differences in temperature ranges and applied fields.

The writer is glad to thank Professor L. P. Smith for many helpful discussions on this subject.

Appendix

1. Surface factor

The measured emission current from thoriated tungsten is the sum of the emission currents from areas of several different work functions. As such, the Richardson plot of the measured emission current should not be a straight line, since the sum of two exponentials is not an exponential. Actually, the curvature of these plots is not detectable. It has meaning therefore within the experimental accuracy to write

$$I=A_1T^2e^{-b_1/T}+A_2T^2e^{-b_2/T}=A_3T^2e^{-b_3/T}, \tag{1}$$

where I=observed emission current from two patches whose constants are A_1, A_2, b_1 and b_2 while A_3 and b_3 are the observed intercept and slope of a plot of $\ln_n I-2\ln_n T$ against $1/T$. A_3 may now be calculated in terms of A_1, A_2, b_1 and b_2 to show that its change with applied field due to the increase of b_2-b_1 is much less than the observed change. The variation computed here is the variation of the surface factor $e^{-\bar{b}(E)}$ which has been omitted in the general analysis.

Let $$b_2-b_1=\Delta b>0;$$

then from (1)

$$I=A_1T^2e^{-b_1/T}(1+A_2/A_1)e^{-\Delta b/T} \tag{2}$$

and $$\ln A_3=\ln I-2\ln T+b_3/T. \tag{3}$$

From (3): $$b_3=-\frac{d(\ln I-2\ln T)}{d\,1/T}=b_1+\frac{\Delta b}{1+(A_1/A_2)e^{\Delta b/T}}. \tag{4}$$

By inserting $\ln I$ from (2) and b_3 from (4) into (3):

$$\ln A_3=\ln A_1+\ln\left(1+\frac{A_2}{A_1}e^{-\Delta b/T}\right)+\frac{\Delta b}{T(1+(A_1/A_2)e^{-\Delta b/T})}. \tag{5}$$

To get the over-all change of A_3 with applied field due to the change of effective emitting area, let: $A_1=A_2$, $b=2000$ degrees at zero applied field, $T=1500°$K. Then from (5)

$$\ln A_3=\ln A_1+0.51. \tag{6}$$

At applied fields greater than the patch field at the surface, $b=4000$ degrees and

$$\ln A_3=\ln A_1+0.24. \tag{7}$$

From (6) and (7):

$$\frac{A_3 \text{ zero field}}{A_3 \text{ high field}}=1.3.$$

This change is small compared with the observed change of the order of a factor of 10.

2. Local patch fields

The electrostatic field in the Z direction was computed for the case shown in Fig. 11, where ΔV=contact potential

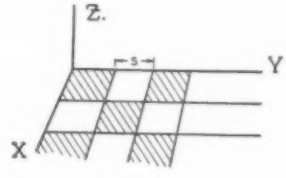

Fig. 11.

difference between the shaded and unshaded square patches and s=length of side of each square. The solution of Laplace's equation

$$\nabla^2V=0$$

is $$V(x,y,z)=\sum_{\substack{m,n\\ odd}}\frac{8\Delta V}{mn\pi^2}e^{-(\pi/s)(m^2+n^2)^{\frac{1}{2}}z}\sin\frac{m\pi}{s}x\sin\frac{n\pi}{s}y,$$

from which it follows that

$$E_z=\frac{8\Delta V}{\pi s}\sum_{\substack{m,n\\ odd}}\frac{(m^2+n^2)^{\frac{1}{2}}}{mn}e^{-(\pi/s)(m^2+n^2)^{\frac{1}{2}}z}\sin\frac{m\pi}{s}x\sin\frac{n\pi}{s}y.$$

Using 16 terms of this series gave the field with an accuracy of several percent up to a distance of about 5×10^{-6} cm from the surface.

The low work function patch was divided into sub-squares for each of which the work function was obtained at various applied fields by graphical methods. The work functions of the various sub-squares differed by sufficiently small amounts to allow the arithmetic mean to be taken with an error not greater than 0.02 volt. To average the work functions of the two different kinds of patches, however, the expression obtained above:

$$b_3=b_1+\frac{\Delta b}{1+e^{\Delta b/T}}$$

was used since here Δb was appreciable.

Self-Consistent Field for Tungsten

MILLARD F. MANNING AND JACOB MILLMAN, *Massachusetts Institute of Technology*

(Received March 19, 1936)

Calculations of the self-consistent field of the tungsten atom have been carried out with the aid of the Massachusetts Institute of Technology differential analyzer. A discussion of the machine set-up and an outline of a method for estimating initial fields are given.

IF the wave-function of a many-electron atom is expressed as a product of one-electron wave-functions, the radial factor of each of these wave-functions is found by solution of the differential equation[1]

$$d^2P/dr^2+(2v-\epsilon-l(l+1)/r^2)P=0. \quad (1)$$

As has been pointed out by Hartree[2] it is convenient to introduce the new independent variable $\rho=\log r$, and the new dependent variables $Q=Pr^{-l-1}$ and $Y=Pr^{-\frac{1}{2}}$. The differential equations which Q and Y satisfy are:

$$d^2Q/d\rho^2+(2l+1)dQ/d\rho+(2rZ_p-\epsilon r^2)Q=0, \quad (2)$$

$$d^2Y/d\rho^2+[2rZ_p-\epsilon r^2-(l+\tfrac{1}{2})^2]Y=0. \quad (3)$$

For $n<4$ and for all of the "s" functions, Eq. (3) was used throughout the range of integration. For the other functions the "Q" equation was used near the origin because in this region Q is nearly constant while Y increases exponentially.

The contribution to Z_p of the electrons of a particular type is found from the relations:

$$\zeta=\int_0^r P^2dr=\int_0^\rho Y^2e^{2\rho}d\rho, \quad (4)$$

$$Z=2(2l+1)\left[1-\int_0^r P^2dr\Big/\int_0^\infty P^2dr\right], \quad (5)$$

$$dZ_p/d\rho=Z_p-Z. \quad (6)$$

The estimation of the initial Z_p's was carried out by a method which, as far as the authors know, has not been described in the literature. Since it proved to be very satisfactory, it will be outlined briefly here. The basis of the method of interpolation is the fact that the Z *vs.* ρ curve for a particular type of electron has the same shape for different elements which are not too far apart in the periodic table. As can be seen from the graph of Fig. 1, one curve can be nearly superposed on the other by a shift parallel to the ρ axis. A reason why this can be expected and a method of utilizing it for interpolations can be seen from the screening constant relation:

$$r_1/r_2=(N_2-\sigma)/(N_1-\sigma) \quad (7)$$

or

$$\rho_1-\rho_2=\log(N_2-\sigma)/(N_1-\sigma), \quad (7a)$$

where N_1 and N_2 are the atomic numbers of the two elements considered and σ is the screening constant for the type of electron considered. This relation is ordinarily assumed to be valid only for the two radii for which the charge densities have their maxima, but the figure shows that it will be valid for any pair of radii corresponding to the same value of Z. Using data from two atoms which have been studied previously, $\rho_1-\rho_2$ and hence σ can be determined. Eq. (7a) can then be used to determine the Z against ρ curve for the same type of electron in another atom. For tungsten the interpolations were based upon Hartree's result for caesium[3] and mercury.[4] For the electrons inside of the $4s$ electron, the original estimates agreed so closely with those computed that it was necessary to determine these functions only once. For the outer electrons the estimates were not as satisfactory. This is because the $4f$ shell occurs in only one of the atoms which were used for interpolation. Since the charge density of the $4f$ electrons overlaps both four and five quantum electrons, it is easy to understand why the screening constants should be affected in a manner difficult to estimate.

[1] Except where stated the notation is that used by Hartree. See Proc. Roy. Soc. **A141**, 282 (1933).

[2] Hartree, Phys. Rev. **46**, 738 (1934).

[3] Hartree, Proc. Roy. Soc. **A143**, 506 (1934).

[4] Hartree, Proc. Roy. Soc. **A149**, 210 (1935).

In determining the Z's by the method described, there is some difficulty about making estimates in the region of the nodes. Even after the Z's have been determined, it is necessary to integrate to obtain the Z_p's. For these reasons, it seems possible that it would be more satisfactory to make the estimates in terms of the Z_p's. Hence tables of $2Z_p$ and $2v_0$ for the separate electrons have been included in the results.

Method of Solution

The solutions of Eqs. (2), (3), and (4) have been carried out on the Massachusetts Institute of Technology differential analyzer.[5] A schematic diagram[6, 7] of the setup for the simultaneous solution of Eqs. (3) and (4) is given in Fig. 2. The solution of Eq. (2) requires only the insertion of an extra set of gears and an adder. This equation is not used beyond the point where contributions to ζ become appreciable. It would be possible to integrate a modified form of Eq. (6) but this would require another input table. It is also difficult to estimate the starting conditions, and hence it was found more convenient to carry out this comparatively easy integration by hand. For the inner electrons and for the earlier approximations to the outer ones, it is not necessary to use different input plots of $2rZ_p$ for different functions having the same value of n but different values of l. The constant $(l+\frac{1}{2})^2$ can be taken care of by the initial setting of the first integrator. The method of generating ϵr^2 by an integrator avoids the necessity of making either a large number of plots or using another input table. In practice, the displacement of this integrator is multiplied by a factor greater than unity at small ρ and less than unity at large ρ. Compensating gears must, of course, be introduced.

The method ordinarily used by Hartree is to integrate from the origin outward to some point near the outer maximum of the wave function and to integrate a transformed equation from large r inward to the same point. The value of ϵ for which these solutions join is the eigenvalue. To carry out this process on an analyzer having six integrators would have required either an additional input table or the hand integration of the ζ equation. It seemed preferable to keep to the same equation and hunt for solutions asymptotic to the ρ axis. In practice this method did not prove too difficult, but some improvement in this part of the integration would probably be necessary before the accuracy could be greatly increased. The tabulated values of Y at large ρ have been smoothed to the correct asymptotic form.

One of the difficulties of any step-by-step process of integration is the accumulation of rounding-off errors. In hand computation this can be partly avoided by carrying extra figures

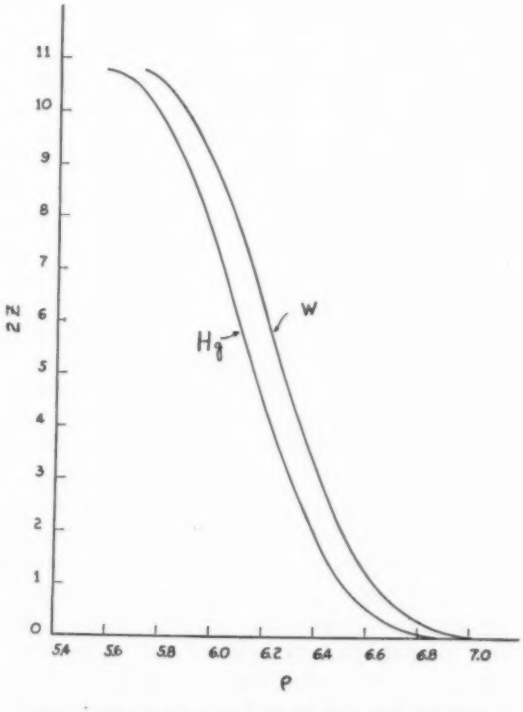

FIG. 1. Plot of $2Z$ as a function of ρ for $4p$ electrons in Hg and W.

[5] The authors wish to express their thanks to Professor S. H. Caldwell of the department of electrical engineering for placing the facilities of the differential analyzer at their disposal, and for making many helpful suggestions about the problem. As Hartree has pointed out, the solution of such a problem without mechanical methods of computation, is very laborious.

[6] For an explanation of the operation of the differential analyzer and the meanings of the symbols used, see: V. Bush, J. Frank. Inst. **212**, 447 (1931).

[7] For other cases where a differential analyzer has been used for the solution of the self-consistent field problem, see: Hartree, Phys. Rev. **46**, 738 (1934); Porter, Proc. Manchester Phil. Soc. **79**, 75 (1935).

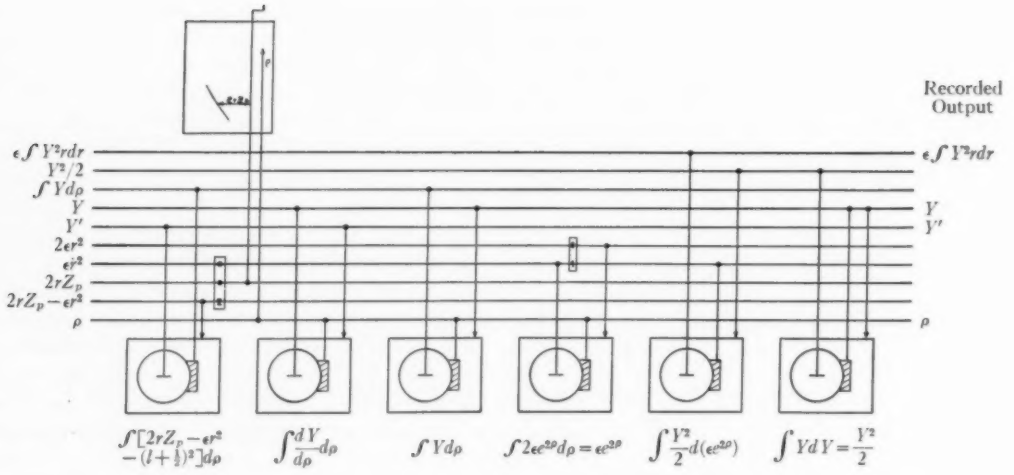

FIG. 2. Schematic diagram for the set-up of the differential analyzer for solution of the equations:

$$d^2Y/d\rho^2+[2rZ_p-\epsilon r^2-(l+\tfrac{1}{2})^2]Y=0 \qquad \text{and} \qquad \zeta=\int_0^\rho Y^2\epsilon^{2\rho}d\rho.$$

for the earlier stages of the computation. With the differential analyzer this method is not possible, and instead a method suggested by Professor Caldwell was used. The essential feature is to run solutions for five different energies which are evenly spaced about a value of the energy estimated from preliminary runs. These solutions are carried forward in stages of about two units in ρ. The solutions are smoothed by a least-squares method at the end of each of these stages and the solutions carried forward with the smoothed values.

As was anticipated, the most troublesome function was the $4f$. This is because $2rZ_p$ is never very much greater than $(l+\frac{1}{2})^2$ and hence small changes in $2rZ_p$ can produce large changes in the coefficient of Y in Eq. (3) in the region where that coefficient is positive. These small changes in $2rZ_p$ can be produced by any of the four or five quantum electrons—most particularly by the $4f$ electrons themselves. The functions are probably not "overstable" in the sense used by Hartree, but any process of using the field found at the end of one approximation as the initial field for the next approximation would probably converge but slowly. A little judicious guessing as to what is likely to happen next speeds up the convergence considerably. The $5d$ functions caused much less trouble than in the case of Hartree's calculations for mercury. This is partly because there are four instead of ten electrons in this shell, and partly because of a fortuitous estimate made at the end of the first approximation. The solution of the problem was of course much easier than it would have been without Hartree's previous work on mercury.

TABLE I. *Values of Y for* $\rho<2.0$.

	$1s$	$2s$	$2p$	$3s$	$3p$	$3d$	$4s$, $5s$, $6s$
0.0	3200	3200	80.0	3200	64.0	5.33	3200
.2	3478	3475	106.5	3477	85.5	8.70	3476
.4	3764	3761	142.0	3765	114.1	14.23	3762
.6	4058	4052	189.2	4058	152.0	23.28	4053
.8	4351	4341	251.5	4348	202.3	38.02	4343
1.0	4634	4617	333.5	4625	268.0	61.91	4620
.2	4896	4868	440.3	4874	353.9	100.50	4868
.4	5121	5074	578.5	5079	464.9	162.3	5071
.6	5293	5215	756	5216	605.8	261.8	5206
.8	5392	5264	980	5267	784.0	420.3	5235
2.0	5395	5188	1258	5174	1006	671.0	5155

TABLE II. *Values of* $Q\times10^{-4}$.

ρ	$4p$, $5p$	$4d$, $5d$	$4f$	ρ	$4p$, $5p$	$4d$, $5d$	$4f$
0.0	329.5	1780	1905	2.4		1393	1586
.4	323.5	1758	1887	2.6		1313	1519
.8	314.7	1727	1862	2.8		1222	1441
1.2	302.0	1681	1824	3.0		1119	1352
1.6	284.0	1615	1770	3.2			1253
2.0	251.9	1522	1694	3.4			1143
2.2		1462	1644	3.6			1024

TABLE III. *Values of Y.*

	1s	2s	2p	3s	3p	3d	4s	4p	4d	4f	5s	5p	5d	6s
2.0	5395	5188	1258	5174	1008	67.1	5155	1600			5155	1600		5155
.1	5353	5094	1420	5073	1135	84.3	5052	1803			5052	1803		5052
.2	5280	4957	1398	4928	1276	106.0	4903	2028			4902	2027		4902
.3	5173	4773	1794	4734	1431	133.0	4704	2273			4702	2272		4702
.4	5031	4538	2006	4488	1397	166.5	4452	2537			4448	2535		4448
.5	4852	4251	2236	4185	1776	208	4144	2820			4137	2817		4137
.6	4643	3910	2481	3825	1996	260	3776	3120			3766	3115		3766
.7	4392	3507	2739	3405	2165	323	3349	3433			3335	3427		3335
.8	4112	3054	3009	2928	2369	399	2864	3754			2844	3745		2844
.9	3803	2545	3286	2395	2576	476	2323	4078			2298	4067		2298
3.0	3471	1988	3565	1817	2781	605	1733	4396	640		1702	4380	640	1702
.1	3121	1390	3841	1188	2976	741	1102	4697	780		1065	4677	779	1065
.2	2761	761	4106	+ 534	3155	896	+ 442	4969	948		+ 400	4944	946	+ 400
.3	2398	+ 114	4352	− 135	3307	1083	− 230	5197	1144		− 276	5167	1143	− 276
.4	2042	− 538	4569	− 799	3424	1301	− 895	5364	1374		− 943	5328	1372	− 943
.5	1702	−1173	4748	−1437	3495	1552	−1527	5454	1638		−1578	5412	1636	−1578
.6	1382	−1775	4879	−2023	3507	1840	−2106	5447	1939	96.0	−2151	5398	1936	−2151
.7	1094	−2320	4952	−2529	3451	2163	−2596	5323	2275	127.6	−2635	5266	2272	−2635
.8	841	−2789	4958	−2927	3314	2524	−2971	5068	2648	169.0	−3001	5002	2644	−3001
.9	625	−3162	4890	−3129	3097	2918	−3201	4667	3049	222.4	−3225	4591	3042	−3225
4.0	448	−3425	4738	−3298	2776	3340	−3265	4112	3470	290.2	−3226	4026	3461	−3226
.1	308	−3566	4517	−3233	2369	3782	−3141	3406	3898	377.4	−3129	3288	3887	−3129
.2	202	−3581	4217	−2975	1875	4229	−2825	2561	4322	485	−2798	2430	4302	−2798
.3	125	−3474	3850	−2559	1305	4670	−2324	1597	4716	618	−2280	1461	4685	−2280
.4	73	−3257	3433	−1971	683	5082	−1660	+ 556	5055	780	1598	+ 416	5010	−1598
.5	39	−2949	2979	−1252	+ 23	5447	− 871	− 523	5708	975	− 796	− 615	5247	− 797
.6	20	−2577	2511	− 448	− 639	5738	− 15	−1565	5446	1205	+ 72	−1676	5363	+ 69
.7	10	−2169	2050	+ 389	−1265	5935	+ 843	−2504	5436	1472	932	−2588	5327	927
.8	4	−1753	1616	1196	−1824	6015	1623	−3264	5249	1776	1704	−3310	5110	1698
.9	2	−1357	1226	1915	−2227	5967	2251	−3777	4865	2115	2307	−3771	4690	2300
5.0	1	−1004	892	2485	−2597	5781	2653	−3986	4276	2483	2671	−3917	4060	2663
.1		− 706	619	2880	−2773	5459	2785	−3857	3477	2874	2743	−3713	3224	2735
.2		− 470	409	3069	−2796	5015	2618	−3386	2503	3274	2502	−3158	2212	2493
.3		− 294	256	3056	−2676	4474	2164	−2603	1388	3670	1964	−2298	+1065	1954
.4		− 171	152	2865	−2441	3863	1467	−1574	+ 192	4047	1184	−1188	− 150	1172
.5		− 94	82	2536	−2120	3222	+ 603	− 392	−1017	4371	+ 254	+ 38	−1356	+ 241
.6		− 49	45	2122	−1751	2587	− 331	+ 828	−2159	4630	− 739	1272	−2458	− 724
.7		− 24	21	1677	−1374	1991	−1228	1967	−3158	4822	−1578	2352	−3371	−1587
.8		− 10	9	1252	−1021	1465	−1991	2915	−3945	4906	−2234	3153	−4014	−2231
.9		− 4	4	873	− 715	1026	−2543	3593	−4475	4885	−2585	3579	−4331	−2564
6.0		− 1	1	571	− 471	679	−2844	3958	−4725	4757	−2586	3580	−4297	−2537
.1				345	− 289	422	−2899	4017	−4710	4534	−2241	3160	−3911	−2154
.2				190	− 164	241	−2737	3806	−4461	4231	−1624	2377	−3218	−1475
.3				88	− 80	134	−2417	3394	−4036	3868	− 763	1331	−2281	− 598
.4				41	− 43	69	−2006	2860	−3494	3465	+ 171	+ 140	−1178	+ 360
.5				18	− 20	33	−1569	2282	−2898	3042	1085	−1068	+ 1	1268
.6				7	− 8	15	−1158	1724	−2303	2616	1880	−2167	1194	2021
.7				3	− 3	6	− 801	1232	−1753	2199	2490	−3077	2305	2535
.8				1	− 1	2	− 520	831	−1274	1810	2864	−3724	3282	2756
.9						1	− 317	529	− 884	1454	2998	−4083	4079	2673
7.0							− 180	319	− 584	1140	2914	−4120	4674	2309
.1							− 96	185	− 365	871	2657	−3991	5058	1708
.2							− 48	100	− 214	646	2288	−3633	5242	949
.3							− 22	51	− 118	467	1867	−3151	5245	+ 106
.4							− 9	23	− 58	326	1446	−2609	5093	− 747
.5							− 4	11	− 30	220	1064	−2064	4816	−1546
.6							− 1	3	− 13	141	747	−1562	4441	−2236
.7								1	− 5	87	497	−1127	3999	−2782
.8									− 2	52	318	− 775	3516	−3162
.9										29	191	− 505	3020	−3369
8.0										16	108	− 311	2532	−3411
.1										8	57	− 183	2071	−3306
.2										3	29	− 101	1652	−3079
.3										1	13	− 53	1282	−2763
.4											5	− 25	967	−2391
.5											2	− 11	708	−1996
.6											1	− 5	500	−1604
.7												− 2	337	−1238
.8												− 1	214	− 915
.9													132	− 645
9.0													77	− 440
.1													42	− 266
.2													22	− 158
.3													11	− 89
.4													5	− 46
.5													2	− 22
.6													1	− 10
.7														− 4
.8														− 1

RESULTS

Tables of Y, $2Z$, and $2Z_p$ for each type of electron are given. For the cases where the Q equation was used near the origin, the values of Q rather than Y are given at small ρ. In the tables $\rho = \log 1000r$. The discrepancy between final estimates and final values of $2Z_p$ for any given type of electron does not exceed 0.06. This is about the same as the discrepancy in Z and is about five times the tolerance allowed by

TABLE IV. *Values of $2Z_\rho$ for the separate electrons and for the complete atom.*

(ρ)	(1s)	(2s)	(2p)	(3s)	(3p)	(3d)	(4s)	(4p)	(4d)	(4f)	(5s)	(5p)	(5d)	(6s)	Total
0.0	3.71	3.93	11.79	3.97	11.92	19.87	3.99	11.97	19.95	27.94	4.00	11.99	8.00	4.00	147.02
.4	3.56	3.89	11.69	3.96	11.83	19.81	3.98	11.95	19.93	27.91	3.99	11.98	7.99	4.00	146.49
.8	3.35	3.84	11.54	3.94	11.83	19.71	3.98	11.93	19.89	27.87	3.99	11.97	7.99	4.00	145.83
1.2	3.05	3.77	11.31	3.92	11.74	19.57	3.96	11.89	19.83	27.81	3.99	11.96	7.98	4.00	144.78
.6	2.62	3.67	10.97	3.87	11.61	19.36	3.95	11.84	19.75	27.71	3.98	11.94	7.98	3.99	143.24
2.0	2.07	3.52	10.47	3.81	11.42	19.05	3.92	11.76	19.63	27.57	3.97	11.91	7.97	3.99	141.05
.2	1.75	3.42	10.13	2.77	11.29	18.84	3.90	11.71	19.55	27.47	3.96	11.89	7.96	3.99	139.64
.4	1.42	3.31	9.72	3.73	11.14	18.58	3.88	11.64	19.45	27.36	3.95	11.87	7.95	3.99	137.98
.6	1.08	3.18	9.22	3.67	10.95	18.26	3.86	11.56	19.33	27.21	3.94	11.84	7.94	3.98	136.03
.8	0.77	3.03	8.62	3.60	10.72	17.88	3.83	11.47	19.18	27.04	3.93	11.81	7.92	3.98	133.07
3.0	.50	2.85	7.90	3.52	10.44	17.41	3.79	11.35	19.00	26.83	3.92	11.77	7.91	3.98	131.15
.2	.29	2.64	7.05	3.43	10.11	16.83	3.74	11.21	18.78	26.57	3.90	11.72	7.89	3.97	128.11
.4	.15	2.38	6.07	3.31	9.71	16.13	3.69	11.04	18.51	26.26	3.87	11.65	7.86	3.96	124.59
.6	.06	2.06	4.99	3.16	9.25	15.28	3.62	10.84	18.18	25.86	3.85	11.58	7.83	3.96	120.50
.8	.02	1.69	3.84	2.99	8.73	14.24	3.54	10.60	17.77	25.39	3.81	11.49	7.79	3.95	115.83
4.0		1.28	2.71	2.79	8.14	12.98	3.44	10.32	17.29	24.81	3.77	11.37	7.74	3.93	110.57
.1		1.07	2.19	2.67	7.82	12.26	3.38	10.15	17.00	24.48	3.75	11.32	7.72	3.93	107.74
.2		0.86	1.72	2.56	7.46	11.49	3.32	9.99	16.70	24.10	3.72	11.24	7.69	3.92	104.77
.3		.68	1.30	2.43	7.09	10.64	3.26	9.79	16.36	23.70	3.69	11.17	7.66	3.91	101.66
.4		.50	0.94	2.30	6.67	9.74	3.20	9.58	15.99	23.24	3.66	11.08	7.62	3.90	98.42
.5		.36	.65	2.15	6.22	8.79	3.11	9.34	15.60	22.75	3.63	10.99	7.58	3.89	95.05
.6		.24	.43	2.00	5.71	7.79	3.02	9.09	15.17	22.19	3.59	10.88	7.54	3.88	91.54
.7		.16	.27	1.82	5.16	6.77	2.93	8.80	14.72	21.58	3.55	10.77	7.51	3.86	87.89
.8		.09	.16	1.63	4.56	5.75	2.82	8.50	14.23	20.91	3.50	10.64	7.44	3.85	84.07
.9		.05	.08	1.42	3.92	4.75	2.71	8.16	13.71	20.17	3.45	10.51	7.40	3.83	80.16
5.0		.02	.04	1.20	3.26	3.80	2.59	7.80	13.16	19.35	3.39	10.35	7.32	3.82	76.11
.1		.01	.02	0.98	2.61	2.94	2.46	7.42	12.57	18.47	3.33	10.19	7.27	3.80	72.05
.2			.01	.76	1.99	2.18	2.32	7.02	11.94	17.49	3.27	10.01	7.17	3.78	68.37
.3				.56	1.45	1.54	2.17	6.59	11.24	16.44	3.19	9.81	7.11	3.75	63.85
.4				.38	0.99	1.03	2.02	6.13	10.48	15.30	3.12	9.59	7.00	3.73	59.76
.5				.25	.63	0.65	1.85	5.63	9.64	14.09	3.03	9.36	6.91	3.70	55.72
.6				.15	.37	.38	1.66	5.08	8.72	12.81	2.93	9.09	6.79	3.67	51.63
.7				.08	.20	.21	1.46	4.47	7.71	11.49	2.83	8.81	6.68	3.63	47.54
.8				.04	.09	.10	1.24	3.81	6.65	10.14	2.71	8.48	6.53	3.59	43.38
.9				.02	.04	.04	1.01	3.13	5.56	8.79	2.58	8.15	6.39	3.55	39.25
6.0				.01	.01	.02	0.78	2.46	4.48	7.47	2.45	7.77	6.22	3.51	35.17
.1							.57	1.83	3.47	6.22	2.31	7.38	6.06	3.45	31.30
.2							.39	1.29	2.56	5.05	2.16	6.96	5.86	3.40	27.66
.3							.25	0.85	1.80	4.01	1.99	6.50	5.66	3.34	24.39
.4							.14	.52	1.20	3.09	1.81	6.00	5.42	3.27	21.45
.5							.08	.29	0.75	2.31	1.61	5.45	5.18	3.19	18.86
.6							.04	.15	.44	1.67	1.40	4.83	4.89	3.11	16.52
.7							.02	.07	.23	1.16	1.17	4.18	4.59	3.02	14.44
.8							.01	.03	.11	0.78	0.94	3.50	4.25	2.92	12.53
.9								.01	.05	.50	.71	2.82	3.89	2.82	10.80
7.0									.02	.31	.52	2.17	3.50	2.70	9.21
.1										.18	.35	1.59	3.11	2.57	7.81
.2										.10	.22	1.11	2.69	2.44	6.56
.3										.05	.13	0.73	2.30	2.29	5.50
.4										.02	.07	.44	1.92	2.12	4.58
.5										.01	.04	.25	1.56	1.94	3.80
.6											.02	.13	1.23	1.74	3.12
.7											.01	.07	0.94	1.53	2.55
.8												.03	.70	1.31	2.04
.9												.01	.50	1.09	1.60
8.0													.35	0.87	1.22
.1													.23	.68	0.90
.2													.14	.50	.64
.3													.08	.35	.43
.4													.05	.23	.28
.5													.02	.14	.16
.6													.01	.08	.09
.7														.04	.04
.8														.01	.01

TABLE V. *Values of ϵ, $\int_0^\infty P^2 dr$, and $2v_0$.*

	ϵ	$\int_0^\infty P^2 dr$	$-2v_0$
1s	4764	7.187×10^3	294
2s	773.5	67.90	74
2p	740.5	93.67	206
3s	175.4	269.6	26
3p	161.8	244.7	78
3d	135.5	851.4	129
4s	34.46	1.318×10^3	10.9
4p	28.30	2.711	32.4
4d	17.33	4.251	49.9
4f	3.378	4.422	57.2
5s	4.865	7.875	4.3
5p	3.125	19.10	11.7
5d	.4870	88.0	4.7
6s	.4293	113.3	1.2
Total			979

Hartree in his calculations for mercury.[8] Much further improvement in the results would require less efficient operation of the differential analyzer and some checking by hand calculations. In this work there has been no direct check of the machine integrations. The only checks are the interval consistency of different runs and the check of estimated and calculated values of Z

[8] Calculations of about the same accuracy have also been made for iron. Since applications to theories of ferromagnetism and atomic spectra require a higher degree of accuracy than the work for which the tungsten results are being used, the results for iron will not be published until their accuracy has been improved.

TABLE VI. *Values of 2Z.*

(p)	$(1s)$	$(2s)$	$(2p)$	$(3s)$	$(3p)$	$(3d)$	$(4s)$	$(4p)$	$(4d)$	$(4f)$	$(5s)$	$(5p)$	$(5d)$	$(6s)$
0.0	4.00	4.00	12.00	4.00	12.00	20.00	4.00	12.00	20.00	28.00	4.00	12.00	8.00	4.00
.4	4.00													
.8	3.98	4.00												
1.2	3.95	3.99												
.6	3.85	3.98		4.00										
2.0	3.61	3.96		3.99										
.2	3.40	3.94	12.00	3.99										
.4	3.10	3.91	11.99	3.98	12.00		4.00							
.6	2.71	3.88	11.97	3.98	11.99		3.99							
.8	2.24	3.85	11.92	3.97	11.98		3.99	12.00						
3.0	1.71	3.83	11.83	3.96	11.96		3.99	11.99						
.2	1.18	3.81	11.64	3.96	11.92	20.00	3.99	11.98						
.4	0.72	3.81	11.28	3.96	11.84	19.99	3.99	11.96				12.00		
.6	.37	3.79	10.65	3.96	11.71	19.98	3.99	11.93	20.00			11.99		
.8	.16	3.68	9.61	3.93	11.52	19.94	3.98	11.89	19.99			11.99		
4.0	.05	3.39	8.13	3.86	11.29	19.84	3.97	11.85	19.97		4.00	11.98		
.1	.02	3.15	7.12	3.82	11.18	19.74	3.96	11.83	19.95		3.99	11.98		
.2	.01	2.85	6.23	3.77	11.10	19.59	3.95	11.81	19.91		3.99	11.98		
.3		2.45	5.20	3.72	11.04	19.37	3.94	11.80	19.87		3.99	11.98		
.4		2.08	4.18	3.68	11.01	19.03	3.93	11.80	19.80	28.00	3.99	11.98	8.00	
.5		1.66	3.21	3.66	11.01	18.56	3.92	11.80	19.71	27.99	3.99	11.98	7.99	
.6		1.27	2.35	3.65	11.00	17.90	3.92	11.79	19.58	27.99	3.99	11.98	7.99	
.7		0.90	1.63	3.65	10.95	17.02	3.92	11.77	19.43	27.98	3.99	11.97	7.99	
.8		.60	1.05	3.63	10.79	15.90	3.92	11.72	19.25	27.96	3.99	11.96	7.99	
.9		.37	0.63	3.58	10.46	14.53	3.90	11.63	19.05	27.93	3.98	11.95	7.98	
5.0		.21	.35	3.46	9.87	12.93	3.86	11.50	18.86	27.87	3.98	11.93	7.98	
.1		.11	.18	3.23	9.00	11.11	3.80	11.33	18.68	27.78	3.97	11.91	7.98	
.2		.06	.08	2.88	7.86	9.19	3.74	11.16	18.56	27.63	3.96	11.89	7.97	
.3		.02	.03	2.44	6.52	7.27	3.67	11.01	18.49	27.40	3.95	11.87	7.97	
.4			.01	1.94	5.10	5.46	3.63	10.92	18.47	27.05	3.94	11.86	7.97	
.5				1.43	3.71	3.86	3.61	10.90	18.46	26.55	3.94	11.86	7.97	
.6				0.97	2.49	2.56	3.61	10.89	18.38	25.84	3.94	11.86	7.97	4.00
.7				.60	1.53	1.57	3.59	10.81	18.10	24.89	3.93	11.84	7.96	3.99
.8				.34	0.84	0.88	3.51	10.54	17.50	23.67	3.92	11.79	7.95	3.99
.9				.17	.41	.44	3.32	9.96	16.48	22.16	3.88	11.70	7.93	3.99
6.0				.07	.17	.20	3.00	9.02	15.01	20.38	3.83	11.58	7.91	3.99
.1				.02	.06	.07	2.54	7.74	13.12	18.35	3.77	11.44	7.88	3.99
.2				.01	.02	.02	2.01	6.23	10.93	16.16	3.73	11.35	7.85	3.98
.3							1.47	4.68	8.64	13.87	3.71	11.29	7.83	3.98
.4							0.98	3.25	6.45	11.39	3.71	11.27	7.82	3.98
.5							.60	2.08	4.52	9.39	3.70	11.27	7.82	3.98
.6							.33	1.22	2.96	7.37	3.65	11.18	7.82	3.98
.7							.16	0.65	1.80	5.57	3.50	10.92	7.80	3.96
.8							.07	.31	1.00	4.06	3.22	10.37	7.75	3.93
.9							.02	.14	0.49	2.83	2.83	9.51	7.64	3.92
7.0							.01	.05	.20	1.89	2.34	8.34	7.45	3.90
.1								.02	.08	1.19	1.81	6.94	7.16	3.88
.2									.02	0.72	1.31	5.45	6.76	3.87
.3										.41	0.87	4.02	6.15	3.87
.4										.22	.54	2.77	5.68	3.87
.5										.11	.31	1.77	5.02	3.85
.6										.04	.16	1.04	4.32	3.80
.7										.01	.08	0.56	3.60	3.70
.8											.03	.29	2.91	3.53
.9											.01	.13	2.26	3.28
8.0												.05	1.70	2.96
.1												.01	1.22	2.57
.2													0.84	2.13
.3													.55	1.69
.4													.34	1.27
.5													.19	0.90
.6													.10	.59
.7													.04	.36
.8													.02	.20
.9														.04
9.0														.01

for the inner electrons.

Tables of total $2Z_p$ and the values of ϵ, $\int_0^r P^2 dr$, and $2v_0$ are also given. The maximum discrepancy between final estimates and final values of the total $2Z_p$ does not exceed 0.10. The last figure of ϵ has significance only as indicating the resolving power of the method of computation. The last figure in the other quantities is also uncertain.

The authors wish to express their thanks to Professors J. C. Slater and P. M. Morse for many helpful suggestions, and to Mr. D. D. Terwilliger for his skillful operation of the differential analyzer.

LETTERS TO THE EDITOR

Prompt publication of brief reports of important discoveries in physics may be secured by addressing them to this department. Closing dates for this department are, for the first issue of the month, the twentieth of the preceding month; for the second issue, the fifth of the month. The Board of Editors does not hold itself responsible for the opinions expressed by the correspondents.

Communications should not in general exceed 600 words in length.

The Specific Ionization of Cosmic-Ray Particles as Determined by Geiger-Müller Counter Efficiency

The efficiency of a Geiger-Müller counter, used in a coincidence arrangement for cosmic-ray counting, is determined, at least in part, by the primary ionization along the path of the particles.

The results here reported seem to show that the efficiency is determined to such an extent by the primary ionization that measurements of the former may serve as a satisfactory means of determining the latter.

The points plotted in Fig. 1 show measured values of efficiency of air-filled and hydrogen-filled counters at different pressures of the counter gas. The smooth curves, however, are calculated on the basis of the indicated values of the primary specific ionization at N.T.P., 21 ion pairs per cm for air, and 6.2 for hydrogen.

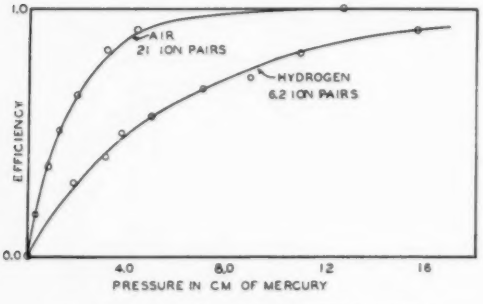

FIG. 1. Efficiency of counter as a function of pressure.

In these calculations we have assumed that (1) the presence of one ion pair is sufficient for the initiation of a discharge, and (2) that negligibly few entities capable of exciting a discharge are ejected by the ray from the inner surface of the counter cylinder. The efficiency is then obtained by subtracting from unity the probability that a particle will traverse the counter without suffering an ionizing collision with a gas molecule. This probability, calculated from the Poisson law of the random sequence, involves the primary ionization and the distribution of path length within the counter.

The fact that the observed points lie satisfactorily about the calculated curves constitutes, in itself, a tentative verification of the two above-mentioned assumptions. Assumption (2) concerning the absence of wall effect has been studied in an independent experiment in which it was found that increasing the path length augments the efficiency to about the same extent as does a proportionate increase in pressure. The path length distribution problem in this auxiliary experiment is, however, so complex, that an exact calculation has not, as yet, been carried out.

One notices that the value obtained for air (21 cm^{-1}) is lower than the cloud chamber results of G. L. Locher[1] and of C. D. Anderson[2] who counted droplets in diffuse tracks and obtained 36 cm^{-1} and 31 cm^{-1}, respectively. On the other hand, our value is somewhat higher than that found by P. Kunze[3] who examined sharp tracks and found 19 droplets per cm. Two circumstances which may render the cloud chamber data uncertain are the following: (1) Diffuse tracks, by including ions which have been produced by secondaries, tend to give too high a value. (2) Sharp tracks, on account of random grouping and coalescing of droplets, tend to give too low a value. Kunze, however, applied a statistical correction to take care of random grouping. Our value for air is slightly lower than that found by E. J. Williams and Terroux[4] for a million-volt beta-particle in oxygen. For hydrogen however, our value is somewhat higher than that given by these authors (5.1 cm^{-1}) for a million-volt beta-particle.

This method should be able to detect inhomogeneity of the radiation as regards specific ionization. Interpreted as homogeneous radiation, a distribution of specific ionization would, at low pressures, give an effective ionization equal to the average, but at high pressures the effective value would be less than the average. The present results show a rather surprising degree of homogeneity.

Counters operating at low efficiency form a means of discriminating between radiations of different primary ionizations. We have in progress an experiment designed to detect, by this means, the presence of low energy protons in the radiation—entities which should exist in measurable numbers if, as has been suggested by Compton and Bethe,[5] protons form an important component of the sea level radiation.

Measurements on different gases are now in progress in the hope that the results will be of use in the theoretical problem of ionization by high energy particles.

W. E. DANFORTH
W. E. RAMSEY

The Bartol Research Foundation of the Franklin Institute,
Swarthmore, Pennsylvania,
May 4, 1936.

[1] G. L. Locher, Phys. Rev. **39**, 883 (1932); J. Frank. Inst. **217**, 39 (1934).
[2] C. D. Anderson, Phys. Rev. **44**, 406 (1933).
[3] P. Kunze, Zeits. f. Physik **83**, 1 (1933).
[4] E. J. Williams and Terroux, Proc. Roy. Soc. **A126**, 289 (1930).
[5] A. H. Compton and H. A. Bethe, Nature **134**, 734 (1934).

Neutrons and Other Heavy Particles in Cosmic Radiation of the Stratosphere

Three sets of Imperial Process Plates, to which the technique of Blau[1] was adapted, were sent to the stratosphere inside the gondola of Explorer II, on the National Geographic Society—Army Air Corps flight of November 1935, to register the tracks of any heavy particles of either primary or secondary origin which may occur in the cosmic radiation of the upper atmosphere. 17 plates (1700 cm²), in a flat nitrogen-filled rubber bag, were covered with materials about 1 cm thick, representing 20 elements: H, Li, Be, B, C, N, O, F, Na, Mg, Al, Si, S, Cl, K, Ca, Br, Cd, I, and Pb. 15 plates (1800 cm²), without covering materials, were packed in two separate boxes of thin wood. These plates remained at 1/2 meter, water-equivalent, below the top of the atmosphere for about 2 hours.

Microscopic examination of 70 cm² of the emulsions under paraffin, aluminum, lead, carbon, and without covering, for α and H tracks at angles between 0° and 45° with the plane of the emulsion shows: (1) no α-particle tracks in plates not covered with materials, other than those tracks originating in radioactive contamination; (2) 4.5 ± 1 proton tracks per cm² in paraffin-covered plates, but only 0.8 ± 0.4 per cm² in emulsions covered with lead and with carbon, *so that these protons are evidently recoils from neutron collisions.* In addition, there is evidence that a small number of α-particles and possibly protons occur as secondaries in plates covered with aluminum.

The radioactive background of the room in which the plates were prepared and developed is low, as measured with an unshielded G–M counter.

All plates examined are compared with control plates of similar sensitive life, covered with the identical materials used with the stratosphere plates. The plates used as controls were originally prepared for the intended flight of July, 1935, and were later left on Pike's Peak (14,000 ft. elevation) for one month. The paraffin-covered plates from Pike's Peak show only 2 proton tracks in 6 cm² of emulsion, as compared with 27 on an equivalent area of stratosphere plates. Although the possibility of a terrestrial neutron source cannot be entirely eliminated, the foregoing constitutes good evidence that the neutron recoil tracks were produced in the stratosphere, and that the intensity of these neutrons at 6 meters of water below the top of the atmosphere is not more than 0.0005 times as great as at 1/2 meter.

Since the recoil tracks in the emulsion represent only a fraction of the total ranges of the protons, it is difficult to assign an average energy to the neutrons producing them. If one assumes neutrons of one energy uniformly distributed in angle, the number of proton recoils of maximum range R_0 having ranges between R and $R+dR$ is given by $dn=-A\,dR/R_0^{2/3}R^{1/3}$. Application of this formula to the distribution of lengths of proton tracks visible under paraffin, or to the relative numbers of proton tracks produced under paraffin and without paraffin, sets a rough lower limit of 6 MEV for the mean energy of the incident neutrons. To a rough approximation, the number of protons appearing below 1 cm of paraffin is proportional to the total energy of traversing neutrons. Hence, the direct energy in the primary cosmic radiation of this region of the stratosphere, attributable to neutrons, is calculated to be 1.2 MEV per cm² per sec. Although probable error cannot be computed, this value is believed to be in error by not more than a factor of 3. The maximum amount of *indirect* energy which could be released by atmospheric transformations would appear from a process similar to the hypothetical one: $N^{14}+n^1\rightarrow N^{15}+h\nu$, where $h\nu\sim9$ MEV. Consequently the maximum possible contribution of neutrons, by both direct and indirect processes, can be of little significance compared with the total cosmic-ray ionization, unless slow neutrons are present in much greater numbers than the distribution of lengths of observable proton recoil tracks indicates.

If these neutrons are primary constituents of cosmic radiation, as the present evidence indicates, the free neutron must be comparatively stable, despite its high mass.[2] Further, the presence of such neutrons suggests that the primary cosmic radiation has been associated with considerable quantities of matter, and should contain considerable gamma-radiation.

The suggestion that primary cosmic radiation at high altitudes contains a strong component of α-particles whose effects are conspicuous at about 1 meter of water,[3] is inconsistent with our observations. From the counting rates obtained with coincidence counter telescopes during the same flight in which the plates were carried aloft,[4] it is calculated that 2×10^5 primary α-particles would have traversed the emulsion examined, if 1/3 of the counter discharges were produced by α-particles. On the assumption that the apparent absorption coefficient for such α-particles is 0.6 per meter of water, and that the plates record α-particles whose energies have been reduced to 100 MEV or less, at least 200 of these particles should have produced observable tracks, whereas none were found. This result is not in conflict with that recently reported by Wilkins and St. Helens,[5] since their tracks are all nearly parallel and came from the horizontal direction; this almost certainly excludes the possibility that their tracks were produced by primary particles. Moreover, the absence of observable primary α-particles cannot be explained by their disappearance through nuclear collisions, since, for a nuclear cross section of 10^{-25} cm², 0.67 of all α-particles suffer no nuclear collisions in passing through 1 meter of water-equivalent of atmosphere. The nuclear cross section for α-particles of energies equal to the potential barrier of nitrogen is 10^{-25} cm² or less, and varies inversely as the velocity for α-particles of greater energies, so most of the suggested primary α-particles[3] would have retained their identity to the end of their range.

L. H. Rumbaugh
G. L. Locher

Bartol Research Foundation of the Franklin Institute,
Swarthmore, Pennsylvania,
May 14, 1936.

[1] M. Blau, J. de phys. et rad. (VII) **5**, 49 (1934); M. Blau and H. Wambacher, Akad. Wiss. Wien, Ber. **134**, 285 (1934).
[2] M. L. Oliphant, Nature **137**, 396 (1936).
[3] A. H. Compton, Rev. Sci. Inst. **7**, 71 (1936).
[4] W. F. G. Swann, G. L. Locher and W. E. Danforth, reported by W. F. G. Swann at the Washington meeting, Am. Phys. Soc., May 1936; Phys. Rev. **49**, 890A (1936).
[5] T. R. Wilkins and H. St. Helens, Phys. Rev. **49**, 403 (1936).

Weather Changes as Indicated by Variations in the Earth's Magnetic Field

In 1927 this department began a series of studies on the astonishing electrical effects that accompany sandstorms in West Texas. The question naturally arose: "Do these sandstorms give rise to, or are they accompanied by, magnetic effects?" In 1932 we constructed a laboratory of non-magnetic materials at a distance of 210 yards from the nearest building, power line, or pipe line; and installed a horizontal Askania magnetometer.

During the winter of 1933–34 J. Preston Conner, one of our graduate students, took some preliminary readings. He read a paper on this subject at the Lubbock meeting of the Southwestern Division of the A. A. A. S. on April 30, 1934. During the summer of 1934 Kimsey Miller made a series of observations in connection with his master's thesis. From October 3, 1935 to May 9, 1936, readings have been taken from three to six times per day with the exception of two periods of two weeks each, and excepting about one-half of the Sundays. Some results of these readings were given in a paper read by Florence Robertson at the Flagstaff meeting of the S. W. Division of the A. A. A. S. on April 28, 1936.

At a meeting of the A. A. A. S., Southwestern Division, Technical section, at Albuquerque in 1930, Mr. Harry A. Aurand read a paper on the relation between variations in the magnetometer readings and changes in the weather. Apparently this paper was not published, and was entirely unknown to the authors until our work was well under way.

Before discussing our results it should be stated that at Lubbock, Texas, the average annual rainfall is 18.6 inches. Most of this comes in the summer and early fall. During November, December, and a good part of January the weather is apt to be fair; a part of this time ideal. During February, March and April sand storms are of frequent occurrence.

As a result of our observations we have arrived at the following conclusions which seem to verify those of Mr. Aurand, and go somewhat beyond them:

(1) In about 95 percent of the cases observed a high magnetometer is followed by bad weather (rain, snow, sleet, hail, thunder, lightning, sandstorms, dust storms, violent winds, cold waves, etc.). In the majority of cases the rise in the magnetometer came about a day in advance of the adverse weather change.

(2) In about 57 percent of the cases observed a low barometer is followed by bad weather. The falling barometer, when it occurred, preceded the bad weather by a much shorter interval of time than the high magnetometer.

(3) It would thus appear, that insofar as West Texas is concerned, the magnetometer is a very much better indicator of bad weather than the barometer.

In addition to the above we have noted the following:

(4) At Lubbock, Texas, the diurnal variation in the horizontal component of the earth's magnetic field is almost the reverse of that found at various observatories in the northern hemisphere.

(5) There are some indications that exceptionally low magnetometer readings accompanied earthquakes in various parts of the earth, particularly those in Montana in the fall of 1935.

Texas Technological College,
Department of Physics,
Lubbock, Texas,
May 9, 1936.

E. F. George
Florence Robertson

Evidence for the Existence of Na^{22}

Sodium is generally considered to be a simple element of mass number 23. The best test of its simplicity has been made by Bainbridge[1] who found that the mass numbers 21 and 25 could not be present to the extent of 1 in 3000 and 22 to the extent of 1 in 800.

Recent mass spectra obtained in this laboratory show a small peak in the 22 position. Representative results are illustrated in Fig. 1.

The peak observed at 22 is proportional to Na^{23}, the abundance ratio being close to $Na^{23}/Na^{22}=5000\pm500$. No peaks were in evidence at 20, 21, 24, and 25, the sensitivity being about 1 in 50,000.

The technique was essentially the same as that employed in the detection of Li^6.[2] The ion source in these experiments was a platinum disk which had been impregnated with sodium by heating in contact with Na_3PO_4. All adhering salt was carefully scraped from the disk before installing in the spectrograph. In the detection of faint peaks of this type it is essential that the disk be smooth and that the slits be free from tarnish since both of these tend to broaden the peaks and increase the background.

It seems probable that the observed peak at mass 22 is due to Na^{22} since it was proportional to Na^{23} and since calcium was completely absent, thus precluding the possibility of the peak being due to doubly charged Ca^{44}. The only peaks observed other than those at 22 and 23 were those due to potassium; the magnitude of the 22 peak, however, showed no relationship to the potassium current.

A similar test was made on caesium but no new isotopes were observed. In the case of rubidium no evidence was obtained for the existence of Rb^{86}; this confirms the results recently obtained by Nier.[3]

A. Keith Brewer

Bureau of Chemistry and Soils,
U. S. Department of Agriculture,
Washington, D. C.,
May 11, 1936.

[1] K. T. Bainbridge, J. Frank. Inst. **212**, 317 (1931).
[2] A. Keith Brewer, Phys. Rev. **49**, 635 (1936).
[3] A. O. Nier, Phys. Rev. **49**, 272 (1936).

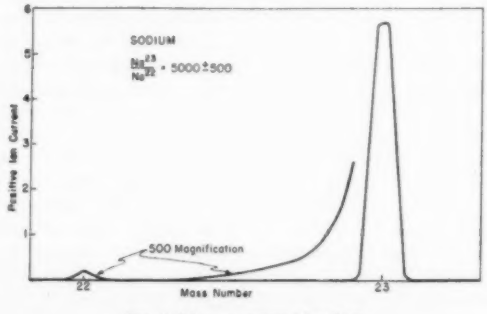

Fig. 1. Mass spectrum of sodium.

The Accuracy of Least-Squares Solutions

In a paper ". . . Parameters Estimated by Least Squares," Dr. Deming claimed[1] that I had discussed[2] my P, related to his P_z, as though it were his P_w. May I explain that there was no confusion of P with P_w, but that I was merely following a certain one of three common and distinct definitions of "probable error" that had been in use before the time of my paper, and giving to that definition a greater precision.

How should one think of the accuracy of estimates, found by least squares, of the unknowns, when σ is not known? In the many applications of least squares with which I am familiar, σ is never known. At times one may have some prior knowledge of σ, obtained from similar runs, or from remeasures of the observational quantities in my equations of condition (1). My analysis is then not at once applicable, but such prior knowledge never furnishes values of σ, but merely estimates s' of σ obtained from various numbers of degrees of freedom. Such prior knowledge can, and should, be incorporated in my Eqs. (1), by pooling all the existing equations of condition, and even if necessary at the expense of increasing the number of unknowns. That done, my analysis is applicable.

The first common meaning of probable error related to the quantity $0.6745\cdots\sigma/w_x^{\frac{1}{2}}$. But in practical cases that quantity cannot be found, because σ cannot be found. My Eq. (9) gives the chance, $p(t)dt$, that the error ϵ of any least-squares value x' lies between $ts'/w_x^{\frac{1}{2}}$ and $(t+dt)s'/w_x^{\frac{1}{2}}$. The factor $s'/w_x^{\frac{1}{2}}$ is the classical expression for the "mean," or "standard" error of x'. It is an estimate, obtained from $n-m$ degrees of freedom, of the unknown quantity $\sigma/w_x^{\frac{1}{2}}$. Let t_p be the value of t for which $P(t)$ is three-fourths. Then the chance that ϵ exceeds $t_p s'/w_x^{\frac{1}{2}}$ numerically is exactly one-half. Instead of adopting the first meaning of probable error, relating to an unknowable quantity, I chose to apply the phrase to the quantity $t_p s'/w_x^{\frac{1}{2}}$, the chance of an error exceeding which, numerically, in any one least-squares solution, has been seen to be one-half. The quantity can be easily computed by multiplying the value of $s'/w_x^{\frac{1}{2}}$, found in the course of the least-squares solution, by the 75 percent value of t found from Student's *Tables*.[3] The course I followed eliminated from the results all reference to the unknown and unknowable σ, and expressed them in terms of the known s'.

The second common meaning of probable error related to the quantity $0.6745\cdots s'/w_x^{\frac{1}{2}}$, usually published after a least-squares value as its "probable error." This quantity is only an estimate, subject to known statistical fluctuations from sample to sample, and obtained from $n-m$ degrees of freedom, of the probable error in the first meaning. To distinguish between them, it would be perhaps well always to refer to the second "probable error" as an "estimated" probable error. If $n-m$ is finite, the chance of an error numerically greater than the estimated probable error exceeds one-half, and equals 0.62 when $n-m$ is unity.

In the third sense, "probable error" related to the error is likely as not to be numerically exceeded. My course preserved this third meaning of "probable error," as the error, in any *single* least-squares solution, the chance of exceeding which is one-half.[4]

Should Dr. Deming wish to continue to use "probable error" in the sense of the unknowable $0.6745\cdots\sigma/w_x^{\frac{1}{2}}$, he is, of course, at complete liberty to do so, but then his use of the term "probable error" is to be distinguished clearly from mine. Dr. Deming cannot bring any fundamental criticism to bear against the theory given in reference 2 merely by adopting, as apparently he does, a different definition of "probable error" from mine. Any dispute would be about a mere matter of a choice of words, and an argument would hardly be profitable.

T. E. STERNE

The Harvard College Observatory,
April 4, 1936.

[1] W. E. Deming, Phys. Rev. **49**, 243 (1936). The reference is to the third paragraph from the end.
[2] T. E. Sterne, Proc. Nat. Acad. Sci. **20**, 565 (1934).
[3] "Student," Metron. **5**, 105 (1925).
[4] In the simple case of two observations of one unknown, for example, my "probable error" is half the separation. This is seen without analysis, for the chance that either observation is too small and the other too large is, with symmetrical parent errors, one-half. Hence the probability is one-half that the unknown lies somewhere between the two observations, as could be seen likewise from the function $p(t)$.

Dr. Sterne has called attention to the fact that my P_z is not numerically his P, but is twice the complement of his P. The slip came about from the fact that I prefer to work with the region of the ϵ, s plane *external* to the z contours (see the figure in my article just cited in Sterne's footnote 1), so that a low value of P_z corresponds to a doubtful hypothesis; and I inadvertently supposed that Sterne had made the same choice.

The probable error of a mean or of any other parameter is that *constant* quantity (constant in the sense of being dependent only on the weight w_s, not on s) for which the odds are 1 : 1 that it exceeds the error in the estimate obtained from any one experiment (sample; set of points). This constant quantity is the constant separation of the *vertical* u contours in the figure aforementioned. I regard as irrelevant the fact that this constant separation cannot be computed without knowledge of σ; it is in any case a concept indispensable for a discussion of test regions, as is evident from a study of Neyman and Pearson's[1] paper of 1928.

Odds can also be laid between the error in an estimated parameter and various *fluctuating* magnitudes, as Sterne says. One of them is the quantity that Sterne designates as $t_p s'/w_x^{\frac{1}{2}}$, and which Deming and Birge[2] designated by ζs. I refer the reader to Fig. 11, p. 141, of the Deming-Birge article for an illustration of the various possibilities. I deplore any deliberate attempt to fuse the fluctuating $t_p s'/w_x^{\frac{1}{2}}$ (or ζs) with "probable error" or estimates of it.

Sterne's P and my P_z are defined by the *diverging* V-shaped z (or t) contours; hence they deal with the *ratio* ϵ/s and not with the numerator alone. It is this that I tried to emphasize in the paragraph cited by Sterne. It is a fact, nevertheless, that in the absence of σ there is no better test region than that defined by the z (or t) contours. But the test is on ϵ/s, and not on ϵ alone; both numerator and denominator are subject to the fluctuations of samplying.

Dr. Sterne urges me to point out that on the last page of my article there should have been some qualification to the statement that the classical procedure of using an estimated σ gives numerical results in the normal integral not essentially different from P_s. The situation might appear otherwise at low odds and few degrees of freedom (k, or $n-m$); thus, with $k=3$, suppose $P_s=0.1$; then the ratio of the error to the *estimated* S. D. is 2.353, and the normal integral with the estimated σ turns out to be 0.019 —only one-fifth the size of P_s. Discrepancies even more glaring could be discovered, but always at low odds and few degrees of freedom. However, my own feeling is, as it was when I wrote the paper, that it is rash to differentiate between odds such as this when the number of degrees of freedom is so small, because of the serious fluctuations to be expected in s, and hence also in P. However, I can readily understand that Dr. Sterne might think differently, and I am glad for this opportunity of explanation.

W. EDWARDS DEMING

Bureau of Chemistry and Soils,
U. S. Department of Agriculture,
Washington, D. C.,
April 10, 1936.

[1] J. Neyman and E. S. Pearson, Biometrika **20a**, 263 (1928); Proc. Camb. Phil. Soc. **29**, 492 (1933); Phil. Trans. Roy. Soc. **A231**, 289 (1933).
[2] W. Edwards Deming and Raymond T. Birge, Rev. Mod. Phys. **6**, 119 (1934).

The Structures of Light Nuclei and the Existence of $_4Be^8$

The existence of $_4Be^8$ as a disintegration product appears to have been postulated for the following reactions:

$$_3Li^7+{}_1H^1\rightarrow{}_4Be^8+\gamma, \quad (1)$$

$$_4Be^9+\gamma \rightarrow{}_4Be^8+{}_0n^1, \quad (2)$$

$$_3Li^7+{}_1H^2\rightarrow{}_4Be^8+{}_0n^1, \quad (3)$$

$$_5B^{10}+{}_1H^2\rightarrow{}_4Be^8+{}_2He^4, \quad (4)$$

$$_5B^{11}+{}_1H^1\rightarrow{}_4Be^8+{}_2He^4. \quad (5)$$

The recent results of Neuert[1] and of Dee and Gilbert[2] on (5) and of Cockcroft and Lewis[3] on (4) suggest a mechanism with which it appears feasible to dispense with $_4Be^8$ as a stable nucleus. In each case two roughly homogeneous groups of α-particles are found, one of which can be attributed to $_2He^4$ recoiling against $_4Be^8$. For (5) Dee and Gilbert suggest that the second, more predominant group, may be due to $_2He^4$ recoiling against an excited $_4Be^8$, the energy of excitation being about 3 MEV. In view of the low mass defect of $_4Be^8$ against two α-particles this is not easy to understand.

Alternatively we may suppose that the nucleus is a structure composed of internal groups, or "sub-nuclei," and that, like a complex molecule, it resonates among the various forms which may be assumed for it. Lacking better information we may suppose the *a priori* probability to be greatest for those groupings giving the lowest binding energies.

On this basis we find the following probable structures for $_5B^{10}$ and $_5B^{11}$:

$_5B^{10}$: (a) $[_3Li^6+{}_2He^4(4.2)]$; (b) $[_2He^4+{}_1H^2+{}_2He^4(6.0)]$

$_5B^{11}$: (a) $[_3Li^7+{}_2He^4(8.5)]$; (b) $[_2He^4+{}_1H^3+{}_2He^4(11.3)]$; (c) $[_5B^{10}+{}_0n^1(11.5)]$.

The numbers in ( ) give the binding energies in MEV. Clearly by this procedure the most probable structures correspond to small numbers of "particles." If we think of the 3-particle structures as linear, we can propose the following mechanism:

$_5B^{10}+{}_1H^2$: (4a) "capture" of $_1H^2$ by $_3Li^6$ gives α recoiling against 2α.

(4b) "capture" of $_1H^2$ by $_1H^2$ gives 2α with high energies and one with zero or small energy.

$_5B^{11}+{}_1H^1$: (5a) "capture" of $_1H^1$ by $_3Li^7$ gives α recoiling against 2α.

(5b) "capture" of $_1H^1$ by $_1H^3$ gives 2α with high energies and one with zero or small energy.

In each case we thus expect two homogeneous groups of α-particles one with 0.67 and the other with about 0.5 of the total energy release. For reaction (5) this mechanism appears to explain the energies of the two groups about as satisfactorily as does the hypothesis of Dee and Gilbert, the total energy release being about 8.7 MEV, the ratios for the two groups being about 0.67 and 0.45 of this value. For (4) the energy release is about 17.5 MEV, the observed fractions for the two groups about 0.68 and 0.57, respectively. The latter value is too high and might be attributed to some error in the determination of the energy release or to a tendency of two α-particles to go off together in process (4b). The hypothesis of Dee and Gilbert seems to work a little better here as it predicts a ratio of 0.55. Reactions (1) and (2) do not appear to demand the existence of $_4Be^8$, while little can be said definitely about (3) because of the difficulty of studying the neutrons.

It can be seen from the energy-momentum relations that the faster α-particles from a reaction such as (5a) should be rather more homogeneous than those from the alternative (5b) as is observed. It is also to be expected that the disintegration may occur in a more or less symmetrical manner, giving a continuous background. Lastly we must emphasize that a division into structures such as is here proposed should not be taken too literally, but only as representing *average* or *preferred* combinations of the nuclear groups. In this sense it does not seem to be out of line with established theories. We can only say for the moment that this seems to provide a possibility for reconciling the disintegration experiments with the lack of direct evidence for a real nucleus $_4Be^8$.

WILLIAM H. WELLS
E. L. HILL

University of Minnesota,
May 12, 1936.

[1] H. Neuert, Physik. Zeits. **36**, 629 (1935).
[2] P. I. Dee and C. W. Gilbert, Proc. Roy. Soc. **A154**, 279 (1936).
[3] J. D. Cockcroft and W. B. Lewis, Proc. Roy. Soc. **A154**, 246 (1936).

Proceedings of the American Physical Society

Minutes of the Washington Meeting, April 30–May 2, 1936

THE 205th regular meeting of the American Physical Society was held in Washington, D. C. at the National Bureau of Standards on Thursday and Friday, April 30 and May 1, and at the National Academy of Sciences and the American Pharmaceutical Association on Saturday, May 2, 1936. There were three parallel sessions for the reading of ten-minute contributed papers on Thursday morning and afternoon, Friday morning, and Saturday morning and afternoon. The presiding officers were F. K. Richtmyer, President of the Society, H. M. Randall, Vice President, F. C. Blake, T. B. Brown, H. L. Curtis, W. P. Davey, J. H. Dellinger, H. G. Dorsey, W. J. Humphreys, E. Karrer, L. W. McKeehan, A. G. Shenstone, and H. W. Webb. The attendance at the meeting was not less than five hundred.

On Thursday evening in the Auditorium of the National Museum there was a joint session with the Institute of Radio Engineers. The speakers at this meeting were V. K. Zworykin of the RCA Manufacturing Company who spoke on *Applied Electron Optics*, and G. C. Southworth of the Bell Telephone Laboratories, Inc. who spoke on *Hyperfrequency Transmission Through Wave Guides*. J. H. Dellinger of the National Bureau of Standards presided at this session.

A symposium of invited papers on *The Scientific Results of the 1935 Stratosphere Flight under the Auspices of the National Geographic Society and the U. S. Army Air Corps* was presented on Friday afternoon. The presiding officer at this meeting was Lyman J. Briggs of the National Bureau of Standards. The program of invited papers was as follows:

1. **The Balloon as a Flying Laboratory.** Captain A. W. Stevens, *U. S. Army Air Corps.*
2. **Stratosphere Altitude, Barometric and Photogrammetric.** W. G. Brombacher, *National Bureau of Standards.*
3. **Cosmic-Ray Measurements.** W. F. G. Swann, *Bartol Research Foundation of the Franklin Institute.*
4. **Electric Conductivity of the Troposphere and the Stratosphere.** O. H. Gish, *Department of Terrestrial Magnetism, Carnegie Institution of Washington.*
5. **High Energy Cosmic-Ray Tracks.** T. R. Wilkins, *University of Rochester.*
6. **Distribution of Ozone from Spectrographic Measurements.** Brian O'Brien, *University of Rochester*, and F. L. Mohler, *National Bureau of Standards.*
7. **Composition of the Stratosphere.** Martin Shepherd, *National Bureau of Standards.*
8. **Strength and Performance of Stratosphere Balloons.** L. B. Tuckerman, *National Bureau of Standards.*

On Friday evening the Society held its dinner at the Raleigh Hotel. President F. K. Richtmyer presided and called upon Harold C. Urey who spoke on the relation of physics and chemistry. He then called upon Captain Williams who told of the meteorological work that had to be done in selecting "the perfect day" for the stratosphere flight. There were two hundred and seventy-three guests present.

Meeting of the Council. At its meeting held on Thursday, April 30, 1936, the death of one member (George Rosengarten) was reported. Two candidates were transferred from membership to fellowship and twenty-five candidates were elected to membership. *Transferred from membership to fellowship:* Dunham Jackson and Ernest J. Jones. *Elected to membership:* Edoardo Amaldi, H. Anjour, Robert A. Becker, Henry J. Bolger, Robert W. Cairns, David W. Carpenter, Don Cornish, Samuel C. Coronite, Irving Emin, Albert C. Erikson, T. R. Folsom, G. Herzog, Hiromi Imahori, Frederick L. Knowles, David G. C. Luck, Raymond D. Mindlin, Charles E. Mongan, Jr., Howard I. Oshry, Melba Phillips, Fred T. Rogers, Jr., L. H. Rumbaugh, E. Neil Shawhan, Robert L. Thornton, Gladys White, and E. G. Witting.

The regular scientific program of the Society consisted of one hundred and sixty-two contributed papers of which numbers 11, 14, 15, 48, 52, 67, 157, 158, and 162 were read by title. The abstracts of these papers are given in the following pages. An *Author Index* will be found at the end.

W. L. Severinghaus, *Secretary*

Abstracts

1. Excess Energy Electrons in High Vacuum Tubes. E. G. Linder, *RCA Manufacturing Co. Inc., Camden, N. J.*—Data have been obtained showing the existence, in certain types of high vacuum tubes, of electrons which are able to pass to an electrode having a more negative potential than the cathode from which they originate. The tubes used had a cylindrical plate with a concentric tungsten wire cathode, and a probe electrode either in the form of a wire positioned near and parallel to the cathode, or in the form of a disk near the end of the plate. A magnetic field was applied parallel to the filament. Excess energy electrons appeared when the magnetic field strength exceeded the cut-off value so that electrons were unable to reach the plate. Probe measurements indicate that the energy distribution is nearly Maxwellian. The average energy increases with plate potential over a large part of the region investigated. As the magnetic field is increased, the excess energy electron current rises to a maximum, then drops off. With a plate voltage of 1000, electrons have been collected by probes 200 volts negative with respect to the filament. The presence of gas, or the existence of oscillations, does not seem to be necessary. Possible explanations will be discussed.

2. A Photographic Study of Lightning. L. B. Snoddy, E. J. Workman and J. W. Beams, *University of New Mexico and University of Virginia.*—A photographic investigation of lightning flashes near Albuquerque, New Mexico (altitude 5000 to 6000 ft.), has been made. The pictures were taken with three separate cameras, the first with photographic film stationary, the second with film moving 80 cm/sec., and the third with film moving 850 cm/sec. In one picture four flashes were obtained approximately 0.01 sec. apart, each progressively lengthening the same path. The first flash reached 0.5, the second 0.6, the third 0.7 of the distance from cloud to ground. The fourth flash was the first to extend all the way from cloud to ground. This main flash was followed by four others at varying intervals. Photographs of flashes similar to those previously reported by Schönland and others were obtained in which the "leader" proceeded from cloud to ground, immediately followed by the "main" flash traversing the same path but from ground to cloud. Two intense flashes taken during unusual atmospheric conditions showed no observable "leaders."

3. Investigations of Vacuum Sparks by Means of a High Speed Rotating Mirror. J. A. Chiles, Jr., *University of Virginia.*—Investigations of vacuum sparks between electrodes of aluminum, bismuth, cadmium, copper, graphite, lead, magnesium, palladium, tin, tungsten, and zinc were carried out by means of a camera and a high speed rotating mirror. In the case of tungsten and palladium photographs were taken both before and after outgassing the electrodes. The images of the sparks were swept across the plate at a speed of about 1.5×10^6 cm/sec. It was found that in each vacuum discharge the anode became luminous before the cathode, except in a few rare cases where very faint spots of luminosity were observed on the tip of the cathode before the initiation of the main discharge. The emission of x-rays from the spark was studied with a pinhole camera. The results support the conclusion that the discharge in high vacuum between cold electrodes is initiated by field electron emission from the cathode.

4. Ionization of Liquid CS_2 by X-Rays. Lauriston S. Taylor, *National Bureau of Standards.*—Continuing studies already reported,[1] measurements of the ionization produced in CS_2 by 160 kv (eff.). X-rays have been made with the view of avoiding the effects of space charge or barrier potential previously encountered. This space charge was such as to reduce the effective voltage across the cell to about 60 percent of the applied value. Applying a variable frequency variable amplitude square wave voltage to give field strengths up to 80 kv/cm, ionization measurements were made at various intervals, from 0.002 to 2 sec. after applying the voltage. Much larger ionization currents resulted at the shorter intervals, before the barrier potential became large enough to be effective. At longer intervals the currents agreed with those previously found for static conditions. An apparent "fatigue" of the cells used under static conditions is absent when the voltage is applied for only short intervals. Under some conditions there appears to be a unipolar conductivity of the cell when applying fluctuating voltages. Calculated values of the saturation current are the same regardless of the cell polarity.

[1] F. L. Mohler and L. S. Taylor, Phys. Rev. **45**, 762 (1934); **47**, 805 (1935).

5. Negative Ions in Oxygen and Hydrogen. Overton Luhr and Charles T. Male, Jr., *Union College.*—Preliminary results are presented on experiments in O_2, H_2 and H_2-O_2 mixtures which were designed to determine the nature of negative ions formed by electron attachment with subsequent aging in these gases. Nernst glowers were found to serve as satisfactory emitters of electrons in O_2 at any pressure, as they are not poisoned like other oxide emitters. Emission currents of about 15 milliamperes were easily obtained from a Nernst glower rated at 0.4 ampere when the heating current was raised to 0.65 ampere. This procedure did not harm the glower over long periods of operation. Only newly formed ions have been investigated so far with the mass spectrograph, but a wide variety have been found, ranging from H^- to complex ions of molecular weight over 100 in H_2. The heavier ions were presumably due to impurities such as water vapor in the H_2. In relatively pure oxygen, four intense peaks appeared, due apparently to O^-, $H_2O_2^-$, O_3^- and O_4^-. The O_2^- ion seemed to appear principally in H_2-O_2 mixtures. The identity of these ions is yet to be definitely checked by careful calibration of the mass spectrograph. Ions of similar nature have been found in the plasma of a glow discharge.

6. A Characteristic of the Copper Arc During the Formative Period. Paul L. Betz and S. Karrer, *Consolidated Gas, Electric Light & Power Company of Baltimore.*—This paper gives the results of an investigation of the voltage

characteristic of the copper arc in air during the process of arc formation. A pair of copper electrodes, initially in contact and carrying current, were separated and the voltage arising across the arc gap was studied. At the instant of electrode separation there developed across the gap a voltage of about 12.2 volts. This value was attained in less than 10^{-8} second. These data were obtained by means of a cathode-ray oscillograph. The rapidly developed voltage was found to be independent of arc current for current values up to 100 amperes, which suggests that the rapidly developed initial voltage corresponds to the cathode fall of the arc. The initial voltage appears to be a prerequisite to the subsequent development of the usual arc characteristics, i.e., dependence of arc voltage upon arc current, arc length, etc.

7. Forces at the Cathode of a Copper Arc. R. M. ROBERTSON, *Massachusetts Institute of Technology.*—Experiments to investigate mechanical forces at a copper arc cathode were undertaken with the object of studying the effects observed by Tanberg[1] in the vacuum arc and by Duffield, Burnham and Davis[2] in the arc in air. Force measurements were taken at various pressures of hydrogen and nitrogen. The cathode was the bob of a pendulum suspended in a tank which could be evacuated to about 10^{-6} mm of mercury. The deflection was measured by means of a mirror and scale and the force was thus determined. Corrections were made for electromagnetic interactions. Convection produced a force tending to bring the electrodes together, which was apparent in nitrogen but not in hydrogen. The measurements revealed a force increasing rapidly with current and increasing with decreasing pressure. These forces were found to be larger for hydrogen than for nitrogen and in the pressure range studied were of the same order of magnitude as those detected by Duffield, Burnham and Davis, ranging from 7 dynes at 50 cm to 17 dynes at 2 cm in nitrogen for a current of 15 amperes. The experimental arrangement permitted much greater accuracy in the measurement of cathode forces than has been previously reported.

[1] Tanberg, Phys. Rev. **35**, 1080 (1930).
[2] Duffield, Burnham and Davis, Proc. Roy. Soc. **A97**, 326 (1920).

8. Theory of the Positive Column of an Arc in Nitrogen at Atmospheric Pressure. E. S. LAMAR, *Massachusetts Institute of Technology.*—A consideration of the energy losses from the positive column shows that thermal conduction and the radial diffusion of atoms out of the arc column account for all but a few percent of the energy generated. If one assumes thermal ionization in accordance with the Saha equation, one can set up an energy balance. The numerical integration of the resulting differential equation determines the radial temperature distribution in terms of the temperature at the center of the column. In the differential equation a change of variable is made from the radius r to a variable $x=Er$ where E is the potential gradient. E appears, therefore, simply as a scale factor for the current, the relationship between current and gradient being of the form $E=C/i$. The integration is carried out for a number of different center temperatures. The arc is believed to operate with that center temperature which makes the constant C, and thus the energy dissipation, a minimum. Thus, with the introduction of no arbitrary constants, it has been possible to determine a center temperature of about 6000°K and a value of C well within reason. The effects of small concentrations of materials having ionization potentials less than that of nitrogen have been considered.

9. The Energy Distribution of Electrons in an Electric Field in a Gaseous Column. HARRY C. KELLY, *Massachusetts Institute of Technology.* (*Introduced by Philip M. Morse.*)—An investigation was made to determine the influence on the distribution function of energy losses due to elastic and inelastic impacts with atoms of helium. The experimental tube consisted of two circular plates between which the field was applied enclosed by a cylindrical container kept midway in potential between the accelerating plates. Electrons from a tungsten filament enter the enclosure through a grid in the first circular plate and a sample of these electrons leaves the enclosure through a grid in the second plate. Electrons were put into the cylindrical container with an average energy calculated from the Morse-Allis-Lamar distribution function.[1] The distribution was determined by measuring the current to a retarding plate placed beyond the second grid. By varying the helium pressure, tests were made to show that sufficient collisions were made to set up a distribution. The Morse-Allis-Lamar and Maxwell's distributions were integrated to compare with the observed probe current *vs.* probe voltage curves. With values of $E/P=5$, 10, 15 volts/cm mm excellent agreement was found with the Morse-Allis-Lamar distribution and a definite departure from the Maxwellian. With $E/P>20$ volts/cm mm where excitation and ionization set in a marked decrease in the number of high energy electrons was observed with discontinuities at the excitation voltages.

[1] Morse, Allis and Lamar, Phys. Rev. **48**, 412 (1935).

10. The Technique of Producing Low Pressure High Frequency Electrical Discharges Due to a Solenoid Immersed in the Gas Under Examination. OTTO STUHLMAN, JR., *The University of North Carolina at Chapel Hill.*—Continuous wave excitation was employed using a balanced push-pull vacuum-tube circuit. Frequency range 1500 to 6000 kc/sec. The solenoid was constructed of 3/16-inch glass tubing with 1/16-inch bore, filled with mercury, loosely wound and fused into cylindrical or spherical glass containers. Internal diameter of solenoid about half the diameter of container. This solenoid, immersed in the gas under spectroscopic examination, formed the plate inductance in the P. P. circuit. Upon reducing the pressure of the gas, the discharge struck at the high potential end of the solenoid and spread along the coil as the pressure was decreased or the potential increased. Standing waves can be identified by the presence of luminous loops along the solenoid. The intensity and character of the discharge can be controlled, along the axis of the solenoid, by changes in pressure of the gas and changes in current, frequency and inductance. Characteristic discharges will be illustrated by photographs.

11. Filtration of Elastic Waves in Solid Rods with Membranes as Side Branches.* R. B. LINDSAY AND T. G. BARNES, *Brown University.*—This paper considers theoretically the propagation of compressional and torsional waves in solid rods having membranes as side branches. An infinite cylindrical rod is loaded at equal intervals with flexible circular membranes attached at their outer edges to the inside of a circular cylinder. The assumption that longitudinal waves in the rod set up symmetrical transverse waves in the membranes leads to the conclusion that the structure is a *high-pass* compressional wave filter. The limiting case of an infinitely rigid membrane is also investigated. There is next considered the case of torsional waves in the rod giving rise to radial torsional waves in the attached membranes which now may be treated either as flexible or rigid diaphragms. When the latter are rigidly clamped at their outer edges, the structure is found to be a *high-pass* torsional wave filter. When the diaphragms are free at the outer edges, a *low-pass* filter results.

* To be read by title.

12. An Optical Stethograph. J. E. SHRADER, *Drexel Institute, Philadelphia, Pa.*—An instrument is described which has characteristics similar to Miller's phonodeik. It differs from Miller's device in that the suspension eliminates pivot bearings, thus preventing friction. This suspension is quite simple and requires only ordinary skill in its construction. The new application is that of a stethograph which may be used for observing and recording all sorts of vibrations. Industrially it can be used in measuring vibrations of walls, plates, structures, machinery, etc. The device provides for observation of vibration by a rotating mirror at the same time that a record is being made photographically.

13. An Interesting Case of Submultiple Resonance. L. B. TUCKERMAN AND WALTER RAMBERG, *National Bureau of Standards.*—In investigating a case of severe vibrations in an airplane it was found that air impulses from a two-blade propeller with a frequency of about 3200 per minute excited resonant vibrations in the wings with a frequency of about 1600 cycles per minute and these in turn excited resonant vibrations in the tail assembly with a frequency of about 800 cycles per minute. The natural frequencies of the wing and tail differed enough from the ratio 2 to 1 to produce strong beats by the interchange of energy between wing and tail. There is a voluminous literature in the field of radio communication on the use of relaxation phenomena in frequency divider circuits, but no discussion of the phenomena of submultiple resonance was found in a search of engineering literature, and no reference at all to any investigation of the subject between the work of Raman and his followers (1911 to 1921) and a discussion by P. O. Pedersen in 1933 of its occurrence in radio loudspeakers. It seems possible that submultiple resonance has been the unrecognized cause of a number of baffling cases of undue vibrations in engineering structures. A mechanical model illustrating the phenomenon has been constructed and will be demonstrated.

F. Melde, "Über die Erregung stehender Wellen eines fadenförmigen Körpers," Poggendorff's Ann. d. Physik u. Chemie, 4th Series, **19**, 193–215 (1860).
C. V. Raman, "On Motion in a Periodic Field of Force," Bull. No. 11, Ind. Assn. Cult. Sci. (1914), pp. 25–42.
P. O. Pedersen, "Subharmonics in Forced Oscillations in Dissipative Systems," J. Acous. Soc. Am. **6**, 227–238 (1935); and **7**, 64–70 (1935).

14. Analysis of Broadening of X-Ray Reflections by Strain.* S. O. RICE, *Bell Telephone Laboratories Inc. (Introduced by T. C. Fry.)*—In the interpretation of x-ray measurements of the reflection of "monochromatic" radiation from a crystal plane it is often desirable to separate two effects, one due to variations in the lattice spacing of the planes and the other due to variations of the wave-length. In the present case it was desired to know the distribution of lattice spacings in a material, having given (1) the function relating x-ray intensity to the angle of reflection, and (2) the distribution of intensity in the x-ray line, which is given by reflection from a material having constant lattice spacing. This involves solution of the integral equation

$$F(\theta)=\int_{-\infty}^{+\infty} f_\lambda(\theta-u)f_d(u)du$$

for $f_d(u)$ when the other two functions are given. The solution may be written as a Fourier integral, which for the special case

$$f_\lambda(\theta)=q/[1+r\theta^2+s\theta^4], \text{ and } F(\theta)=Q/[1+R\theta^2+S\theta^4]$$

becomes

$$f_d(u)=\frac{(M+N)n}{\pi(m+n)N}\times\sum_{k=0}^{\infty}z^k\left[\frac{p+2kn}{(p+2kn)^2+u^2}-\frac{Z(p+2N+2kn)}{(p+2N+2kn)^2+u^2}\right].$$

Here $q=2ms^{\frac{1}{2}}/\pi$, $r=2(m^2+n^2)s$, $s=1/(m^2-n^2)^2$, $z=(m-n)/m+n$; Q, R, S and Z are similar expressions in M and N; and $p=(M-N)-(m-n)$. The mean square values of the functions $f_\lambda(\theta)$, $F(\theta)$ and $f_d(\theta)$ are, respectively, m^2-n^2, M^2-N^2, and $(M^2-N^2)-(m^2-n^2)$. The fact that the mean square value of $F(\theta)$ is the sum of the mean square values of the other two functions is also given by a more general argument known previously.

* To be read by title.

15. Energy and Lattice Spacing in Strained Solids.* G. R. STIBITZ, *Bell Telephone Laboratories Inc. (Introduced by R. M. Bozorth.)*—If an elastically isotropic substance is strained by means of principal stresses F_x, F_y, F_z, the distance d between a pair of planes having direction angles θ and ψ will become $d+\Delta d$, where

$$E\Delta d/d=(F_x-\nu F_y-\nu F_z)\sin\psi\cos\theta+(F_y-\nu F_z-\nu F_x)\sin\psi\sin\theta+(F_z-\nu F_x-\nu F_y)\cos\psi.$$

E is Young's modulus and ν Poisson's ratio. From this formula we may deduce a relation between the distortion of the lattice and the potential energy of internal strain in cold worked crystals. In particular, if the stresses are assumed independent, and oriented at random (which implies that $\overline{F_x^2}=\overline{F_y^2}=\overline{F_z^2}=\overline{F^2}$ and $\overline{F_xF_y}=\overline{F_xF_z}=\overline{F_yF_z}=0$, and also that the mean values of the trigonometric func-

tions are all zero), the mean square percentage change in spacing comes out at once to be

$$E^2\overline{\Delta d^2}/d^2 = \overline{F^2}(1+2\nu^2).$$

But under these conditions the potential energy due to the strain is $V = 3\overline{F^2}/2$. Hence

$$\overline{\Delta d^2}/d^2 = (2V/3E)(1+2\nu^2).$$

As the broadening of x-ray lines, due to strain, is deducible from $\overline{\Delta d^2}/d^2$, this formula is equivalent to a relation between such broadening and the potential energy of strain acquired in the process of cold working.

* To be read by title.

16. Energy of Lattice Distortion in Hard Worked Permalloy. F. E. HAWORTH, *Bell Telephone Laboratories Inc.*—By using a focusing camera and Fe radiation, the lattice distortion produced by severe cold working of permalloy of 70 percent Ni content has been studied by measuring the broadening of the reflection of the $K\alpha$ doublet by the (311) planes. The broadening decreases upon annealing and recovery is complete at 650°C, when the breadth of the x-ray intensity curve at half-maximum is as small as that obtained by use of the two crystal spectrometer. The mean square distortion in the lattice spacing due to cold work is derived from the x-ray measurements after photometering the x-ray film, converting the curve into an x-ray intensity curve, fitting the latter with an empirical equation and using the analysis given by Rice in the second abstract above. The energy of the distortion is then calculated by using Stibitz's equation given in the preceding abstract. The root-mean-square distortion was found to be 0.31 percent of the lattice spacing after the material had been reduced 96 percent in area by cold working. After annealing at 650°C, no distortion was detectable (accuracy about 0.01 percent of the lattice spacing). The energy of distortion in the hard worked condition is found to be 23×10^8 ergs/cm³ or 0.068 calorie/gram.

17. Effect of Annealing on the Properties of Hard-Worked Permalloy. J. F. DILLINGER, *Bell Telephone Laboratories Inc.*—An alloy containing 70 percent nickel and 30 percent iron was hard-worked until its original cross section was reduced 96 percent, and the changes in various properties were observed after annealing for various lengths of time at temperatures between 200° and 1100°C. The properties measured were initial and maximum magnetic permeabilities, the "magnetic hardness" in high fields, the electrical resistivity and the mechanical hardness. The changes are practically complete after annealing for one hour at 650°C, and are exponential with time and the reciprocal of the absolute temperature. The results are interpreted in terms of the energy which atoms must have in order to diffuse in the crystal lattice, and this energy is found to be 1.7 electron volts, in agreement with that found in alloys having superstructure. Results are correlated with the relief of internal strains as measured by x-rays (see preceding abstract).

18. The Variation of Young's Modulus with Magnetization in Permalloy. SIDNEY SIEGEL AND SEYMOUR ROSIN, *Columbia University.*—Data are reported which show the variation of Young's modulus with magnetization in three specimens of 81 permalloy. The specimens were prepared by subjecting a single rod of material to the following consecutive processes: (1) annealing at 1100°C in hydrogen and slow cooling; (2) stretching beyond the elastic limit with a resultant permanent elongation of 2 percent; (3) quenching in water at 1050°C. The percent increase in Young's modulus between zero and saturation magnetization was 0.26 percent for the first specimen, 0.15 percent for the second, and 0.11 percent for the third. The magnitude of this effect in annealed 81 permalloy is thus very nearly the same as it is in annealed Armco iron, and so is larger than might have been predicted, on the basis of Akulov's theory, from the known absence of magnetostriction in this material. We wish to thank Dr. R. M. Bozorth of the Bell Telephone Laboratories for the gift of the permalloy rod.

19. Variation of Rigidity and of the Decrement of Torsional Vibrations with Magnetization in Iron. W. F. BROWN, *Columbia University.*—Results obtained by a method previously described by W. T. Cooke[1] are compared with Cooke's results for longitudinal vibrations. From demagnetization to saturation, the rigidity of annealed material increases about 0.26 percent and Young's modulus about 0.30 percent. Both changes are about 50 percent greater than before annealing. The decrement before annealing varies with magnetization much as described by Cooke for longitudinal vibrations. The demagnetized value is practically the same for both types of vibration, and in both cases is increased from 2×10^{-4} to 2.6×10^{-3} by annealing. The decrement for annealed material drops rapidly above the knee of the magnetization curve. The effect of eddy currents of magnetostrictive origin[2] has been calculated and is negligible except for longitudinal vibrations at high fields.

[1] Phys. Rev. **45**, 742 (1934).
[2] M. Kersten, Zeits. f. tech. Physik **11**, 463 (1934).

20. The Temperature Variation of the Elastic Constants of NaCl, KCl and MgO Crystals between 80°K and 560°K. MILO A. DURAND, *Columbia University.*—The piezoelectric method developed by Balamuth and Rose has been extended to permit the measurement of the elastic constants of solids at temperatures at least as high as 560°K. Data are reported which exhibit the temperature variation of the three elastic constants of NaCl between 80°K and 480°K, of KCl between 80°K and 280°K, and of MgO between 80°K and 560°K. The behavior of these three substances can be correlated in the following manner: If c_{rs} denote one of the elastic constants c_{11} or c_{44}, then

$$A_{rs}\log\{(c_{rs})_0/(c_{rs})_X\} = f_{rs}(X),$$

where A_{rs} is a constant characteristic of the substance, X = (absolute temperature)/(characteristic temperature), and $f_{rs}(X)$ is a function which is identically the same for all three substances. The value of c_{12} is independent of temperature over the specified ranges for all three substances. Plausible extrapolations to lower and higher temperatures yield values of the constants at absolute zero and approximately correct values of the melting points.

21. Magnetic Susceptibility of Oxides of Lead. LARS WELO AND MAX PETERSEN, *Tottenville, N. Y., and Lehigh University.*—The measurement of the magnetic susceptibility of the product of vacuum decomposition of lead oxalate at 200–300°C fails to confirm the interpretation given by Pascal and Minne[1] that the phenyl-hydrazine reduction of lead oxide produces some, but not pure lead suboxide. Their conclusions rest on the assumption of a susceptibility value -0.09×10^{-6} for the supposed suboxide produced by vacuum decomposition of PbO at 265°C. The authors' measurements, made by the Gouy method, fail to confirm this datum. The measured values for a number of specimens, uncorrected for ferromagnetic contamination, considerably exceeded, absolutely, the value 0.09 and the extrapolated values were not significantly different from that which they should have given if they consisted of a mixture of Pb and PbO having the same free lead (12–60 percent) content that chemical analysis showed them to have. In all samples, prepared by pumping and temperature variants of that prescribed by Pascal and Minne, appreciable ferromagnetic impurities were found, apparently aggravated by the process of decomposition of the oxalate. Observations on pure PbO confirm the accepted value of its susceptibility, namely, -0.19. Observations of the reduction product by phenyl-hydrazine showed low susceptibility values not unlike Pascal's; but unsolved chemical complexities were clearly involved. The conclusion seems unavoidable that in these measurements there is no evidence for the existence of a stable suboxide of lead.

[1] Comptes rendus **193**, 1303 (1931).

22. The Inverse Piezoelectric Properties of Rochelle Salt at Audiofrequencies. OSCAR NORGORDEN, *University of Minnesota.*—Measurements of the inverse piezoelectric dilatation were made as a function of the temperature and of the frequency and intensity of the applied electric field. It was found to be proportional to the intensity of the electric field from 5 to 47 peak volts/cm for temperatures above the upper Curie point and from 5 to 40 peak volts/cm for temperatures below the Curie point; also it was found to be practically independent of the frequency from 100 to 4000 cycles/sec. and for temperatures from 13.3°C to 35.4°C. For temperatures below the Curie point the inverse piezoelectric dilatation increased as the frequency was decreased from 100 cycles/sec. This increase was explained in terms of Schulwas-Sorokin and Posnov's theory of relaxation time. For temperatures above the Curie point the inverse piezoelectric dilatation decreased as the frequency was decreased from 100 cycles/sec. Mueller's theory explained the experimental results for frequencies from 100 to 4000 cycles/sec. and temperatures above the upper Curie point. This theory was approximately in agreement with experiment for temperatures from 13.3°C to the Curie point and for frequencies from 100 to 4000 cycles/sec. Below 100 cycles/sec. the theory is not in good agreement with the experimental results.

23. Electron Image Tubes: Focusing Properties. G. A. MORTON AND E. G. RAMBERG, *RCA Manufacturing Company, Inc., Camden, N. J.*—The variation of image distance and magnification with object distance is investigated experimentally and theoretically for systems consisting of two cylinders of equal diameter, one of which is at cathode potential. Furthermore, the effect on both quantities of replacing this latter cylinder by a system of rings simulating a cylinder at linearly increasing or decreasing potential is studied. It is found that in both cases, for a large range of object and image distances and accelerating or decelerating potentials, the magnification is given to a fair approximation by one-half the ratio of image and object distance measured from the plane separating the two cylinders. Tables are shown giving the principal optical parameters of the systems.

24. Electron Image Tubes: Aberrations. E. G. RAMBERG AND G. A. MORTON, *RCA Manufacturing Company, Inc., Camden, N. J.*—Curvature of the image field, astigmatism, and distortion are calculated and measured for an electron-optical system consisting of a flat cathode and two cylinders, one at cathodic potential. Their correction by suitably curving the cathode is demonstrated and discussed. Furthermore, the chromatic and spherical aberrations on the axis and their relation to the initial velocities of the electrons leaving the cathode are considered.

25. Spontaneous Resistance Fluctuations in Carbon Microphones and Other Granular Resistances. G. L. PEARSON AND C. J. CHRISTENSEN, *Bell Telephone Laboratories, Inc.*—Voltage fluctuations which occur in resistance elements of the granular type when a direct current is flowing have been measured in the granular carbon microphone, commercial grid leaks, and sputtered or evaporated metal films. The results can be expressed by the formula, $\overline{V_e^2}=KV^\alpha R^\beta \log(F_2/F_1)$, where $\overline{V_e^2}$ is the mean square fluctuation voltage, V is the d.c. voltage across the granular resistance R, α and β are constants having values of about 1.85 and 1.25, respectively, and F_2 and F_1 are the limits of the frequency range over which the fluctuation voltage is measured. The constant K depends, among other things, on the temperature, the surrounding medium, and the dimensions and material of the resistance element; for a commonly used carbon transmitter at ordinary operating conditions its value is about 1.3×10^{-11}. In the carbon microphone the spontaneous voltage fluctuations and the signal due to acoustic modulation are affected in almost an equivalent manner by the applied d.c. voltage which suggests that the two effects arise from the same type of mechanism, namely, a fluctuating resistance at the points of contact between granules. The spontaneous resistance fluctuations are random, unlike the resistance modulation produced by the acoustic signal which is in phase at all contacts.

26. Spontaneous Resistance Fluctuations and the Nature of a Microphonic Carbon Contact. C. J. CHRISTENSEN AND G. L. PEARSON, *Bell Telephone Laboratories, Inc.*—A partial explanation of the experimental results outlined in the previous abstract (Pearson and Christensen) is possible when we assume carbon granular surfaces with a fine grained roughness such as demonstrated from elastic measurements and other considerations.[1] Goucher showed

that this roughness is equivalent to a layer of small hemispherical hills distributed in height according to the function $N_x = \text{const.}\ x^n$, and that electrical conduction is primarily between hills in intimate contact, which conduction, we have reason to believe, does not contribute to the resistance fluctuations. If we further assume a fluctuating secondary conduction in the regions adjacent to each area of intimate contact then calculation shows that $\overline{V_c^2} = \text{const.}\ R^{(2n+4)/(2n+3)}$. Comparing this with the empirical equation we find $n = 0.5$. From elastic measurements it was found that $n = 0.6$, a satisfactory agreement. Assuming that the secondary conductance is due to thermal agitation of the particle surface, causing minute momentary electrical contacts, we derive the observed frequency characteristic and show that $\overline{V_c^2}$ should vary as the square root of temperature. It has not been possible to make satisfactory temperature experiments but the observed results are not inconsistent with this relationship.

[1] F. S. Goucher, J. Frank. Inst. **217**, 407 (1934).

27. Piezoelectric Ultramicrometer. J. C. HUBBARD, *The Johns Hopkins University.*—An electrical circuit with a piezoelectric quartz plate connected as in the well-known work of W. G. Cady and of D. W. Dye in their studies of the piezoelectric resonator, gives a response curve of current *vs.* frequency cleft by a deep cut, or *crevasse*, at the response frequency of the plate. The extraordinary steepness of the sides of the *crevasse* is due to the very small decrement of the quartz resonator as compared with that of ordinary circuits. At an exciting frequency corresponding to a point of steepest slope of the *crevasse* the system is sensitive to a change of exciting frequency in general much smaller than can be detected by usual beat-tone methods, as by R. Whiddington with the ultramicrometer. A number of applications of this sensitivity to frequency variation suggest themselves, perhaps the most interesting applying to measurement of small displacements of an ultramicrometer plate in the exciting circuit. Displacements of 10^{-9} cm have been measured to a few percent, the accuracy depending upon the absence of mechanical disturbances. By suitable mechanical insulation it is expected that one order less in magnitude of displacement may be measured.

28. The Measurement of Dielectric Constants at Ultra-High Frequencies. RONOLD KING, *Lafayette College.*—A new parallel-wire method for the measurement of dielectric constants of solids and liquids at ultra-high frequencies has been developed. It depends upon the solution of the telegraphist's equations for a parallel wire system of which a part passes through the medium of unknown dielectric constant ϵ. By comparing the input admittance of a section of parallel wires in air with a similar section of which a part is in air and a part in the medium to be tested, a useful and simple expression involving ϵ has been derived. The experimental procedure is simple and accurate. For a suitably shaped sample it is merely necessary to observe the shift in the position of a bridge with and without the sample in place. Only a relatively small sample is required. Up to the present the method has been tested by determining the temperature coefficient of the index of refraction of water, the dielectric constants of solutions of ethyl alcohol in water, and the dielectric constant of rubber. These measurements were made at a wave-length of 188.8 cm. Other measurements are in progress. The method would seem especially well suited to measurements in the wave-length range from five meters down to a few centimeters. Mathematically and experimentally the method is also readily specialized to permit the measurement of reactances of coils or condensers in the range from several thousand ohms to infinity. It thus supplements other methods already outlined.[1]

[1] Proc. I.R.E. **23**, 913 (1935).

29. The Production of Short Electrical Pulses. R. C. COLWELL, A. W. FRIEND AND N. I. HALL, *West Virginia University.*—In the exploration of the ionosphere, the pulse delay method of Breit and Tuve has given results of very great value. We have tried to improve the shortness and sharpness of the pulses by various devices which will be described: (1) The mechanical chopper; (2) the cam and breaker contact; (3) the interrupted conducting fluid; (4) synchronous motor with telephone magnet; (5) resistance "motorboating"; (6) the resistor-condenser combination.

30. The Rochester Cyclotron. L. A. DUBRIDGE AND S. W. BARNES, *University of Rochester.*—A magnetic resonance accelerator designed to produce 6 MV protons is nearing completion. The 17-ton magnet, now installed, was designed to produce a field of 20,000 gauss with pole faces 20 inches in diameter. In designing the magnetic circuit we were guided by the theoretical calculations of Bethe and by preliminary tests on a model built to a 3/16 scale. The yoke is built of 4 Armco iron forgings 12 inches by 26 inches in cross section. The pole pieces, also of Armco, are 26 inches in diameter tapered at 45 degrees to a 20 inch diameter; or the full 26 inch diameter can be used. Experiments with the model showed that a field of 20,000 gauss in a 3-inch air gap could be obtained with 240,000 ampere-turns excitation. The two exciting coils of 1200 turns each are wound of copper strip with intermediate layers of square copper tubing for water cooling. The exciting current will be controlled through the field of a 50 kw motor-generator set. Tests indicated that the area of the uniform field region could be considerably increased by shaping the pole faces so that the air gap is thicker in the middle than at the edges. The best form of pole face has been determined empirically and it seems probable that this shaping will materially decrease the amount of "shimming" required to secure resonance. The vacuum chamber follows closely the design of Lawrence and Livingston. High frequency power will be supplied by a 20 kw oscillator using commercial tubes.

31. The Design and Performance of the Round Hill Electrostatic Generator. L. C. VAN ATTA, D. L. NORTHRUP, C. M. VAN ATTA AND R. J. VAN DE GRAAFF, *Massachusetts Institute of Technology.*—The design of belt charging systems and the technique of voltage measurement are discussed. Performance data for the Round Hill electrostatic gener-

ator are presented. The original belt charging system, with the belts operated at saturation charge density, is described and its range of usefulness is indicated. A consideration of the problems of voltage control and voltage steadiness at reduced charging currents leads to two modified designs of the belt charging system. The measurement of voltage by means of the generating voltmeter is discussed with special emphasis on the precautions necessary to eliminate or to correct for sources of systematic error. Under the conditions realizable with the Round Hill generator the probable error in voltage measurements is less than 1 percent on a relative scale and about 2 percent on an absolute scale. The magnitude of voltage fluctuations is less than 0.1 percent. The generator performance data for the positive and negative terminals are given in graphical form. The maximum charging current is 2.1 ma and is practically independent of voltage. The highest voltage obtained consistently without sparking is 2.4 megavolts positive and 2.7 megavolts negative, giving 5.1 megavolts between the terminals. At this voltage there is 1.1 ma of current available for application to an accelerating tube.

32. Modified Design of the Linear Accelerator for High Intensities. LLOYD P. SMITH AND PAUL L. HARTMAN, *Cornell University*.—A mathematical analysis of the action of the linear accelerator in producing high voltage ion beams has been made in order to determine the number and velocity distribution of ions in the beam after n accelerations. The analysis indicates how to modify the usual design so that a nearly homogeneous ion beam of considerably greater intensity could be produced. The questions of focusing and the separation of ions of different mass have been considered.

33. Six Million Volt Magnetic Resonance Accelerator with Emergent Beam. DONALD COOKSEY AND ERNEST O. LAWRENCE, *University of California*.—Changes have been made in the design of the Berkeley magnetic resonance accelerator, in order to bring the ion beam out of the accelerating chamber and the magnetic field. A six million volt beam of several microamperes, thus brought out into the air, produces a column of bright luminosity 28 cm long.

34. The Scattering of Protons by Protons. M. A. TUVE, N. P. HEYDENBURG AND L. R. HAFSTAD, *Department of Terrestrial Magnetism, Carnegie Institution of Washington*.—Observations described in a recent letter to the *Physical Review* under the same title will be discussed, together with refined and extended measurements now in progress.

35. Interaction Between Protons as Indicated by Scattering Experiments. G. BREIT AND E. U. CONDON, *Institute for Advanced Study and Princeton University*.—A preliminary analysis of experiments by Tuve, Heydenburg and Hafstad indicates an interaction between protons of nearly the same magnitude as that obtained from mass defects by Bethe, Feenberg and Young. The potential between protons in a ^1S state is 10 or 20 percent less than that between a proton and a neutron in a similar state. With only the phase shift for $L=0$ the variation of the scattering anomaly with energy is not accounted for by a simple short range potential and requires either a stable He^2 or a special combination of attractive and repulsive regions. With phase shifts for $L=0$, 1, 2 the data can be accounted for approximately without these assumptions; on this view the interaction energy is allowed to extend to 10^{-12} cm or more and is made equal in that region to an appreciable but small fraction of the Coulombian energy. Attractions for $L=0$, 2 and repulsions for $L=1$ appear to fit the data better on the whole than other possibilities. The interpretation is sensitive to errors in the angular distribution.

36. Widths of Nuclear Resonance-Levels and the Calibration of Ion-Beam Energies. L. R. HAFSTAD, N. P. HEYDENBURG AND M. A. TUVE, *Department of Terrestrial Magnetism, Carnegie Institution of Washington*.—The development of a corona-free, 10,000-megohm voltmeter-resistor has brought the accuracy of our voltage-measurements to approximately two percent on an absolute scale and to about one percent on a relative scale. Oscillograph-studies of voltage-fluctuations have shown that up to 1000 kv the voltage is constant to ± 1.4 percent "peak-ripple" (fluctuation half-width 1.0 percent). The resultant homogeneity of our ion-beam permits us to conclude that the observed width of the 440-kv Li resonance is greater by about 11 kv than can be accounted for by voltage-fluctuation. Similar though less precise observations have been made on the fluorine resonances giving the following as points available for the calibration of ion-beams of unknown energy or distribution.

VOLTAGE IN kv	ELEMENT	HALF-WIDTH
328	F	< 4 kv
440	Li	11 kv
892	F	<12 kv
942	F	<15 kv

While no sharp resonances are available at present for the region between 440 and 892 kv, there is an indication of a weak multiplet structure in fluorine in the region between 500 and 700 kv, with a broad but fairly prominent "resonance" at 650 to 700 kv.

37. The Paschen-Back Effect of Hyperfine Structure. III. Separation of Hg_{199}. J. B. GREEN, *Ohio State University*.—It has been possible, by a judicious choice of field strength, to separate the magnetic components due to the 199 isotope of mercury. Five lines have been studied, λλ 3125 ($^3P_1$ $^3D_2$), 5790 ($^1P_1$ $^1D_2$), 5461, 4358, 4047 (^3P ^3S). A practically complete Paschen-Back effect is observed, each ordinary Zeeman component being accompanied by two satellites due to the nuclear spin $i=\frac{1}{2}$ of Hg_{199}. There is excellent agreement between theory and experiment, even to the slight asymmetries observed.

38. The Zeeman Effect in N II. H. N. MAXWELL AND J. B. GREEN, *Ohio State University*.—The Zeeman effect in N II has been observed and is in excellent agreement with the classifications assigned by Fowler and Freman. The nitrogen was present as a 4 percent impurity in a 3 cm helium atmosphere and the spectrum was excited probably by collisions of the second kind in an arc between gold electrodes, in a magnetic field of about 35,000 gauss.

39. An Estimation of the Atomic Weights of Lithium, Potassium and Rubidium from Isotope Abundance Measurements. A. KEITH BREWER, *Bureau of Chemistry and Soils, U. S. Department of Agriculture, Washington, D. C.*—The abundance ratios of the isotopes of lithium, potassium and rubidium have been estimated from positive thermions emitted from platinum disks impregnated with the alkali in question. The ratios so obtained are $Li^7/Li^6 = 11.60 \pm 0.06$, $K^{39}/K^{41} = 14.20 \pm 0.003$, and $Rb^{85}/Rb^{87} = 2.59 \pm 0.01$. These values are necessarily complicated by a possible isotope effect of free evaporation. The extent to which the positive ion currents represent the atom abundance within the source was determined by measuring the change in the abundance ratio as a function of the percent of alkali evaporated. Lithium obeyed the law for free evaporation until the source was 40 percent depleted; potassium and rubidium showed no appreciable isotope effect. In the two latter cases, therefore, the positive ion ratios represent the true abundance ratio; in the case of lithium, however, the positive ion ratio must be multiplied by $(7/6)^{\frac{1}{2}}$, to obtain the atom ratio within the source $(11.60 \times (7/6)^{\frac{1}{2}} = 12.52)$. The atomic weights computed from the above abundance ratios, assuming the most probable values for the packing fractions, are Li = 6.939, K = 39.094, and Rb = 85.46.

40. The Nuclear Spin and Magnetic Moment of K^{41}. J. H. MANLEY, *Columbia University*.—The spin of the K^{41} nucleus and the h.f.s. separation of the $^2S_{\frac{1}{2}}$ normal state have been measured by the method of zero moments. The high resolution necessary to secure sufficient separation of the two isotopes was obtained by passing a beam of neutral potassium atoms through a weak inhomogeneous magnetic field 153 cm long. The total beam length was 201 cm. A new method of analysis of the zero moment peak of K^{41} relative to that of K^{39} was employed in the determination of the spin. The spin was found to be 3/2 and the h.f.s. separation to be 0.554 ± 0.2 percent of that of K^{39}. The same ratio applies to the magnetic moments, hence this ratio and the values for K^{39} given by Fox and Rabi[1] yield

$$\Delta\nu(K^{41}) = 0.00853 \pm 0.0001 \text{ cm}^{-1},$$
$$\mu(K^{41}) = 0.220 \text{ nuclear Bohr magnetons.}$$

From the intensities of the K^{41} and K^{39} peaks it is possible to give the abundance ratio, K^{39}/K^{41}, as 13.4 ± 0.5 which is in fair agreement with 13.88 ± 0.4 given by Brewer and Kueck,[2] and the ratio 13.96 ± 0.1 found by Nier.[3]

[1] M. Fox and I. I. Rabi, Phys. Rev. **48**, 746 (1935).
[2] Brewer and Kueck, Phys. Rev. **46**, 894 (1934).
[3] A. O. Nier, Phys. Rev. **48**, 283 (1935).

41. Nuclear Spins and Magnetic Moments of Rb^{85} and Rb^{87}. S. MILLMAN AND M. FOX, *Columbia University*.—The atomic beam method of "zero moments" has been applied to the measurement of the nuclear spins and h.f.s. separations, $\Delta\nu$, of the $^2S_{\frac{1}{2}}$ states of Rb^{85} and Rb^{87}. We find the spin of Rb^{85} to be 5/2 and that of Rb^{87} to be 3/2, in agreement with the most probable values given by Kopfermann.[1] With the value of $\Delta\nu$ for sodium as a standard we were able to measure the $\Delta\nu$'s of the rubidium isotopes with a precision of 1 percent, the same as that given for the sodium measurement.[2] We find these values to be 0.1018 cm^{-1} for Rb^{85} and 0.229 cm^{-1} for Rb^{87}, as compared with Kopfermann's values of 0.105 cm^{-1} and 0.240 cm^{-1}, respectively. The magnetic moments calculated from the modified Goudsmit formula are 1.44 nuclear magnetons for Rb^{85} and 2.92 for Rb^{87}. The ratio of these magnetic moments, μ^{87}/μ^{85}, is found to be 2.026, with a precision of 0.2 percent. The $\Delta\nu$ for Cs was also measured with a precision of 1 percent. The result, 0.307 cm^{-1}, is in excellent agreement with the value of 0.3067 cm^{-1} of Granath and Stranathan.[3]

[1] Kopfermann, Zeits. f. Physik **83**, 417 (1933).
[2] Fox and Rabi, Phys. Rev. **48**, 746 (1935).
[3] Granath and Stranathan, Phys. Rev. **48**, 725 (1935).

42. The Magnetic Moment of Li^7. J. H. BARTLETT, JR., AND J. J. GIBBONS, JR., *University of Illinois*.—The recent measurement by Fox and Rabi[1] of the h.f.s. separation of normal lithium makes possible the calculation of values of the nuclear magnetic moment. Fock and Petrashen[2] have found a self-consistent wave function, and calculation with this results in a value of 4.58 nuclear magnetons for the magnetic moment. This is to be compared with the value 3.28 n.m. as found by Breit and Doermann[3] on the basis of h.f.s. measurements in the spectrum of Li^+. The functions of Fock and Petrashen might be supposed to be less accurate than functions calculated by a variational method and involving the interelectronic distances. An investigation of this is being made.

[1] Phys. Rev. **48**, 746 (1935).
[2] Physik. Zeits. Sowjetunion **8**, 547 (1935).
[3] Phys. Rev. **36**, 1262 (1930).

43. The Magnetic Moment of the Deuteron. J. M. B. KELLOGG AND I. I. RABI, *Columbia University*, J. R. ZACHARIAS, *Hunter College of the City of New York*.—Under the title of "Deflection and Focussing of a Beam of Hydrogen Atoms" we reported at the Baltimore meeting a method by which it is possible to measure the h.f.s. separation of the normal state of hydrogen. We have applied this method to the deuteron and find the h.f.s. separation to be 0.0108 cm^{-1}. From this value we calculate the deuterium moment to be 0.85 ± 0.03 nuclear magneton. This value coincides very closely with the value of the magnetic moment of the Li^6 nucleus calculated from the measurements of Fox and Rabi under the assumption that its spin is 1. We wish to acknowledge the aid of a grant from the Carnegie Foundation in support of this research.

44. Hyperfine Structure and Nuclear Moment of Barium. ALBIN BENSON AND R. A. SAWYER, *University of Michigan*.—In recent compilations of nuclear moments, White gives for the odd isotopes of barium 5/2?, while Darrow gives 5/2, and Schüler 3/2. Schüler refers to his unpublished analysis of the data of Ritschl and Sawyer on the resonance lines of Ba II; the other values are probably based on the intensity measurements of Kruger, Gibbs and Williams on the h.f.s. of Ba II $6s\,^2S_{\frac{1}{2}} - 6p\,^2P_{\frac{1}{2}}$. The only other work is an intensity study by Murakawa of the h.f.s. of Ba II $6s\,^2S_{\frac{1}{2}} - 6p\,^2P_{\frac{1}{2}}$, who concludes $i = 3/2$. The conflict

arises from the fact that the even isotopes of barium (136, 136) with no nuclear moment make up 83 percent of the total and so give in each h.f.s. pattern a powerful central component superimposed on the h.f.s. of the odd isotopes (135, 137), which have a moment, so the h.f.s. patterns can never be completely observed. In a study of new experimental material on the h.f.s. of both Ba I and Ba II lines as well as of the previously published material, use has been made of the interval rules and of the centroids of the h.f.s. patterns. Several independent evaluations of the nuclear moments of the odd isotopes can be made and the evidence shows quite conclusively that for $Ba_{135,137}$ $i=3/2$.

45. Surface Ionization of Barium on Tungsten. ALBERT N. GUTHRIE, *Columbia University.*—A molecular beam of barium is formed by heating the metal in a nickel oven to a temperature near 1000°K. Alkali metal atoms present are deflected out of the beam by passage through a strong inhomogeneous magnetic field. The beam then strikes a tungsten filament and the positive ion current produced by surface ionization of the barium on the tungsten is measured. At a filament temperature near 1700°K the current becomes detectable and increases with increasing filament temperature up to 2000°K. From this temperature up to 2600°K, the highest temperature at which measurements have been made, the current remains constant. Filaments are given a prolonged heating at 2800 to 2900°K before measurements are made. By calculating the intensity of the beam from the oven temperature and the dimensions of the apparatus, an estimate of the ionization efficiency is obtained. It is of the order of 100 percent in the range of filament temperatures 2000 to 2600°K.

46. Direct Partition of Energy Metabolism by Differential Calorimetry. A. P. GAGGE, *John B. Pierce Foundation and Yale University.*—A new experimental arrangement, whereby the energy exchange due to radiation and convection with the environment may be differentiated, is described; the subject, at rest, is placed inside a nine-sided booth of polished copper whose effective black-body wall temperature is controlled by the reflected radiation from three electric heaters and whose air temperature and humidity are controlled by air-conditioning equipment. The wall temperature (1), the air temperature (2), and the body skin temperature (3) (as measured by a thermopile) are sufficient to describe the radiation and convection exchange for constant air movement. The partition elements, metabolism, storage, and evaporation, are assumed to be measured by O_2-consumption (4), rate of change of rectal temperature (5), and rate of weight loss (6), respectively. By the application of the first law of thermodynamics to the five elements of partition it is shown that a linear relationship exists between certain groups of these basic measurements only when the above assumptions hold. Where this "linearity criterion" is satisfied a partition of energy metabolism into storage, evaporation loss, total radiation (including radiation surface area) and convection may be evaluated directly from the *six* basic measurements above. Formulae for the convection are given to extend partitions to conditions where the criterion fails.

47. The Response of the Skin to Radiation. J. D. HARDY AND T. W. OPPEL, *Russell Sage Institute of Pathology in Affiliation with the New York Hospital, New York.*—The response of the white human skin to the heating effects of visible light (0.4μ to 0.8μ), near infrared light (0.8μ to 2.5μ), and far infrared radiation (3μ) has been studied. It has been found that the smallest amount of visible radiation which can be perceived as heat by the face is 0.0014 gram cal. per sec. per cm²; of near infrared 0.00096; and of far infrared 0.00063. The rise in skin temperature caused by these radiations is practically the same and is at the rate of 0.001°C per second. The sensitivity of the skin to radiation is found to be related to the area of skin exposed in a very definite way but for areas larger than 200 cm² very little increase in absolute sensitivity is obtained. The minimum amount of radiation required for the stimulation of the heat sense is 0.00033 gram cal. per sec. per cm²; the skin temperature rise thus caused is 0.0005°C per second.

48. The Extreme Ultraviolet Spectrum of the D_2 Molecule.* C. R. JEPPESEN, *The Johns Hopkins University.*—The emission spectrum of the D_2 molecule has been photographed in the extreme ultraviolet region by use of a grazing incidence vacuum spectrograph with 2-meter grating. In the $2p\,{}^1\Sigma - 1s\,{}^1\Sigma$ system 37 bands have been analyzed. In the $2p\,{}^1\Pi - 1s\,{}^1\Sigma$ system 29 bands were obtained. Values of the important molecular constants in cm^{-1} units for the three electronic states involved are as given in the table. Electronic shifts (T_e for D_2 − T_e for H_2)

	$1s\,{}^1\Sigma$	$2p\,{}^1\Sigma$	$2p\,{}^1\Pi_{cd}$
B_e	30.429	10.186	15.665
$B_e z$	—	9.994	15.857
a_e	1.0492	0.35092	0.5739
$\Delta G_{\frac{1}{2}}$	3118.8	963.5	1736.2
$2x_{e\omega_e}$	128.3	21.96	78.215
T_e	0	91698.4	100092.1

of 4 cm^{-1} and 23 cm^{-1} are observed for the $2p\,{}^1\Sigma - 1s\,{}^1\Sigma$ and $2p\,{}^1\Pi_{cd} - 1s\,{}^1\Sigma$ systems, respectively.

* To be read by title.

49. Infrared Dispersion of Chloroform and Bromoform. M. A. PITTMAN, *The Johns Hopkins University.* (*Introduced by A. H. Pfund.*)—Dispersion of $HCCl_3$ and $CHBr_3$ has been studied from visible light to about 12μ. The apparatus used consisted of a rocksalt monochromator and a hollow rocksalt prism spectrometer. Particular attention was paid to the C–H vibrations and their harmonics and it is hoped that the relationship between these harmonics and "transition probabilities" can be shown. Of special interest is that the dispersion of these liquids was measured directly through the principal absorption bands near 8μ where it is greater than for visible light. This direct measurement was made possible by means of a highly amplified Photronic cell system. The new Pfund design "vibration-free" support was of vital importance in this work.

50. Infrared Absorption Spectra of Aqueous Solutions of Acetic Acid and Its Chlorine Derivatives. E. K. PLYLER AND E. S. BARR, *University of North Carolina.*—The infrared absorption spectra of aqueous solutions of acetic

acid, monochloroacetic acid, and trichloroacetic acid have been measured from 2.8μ to 6.5μ. In the region from 4.5μ to 6.0μ intense absorption was observed. In the acetic acid solution the maximum of absorption was at 5.75μ and in the trichloroacetic acid solution the band occurred at 5.4μ. This change in position of the band was attributed to the greater dissociation present in the trichloroacetic acid solution. With the same cell thickness, absorption curves were obtained for 8 concentrations ranging from $1/4N$ to $8N$. The coefficient of absorption was not proportional to the concentration for different concentrations, which shows that the number of absorbers present in the solution was not directly proportional to the concentration. The percent dissociation for each concentration has been calculated by using the intensity of the band.

51. Infrared Absorption Spectrum of Liquid Water. DUDLEY WILLIAMS, *University of North Carolina.*—A detailed study has been made of the absorption spectrum of liquid water in the region between 4μ and 10μ. Bands have been discovered at 6.8μ and near 8.6μ. These bands do not fall readily into any of the early classifications of the bands of liquid water. However, it has been pointed out by Cartwright that there are bands at 20μ and 60μ which arise from hindered rotation and mutual vibration, respectively. By considering the combinations which may be formed between these frequencies and the fundamental vibrational frequency, it is found that the frequencies of the two observed bands check satisfactorily with the calculated values. Also, there are two bands on the high frequency side of the 6μ fundamental with frequencies in close agreement with calculated combinations. In the 3μ region the absorption is so intense that not all of the separate maxima have been well resolved. However, the bands which have been observed agree satisfactorily with the above classification.

52. The Infrared Absorption Spectrum of Deuterium-Containing Stearic Acid. W. W. COBLENTZ AND R. STAIR, *National Bureau of Standards.*—It is of interest to compare the infrared absorption spectrum of stearic acid-containing deuterium, 6–7–9–10 d_4 with that of stearic acid, $C_{18}H_{36}O_2$ previously examined.[1] The sample containing deuterium was kindly supplied by Dr. Rudolf Schoenheimer.[2] Examined to 9μ with a mirror spectrometer and fluorite prism the material shows a strong absorption band at about 4.65μ not present in stearic acid. Other strong absorption bands, found in both substances, occur at 2.4, 3.43, 3.8, 5.9, 6.86, 7.1, 7.7, 8.2, and 8.4μ.

[1] Pub. No. 35, Carnegie Institution of Washington, 1905.
[2] J. Biol. Chem. **111**, 163 (1935).

53. Applied Electron Optics. V. K. ZWORYKIN, *RCA Manufacturing Co., Victor Division, Camden, New Jersey.*—(45 minutes.) The application of electron optics to the problem of image formation is discussed. Electrostatic lenses may be used for this purpose, but suffer from aberration and distortion similar to that existing in simple optical systems. The causes of these faults are considered and various means of correcting the "lenses" are given. The corrected "electron lens" may be used in an image tube which is capable of giving a faithful reproduction of an image projected onto its photosensitive cathode. The performance of this type of tube is illustrated. Other applications of electron optics are also considered.

54. Hyperfrequency Transmission Through Wave Guides. G. C. SOUTHWORTH, *Bell Telephone Laboratories, Inc.*—(45 minutes.) This paper will be a nonmathematical description of a novel form of electric wave propagation through dielectric rods or through metal pipes either hollow or filled with insulation. Quantitative data based on calculation but verified by experiment will be presented and discussed. The data will relate to four of the many possible forms of waves that may be propagated. Extremely short wave generators and receivers of a very elementary character but utilizing some of the properties of wave guides will be described along with some of the methods of measurement.

55. Energies of Selectively Absorbed Neutron Groups. F. RASETTI, G. A. FINK, H. H. GOLDSMITH AND D. P. MITCHELL, *Columbia University.*—Since resonance capture of neutrons by light nuclei, e.g., boron and lithium, is improbable, the capture cross section for slow neutrons should be inversely proportional to the neutron velocity, and therefore the relative velocities of neutron groups may be estimated from their absorption coefficients in boron, as by Weekes, Livingston and Bethe.[1] The expected value of 1/40 ev for the mean energy of the thermal neutron group (C) has been verified by use of a mechanical velocity selector.[2] The measured absorption coefficients in boron and the corresponding relative velocities for the various neutron groups are shown in the table, the reliability of the measurements decreasing with lower absorption. Using the value of 0.025 ev for the C group we obtain the energies given in the last column. Relative absorption coefficients for the C, D and A groups have also been measured in Li and the estimated energies are in agreement with those obtained from absorption in boron.

Fermi-Amaldi Neutron Group	Detector	Filter	Mass Abs. Coef.	V/V_c	Energy (ev)
C	Mn	none	34	1.0	0.025
D	Rh	0.4g/cm Cd	7.0	4.9	0.6
A	Ag	"	3.4	9.9	2.5
I	I	"	0.45	75	140

[1] Weekes, Livingston and Bethe, Phys. Rev. **49**, 471 (1936).
[2] Phys. Rev. **48**, 704 (1935).

56. Evidence for Neutron-Proton Shells from Nuclear Masses. H. A. BETHE, *Cornell University.*—If the particles in a nucleus are considered to move independently in a suitable central field, periodicities analogous to the periodic system should be expected. The first shell of neutrons and protons is completed in the α-particle, the second in the O^{16} nucleus. Therefore any particle added to the O^{16} nucleus should be less strongly bound than the same particle added to an "analogous" nucleus, e.g., C^{12}. This is actually the case; e.g., if two neutrons and one proton are added to C^{12} (giving N^{15}), the atomic weight increases by $15.0053 - 12.0037 = 3.0016$. If the same particles are added to O^{16}

(result F^{19}), the increase in weight is 3.0040, i.e., 2.2 MV more than for $C^{12}-N^{15}$. This is the more significant in view of the general trend of the binding energy of nuclear particles to increase with the size of the binding nucleus. Any conceivable experimental errors are such that their correction could only make the experimental values more favorable for our argument. The binding energies of other particles and groups of particles added to C^{12} and O^{16} show the same phenomenon. There seems thus some justification for the individual-particle approximation in nuclear theory.

57. Scattering of Fast Neutrons by Heavy Nuclei. CHARLES H. FAY, *Harvard University.*—Van Vleck's[1] approximate treatment of s neutron scattering by heavy nuclei, considering neutron-proton forces of the Majorana exchange type, is extended to the higher partial cross sections, the effective potential hole being found the same for all angular momenta. For fast neutrons the scattering problem lies in the annoying region where the Born approximation is invalid and yet partial cross sections as high as the sixth are important. Exact calculation shows important variations of cross section with hole radius R and energy, so that the monotonic variation of cross section with atomic number found experimentally for fast neutrons by Dunning[2] can be fitted by this approximate theory only by taking into account the distribution of neutron energies over a wide range in the experiment, and the fact that small-angle scattering is not measured. The existing data seem inadequate to test the validity of the theory, and work using beams of sharply defined velocity is desirable and should give interesting results. Phases and cross sections/R^2 have been computed for a range of values of kR and of $k_0'R$ for use in future applications.

[1] J. H. Van Vleck, Phys. Rev. **48**, 367 (1935).
[2] J. R. Dunning, Phys. Rev. **A45**, 586 (1934).

58. The Scattering and Capture of Neutrons by Protons. J. B. FISK, P. M. MORSE AND L. I. SCHIFF, *Massachusetts Institute of Technology.*—An exact solution for both negative and positive energies has been obtained for the potential field

$$-2D\exp[2(r_1-r)/r_0]+D\exp[4(r_1-r)/r_0].$$

When $r_1>0$ the field is repulsive at small distances. The value of D is set so that the deuteron binding energy is $4mc^2$, hence, the results depend only on the parameters r_0 and $(2r_1/r_0)=X_0$. The elastic cross section ($l=0$) for very slow neutrons is practically the same for X_0 from 0 to 1, rising to a maximum of 6×10^{-24} cm^2 at $r_0=3\times10^{-13}$ cm, dropping to zero at $r_0=7\times10^{-13}$, and rising rapidly to very large values for larger r_0. The $l=1$ cross section is negligible for $X_0=0$, but becomes important for $X_0=1$, for neutron energies about 100,000 volts. For instance, at $r_0=5\times10^{-13}$ cm the cross section shows a "Ramsauer effect" and a considerable dependence of scattering on angle. The capture cross section is expressed in terms of the inverse mean life, $1/\tau$, in paraffin. The fraction of this due to electric dipole radiation is negligible compared to that due to magnetic dipole for very slow neutrons. The quantity $1/\tau$ shows the same general variation as the elastic cross section, having a first maximum of about 500 sec.$^{-1}$ at $r_0=3\times10^{-13}$ cm, and rising rapidly for $r_0>7\times10^{-13}$.

59. Scattering of Slow Neutrons. ALLAN C. G. MITCHELL, EDGAR J. MURPHY AND MARTIN D. WHITAKER, *New York University, University Heights.*—The work on the scattering of slow neutrons has been continued with a view to obtaining information about the scattering cross sections for the various groups. We have measured the scattering from Ag using an Ag detector when the neutrons had been filtered through sufficient Cd to cut out the C group. The scattering at 2 cm in this case is 16 percent, which compares to a maximum scattering of 8 percent for the unfiltered neutrons. The influence of various detectors has been further investigated by running full scattering curves using Cu as detector. As an example the scattering cross section for carbon using the detectors Ag, Rh, Cu has been found to be 3.2, 2.2, and 2.0×10^{-24} cm^{-2}, respectively. Similarly, the scattering cross section for Cu using Ag and Cu detectors is 7.7 and 9.0×10^{-24} cm^{-2}. Finally, using an arrangement like that of Moon and Tillman we have measured the temperature coefficient of the C and D neutrons using an In detector. The value of J_{80} for the C neutrons is 1.27 while that for the D neutrons is 1.08. The latter figure is in agreement with the value for the D neutrons obtained by Rasetti and Fink using a Rh detector.

60. The Diffusion of Slow Neutrons. D. S. BAYLEY, B. R. CURTIS, E. R. GAERTTNER AND S. GOUDSMIT, *University of Michigan.*—A radon beryllium source was placed at the center of a large cylindrical tank filled with water. A solid sphere of cadmium was suspended a distance away from the source and its influence on the distribution of the diffusing slow neutrons was measured by means of the activity induced in rhodium. It was found that the cadmium sphere acts as a "sink" for the slow neutrons. Other elements also have the effect of lowering the density of the neutrons. Layers of silver, copper and carbon were placed against one side and also against both sides of the rhodium foil and the decrease in induced activity was measured. Whereas thick layers of carbon had nearly no influence on the induced activity, thin layers of silver reduced it considerably, copper had an intermediate effect. An attempt was made to discover some temperature effect on the boundary between hot and cold blocks of paraffin, with rhodium as a detector. The effect, if present, is very small.

61. Beta-Ray Spectra of Several Slow Neutron-Activated Substances. E. R. GAERTTNER, J. J. TURIN AND H. R. CRANE, *University of Michigan.*—By means of a 200 millicurie radon-beryllium source of neutrons we have been able to activate rhodium, silver, manganese, dysprosium and indium (2 periods) with sufficient intensity to obtain their beta ray spectra by the cloud chamber method. About 2500 photographs were taken, yielding about 4500 measurable tracks in all. The plots of the energy distributions were transformed into straight lines according to the Konopinski-Uhlenbeck formula and extrapolated to find the upper energy limits. This gave for silver (22-sec. period) 2.8 MEV; rhodium (44-sec. period) 2.8 MEV; manganese (2.5-hour period) 2.8 MEV; indium (54-min. period) 1.3 MEV; indium (13-sec. period) 3.2 MEV; dysprosium (2.5-hour period) 1.4 MEV, which are on the average about 200 kv greater than the energy limit which would be estimated by inspection of the plot of energy against intensity.

62. The Scattering of β-Rays. J. A. GRAY AND A. G. WARD, *Queens University.*—In 1931 (see Trans. Roy. Soc. Canada), one of us concluded that β-rays were modified in the scattering process, this modification or loss of energy appearing to be greater the greater the angle of scattering and the smaller the atomic number of the scattering material. As a result, however, of experiments carried out by J. S. Marshall in this laboratory, in addition to those now to be reported, we have been led to the conclusion that when β-rays are scattered by nuclei, some of them are modified in the process, the percentage of modified rays increasing with the angle of scattering and as the atomic number of the scattering material is diminished. During the course of our experiments we have had to determine the end point of the β-ray spectrum of radium E. We find it to be near HR 5200.

63. Portable Counter-Controlled Wilson Cloud Machine of New Design. GORDON L. LOCHER, *Bartol Research Foundation of the Franklin Institute.*—A semi-automatic cloud machine of rugged construction, light weight (76 lbs.; Dowmetal), and small power consumption (10 watts), initially designed for stratosphere balloon flights, has been developed for portable use. Actuating force is provided by a fixed partial vacuum that acts on an 8-inch sylphon bellows placed between the vacuum chamber and cloud chamber. The machine is thus independent of external pressure. No diaphragm or piston is used. Two baffles: a gauze and a perforated metal plate, completely remove turbulence from the cloud chamber. The apparatus is held compressed by a small electromagnet which acts centrally along the moving system; this allows quick release, as required for counter-controlled expansions. Cloud chambers of various forms can be used with the machine. The present chamber, which consists of a rectangular metal box (12 cm×13 cm×5 cm), with two parallel glass sides, makes possible the photography of the tracks with weak illumination. Stereo-pictures have been made on Eastman sound-recording positive film, at apertures as low as f: 18, with No. 10 Photoflash bulbs as the source of illumination. Expansions of 18.5 percent and 11.7 percent, with alcohol-air and alcohol-argon, respectively, give excellent tracks. An injector and wick system make possible the introduction and rapid distribution of controlled amounts of vapor-generating liquids into the chamber, even while in use. A variable delay circuit is provided for adjusting the interval between the expansion and the instant of illumination. Pictures of beta-ray tracks in air and in argon, and some counter-controlled photographs of cosmic-ray bursts will be shown.

64. Cloud Chamber Study of the Ionization Produced by Cosmic Rays in the Neighborhood of a Block of Lead. EDWIN G. SCHNEIDER, *Harvard University.*—Since any geometric arrangement of Geiger counters is highly selective for a particular type of cosmic-ray phenomenon and an ionization chamber integrates all sources of ionization, random photographs taken with a cloud chamber give the most reliable picture of the relative occurrence of cosmic-ray phenomena in a piece of material. A cloud chamber containing a plate of lead 0.6×7×25 cm was placed between Helmholtz coils giving a field of 600 gauss. The magnetic field served to distinguish ionizing particles produced by radioactive contamination from cosmic-ray particles. In order to avoid secondary rays from material outside the chamber, the apparatus was placed in a building having only a light wooden roof. Stereoscopic photographs taken at random in time show that for N electrons with sufficient energy to pass through the lead there are about $N/2$ electrons stopped by the lead, $N/2$ electrons created in the lead presumably by photons, $N/10$ electron pairs produced by photons and $N/100$ showers of a more complicated nature. About three-quarters of the electron pairs have total energies between 3 and 10 MEV.

65. Shower Production and Absorption in Various Materials. J. E. MORGAN, *Duke University.* (*Introduced by W. M. Nielsen.*)—Shower production has been studied by means of G.M. counters on a series of elements, carbon, aluminum, copper, tin and lead. In addition to the non-linearity of increase in triple coincidences previously noted[1] the following additional results have been obtained: (1) With a producing material thickness of 0.58 cm lead equivalent the ratio of observed triple coincidences per unit time to observed double coincidences per unit time is a markedly increasing function of Z. (2) The departure from linearity (shower producing material thickness of 0.58 and 0.29 cm lead equivalent) in the increase in counting rate for triples is a markedly increasing function of Z. (3) With a producing material thickness of 0.58 cm lead equivalent the increased counting rate for doubles per atom of producing material varies as a power of Z slightly less than two. (4) Direct determination of absorption coefficients with various experimental arrangements indicates that the penetrating power of the shower particles varies considerably with the solid angle included in the measurements. The more penetrating showers are observed most frequently in the vicinity of the vertical direction.

[1] J. E. Morgan and W. M. Nielsen, Phys. Rev. **48**, 773 (1935).

66. New High Altitude Measurements on Cosmic-Ray Intensities. R. A. MILLIKAN, H. V. NEHER AND S. KORFF, *California Institute of Technology.*—Airplane measurements on cosmic-ray intensities to altitudes up to more than 26,000 feet have been made both in South America and in Asia, with results which show close agreement on the two sides of the earth, the apparent absorption coefficient in both localities being only slightly different from its value in the temperate latitudes. These results remove one of the chief arguments that has in the past been advanced for the great predominance of the corpuscular component of the incoming cosmic rays.

67. The Influence of Optical Excitation Energy on Transitions Involving the 2^3P_0 Level of Mercury.* G. A. ROSSELOT, *The Ohio State University.*†—Mercury vapor, with admixed purified nitrogen, at room temperature was optically excited by the radiation from 2 water-cooled quartz mercury arcs and the optical excitation energy varied from maximum to one-sixteenth maximum by means

of neutral screens. Nitrogen pressures up to 720 mm Hg were used. The intensity, I, of the "forbidden line" 2656.6 was found to vary with the excitation energy, E, approximately according to the equation, $\log I = kE$ for all pressures of N_2. Emission of 2656.6 was greatest at pressures of 300 mm, falling off gradually to about 65 percent of the maximum at 720 mm. Absorption of 2967 rose rapidly to a maximum at a nitrogen pressure of 100 mm, falling off to less than half-maximum at 720 mm. Absorption of 4047 showed a similar curve with its maximum at much lower pressure. The ratio of emission from 2^3P_0 to the number of metastable atoms as calculated from the absorption of 2967 rises sharply up to 250 mm pressure with a slower uniform rate of increase up to 720 mm. A similar ratio involving the 4047 absorption gives a sharp increase in value up to 250 mm, with a uniform drop to about 20 percent maximum at 720 mm. A third ratio between the number of metastable atoms as evidenced, respectively, by the 2967 and 4047 absorptions gives a curve similar to the last above, but with its peak at 200 mm pressure. The $Hg_2(2^3P_0)$ bands at 4800A increased sharply in intensity at low excitation energies, but slowly after approximately 1/4 the full optical excitation energy had been reached. The manner of increase was independent of the nitrogen pressure. The intensity of the bands was nearly proportional to the nitrogen pressure for a given energy of excitation.

* To be read by title.
† Now at the Georgia School of Technology.

68. Isotope Abundance and Atomic Weight of Lead from Hyperfine Structure. JOHN L. ROSE AND R. K. STRANATHAN, *New York University, University Heights.*—The relative abundance of the isotopes of lead was determined from intensity measurements of the hyperfine structure components of the lead spark line λ5372. With eleven calibrated wire screens a single order of the Fabry-Perot interference pattern was photographed with the same exposure time for each screen. The following results from densitometer measurements were obtained for the percentage abundance of the isotopes of ordinary lead: 51.5, 26.3, 21.3, and 0.8 for Pb^{208}, Pb^{206}, Pb^{207}, and Pb^{204}, respectively. The mean mass number 207.22_8 calculated from the above figures on the assumption that the masses of the isotopes are integral, agrees very well with the international chemical atomic weight 207.22. Because of the interest in the atomic constitution of the isotopes of radiogenic leads in the determination of geologic time and the origin of actinium, leads from various radioactive deposits were investigated. These results will be reported.

69. Intensity Measurements in the Arc Spectrum of Copper. HAROLD T. SMYTH, *Massachusetts Institute of Technology.*—By means of photographic photometry intensity measurements were made on a number of Cu I lines in the region 3100A–3700A. The light source was an arc run at different current strengths between pure copper electrodes and between electrodes of alloys containing different proportions of copper in order to enable reversal effects to be studied. The lines measured belong to the doublet-quartet spectrum of copper and consist mostly of transitions from negative terms to a^4P, a^4D, a^4F and m^2D using Shenstone's notation. The spectrograms were taken with a normal incidence 15,000 line per inch 21-foot concave grating used with a cylindrical lens between the slit and the grating. It was found that at the point where the locus of the vertical focus (a hyperbola) intersects the locus of the horizontal focus (the Rowland circle) a region of 1200–1500A along the Rowland circle was so nearly stigmatic that a rotating stepped sector disk in front of the slit could be used to imprint the calibration marks on the plate. A calibrated mercury arc was used for standardization.

70. Wave-Lengths of the Spectrum of H_2 from λλ3612 to 4224. NORTON A. KENT, *California Institute of Technology and Boston University.*—The wave-lengths of 511 lines are given. These were obtained from concave grating plates by using the secondary iron standards and tertiary H_2 interferometrically determined wave-lengths. A method is described by which the iron arc spectrum is photographed concomitantly with that of the hydrogen vacuum tube, thus securing greater accuracy. The plates were measured in a thermostatically controlled case. The average probable error of the means of the determinations is less than 0.002A and the results agree more closely with those of Gale, Monk and Lee[1] than of Finkelnburg.[2]

[1] Astrophys. J. **67**, 89 (1928).
[2] Zeits. f. Physik, Nov. 16, 1928, p. 27.

71. The Hyperfine Structure Interval Rule as a Means of Classifying Unidentified Spectrum Lines. H. E. WHITE, *University of California.*—The value of Zeeman effect data as an aid to the classification of spectrum lines is well known to every spectroscopist. In many atomic spectra suitable Zeeman patterns will not be easily attainable. This is particularly true in complex spectra where the hyperfine structure is large. It is in just these cases that the hyperfine structure itself, even though incompletely resolved, may be used to determine the J values of the levels involved. This method can be demonstrated by examples from various spectra, e.g., Co, La, Cb, and Mn, where both the I and J values are known for many of the stronger lines. In applying the method to the praseodymium spectrum, where attempts at an analysis have as yet proved futile, the J values involved in many lines have been determined by means of the hyperfine structure patterns. By measuring the diagonal components of a pattern the F values have been determined with reasonable certainty. Knowing the nuclear spin to be $I=5/2$ the J value of the widely split level can be determined. These results will be a valuable aid in analyzing this extremely complex rare earth spectrum. In practically all of the lines studied in Co, La, and Pr the interval rule holds to within 2 or 3 percent, which is the limit of experimental error.

72. Deep Terms in Ti VI, V VII, Cr VIII and Mn IX. S. G. WEISSBERG AND P. GERALD KRUGER, *University of Illinois.*—The deepest terms in the ions of the Cl I isoelectronic sequence are $3p^5\,{}^2P^0_{\frac{1}{2}\frac{1}{2}}$. The strong PP^0 multi-

plet arising from transitions between the $3p^4\,4s\,{}^2P_{\frac{1}{2}\frac{1}{2}}$ and the ground level has been identified in V VII, Cr VIII, and Mn IX, with the aid of constant second difference displaced frequency diagrams. The splitting in the ground level has been verified in Ti VI, V VII, Cr VIII and Mn IX by the identification of the transitions $3p^5\,{}^2P^0_{\frac{1}{2}\frac{1}{2}}-3s3p^6\,{}^2S_{\frac{1}{2}}$. These more complete data have necessitated a revision of our previous identification in Mn IX.[1] Table I gives the PP^0 multiplets and Table II gives the $^2P-{}^2S$ lines.

TABLE I. *Radiated frequencies (PP^0 multiplet).*

	Int.	$^2P^0_{1/2}-{}^2P_{3/2}$	Int.	$^2P^0_{1/2}-{}^2P_{1/2}$	Int.	$^2P^0_{3/2}-{}^2P_{3/2}$	Int.	$^2P^0_{3/2}-{}^2P_{1/2}$
V VII	(2)	612982	(5)	617902	(10)	620651	(3)	625586
Cr VIII	(8)	739634	(3)	745757	(5)	749591	(10)	755687
Mn IX	(0)	876993	(4)	884337	(5)	889568	(2)	896941

TABLE II. *Radiated frequencies ($^2P-{}^2S$).*

	$^2P_{1/2}-{}^2S_{1/2}$	Int.	$^2P_{3/2}-{}^2S_{1/2}$	Int.
Ti VI	190800	(12)	196620	(10)
V VII	211504	(5)	219161	(9)
Cr VIII	232175	(15)	242131	(20)
Mn IX	252715	(3)	265291	(7)

[1] Phys. Rev. **47**, 798 (1935).

73. Series Spectra in Mn VII and Fe VIII. P. GERALD KRUGER AND S. G. WEISSBERG, *University of Illinois.*—Lines in the extreme ultraviolet region involving the $3d\,{}^2D$, $4p\,{}^2P$, $5s\,{}^2S$, $6s\,{}^2S$ and several $nf\,{}^2F$ terms have been identified in the spectra of Mn VII and Fe VIII. These spectra have been photographed with a 21-foot grazing incidence vacuum spectrograph. Identification was facilitated by the use of displaced frequency diagrams. The values of the $3d\,{}^2D_{\frac{1}{2}}$ term and the corresponding ionization potentials are shown in Table I.

TABLE I. *Ionization Potentials in the Isoelectronic Sequence K I–Co IX.*

Ion	$3d\,{}^2D_{3/2}$ (cm^{-1})	Ionization Potential	1st Diff. (volts)	2nd Diff. (volts)
K I	13470.26	1.6618		
			8.4662	
Ca II	82097.8	10.1280		6.024
			14.4899	
Sc III	199496	24.6109		3.88
			18.3736	
Ti IV	348433	42.9845		3.53
			21.9065	
V V	526006*	64.891		3.37
			25.279	
Cr VI	(730940)	(90.17)		3.23
			28.507	
Mn VII	962001	118.677		3.24
			31.750	
Fe VIII	1219360	150.427		3.22
			34.97	
Co IX	(1503000)	(185.4)		

* Our estimate.

74. Absolute Resistivity of Na. E. PETERSON AND L. W. NORDHEIM, *Purdue University.*—The interaction of electronic motion and heat vibrations of the ionic lattice (responsible for the resistivity of metals) cannot be formulated without ambiguity as a perturbation problem. This is illustrated by the fact that with the usual model of deformable ions[1] and the Wigner-Seitz eigenfunctions now available, a resistance for Na is obtained which is 5 to 6 times the experimental value. By interpreting the transitions between progressing (exponential) electronic waves as beats between stationary (sin and cos) waves in a crystal deformed by a "frozen in" elastic wave, the problem can be attacked in a more direct way by calculating the beat frequency as energy difference between those two stationary waves. For Na the calculations can be carried out owing to its simple properties. The eigenfunctions are formed of suitable combinations of s, $p\cdots$ *W.–S.* functions in the different deformed elementary cells. A preliminary computation of the resistivity gave a result within 30 percent of the actual value. The dominating factor for the resistivity is found to be the change of volume of the ionic cells. The volume determines the normalization since, for reasons of self-consistency, the cells have to be neutral. From this it follows that a type of disorder which does not change the volume of the cells will not cause a resistance, thus confirming a supposition of Mott[2] about the resistivity of liquid metals.

[1] A. Sommerfeld and H. Bethe, *Handbuch der Physik*, Vol. 24/2, 2nd ed., paragraph 34, 36.
[2] N. F. Mott, Proc. Roy. Soc. **A146**, 465 (1934).

75. Simultaneity in the Compton Effect. LOUIS A. TURNER, *Princeton University.*—Shankland's paper[1] raises interesting fundamental questions. Consideration of the probabilities involved, more detailed than in that paper or in the one of Bothe and Geiger,[2] leads to the following results. The probability that an observed number of coincidences shall have occurred purely by chance is approximately $(2\pi n^2)^{-\frac{1}{2}}\exp(-n^2)$, (for $n>1$), n being the ratio of the excess of observed coincidences above expected random ones to the square root of the latter (root mean square fluctuation). The existence of true coincidences is indicated by a large value of n. n becomes

$$\{(1+R_{cn}/R_{ca})(1+R_{pn}/R_{ps})\}^{-\frac{1}{2}}\{R_0 ft/R_{ca}\tau\}^{\frac{1}{2}}.$$

R_{cn} and R_{ca} are, respectively, the natural rate of the electron counter and the increase in that rate attributable to source and scatterer. R_{pn} and R_{ps} are similar rates for the photon counter. R_0 is the rate of occurrence of true coincidences. $f=R_0/R_{ps}$. t is the time of observation. τ is the resolving time of the indicator of coincidences, suitably defined. The implications of the last factor would be fairly obvious by general considerations. (Necessity of large R_0/R_{ca}, f, and t and small τ to get large n.) The first factors show that n is nearly independent of the strength of the source used, provided that $R_{cn}/R_{ca}\ll 1$ and $R_{pn}/R_{ps}\ll 1$.

[1] Shankland, Phys. Rev. **49**, 8 (1936).
[2] Bothe and Geiger, Zeits. f. Physik **32**, 639 (1925).

76. Relativity and Light Nuclei. HENRY MARGENAU, *Yale University.*—The binding energies of light nuclei, as calculated with the use of neutron-proton interactions of various types (Wigner, Heisenberg, Majorana), appear as differences between large potential energies and slightly

smaller kinetic energies of the particles involved. In the case of the deuteron, for example, if the range of the neutron-proton force is taken to be about 10^{-13} cm, the relative kinetic (zero-point) energy of the particles which is necessary to account for the observed binding energy corresponds to a relative speed greater than half the velocity of light. Thus arises the question as to the error committed in using a nonrelativistic wave equation. A relativistic formalism for the two-body problem does not exist; in particular, it is not permissible to use reduced masses. It seems probable, however, that the magnitude of the error may be correctly estimated by employing the simple relativistic Schrödinger equation, which takes account only of the change in mass. The results of such a calculation are presented. For ranges around 2×10^{-13} cm the "relativistic" depth of the potential well differs from the ordinary depth by only three percent, but for ranges of 10^{-13} cm, by more than ten percent. A "relativistic" calculation of the binding energy, based on the ordinary depth of the well (which is 10 percent too low), yields a result which may be in error by a factor 3.

77. The Approximate Solution of Nuclear Three and Four-Body Problems. EUGENE FEENBERG AND SIMON S. SHARE, *University of Wisconsin.*—It is possible to compute the normal state eigenvalues of nuclear three and four-body problems with reasonable accuracy by solving suitably chosen separable wave equations. The potential function in the separable problem is determined by the conditions: (a) that it fits the actual physical potential as closely as possible when all the particles are close together and (b) has the same average value as the physical potential when averaged over a simple approximate wave function. Condition (a) can be satisfied without difficulty if the power series expansions of the potentials contain only even powers of the distances between the particles. The usual first and second order perturbation theory is applicable when the effective range of the forces is sufficiently great and yields simple expressions for the eigenvalues in terms of the effective breadth and depth of the potential wells. The normal state eigenvalue of the actual physical problem lies above the corresponding eigenvalue of the related separable problem. If the potential is symmetrical in the coordinates of all the particles the two eigenvalues do not differ appreciably. In this last case the results obtained from the separable equation are identical with those given by the "equivalent" two body method.[1]

[1] Feenberg and Knipp, Phys. Rev. **48**, 906 (1935).

78. Interaction of Nuclear Particles. LLOYD A. YOUNG, *Carnegie Institute of Technology.*—Recent experiments on proton-proton scattering throw considerable light on the magnitude of the interaction of like nuclear particles (antiparallel spins), and from these results a new calculation of the effective potential hole has been made. This, when combined with the author's previous estimate, allows one to make an estimate of the magnitude of the higher order effects to which Weizsaecker has called attention. The question of the existence of α-particles in heavy nuclei will be discussed.[1]

[1] See Bohr's article in Nature **137**, 344 (1936).

79. Wave Functions in Halite. W. SHOCKLEY, *Massachusetts Institute of Technology.*—The Wigner and Seitz method of cellular potentials has been applied to the calculation of wave functions in NaCl. A renormalized Hartree field has been used around the Cl and the Prokofjew field around the Na. The relative heights of the potentials are determined by use of Madelung's number. The problem of joining the functions at the cell boundaries has been treated by the Slater method of fitting ψ and ψ' at midpoints. For the outer Cl electrons a reasonable approximation is to join at Cl–Cl midpoints only. This gives rise to a face-centered lattice for which solutions of the Slater conditions have been found by Krutter. Several new solutions have been derived which allow fairly accurate energy contours in momentum space to be drawn for the Cl $3p$ band. If the joining is made at Cl–Na midpoints alone, a large number of unsatisfactory zero-width bands arise; while if both Cl–Cl and Cl–Na are used, the equations become too complicated to handle very satisfactorily. For all three cases it can be seen, however, that there are no partially filled bands, which is consistent with the absence of conductivity.

80. Stability of Degenerate Electronic States in Polyatomic Molecules. H. JAHN, *Davy Faraday Laboratory, Royal Institution, London,* AND E. TELLER, *George Washington University, Washington, D. C.*—As a general rule the electronic state of a polyatomic molecule can be degenerate only if the atomic configuration has a sufficiently high degree of symmetry. If the atomic nuclei are displaced the degenerate state may split up and if the splitting is a linear function of the displacement the original symmetrical configuration, and with it the original degenerate state, does not correspond to an equilibrium state of the molecule. A group-theoretical investigation shows that except for molecules in which all atoms lie on a straight line only undegenerate states or the doubly degenerate states of molecules with an odd number of electrons can correspond to stable configurations. However, in the case of spin degeneracy and small spin-orbit interaction a nearly symmetrical configuration might be stable and the electronic state is then split to a very small extent. The same is true for degenerate orbits of electrons in inner incomplete shells if their interaction with the other atoms is small.

81. Some Theorems Concerning Approximate Wave Functions. HUBERT M. JAMES, *Harvard University.*—Let an approximate wave function, ψ^1, for the ground state of a system be expressed as $\psi^1=a_1\psi_1+(1-a_1^2)^{\frac{1}{2}}\psi_E$, where ψ_1 is the correct function for this state, and ψ_E is orthogonal to ψ_1 and indicates the character of the error in ψ^1. The quantities, $\epsilon_1=\int\psi^1(H-E_1)\psi^1 dv$, and $(\delta_1)^2=\int[(H-E^1)\psi^1]^2 dv$, which vanish as ψ^1 approaches ψ_1, may serve as criteria for the accuracy of ψ^1. Between these quantities and ϵ_E and δ^2_E, computed by replacing the function ψ^1 by ψ_E in the above definitions, there exists the relation $\delta_1^2=\epsilon_1[\epsilon_1+(\delta^2_E-\epsilon_1^2)/\epsilon_E]$. The use of ϵ_1 and δ_1 as criteria for the goodness of ψ^1 is discussed in connection with this relation and the results of computations on the helium atom. A lower limit for the energy of the

ground state of a system can be obtained from the inequality, $\epsilon_1 \leq \delta_1^2/(E^2-E^1-\delta_2)$, where $E^2=\int\psi^2 H\psi^2 d\tau$ and $\delta_2=\int[(H-E^2)\psi^2]^2 d\tau$, ψ^2 being a sufficiently good approximation to the function for the first excited state. This lower limit converges more rapidly on the correct value than that previously available; the problem of further improving this convergence will be considered. Theorems relating to variational methods of treating excited states will be presented.

82. Theory of Brillouin Zones and Symmetry Properties of Wave Functions in Crystals. L. BOUCKAERT AND R. SMOLUCHOWSKI, *Institute for Advanced Study, Princeton.*—It is well known that if the interaction between the electrons in a metal is neglected, the energy spectrum has a zonal structure. The problem of these "Brillouin zones" is treated here from the point of view of group theory. In this theory, a representation of the symmetry group of the underlying problem is associated with every energy value. The symmetry, in the present case, is the space group, and the main difference as compared with ordinary problems is that while in the latter the representations form a discrete manifold and can be characterized by integers (as, e.g., the azimuthal quantum number), the representations of a space group form a continuous manifold, and must be characterized by continuously varying parameters. It can be shown that in the neighborhood of an energy value with a certain representation, there will be energy values with all the representations, the parameters of which are close to the parameters of the original representation. This leads to the well-known result that the energy is a continuous function of the reduced wave vector (the components of which are parameters of the above mentioned kind), but allows in addition to this a systematic treatment of the "sticking together of Brillouin zones." The treatment is carried out for the simple cubic and the body centered and face-centered cubic lattices, showing the different possible types of zones.

83. Interpretation of the Absorption Spectra of Crystals and Solutions of Rare Earth Salts. CECIL B. ELLIS, *University of Michigan.*—It is believed that the first definite identification of the electronic transition causing the color of a solid has been made. Analysis of the data of Prandtl and of Spedding shows that the absorption lines of crystals and solutions of trivalent rare earth salts are due to "forbidden" transitions between the ground state of the metal ion and the higher levels of the normal configuration, $4f^n$. The regular progression with Z of the long wave end of the absorption, from Pr in the infrared to Gd in the ultraviolet and back to the red with Tm, is a counterpart of the variation of the distance from the lowest to the next highest level in the sequence of $3d^n$ configurations of gaseous spectra. The only gaseous f^n configuration yet analyzed, La II $4f^2$, exactly matches the Pr ($4f^2$) absorption spectrum. Calculation of the expected multiplet separations by Goudsmit's formulas, and the use of Bethe's predictions as to the splitting of the levels by the crystal fields, have led to the identification of the lowest excited terms (causing the longest wave bands) of the following elements (the normal states being known from Hund's magnetic work): Pr, $^3I_4$, $^3P_{0,1,2}$; Nd, $^4I_{3\frac{1}{2}}$, $^4G_{2\frac{1}{2},3\frac{1}{2},4\frac{1}{2},5\frac{1}{2}}$, $^2L_{7\frac{1}{2},8\frac{1}{2}}$; Sm, $^6F_{1\frac{1}{2},2\frac{1}{2},3\frac{1}{2}}$?; Eu, $^8L_{6,7}$; Gd, $^9H_{2\frac{1}{2},2\frac{1}{2}}$, $^6I_{3\frac{1}{2},4\frac{1}{2}}$; Tb, $^5K_{7,8,9}$; Dy, $^6H_{4\frac{1}{2},3\frac{1}{2},2\frac{1}{2}}$; Ho, $^5I_{8,9,10}$. LS coupling holds well near the beginning of the series (strict interval rule in Pr and Nd), but not so strongly further on. Transitions up to $\Delta J=5$ seem certain but those with small ΔJ are strongest. The Zeeman patterns for Gd are also in accord with the above interpretation.

84. A Model for the One-Dimensional Schrödinger Equation. E. M. PURCELL, *Harvard University.*—A simple electrical and mechanical system has been set up, which is described by: $\ddot{\theta}+Cf(t)\theta=0$. Here $f(t)$ is an arbitrary function of the time which may have both positive and negative values. The model consists of a small coil suspended in a uniform magnetic field, with its axis normally parallel to this field, together with a means for varying the current in the small coil according to some specified $f(t)$. In particular, if we take $f(t)=k(E-V(t))$, where $V(x)$ is the potential in a one-dimensional Schrödinger problem, and k is an appropriate scale factor, the movement of the coil gives directly $\psi(t)$, where $\psi(x)$ is a solution of the wave problem. The apparatus permits the initial conditions to be controlled, and a given $V(t)$ to be repeated at will. E (corresponding to a constant current in the small coil) is then adjusted until satisfactory behavior is obtained at the final boundary. Such "good" values of E lie close to the eigenvalues of the wave problem; the error arises from the fact that one can use only a finite range of the independent variable. It is convenient to locate the proper E values visually, but the corresponding curves of ψ have also been recorded photographically on a revolving drum

85. Influence of Certain Ions on the Structural Temperature of Liquid Water. J. R. COLLINS AND C. MORAN, *Cornell University.*—In their paper on the structure of liquid water, Bernal and Fowler[1] predicted that the effect of small dissolved ions is to reduce the *structural temperature* of liquid water, and that large ions should increase the structural temperature. The authors have investigated the effect of dissolving the chlorides of a number of metals on the spectral position and intensity of certain near infrared absorption bands of liquid water. Since these bands change their character when the temperature of the water is changed, their changes were taken as an indication of the structural temperature of the water in the solutions. It was found that small ions such as those of lithium and magnesium caused a decrease in the structural temperature of the water while large ions such as those of caesium and barium caused an increase in the structural temperature of the water. The structural temperature of the water in the solutions was found to be in the same order as the quotients of the charge and radius of the ions in solution in general agreement with the predictions of Bernal and Fowler.

[1] J. Chem. Phys. 1, 515 (1933).

86. Artificial Radioactivity of Very Long Life. EDWIN MCMILLAN, *University of California.*—It has been known for some time that Be^{10} is produced by the bombardment of beryllium with deuterons, that its mass is probably slightly

above that of B^{10}, and that it is not radioactive with any "ordinary" decay period. Last June a beryllium-aluminum alloy target used as a neutron source for about a year in the Berkeley magnetic resonance accelerator was removed, after having had enough exposure to deuterons to build up an appreciable amount of even a very long period activity. Electroscope observations since then show that there is a long period present. During the past four months (after the decay of the inevitable P^{32} contamination) there has been no certain change in the amount of activity within the accuracy of the measurements (about 3 percent), leading to a lower limit of about 10 years for the half-life. The assignment of this activity to Be^{10} is as yet based only on reasonableness, but chemical tests will be made later. The yield is compatible with a very much longer life. Another long period was found on pieces of Mo and brass taken from parts of the apparatus struck by the deuteron beam. This has a half-life of about 3 months, and probably arises from some common contaminant, perhaps $C^{13}+H^2 \rightarrow C^{14}+H^1$. The electrons from both of these active substances are very slow. The ionization produced by the beryllium target is reduced to 1/3 by 0.0008 g/cm² of Al, and to zero by 0.08 g/cm². The thicknesses required to produce the same absorptions of the Mo brass electrons are 0.003 and 0.08. The absorption curves are seen to differ greatly in shape, although they have the same end point.

87. Variation of Range with Angle of the Disintegration Alpha-Particles of Li. A. ROBERTS, T. ZANDSTRA, R. CORTELL AND F. E. MYERS, *New York University, University Heights.*—The range of the alpha-particles emitted by Li^7 under proton bombardment has been measured at several angles to the incident beam of protons. Measurements were made at bombarding voltages of 200 and 240 kv, and the results have been found to be fully in accord with the predictions of the principle of conservation of momentum, when the straggling due to the penetration of the target by the proton beam is taken into account. A method of calculating the straggling is given, and the observed and calculated results are compared. The question of the formation of $_4Be^8$ in this reaction is discussed in view of the results obtained. It is shown that if $_4Be^8$ is formed and subsequently disintegrates into two alpha-particles without the emission of a gamma-ray, it must have a mean life of not more than $3 \cdot 10^{-14}$ second.

88. The Artificial Radioactivity of Copper, a Branch Reaction. S. N. VAN VOORHIS (National Research Fellow), *University of California.*—The artificial radioactivity produced in copper by bombardment with approximately six million volt deuterons has been studied. Two radioactive substances are produced, corresponding to the two stable isotopes of copper. The half-life of the longer component, which has been studied, is found to be 12.8 ± 0.1 hours. Examination in the Wilson chamber showed both positrons and electrons in roughly equal numbers. By covering the sample with paraffin, the annihilation radiation produced by the positrons could be measured with a pressure ionization chamber. The positrons are found to have exactly the same half-life as the total beta-activity. An absorption curve in lead shows no evidence of any gamma-rays other than the annihilation radiation. An excitation curve was also measured by the method of stacking thin foils. This is found to be the same for positrons and total activity, and to follow the theoretical curve of Oppenheimer and Phillips[1] quite accurately through the range of applicability (approximately one to four million volt deuterons). Since stable isotopes of both zinc and nickel of mass 64 have been reported, it seems likely that this is a case of branching, radio-copper of mass 64 going either to nickel or zinc with the emission of a positron or an electron. Analysis of Wilson chamber photographs in a magnetic field by the method described by Kurie, Richardson, and Paxton[2] gives a value for the upper limit of 0.8 MEV for both positives and negatives on the basis of the Konopinski-Uhlenbeck modification of the Fermi theory. The ratio of negatives to positives in the photographs is about three to two.

[1] Oppenheimer and Phillips, Phys. Rev. **48**, 500 (1935).
[2] Kurie, Richardson and Paxton, Phys. Rev. **49**, 368 (1936).

89. Deuteron-Induced Radioactivity in Bismuth. J. J. LIVINGOOD, *University of California.*—Bismuth bombarded with 22-cm range deuterons exhibits an electronic radioactivity with a half-life of 5 days, as measured with a quartz-fiber electroscope. Linear amplifier observations show an alpha-particle activity which increases daily for about three weeks and then is sensibly constant. The range of these particles has been compared to that of natural polonium and is found to be the same, within the half-mm error of measurement. Inasmuch as radium E emits electrons with a half-life of 5 days, and since the alpha-activity of polonium growing in fresh Ra E is known to rise to a maximum in 23 days and then to decline to half-value in 140 days, these experiments are interpreted as the formation of Ra E by bismuth capturing the neutron out of the deuteron, according to the equation $_{83}Bi^{209}+{}_1H^2 \rightarrow {}_{83}Bi^{210}$ (i.e., Ra E)$+{}_1H^1$, followed by the natural decay of Ra E into polonium by the emission of an electron and the subsequent decay of this into lead by the loss of an alpha-particle. As far as the half-lives and the range of the alpha-particle are concerned, these synthetic elements appear to be identical with the natural varieties. The shape of the alpha-particle range curve gives no suggestion of resonance capture.

90. Transmutation of Chlorine and Potassium by Th C′ Alpha-Particles. E. POLLARD AND C. J. BRASEFIELD, *Yale University.*—Under bombardment by fast alpha-particles from Th C′ the elements chlorine and potassium are found to emit protons. In the case of potassium these are most probably due to the reaction

$$_2He^4+{}_{19}K^{39} \rightarrow {}_{20}Ca^{42}+{}_1H^1+Q.$$

The presence of two chlorine isotopes renders the interpretation of the chlorine reaction uncertain, but it is likely that the more abundant isotope $_{17}Cl^{35}$ is responsible for the protons observed, according to the equation

$$_2He^4+{}_{17}Cl^{35} \rightarrow {}_{18}A^{38}+{}_1H^1+Q.$$

The chlorine protons are emitted in three well-defined groups and those from potassium show two clearly-defined groups with indications of a third. Experiments with reduced energy alpha-particles show that none of these groups is due to resonance levels and therefore that they afford measures of the transmutation energy changes Q for ground and excited states of the nuclei. The values of this energy change in MEV are given in the table together with values for the transmutation of phosphorus as found by Paton.

Potassium	Chlorine	Phosphorus
−3.3	−4.0	−3.0
−2.2	−2.2	−1.5
−1.0	0.0	0.0

There is therefore a broad similarity between the three elements which may be linked with the fact that their nuclear masses are of the form $4n+3$. The maximum proton ranges from potassium and chlorine enable the masses of $_{20}Ca^{42}$ and $_{18}A^{38}$ to be calculated. These are, respectively, 41.956 ± 0.003 and 37.9753 ± 0.0016.

91. Apparatus for the Automatic Analysis of Fluctuations in Radioactive Disintegration. Raymond L. Driscoll, *University of North Carolina.* (*Introduced by Arthur E. Ruark.*)—On the basis of a design suggested by Dr. Lee Devol, a circuit has been developed which records the total number of counts produced by a radioactive source, and also the number of intervals between counts which exceed a chosen interval length t. Several such units can be operated in parallel to record the number of intervals greater in length than the chosen values t_1, t_2, etc. This device eliminates the labor involved in measuring intervals recorded on a chronograph sheet; it makes it possible to use very large numbers of counts, in experiments designed to test either the Bateman fluctuation law, or the ability of a detector to record random events correctly.

92. Time Distribution of Counts Due to a Constant Source and a Radioactive Substance Which It Produces. Lee Devol, *University of Pittsburgh,* and Arthur Ruark, *University of North Carolina.*—An expression is obtained for the size-distribution of the time intervals between counts caused by a constant source and a radioactive substance which it produces, on the assumption that the detecting device (a Geiger counter, for example) is out of operation for a definite time τ after a count but has constant efficiency, for rays or particles of given characteristics, at all other times. It is assumed that each artificially radioactive atom, of decay constant λ, gives only one ray (or particle), and that the rays from the constant source are homogeneous. Let F be the average rate of arrival of rays from the constant source alone. Then the number of intervals between counts which are greater than a chosen value t, divided by the total number of intervals, is

$$[1-\delta(e^{-\lambda\tau}-e^{-\lambda t})/D]\exp[-\alpha F(t-\tau)-\beta F(1-e^{-\lambda(t-\tau)})/\lambda].$$

In this formula δ, D, α and β are functions depending on the counter efficiency, the probabilities that rays of the various classes involved will produce ionization within the counter, and the probability that a primary ray striking the experimental arrangement will produce an artificially radioactive atom.

93. Protection Against the Harmful Effects of Ionizing Radiations. G. Failla, *Memorial Hospital, New York City.*—In view of the rapidly increasing number of physicists working with radioactive substances (natural or artificial), neutrons, etc., it is timely to point out the dangers of overexposure to ionizing radiations, and to suggest precautionary measures, based on our experience in the handling of large quantities of radium at the Memorial Hospital. The desirability of this warning is apparent from the number of students and instructors who have been burned by x-rays in recent years, in spite of the fact that the danger of overexposure to x-rays is generally known.

94. The Temperature Coefficient of the Photoelectric Work Function of Barium. R. J. Cashman and N. C. Jamison, *Northwestern University.*—In work previously reported,[1,2] application of Fowler's method was made to determine the photoelectric work functions of barium and calcium surfaces. Further refinement in the technique of making measurements has increased the accuracy so that an estimation of the temperature coefficient of the work function may be obtained for the temperature interval, 20° to 120°C. The results of several determinations yielded a positive value of $(1.4\pm0.7)\times10^{-5}$ volt/deg. C. The extreme constancy of the photo-emission properties of the surface, even though it repeatedly experienced 100 and 140-degree temperature changes, was of primary importance in the work. The mean value of the work function at room temperature was 2.5067 volts, the average deviation from the mean for a series of five plots being 0.0004 volt. That this value is not fully in accord with that previously reported[1] might well be attributed to a difference in crystal structure of the surface or slightly different chemical purity.

[1] R. J. Cashman and N. C. Jamison, "Photoelectric Work Function of Barium," Phys. Rev. **49**, 195 (1936).
[2] N. C. Jamison and R. J. Cashman, "The Photoelectric Work Function of Ca and Photoemission from Non-Homogeneous Surface," Phys. Rev. **49**, 201 (1936).

95. The Energy Distribution of Photoelectrons from Sodium. A. G. Hill and L. A. DuBridge, *University of Rochester, Rochester, N. Y.*—Experimental energy distribution curves have been obtained from clean sodium over a range of wave-lengths from 2400A to 4350A. These are compared with the theoretical curves derived from various models proposed for the photoelectric effect,[1] and the agreement between theory and experiment is good for all wave-lengths for the high energy end of the curve where the Fermi function is the controlling factor. A discussion will be given of the possibility of improving the agreement between theory and experiment in the low energy region. If impurities are introduced in the photo-cell the threshold shows a large shift toward the red and the curves no longer agree with the theory, but show quite large "tails" as though the surface were at a much higher temperature. An investigation is now being made of the possibility of a photoelectric determination of h/e taking into account the temperature effect previously ignored.

[1] See, for instance, Rudberg, Phys. Rev. **48**, 811 (1935).

96. Photoelectric Emission from Alkali Deposits on Other Metals. H. C. Rentschler and D. E. Henry, *Westinghouse Lamp Co., Bloomfield, N. J.*—The progressive

change in sensitivity to the light through various filters was noted as the alkali distilled and deposited on sputtered surfaces of different metals prepared as previously described.[1] The long wave-length sensitivity so obtained and generally attributed to the formation of a thin film of the alkali was surprisingly small. Thus the maximum red sensitivity of potassium on a sputtered molybdenum surface was many times smaller than for a similar deposit on a molybdenum surface cleaned by electron bombardment. When the potassium was similarly deposited on a metal surface at sufficiently low temperature no red sensitivity was obtained. These tests indicate that the red sensitivity is the result of a reaction between the alkali and the residual impurity on the base metal and not due to the physical nature of the film.

[1] Rentschler and Henry, Rev. Sci. Inst. **3**, 794 (1932).

97. Collisions of Fast Electrons with Helium Atoms. A. L. HUGHES AND S. S. WEST, *Washington University.*—When a charged particle is scattered by another particle which has a Coulomb field, quantum mechanics and classical mechanics give the same formula when the particles are different, and different formulas when they are identical. In the particular case of scattering of electrons by electrons, quantum mechanics predicts a smaller scattering than does classical mechanics, in a ratio which has a minimum of 1 : 2 at 45°. We have investigated the scattering of 2000-volt electrons by helium atoms. For this energy value we can consider the incoming electron to be deflected by the nucleus, *or* by an atomic electron, and disregard the binding energy of the atomic electron, and so use the experimental results to compare the scattering by the nucleus with that by an atomic electron. An electron scattered by the nucleus loses practically no energy, while that scattered by an atomic electron loses more energy the greater the angle of scattering. The ratio of the number of electrons scattered by the nucleus to that scattered by the atomic electrons has been compared with the values predicted by the theories. The results are decisively in favor of the quantum-mechanical theory.

98. The Positive Ion Work Function of Molybdenum. H. J. GROVER, *Cornell University.* (*Introduced by L. P. Smith.*)—A method of utilizing a mass spectrograph for the measurement of positive ion currents from molybdenum as a function of temperature is described. These measurements yield a value for the positive ion work function Φ_{+0}, which is higher than any previously reported. This value is found to balance the familiar energy cycle, $\Phi_{+0}+\Phi_{-0}=V+U$, within experimental error when standard values for the electron work function Φ_{-0}, the ionization potential V, and the latent heat of condensation of neutral atoms U are used.

99. Equations of State of One- and Two-Dimensional Gases of Hard Elastic Spherical Atoms of Finite Size. LEWI TONKS, *General Electric Company.*—The attempt to solve the ideal two-dimensional case in connection with monatomic-film theory led to the consideration of the one-dimensional case also. Rigorous integration in generalized space gives $f=nkT/(1-\theta)$ for the force exerted by the linear array, where $n=$atoms cm^{-1} and $\theta=n/n_0$, $n_0=$atoms cm^{-1} for close packing. The probability distribution of the distance between an atom and its next but one neighbor is what would be calculated from treating the surrounded atom like a (simple atom) gas and by using Boltzmann's equation. The plane gas at low concentrations follows the law $\tau=nkT(1+1.813\theta+2.57\theta^2)$. At high concentrations ($\theta\rightarrow 1$) the atoms tend toward a hexagonal array, but a square array can be arranged for by proper choice of boundary. In that case $\tau=nkT/(1-\theta^4)$. The same law is found for the hexagonal case when all atoms are thought of as confined within equal regular hexagons (noting that θ(hexagon) differs from θ(square) for the same n). This is not thought to affect the equation of state beyond the first order of small quantities, for confinement of the atoms of the linear gas in equal cells leaves its equation of state unchanged; and confinement of the atoms of the square array in square cells leaves its equation of state unchanged to the first order of small quantities.

100. The Temperature Dependence of Field Current Emission. R. T. K. MURRAY, *Johns Hopkins University.*—By the use of a Geiger-Müller counter previously described for recording field current electrons, the dependence of field current emission on temperature has been measured. The cathode consisted of a hollow brass sphere which could be varied over the temperature range from liquid air to boiling water and the electron emission was studied as a function of temperature, the field being kept constant. Current temperature curves were obtained of the form $i=a+bT^2$ which is in agreement with the theoretical calculations of Houston.[1] The constant a in the above expression gives the electron current to be obtained under the given field at the absolute zero. Calculations showed that the effect of thermal expansion on the current was negligible. The distance of the sphere from the plane was so adjusted that the change of the field with the temperature due to thermal expansion was a minimum over the temperature range used. Difficulty was encountered, however, by the effect of temperature on the microscopic geometry of the surface.

[1] W. V. Houston, Phys. Rev. **33**, 361 (1929).

101. Some Properties of Caesium and Oxygen Films on Tungsten. JOHN BRADSHAW TAYLOR AND IRVING LANGMUIR, *General Electric Company.*—A pure tungsten filament was coated with oxygen at low pressures (10^{-8} to 10^{-10} mm), the oxygen being admitted by diffusion through the walls of a heated silver tube. Oxygen films prepared in this way require no "activation" to allow increased electron emission when caesium is adsorbed on them. OW films undergo a rearrangement when heated in the presence of adsorbed Cs, with accompanying changes in electron emission from the Cs–O–W film. Measurements of the amount of Cs adsorbed indicate that the concentration of oxygen in these films is much less than that corresponding to a single layer. The heat of evaporation of oxygen from these dilute films varies from 143 kcal. to 168 kcal. as the oxygen concentration approaches zero. Oxygen diffuses into tungsten at temperatures as low as 1200°K at oxygen pressures lower than

10^{-7} mm. After such diffusion has taken place, the filament can be cleaned in the absence of oxygen and then deactivated by diffusion of oxygen to the surface. A preliminary value for the heat of diffusion is 83 kcal.

102. Thoriated Tungsten Activation as Revealed by the Electron Microscope. A. J. AHEARN AND J. A. BECKER, *Bell Telephone Laboratories, Inc.*—An electron microscope was used to study the activation of thoriated tungsten ribbons. After flashing at 2600°K the electron image at 1500°K shows that only a few small areas emit profusely, the rest of the filament being barely visible. By heating the filament at 1700°K these areas first grow greatly in intensity and in size. Then as they continue to grow in size their intensity decreases. These active spots are thought to be produced by the eruption and migration over the surface of pockets of thorium. From estimates of the sizes of the spots and the current densities therefrom the number of thorium atoms in an eruption is found to be 5×10^{10}. Optical microphotographs of the same filament show many pocketlike dots the size and number of which account for the known thoria content of the filament. On this basis, there are from 1×10^{10} to 200×10^{10} thorium atoms per pocket in good agreement with that calculated from the eruptions. The experiments show that (1) a large part if not all of the thoriation occurs in the form of eruptions; (2) when an eruption occurs all the thorium of a thorium oxide granule escapes.

103. Anomalous Secondary Electron Emission. LOUIS MALTER, *Cornell University.*—Aluminum which has been oxidized electrolytically is coated with a monomolecular layer of caesium oxide. If this surface is now bombarded with an electron beam, it charges positively because of the high normal secondary emission ratio of caesium oxide. This positive charge cannot escape through the highly resistant aluminum oxide. If the normal secondary electrons are collected by an adjacent positive electrode, the surface of the target can be made sufficiently positive to cause "cold emission" from the underlying aluminum. This emission, which may be thousands of times greater than the current in the primary beam, is referred to as anomalous secondary emission. It is found that the anomalous emission is a power function of the collector potential and primary beam current density. The anomalous emission persists even after the removal of the primary beam, decaying very slowly in certain cases. Light from a tungsten filament causes a decrease in the anomalous emission as well as a speeding up of decay characteristics. Reversal of the collector potential while the beam is incident upon the target causes the anomalous emission to build up very slowly when the collector potential is restored to its normal positive potential.

104. A Macroscopic Theory of Metallic Conduction. ERNST WEBER, *Polytechnic Institute of Brooklyn.*—Electric conduction is conceived as analogous to the flow of a viscous compressible fluid in a tube. The theory leads to expressions for the resistance change in a magnetic field which agrees well with the experimental results of Kapitza, of Bridgeman and of the author. The hypothesis of compressibility is supported by experiments from which also first numerical values for the compressibility coefficient as well as the coefficient of viscosity can be obtained. In the theory it is assumed that the viscosity effects are proportional to the square of the magnetic field strength, a reasonable assumption amply supported by the excellent agreement with experimental results.

105. Soft X-Ray Absorption of Lithium and Its Halides. H. M. O'BRYAN, *Harvard University.*—The absorption spectra of LiF, LiCl, LiBr, LiI, and lithium metal have been photographed over the region 170A to 700A on a small plane grating vacuum spectrograph. The absorbing materials were less than 1μ thick and were prepared by distilling onto celluloid films which were about 200A thick. The absorption bands were found by comparing the spectra of a hot spark transmitted by celluloid with that transmitted by an absorbing film on celluloid. The bands show a width of from 2 to 4.5 volts at the head with less intense continuous absorption extending to shorter wave-lengths. The intensities of the higher orders of short wave-lengths obscure the details of absorption above 700A shown by the valence electrons of these substances. The wave-lengths in Angstroms for the centers of these bands are listed below.

	K of Li		
Lithium	214A		
LiF	192A		
LiCl	205A	M_I of Cl 417A	
LiBr	200A	N_I of Br 399A	
LiI	204A	O_I of I 444A	$M_{IV\ V}$ of I 224A

106. Energy Levels of the Hydrogen Molecule. G. H. DIEKE, *Johns Hopkins University.*—The analysis of the spectra of HD and D_2 has led to a number of interesting results which could not have been obtained at all or only with great difficulties from the H_2 spectrum alone. Of the important low-lying levels with one electron in the ground state $1s$ and the second electron in a one or two quantum state all have been satisfactorily identified in H_2 by Richardson and others except $1s\sigma\ 2s\sigma\ {}^1\Sigma$. An empirical level ${}^1X$ was identified with this state by Richardson and the author but there were several difficulties to this so that Weizel classified it as $(2p\sigma)^2\ {}^1\Sigma$. The complete analysis of the system ${}^1X\rightarrow 2p\ {}^1\Sigma$ for H_2, HD and D_2, of which a part had been previously found by Richardson and Davidson, has removed the difficulties. The fact that the $V=0$ level is completely normal shows that the irregularities occurring in the higher vibrational levels must be true perturbations and not Λ-decoupling. It is very probable that the perturbations arise from interaction with the $(2p\sigma)^2\ {}^1\Sigma$ level the approximate position of which is thus located. This level must be absent in the triplet system which accounts for the absence of perturbations in $1s\sigma\ 2s\sigma\ {}^3\Sigma$.

107. The Magnetic Rotation Spectra of Polyatomic Molecules in the Ultraviolet. P. KUSCH AND F. W. LOOMIS, *University of Illinois.*—The apparatus previously used for the study of magnetic rotation spectra in the visible and infrared has been modified for use in the ultraviolet. The polarizing device is a pair of quartz Rochon prisms with components in optical contact. The object is to see whether the simplification often found in magnetic rotation spectra

will help in the analysis of the complicated electronic spectra of polyatomic molecules, most of which occur in the ultraviolet. The spectra of this type which have been found so far are those of CS_2, SO_2 and formaldehyde. In each case the extremely complicated structure observed in absorption is replaced by a spectrum consisting of fairly sharp lines which may readily be correlated to band heads. In the case of CS_2 the magnetic rotation spectrum occurs in the region 3100–3600A, where the absorption heads themselves are well defined. In the region to shorter wavelengths, where the band heads are diffuse, the magnetic rotation spectrum has not been observed. The apparatus is being further modified to permit the investigation of spectra below 3000A.

108. The Band Spectrum of As_2. G. D. KINZER AND G. M. ALMY, *University of Illinois.*—The band spectrum of As_2, previously photographed between 2400A and 3700A, has been extended to 7000A by the use of a quartz discharge tube operating in a furnace. The $A \rightarrow X$ and $B \rightarrow X$ systems have thus been photographed and analyzed to $v''=72$, corresponding to a vibrational energy (G) of 3.1 volts, at which $\Delta G=243$ cm^{-1}. The new intervals ($v''=44$ to $v''=72$), when fitted to a power series in $(v+1/2)$, converge at $G=3.8$ volts. The appearance of predissociation in state A at $v=9$ had indicated a heat of dissociation of the ground state of 3.9 volts, or 3.0 volts, depending upon assumptions as to atomic states near predissociation. The extension of the spectrum definitely excludes the latter value, supports the former, and indicates that states A and B dissociate into $^4S+^2D$.

Two new systems of bands, called D and E, of the As_2 molecule have been observed. The D system whose origin is $\nu_{0,0}=24{,}599.4$ cm^{-1} has the same ground state as the A, B and C systems while in the excited state $\omega_e'=337$ cm^{-1}. The E system is composed of two sets of bands. Either set can be arranged into a square array yielding the same vibrational constants, $\omega_e'=335$ cm^{-1} and $\omega_e''=311$ cm^{-1}. Corresponding bands in either set are separated by an interval of 163 cm^{-1}, and are matched in intensity. The origins of the two sets are at 16,348.2 cm^{-1} and 16,185.0 cm^{-1}. The bands of the E system are degraded to the violet while the bands of the A, B, C and D systems are degraded to the red.

109. Band Spectra of BH and BH^+. G. M. ALMY AND R. B. HORSFALL, *University of Illinois.*—The boron hydride spectrum was excited in a water-cooled hollow cathode and photographed with a 21-foot grating. Three prominent systems were observed. One, with principal R head at 3768A (presumably the (0,0) band), consisting of narrow doublet P, Q and R branches, is new. It is due to a $^2\Pi$ (reg.)$\rightarrow ^2\Sigma$ transition. For $K<10$ the $^2\Sigma$ doubling is negligible, since $\Delta_2F_1''(K)=\Delta_2F_2''(K)$. $B_0''=12.36$ cm^{-1}, $r_0''=1.22$A. For the $^2\Pi$ state, $B_0'=11.57$ cm^{-1}, $A=12.2$ cm^{-1}, $A/B_0'=1.05$. It is therefore between the two possible values of A/B corresponding to pure case b according to Hill and Van Vleck. Consideration of missing lines supports this analysis. This system is due to BH^+ and is analogous to the green BeH system and the AlH^+ bands near 3600A. The previously reported[1, 2] singlet and triplet systems were also found. The analysis of the $^1\Pi \rightarrow ^1\Sigma$ system has been extended to include the (2,2) band. No off-diagonal bands have been found. The (0,0), (1,1) and (2,2) bands exhibit dissociation by rotation at $K'=25$, 21, 14, respectively. The heat of dissociation of the $^1\Pi$ state must be less than 0.75 volt. In the triplet system, previously reported[1] as $^3\Pi \rightarrow ^3\Sigma$, the P and R branches have been resolved into very narrow equally spaced triplets (total width, 4 cm^{-1} at $K''=2$), and the Q branch into doublets. The behavior of the Δ_2F's for low K requires that the transition be $^3\Sigma \rightarrow ^3\Pi$. For this system $B_0'=12.13$, $B_0''=12.72$.

[1] W. Lochte-Holtgreven and E. S. Van der Vluegel, Zeits. f. Physik **70**, 188 (1931).
[2] R. F. Paton and G. M. Almy, Phys. Rev. **37**, 1710 (1931).

110. The Brillouin Effect of Benzene as Obtained with the Concave Grating. D. H. RANK, *Pennsylvania State College.*—E. Gross has shown that when light is scattered by liquids one obtains in addition to the main unmodified line satellites which are symmetrically spaced with respect to the line and separated from it by about 0.04 Angstrom. The few observations which have been made on this phenomenon employed interferometers as the instruments of high resolving power. By making some obvious modifications to the apparatus which I had used several years ago to produce Raman spectra of gases at atmospheric pressure it was possible to obtain sufficient intensity (of the light scattered by pure benzene through an angle of 90°) to use a 21-foot concave grating as the instrument of high resolving power. The λ4358 and λ3650 lines of Hg scattered by benzene were photographed in the fourth order of the grating. Comparison of the structure of these lines scattered from benzene and the same lines obtained directly from the source shows the so-called Brillouin components quite clearly.

111. A Source for Quantitative Spectrographic Analysis of Solutions. K. B. THOMSON AND O. S. DUFFENDACK, *University of Michigan.*—A source has been devised for the quantitative spectrographic analysis of solutions, and applied to the analysis of certain biological fluids. The source is an uncondensed spark between two electrodes of the solution to be analyzed. These electrodes consist of two horizontal quartz jets rigidly attached to one another with their nozzles separated by a distance of 4½ to 5 mm. The solution flows through the jets from two reservoirs attached by quartz tubing. These reservoirs are circular in form, the centers of the circles lying on the axis of the jets. The flow of solution is produced and regulated by rotating the apparatus about this axis. Electrical contact is made through gold wires that enter the system at some distance from the jets. The effects of various changes in conditions, such as changes in spark current, rate of flow of solution through the jets, separation of the jets, etc., have been investigated. Analyses have been made over the following ranges of concentration: magnesium 0.0001 to 0.05 percent; sodium 0.01 to 1.0 percent; potassium 0.025 to 0.8 percent; calcium 0.005 to 0.1 percent. The errors in the results obtained for sodium and potassium are of the same magnitude as the errors in measuring relative intensities

of spectral lines with the microphotometer. Slightly greater errors occur in the analyses for calcium and magnesium. This work has been supported by the Rockefeller Foundation.

112. Vibration-Rotation Energy Levels of Ethane-Type Molecules. J. B. HOWARD AND E. BRIGHT WILSON, JR., *Harvard University.* (*Introduced by J. H. Van Vleck.*)—The vibration, over-all rotation, and internal rotation of the ethane molecule have been treated by a straightforward quantum-mechanical method on the assumption of unhindered internal rotation. The two methyl groups are described by separate rotating coordinate systems with a common axis. The approximate Hamiltonian operator is

$$H=\tfrac{1}{2}\{(P_x-p_x)^2/A_0+(P_y-p_y)^2/B_0 +(P_z-p_z)^2/C_0+(P_\gamma-p_\gamma)^2/C_0+\sum_{k=1}^{3N-7}p_k^2\}+V,$$

in which P_γ is the momentum conjugate to the internal angle γ, p_γ is a corresponding quantity arising from the vibrational motion, p_k is the momentum conjugate to the normal coordinate Q_k; the other quantities have their usual significance. The concept of normal coordinates has been extended to apply to a molecule of this sort which has free internal rotation. There are found to be two types of normal coordinates, one type depending only on the displacement coordinates, the other on the displacement coordinates and the internal angle γ. The first type corresponds to nondegenerate frequencies; the second to doubly-degenerate frequencies. During the free internal rotation of the molecule the normal coordinates for each value of the angle γ are the same as the corresponding normal coordinates of the semirigid molecule in which the free internal rotation is replaced by a torsional normal vibration about an equilibrium position given by that value of γ. The selection rules for the vibration-rotation spectrum and the statistical weights of the energy levels have also been determined.

113. Electronic Structures of Simple Polar Diatomic Molecules. ROBERT S. MULLIKEN, *University of Chicago.*—Electronic structures of the low energy electronic levels of diatomic molecules MH, HX and MX are considered, using band spectrum data, in the light of possible electron configurations and approximate wave functions (M = univalent metal, X = halogen). The empirical potential energy curves of the two $^1\Sigma^+$ states of MH can be explained starting from two hypothetical curves (one homopolar M : H, one ionic M^+H^-) which cross. Quantum-mechanical interaction between these, using a resonance integral varying reasonably with r, gives the observed curves. The anomalous band spectrum constants and shape of the upper curve are made understandable. They are attributable mainly to transition from predominantly homopolar to nearly pure ionic character as r increases. The abnormally small normal state dissociation energies D indicate that the additivity theorem for homopolar bond energies (i.e., $D(M:H)=\frac{1}{2}D(M_2)+\frac{1}{2}D(H_2)$ in the present case) fails badly in MH; complete failure appears practically certain in MX, band spectrum data indicating that $D(M:X)$ is approximately zero. For AgX, it is concluded that the upper potential energy curve of the observed bands contains a shallow minimum followed, as r is increased, by a maximum, after which the curve sinks to an asymptote about 1 ev lower.

114. The Emission of Visible Light from Pure Liquids During Acoustic Excitation. L. A. CHAMBERS, *Johnson Foundation.* (*Introduced by D. W. Bronk.*)—Of 36 pure liquids examined, 14 were observed to emit visible light during cavitation by audible sound waves of 1000 and 9000 c.p.s. The emission was most intense (visual comparison) in the case of glycerol and nitrobenzol. A correlation has been found between the apparent intensity of the radiation and the numerical product of molecular dipole moment μ and viscosity η such that the intensity increases with $\mu\eta$. The emission from pure water is of such an intensity that it constitutes an exception to the rule, the only exception thus far encountered. The intensity of the light varies inversely as the temperature in all of the liquids studied. From solutions of polar compounds in nonpolar solvents the emission intensity was found to vary with concentration of the polar constituents. While no explanation of the phenomenon is available at present it is suggested that the existence of a quasi-crystalline structure in the liquids would make possible a theory of excitation by sudden distortion of a space lattice. Thus sonic-luminescence might be related to the tribo-luminescence exhibited by certain crystals.

115. Filament Ion Sources for Mass Spectroscopy. E. J. JONES, *U. S. Department of Agriculture, Washington,* AND J. P. BLEWETT, *Princeton University.*—Efficient sources of ions of the alkali metals have been produced by heating synthetic alkali aluminum silicates. The ternary system (Li_2O) (Al_2O_3) (SiO_2) has been studied thermodynamically and the eutectics having ratios 2 : 1 : 1 and 3 : 1 : 3 of the components have been found to provide satisfactory lithium ion sources. Similar alloys serve for the other alkalis. The salt is prepared by mixing the alkali carbonate with aluminum nitrate and powdered quartz in the correct proportions. This mixture is reduced by heating and is then painted on a platinum strip or mesh filament with water as a binder. Sources of this type yield ion currents of 10^{-4} amp. per sq. cm for 30 hours or longer. Mass spectrograph analyses show that impurities of other alkalis in the ion emission can be reduced to less than one percent. Magnesium, calcium and aluminum ions have been produced in fairly copious amounts by heating oxides, carbonates or nitrates of these metals to a white heat. The salts were supported on a tungsten spiral filament. In the case of aluminum, negative ions of mass 27—presumably Al^-—were observed. Similar salts of other metals are being investigated.

116. Negative Atomic Hydrogen and Deuterium Ions. PAUL F. DARBY AND WILLARD H. BENNETT, *Ohio State University.*—The source of negative atomic hydrogen ions previously reported[1] has been further improved and simplified by the introduction of a little mercury vapor and

the use of a transverse magnetic field on the arc itself. Mercury vapor at 0.0013 mm pressure makes the performance of the oxide coated filaments steady and also greatly decreases the amount of water dissociated into gaseous products. The transverse magnetic field cuts off all of the electrons from the arc, thus avoiding the more difficult elimination of them later. The transverse magnetic field also increases the intensity of the negative ion beam, possibly because the field captures the slow electrons produced by collision from the vapors in the arc and thus tends to reverse the direction of the anode drop which otherwise opposes the emergence of the negative ions. By using fifty percent heavy water, only six-tenths as much negative deuterium as negative hydrogen was obtained.

[1] Darby and Bennett, Phys. Rev. **49**, 97, 422 (1936).

117. Low Voltage Proton Sources. W. W. BUECHNER AND E. S. LAMAR, *Massachusetts Institute of Technology.*—Further experiments have been carried out with a view towards increasing the proton percentage obtainable from capillary arc sources previously described. The collision method of breaking up molecular ions has been investigated. Although no difficulty was experienced in refocusing the scattered ions, no evidence was found for break-up in the absence of magnetic fields. Rather than investigate these possibilities further, a quartz capillary was tried using a simple beveled outlet. This eliminated the rapid disintegration of the quartz by secondary electrons from any probe electrode but there was still evidence of gradual disintegration of the quartz by low speed electrons in the discharge. The absence of excessive heating indicated that the capillary might as easily be made of Pyrex. A Pyrex capillary source was therefore tried. In a 3-mm capillary, heating was not excessive at arc currents below 0.3 ampere. The proton percentages ranged up to 20 percent. Following the experience of Wood, water vapor was introduced and resulted in a marked increase in the proton percentage (a factor of about 2). Experiments are still in progress to determine the maximum possible increase. This source possesses the advantages of slightly greater ion current efficiency, requires no cooling, is easily constructed, and is free from impurities.

118. A Lithium Ion Source. C. A. WHITMER AND M. L. POOL, *Ohio State University.*—A lithium ion source for nuclear work has been developed capable of delivering more than 15 microamperes of useful current on a collector two feet away. The current near the source is many times that value. The lithium is in a steel boiler held at a red heat. The jet of lithium coming from the gun passes between two tungsten points across which a condensed discharge takes place. Multiply charged lithium ions then pass through diaphragms and focusing potentials onto the collector. The maximum potential used is 150 kv. The ion source is at ground potential and observations are made in a Faraday cage held at high potential. A magnetic analysis of the lithium ion beam shows that the hydrogen contamination is less than one part in ten thousand.

119. Mass Ratio of the Carbon Isotopes from the Spectrum of CN. F. A. JENKINS, *University of California,* AND DEAN E. WOOLDRIDGE, *California Institute of Technology.*—By using a source containing methane with approximately 10 percent of C^{13}, the violet CN bands have been photographed in the second order of the 21-foot grating with a dispersion of 0.63 A/mm. As recently reported, the enriched methane was produced by the second author in a Hertz diffusion apparatus. It was mixed with argon and a trace of nitrogen to produce the CN spectrum. The entire band system due to $C^{13}N^{14}$ appears on the plates. Measurements on the 0,0 and 0,1 bands have thus far been made, and yield an accurate evaluation of the vibrational differences by methods previously used by the first author. We obtain $\Delta G_{\frac{1}{2}} = 2042.416$, $\Delta G_{\frac{1}{2}}' = 2000.016$. By using the known vibrational constants of the main system, and assuming the theoretical ratio ρ^2 for the anharmonic term $x_e\omega_e$, these give the isotopic mass coefficient $\rho = 0.97897$, with an estimated limit of error (*l.e.*) of 0.00002. With Aston's latest value 12.0035 for C^{12}, this corresponds to $C^{13} = 13.0089$, *l.e.* 0.0005. This is slightly higher than the value 13.0073 (*l.e.* 0.0003) recently estimated from disintegration data by Oliphant. Our result is to be considered as preliminary, and further measurements will considerably increase its precision. From the isotope shift in the 0,1 band, we find $C^{13} = 13.0069$, but an electronic shift of only 0.06 cm^{-1} would bring this into agreement with the above value.

120. The Isolation of Lithium Isotopes with a Mass Spectrometer. L. H. RUMBAUGH, *The Bartol Research Foundation of the Franklin Institute.* (*Introduced by W. F. G. Swann.*)—A special form of mass spectrometer has been constructed, by means of which lithium isotopes can be deposited at rates exceeding one milligram per day. The essential features of this instrument are: (1) an extended source of positive ions, 20 cm^2 or more in area; (2) an electric lens for accelerating and collimating the ion beam; (3) a magnetic lens[1] which separates and focuses the different masses; (4) a system of targets of small areas upon which the isotopes are collected simultaneously. A low temperature source of lithium ions, capable of emitting 2×10^{-4} amperes per cm^2, has been developed. Over 20 specimens of the lithium isotopes, ranging from 5 to 1000 micrograms in mass, have been collected and deposition rates of 100 micrograms of Li^7 per hr. have been maintained for as long as 8 hr. Deposited masses have been checked chemically with an accuracy of ± 2 micrograms with various samples of 100 to 750 micrograms of lithium isotopes. The amounts obtainable are sufficient for certain spectroscopic and chemical investigations and are more than ample for the study of nuclear transformation and excitation. The separation of the isotopes is complete except for a general background of unknown constitution amounting to about 0.1 percent of the Li^7 current at the collector.

[1] W. R. Smythe, L. H. Rumbaugh and S. S. West, Phys. Rev. **45**, 724 (1934).

121. Separation of Isotopes by Diffusion. RUBBY SHERR AND WALKER BLEAKNEY, *Princeton University.*—A set of diffusion pumps of the Hertz type[1] was constructed to

fractionate the isotopes of certain gases. The behavior of the pumps under various conditions of pressure and heat supply was investigated by using as a test gas a 50–50 mixture of H_2 and D_2. The progress of separation was observed with an electrodeless discharge and Fabry-Perot interferometer. Ninety-nine percent D_2 was secured in one operation. Mass spectrographic analyses by our colleagues indicated separation factors (ratio of heavy to light in enriched sample)/(ratio of heavy to light in original) about 100 for the 50–50 H_2–D_2 mixture, 10 for tank hydrogen, and 3.7 for neon. The drop in the separation factor with decreasing concentration is probably to be attributed to unfavorable ratios of the volumes used and to lack of complete equilibrium. Runs taken with oxygen gave a value of 165 for the ratio $O^{16}O^{16}/O^{16}O^{18}$ as compared with 250 for normal oxygen indicating a separation factor of 1.5. This value is roughly the same for all pressures between 1.5 and 9 mm. The system comes to equilibrium in 1½ hours for an enriched sample of 200 cc. Runs with five and ten pumps show that the separation factor increases exponentially with the number of pumps.

[1] G. Hertz, Zeits. f. Physik 91, 810 (1934).

122. Distilling Apparatus for Separation of Isotopes. G. B. PEGRAM, H. C. UREY AND JOHN HUFFMAN, *Columbia University.*—This distilling apparatus, adapted to the separation of liquid constituents having boiling points very close together, such as H_2O and D_2O, or H_2O^{16} and H_2O^{18}, consists of a vertical counter-flow column connected with a boiler below and a reflux condenser above. The counter-flow column is a vertical metal cylinder 15 cm diameter, containing a succession of truncated sheet metal cones fitting, small ends down, into the cylinder and fixed peripherally to the cylinder wall. The axial hole in the small end of each cone is 4.5 cm diameter. The cones are spaced 1.6 cm apart. A rotatable shaft with bearings at top and bottom is placed axially in the cylinder and has fastened on it a similar succession of cones, the outer edges of which do not reach the cylinder wall by 1 cm. The rotating cones are spaced half-way between the stationary cones. Vapor from the boiler traverses the spaces between successive fixed and rotating cones which act as baffles. Reflux liquid from the condenser counterflows down a fixed cone by gravity, drops to the next rotating cone, by centrifugal action runs up it and flies off, flows down the next fixed cone, and so on. A column with 15 fixed and 15 rotating cones proved the equivalent of 14 "theoretical plates." A column 150 cm high with 105 pairs of cones operating at atmospheric pressure changed the ratio of concentration of H_2O^{16} to H_2O^{18} by a factor of 1.31.

123. The Mass-Spectrographic Determination of Mass Changes in Some Carbon Transmutations. KENNETH T. BAINBRIDGE AND EDWARD B. JORDAN (National Research Fellow), *Harvard University.*—The mass differences of the matched doublets C^{12} H^1-C^{13} and $H_2^1-D^2$ have been measured with the new mass spectrograph as 4.5 ± 0.1 and $1.53\pm0.04\times10^{-3}$ units, respectively. The $C^{12}+H^1-C^{13}$ separation, taken with Tuve and Hafstad's data for the energy of the bombarding proton, yields 3.6 MV energy available for the gamma-ray, positron, and neutrino in the radiative capture of a proton by C^{13} and the subsequent disintegration of N^{13}. Using both doublet separations, one obtains for the energy of the proton and recoil nucleus in the $C^{12}+D^2\rightarrow C^{13}+H^1$ reaction 2.76 MV, which is in excellent agreement with the disintegration figure. The most interesting result from these mass measurements is the proof that in the carbon plus proton and deuteron reactions involving the transmutation of C^{12} to C^{13}, there is not sufficient energy for a 3.5 to 4 MV gamma-ray in addition to the known products and their energies. This problem, which is of great importance to the reliability of the disintegration mass-scale, has been discussed by Bethe, Tuve and Hafstad, and Cockcroft. Reproductions of the mass spectra will be shown.

124. The Mass-Spectrographic Measurement of the Mass Separation of Certain Doublets. EDWARD B. JORDAN (National Research Fellow) AND KENNETH T. BAINBRIDGE, *Harvard University.*—The $O-CH_4$ and the $N-CH_2$ doublets have been obtained, matched in intensity, in a large number of spectra. The measurements of these doublets were made on three different comparators and checked by means of densitometer records. The mass differences obtained are:

$$CH_4-O=0.0369\pm0.0002$$
$$CH_2-N=0.0130\pm0.0002.$$

These values have been checked by determining the mass difference of the CO–N_2 doublet and the OH–NH_2 doublet. Values of the above mass differences as determined by means of disintegration experiments are in good accord with those measured in these experiments. Densitometer records and slides of the mass spectra will be shown.

125. Ionization Potentials of H_2, N_2, CH_4 and H_2O. LINCOLN G. SMITH AND WALKER BLEAKNEY, *Princeton University.*—A method has been found for measuring ionization potentials with a mass spectrograph which is nearly independent of sensitivity, pressure, current density, and the shape of the theoretical ionization efficiency curve near the foot. The method is based upon approximate theoretical calculations which take account of the Maxwellian velocity-distribution of electrons emitted from an equipotential oxide coated cathode. Measurements of the minimum energies of electrons to produce ions of H_2^+, N_2^+ and H_2O^+ gave 15.37, 15.57 and 12.59 volts, respectively. The estimated error in these measurements is ±0.05 volt. These values agree with other observers but we believe the method is more sound than the usual one. Further studies in methane with a more sensitive mass spectrograph have shown that in addition to the ions CH_4^+, CH_3^+, CH_2^+, CH^+, C^+, H^+ and H_2^+ ions of H_3^+ are formed. All ions are formed by single electron impact with the possible exception of H_3^+, but even this one has a linear component with pressure. The ionization potential of CH_4^+ has been measured by the new method as 12.72 volts, a value somewhat lower than that previously reported. The appearance potentials of H^+, H_2^+, and H_3^+ are, respectively, 22.7, 27.8 and 26.0 volts.

126. The Perfect e/m Filter as a Mass Spectrograph. J. A. HIPPLE, JR., AND WALKER BLEAKNEY, *Princeton University.*—It is well known that the trajectory of a charged particle in uniform crossed electric and magnetic fields is a trochoid in the plane perpendicular to the magnetic field plus a uniform motion in the direction of this field. A family of such trochoids emanating from a slit comes to a perfect focus when the argument is increased by 2π for a given e/m regardless of the initial conditions of direction and velocity. The image is of course an astigmatic one in the direction of the magnetic field. The arrangement therefore serves as an ideal e/m filter and may be used as a mass spectrograph with linear mass scale. The uniform fields are difficult to realize in practice but we have succeeded in constructing a model which meets the theoretical requirements very well. The electric field is secured with a rectangular solenoid of high resistance wire mounted between the poles of a magnet and gives, when carrying a small current, a uniform electric field parallel to the pole faces. Measurements on potassium ions gave the resolving power expected.

127. A Seeman-Bohlin X-Ray Camera for High Temperatures. R. F. BOYER AND C. NUSBAUM, *Case School of Applied Science.*—In the x-ray analysis of the cementite and graphite precipitation in cast iron at high temperatures, the mechanical properties of the material are such as to preclude the use of a sample either in the form of powder or wire. The Seeman-Bohlin Camera, in which the slit, sample, and photographic film are on the circumference of the same circle, permits the placing of the sample, suitably faced, on this circumference. The sample in the form of a T has the front face of the cross arm shaped to the circumference of the cassette. On its stem, suitably insulated, is wound a heating coil. These are mounted so that the axis of the stem of the sample coincides with the axis of a cylindrical shell in which it is held by heat insulating cement. This shell, with the front face of the sample on the circumference, is placed in a water-cooled jacket which is an integral part of the cassette, and held securely in place by four contact points. Displacement of the face of the sample from the circumference, due to thermal expansion, can readily be prevented by suitable use of silica rods. The part of the circumference against which the film rests is also water-cooled. This camera has the additional advantage of short exposures and high resolving power.

128. The Determination of the Size and Shape of Crystal Particles by X-Rays. A. L. PATTERSON, *Massachusetts Institute of Technology.*—By means of a new method, based on Fourier analysis, it is shown that the x-ray interference functions for particles of very general shapes can be obtained. In particular, such functions are given for the known cases of the parallelepiped, and the octahedron; and in addition for the tetrahedron, the ellipsoid, and the elliptic cylinder; all referred to general triclinic axes. An exact derivation of Scherrer's equation is then given for spherical particles of a cubic crystal. Scherrer's original derivation of this equation and W. L. Bragg's simplified derivation are compared with the exact solution and are found to be in reasonable agreement. Bragg's method is then used to discuss the problem of the shape of particles from x-ray data.

129. The Complete Crystal Structure of KNO_2. GEORGE E. ZIEGLER, *Central Y. M. C. A. College, Chicago.*—KNO_2 is one of the nitrite structures being investigated by the author for NO_2 group information. $NaNO_2$ was presented previously (Washington, 1931), $LiNO_2 \cdot H_2O$ has not been completed. The KNO_2 unit cell contains 2 molecules and is face-centered monoclinic with dimensions $a = 4.45$A, $b = 4.99$A, $c = 7.31$A, $\beta = 114° 50'$. The space group is C_s^3. Parameter values are determined on the basis of agreement between calculated and observed intensities. Calculations for the $(h00)$, $(0k0)$, $(00l)$ zones first limit the parameters to definite ranges, then final values are obtained by trial calculations. The final parameters in degrees are:

	x	y	z
K	0	0	0
N	180	0	175
O	160	75	150

Six oxygen atoms surround potassium at average distance of 2.80A. The O−N−O angle is 132°, with the O to O distance 2.08°. The closest approach of O's from different NO_2 groups is 2.91A. The structure may be considered a distorted $NaNO_2$ type structure. From the structure it is concluded that the crystal has large birefringence with the vibration direction of γ parallel to the b axis and the vibration direction of α nearly perpendicular to $(10\bar{1})$. The author wishes to thank the Staff of the Physics Department, Ryerson Physical Laboratory, University of Chicago, for the use of their research facilities and for their advice throughout the investigation.

130. The Crystal Structure of Germanium Disulphide. W. H. ZACHARIASEN, *University of Chicago.*—Crystals of GeS_2 are orthorhombic, $a = 11.66$A, $b = 22.34$A, $c = 6.86$A. There are 24 molecules in the unit cell and the space group is Fdd (C^{19}_{2v}). Eight germanium atoms occupy special positions, (000), $(\frac{1}{4}\frac{1}{4}\frac{1}{4})$. All the other atoms are in general positions. The twelve parameters involved were determined:

	$2\pi x$	$2\pi y$	$2\pi z$
Ge	45°	50°	0°
S_I	8	29	66
S_{II}	55	− 5	− 66
S_{III}	22½	45	−100

Every germanium atom is bonded to four sulphur atoms, the bonds being directed towards the corners of a tetrahedron. Every sulphur atom is linked to two germanium atoms, the bond angle being 103°. The Ge–S distance is 2.19A. The GeS_4-tetrahedra have only corners in common and form a three-dimensional tetrahedral network similar to the networks found in the various forms of SiO_2.

131. Effects of Chemical Combination on the Widths and Asymmetries of X-Ray Lines. H. H. ROSEBERRY AND J. A. BEARDEN, *Johns Hopkins University.*—Previous investigations concerning the effects of chemical combination on x-ray emission spectra have been limited almost entirely to specific lines. Practically all of this work has been done with a vacuum photographic spectrometer in which the uncertainties of such results are well known. In the present work precision measurements have been made on the effects of chemical combination for the complete K series using a double crystal spectrometer and ionization

chamber. Changes of width, indices of asymmetry, separation of the alpha doublet, and the ratio of peak intensities as function of chemical combination have been observed for the oxides of Ti, Cr, Mn, Fe, and zinc. The alpha-lines were broadened 3 to 35 percent and the beta-lines 0 to 30 percent. In no case were the gamma-lines affected by chemical combination within experimental error. No effect was noted on the separation of the alpha-doublet. With a few exceptions the asymmetries of the lines observed remained the same as that of the pure metal.

132. Small Angle X-Ray Scattering. B. E. WARREN, *Massachusetts Institute of Technology.*—A study has been made of the small angle x-ray scattering from very small particle materials such as carbon black and a fine grained silica flour. The patterns were made with Cu $K\alpha$ monochromated by crystal reflection, and using evacuated cameras. Sample to film distances up to 28.3 cm were used. With the silica flour the small angle scattering begins at about $(\sin\theta)/\lambda = 0.05$ and increases rapidly in intensity with decreasing angle. At $(\sin\theta)/\lambda = 0.014$ it is already 4000 e.u. per SiO_2 or ten times the intensity of the strongest peak in the diffraction pattern. That the effect is really one of scattering by the sample was checked by substituting a thin slip of SiO_2 glass; small angle scattering was then absent although the rest of the patterns were the same. The effect is interpreted in terms of scattering and interference between the individual particles in the fine grained material. At sufficiently small angle all the atoms of one particle scatter essentially in phase and for a certain range of angle there is partial reenforcement between the resultant amplitudes from the particles. The application of the effect to particle size measurement is discussed.

133. An Experiment on the Compton Effect for Gamma-Rays. H. R. CRANE, E. R. GAERTTNER AND J. J. TURIN, *University of Michigan.*—A progress report will be presented on an experiment designed to test the photon theory of scattering in the region between 1 and 2.6 MEV. A small pencil of radiation from thorium C″ is shot through a cloud chamber having a thin mica window in each side so that very little radiation is scattered in entering and leaving the chamber. A mica scatterer 0.2 mm thick is placed in the beam at the center of the chamber, and two thin lead sheets are placed parallel to, and on each side of, the primary beam, to absorb the scattered photons. A magnetic field is applied to determine the energies of the electrons. From the energy and direction of an electron ejected from the mica scatterer, the direction of the scattered photon expected on the Compton theory can be calculated. This eliminates any assumption as to the energy of the primary photon. Out of 400 pictures about 200 electrons appeared singly and in the forward direction from the mica scatterer. Twenty of these were accompanied by one or more electrons from the lead sheets. This indicates a low background. It will not be possible to advance an opinion as to the results until considerably more data have been obtained.

134. The Enhancement of the Satellites of the X-Ray Diagram Line $L\beta_1$ by the Auger Effect. F. R. HIRSH, JR., *Cornell University.*—Druyvesteyn[1] tentatively assigned the $L\beta_1$ satellites to a single electron transition in a doubly ionized atom: $L_{II}M \rightarrow MM_{IV}$. Coster and Kronig[2] have pointed out that ionization of the $M_{IV, V}$ shell caused by the radiationless transition $L_I \rightarrow L_{II}$ is impossible if $Z > 40$. However, below $Z = 40$, the atom may be left doubly ionized by the Auger effect, L_{II} and $M_{IV, V}$ electrons lacking, and in the initial state for the emission of satellites. The present author[3] recently reported an intensity anomaly for the $L\beta_1$ satellites at $Z = 40$. This work has now been extended by the same photographic method to include the $L\beta_1$ lines of practically all the elements from Zn(30) to Cd(48). With increasing atomic number, the ratio of the energy of the satellites $L\beta_1'$ and $L\beta_1''$, with respect to that of their parent $L\beta_1$ line, rises to a maximum value of 0.34 at $Z = 38$ and then falls off sharply to less than 0.01 at $Z = 41$. From $Z = 41$ on through $Z = 48$, the value of this ratio remains at less than 0.01. Below $Z = 40$ the enhancement of the satellites is due to the Auger effect; above $Z = 40$ the satellites persist because of double ionization arising from single electron impacts. The present work definitely confirms the suggestions of Druyvesteyn[1] and Coster and Kronig[2]: the single electron transition between doubly-ionized states is $L_{II}M_{IV, V} \rightarrow (M_{IV, V})^2$.

[1] M. J. Druyvesteyn, Dissertation, Groningen (1928).
[2] D. Coster and R. DeL. Kronig, Physica 2, 13 (1935).
[3] F. R. Hirsh, Jr., Phys. Rev. 48, 776 (1935).

135. Strain in Galena Crystals Produced by Abrasion. L. H. GERMER, *Bell Telephone Laboratories, Inc.*—Filing or grinding a galena crystal to a cube face tears out large blocks of the mineral. Such an abraded surface gives an electron diffraction pattern consisting of the Debye-Scherrer rings of galena (PbS). Etching rather lightly in *aqua regia* changes the surface so that it gives a complex diffraction pattern. Two superposed patterns are actually present. These can be identified as arising from different parts of the surface. The parts from which large blocks were torn out give the pattern of an almost perfect crystal. Other areas produce a pattern characteristic of a mass of minute crystallites which have been rotated about an axis in the surface normal to the direction of grinding and in the sense determined by imaginary "rollers" which would be turned by slipping on the (100) plane. The magnitude of the rotations varies for different crystallites over a range from 5° to 35°. By alternate etching and examination by electron diffraction it is found that this layer of rotated crystallites extends beneath the surface for a depth of 0.003 mm. Below this layer the crystal is nearly perfect. Rotation of crystallites along slip planes is the mechanism reported to account for strain hardening of metals.

136. Preferred Orientation of Low Carbon Strip Steels. C. B. POST, *The Pennsylvania State College.* (*Introduced by Wheeler P. Davey.*)—The range of orientation existing in cold-rolled strip steels is shown to be a function of the working roll diameter. Experimental results from three sizes of rolls, *viz.* 19¼, 12, and 5¼ inch diameters, show that for any given percent reduction above 40 percent the angular deviation of a cube face diagonal, [110], from the direction of rolling is greater the smaller the roll diameter. Tandem and Steckel type mills were used and the results

point to the conclusion that tension in the coil as rolled has only a small effect, if any, on the final degree of preferred structure. This structure can be specified by having a [110]-direction of the unit cell along the direction of rolling with a rotation of the cube about this direction as an axis. This rotation is not completely random, but, starting with reductions in the neighborhood of 40 percent, the angle of rotation steadily decreases to about 55 degrees in the neighborhood of 85 to 90 percent reduction. The angle of deviation of the [110] direction from the direction of rolling is found to be a function of the percent reduction and roll diameter. For the 19¼ inch rolls this deviation was 20 degrees for 40 percent reduction and 7 degrees for 90 percent reduction.

137. The McLachlan Machine for Drawing Pole-Figures. WHEELER P. DAVEY, *The Pennsylvania State College.*—This paper describes a very simple machine developed at The Pennsylvania State College by Dan McLachlan, Jr., by which pole-figures showing the preferred orientation of crystals in rolled metal sheets may be drawn directly from the x-ray diffraction patterns. It is inherent in the design of the machine that all the conditions for stereographic projection are fulfilled and that the actual experimental set-up of the diffraction experiment can be simulated, thus taking account of (a) the angle between the x-ray beam and the sheet and (b) the orientation of the sheet itself. All the contributions of a single diffraction pattern to a given pole-figure may be charted mechanically within five minutes from the time the diffraction pattern is inserted into the machine. Any of the three customary planes of projection may be employed, i.e., normal-transverse, normal-rolling, or rolling-transverse. The finished pole-figure is of ample size (about nine inches in diameter) for reproduction. If time permits, the machine will be demonstrated.

138. A Combination Impedance-Wheatstone Bridge. T. M. HAHN AND BEN RAGLAND, *University of Kentucky.*—The use of the double vacuum tube voltmeter as usually constructed involves the assembly of much accessory apparatus. It is also necessary in measuring an inductance to make a separate measurement of the d.c. resistance. By incorporating a multipole switch and small dry cell in the assembly, along with a rectifying unit, a completely self-contained a.c. impedance bridge and d.c. Wheatstone bridge is constructed. Any impedance within the range of this instrument may be measured as conveniently as resistance is determined with the usual self-contained Wheatstone bridge. A full description of the apparatus with the results of typical measurements will be presented.

139. A New Voltage Regulator Circuit. J. A. ASHWORTH AND J. C. MOUZON, *Duke University.*—A circuit has been designed for the supply of constant high voltage to a mass spectrograph. It is equally useful in all types of work requiring constant voltage. The particular feature of the circuit is the operation of the control grid of a type 78 tube at a positive potential. The constants of this grid circuit may be adjusted so that all detectable transients are eliminated. Another important feature is that the current through the load resistor in the plate circuit is large enough for one to vary the output voltage continuously and to measure it without destroying the balance of the circuit. The high voltage input is supplied from a half wave rectifier. With the circuit balanced no fluctuations whatsoever can be detected in the output from the regulator with an L & N potentiometer when the line voltage is varied from 108 to 113 volts. The theory of the operation of the circuit has been developed.

140. A Direct Reading Vacuum Tube Speedometer for Random Counting. NEWELL S. GINGRICH AND ROBLEY D. EVANS, *Massachusetts Institute of Technology.*—Impulses such as are obtained from Geiger counters are generally recorded through a multi-stage amplifier by some form of mechanical counter. The average rate of counting is computed by determining the total number of counts in an interval timed with a clock. This procedure is supplanted and simplified through the use of a frequency meter together with a capacity-resistance tank circuit. Hunt's[1] frequency meter is modified so as to have a condenser input similar to that of Lewis's[2] scale of eight, with the tank circuit in place of the meter of Hunt's circuit (Fig. 3).[1] Voltage across the tank circuit is measured with a vacuum tube voltmeter, and the reading of the meter in this circuit is a direct measure of the mean rate of counting, averaged over about 2CR of the tank circuit. Since the frequency meter responds to frequencies of several thousand per second, the resolving time is limited only by the single amplifier stage and is of the order of 0.001 second. This circuit is suitable for counting rates of less than 50 per minute to at least 2000 per minute, and greatly simplifies the determination of counting rates.

[1] F. V. Hunt, Rev. Sci. Inst. **6**, 43 (1935).
[2] W. B. Lewis, Proc. Camb. Phil. Soc. **30**, 543 (1934).

141. A Hydrodynamical Theory of Piston Ring Lubrication II. R. A. CASTLEMAN, JR., *East Falls Church, Va.*—At the annual meeting of the American Physical Society at St. Louis on January 1, 1936, a hydrodynamical theory of piston ring lubrication was outlined. It was pointed out that, assuming that (a) the outer face of the ring, no matter how "straight" initially, is soon worn down to some gently rounded form, with thick part in the middle; and (b) that oils as used in engine lubrication cannot stand absolute tension, then it follows that the ring will ordinarily be borne on a "thick" (compared to the molecular size) film of lubricant. A crucial test of the theory thus seemed to lie in measurements of the profiles of the outer faces of worn rings. Six worn Ford rings were thus measured, each at three well-separated points along the circumference of the ring, by the Gage Section of the Bureau of Standards. Of the *18* points thus considered, *all showed wear of the general form assumed*, though of various degrees. The unexpected were: (1) the worn surfaces are sensibly plane, not curved; (2) their angle of mutual inclination is much smaller than expected,—of the order of 30 minutes of arc; (3) the line of intersection of the two surfaces averaged about ¾ of the distance below the "top" of the ring. These results are in line with the present theory.

142. The Faraday Effect Near Isolated Band Lines. THOMAS CARROLL, *Yale University.*—It is usually assumed that the Faraday effect observed in the vicinity of some band lines consists of a rotation of the plane of polarization which is symmetrical about the no-field frequency of the line. If, however, the first order perturbation of the intensities of the various Zeeman components by the field is taken into account, plane polarized light with frequency near the absorption line propagated along the field becomes elliptically polarized. The major axis of the ellipse is rotated through an angle which is greater for frequencies on one side of the line than for those on the other. This perturbation of the intensities is important mainly for heavy molecules, since it is proportional to the ratio of the Larmor frequency to the B value of the molecular level in question. Essentially the magnetic field produces dichroism, that is, unequal absorption and coherent scattering for right and left-handed circular polarizations. The observations of Wood on the asymmetrical magnetic rotation near several I_2 lines confirm the theory. New observations of magnetic rotation in the infrared K_2 system indicate that the rotation is predominant on one side of the absorption line.

143. The Optical Constants of Liquid Gallium. J. B. NATHANSON, *Carnegie Institute of Technology.*—A mirror of liquid gallium was produced by filling a previously heated glass cell with the metal, under vacuum. Polarimetric observations were made through a small Pyrex window of the glass cell. By means of suitable glass prisms placed in optical contact with the window of the cell, the phase difference and the angle of restored plane polarization were determined for angles of incidence of 45° and 60°. The optical constants were computed by means of Drude's formulae. For wave-lengths of 4358A, 5461A, and 6708A, the coefficients of absorption were found to be 7.3, 5.9, and 5.4, respectively, while the refractive indices relative to air were 0.58, 0.88, and 1.10, respectively. The reflecting powers for normal incidence varied only slightly with the wave-length, the values for the above wave-lengths being 88.7, 88.3, and 88.5 percent, respectively. Within the limits of experimental error, there did not seem to be any variation of the above constants with respect to temperatures varying from 24°C to 40°C.

144. Evaporated Aluminum Coatings for Interferometer Plates for Use in the Ultraviolet. J. E. RUEDY, *Evaporated Films Co.*, AND GEORGE BURR SABINE, *Cornell University.*—Partially transmitting films of aluminum evaporated upon Corex and fused quartz have been measured for reflection and transmission over the wave-length range 2380–4080A with the purpose of determining their suitability for interferometric use in the ultraviolet. Numerous samples were made having transmissions ranging from 2 to 50 percent in the visible. All of these show the same general behavior: namely, a slow decrease in reflectivity and a nearly corresponding increase in transmissivity with decreasing wave-length. The thicker films have the higher efficiency (efficiency = reflection + transmission) with the opaque film reflectivity of about 90 percent throughout this entire range as the upper limit. A film suitable for use in a Fabry-Perot interferometer might have the following characteristics: at 4000A: $T=2$ percent, $R=84$ percent; at 2400A: $T=16$ percent, $R=70$ percent. Negligible change in the behavior of these films is produced by washing them, and no deterioration with time has been evident over the two-months' period during which they have been under observation.

145. The Theory of the Michelson Interferometer. W. B. CARTMEL, *Université de Montréal.*—In the theory of the interferometer as developed by Michelson, no account was taken of the part played by the lens system, except to some slight extent in deriving the important circular fringe formula used in his determination of the meter in wave-lengths of light. The formulas developed in the present paper are based on the idea that the fringes are formed in the focal plane of the observing telescope, where two images of the flame are seen, which coming from the two end mirrors arrive by different paths. If the observing telescope is perfectly normal to the end mirror and the arms of the interferometer are of exactly equal length l_0, it is found that the central black fringe will arrive at the center of the crosswires. The angular separation between the nth fringe and the crosswires is given by $\phi = n\lambda/2l_0(\alpha-\beta)$, the angle $(\alpha-\beta)$ being the mirror angle as usually defined. If f is the focal length of the observing telescope, the width W in centimeters of the fringes is given by $W = f\tan\phi = f\tan\lambda/2l_0(\alpha-\beta)$. The foregoing theory was developed from ideas that arose in connection with the ether drift problem, it being necessary to take into account small angles that are found to play a small part in ordinary interferometer work and are of the greatest importance in connection with the fringe shifts produced by the ether drift. The paper gives more complete formulas than those given above which are only approximate, and it will be shown how these new formulas may possibly be of value to those engaged in metrological work.

146. Photographs of Unusual Interference Fringes. F. A. MOLBY, *West Virginia University.*—Photographs will be shown (a) of fringes which appear to have the combined features of equal thickness fringes and of equal inclination fringes. These are obtained from a "half" platinized convex side of a "Plano" lens resting on a platinized plane surface. Surfaces were platinum sputtered. These fringes are very similar to those obtained with a Fabry and Perot Interferometer, several hundred rings being visible in the photograph, sharp to the edge of the plate of about 3×3 cm.; (b) of fringes seen by an eye looking at its own image as seen in the multiple images formed by a "half" platinized front surface and a platinized rear surface of a plane parallel glass 3.5 mm in thickness. These fringes have the appearance of perfect circles centered about the eye and located on the face of the observer, which proves to be a deceptive illusion for they are actually at or near an infinite distance, and the multiple images of the eye and face result in no very good image. The light of a Cooper Hewitt mercury lamp, or that of a sodium electric arc, and the platinized plate only are needed for viewing these fringes.

147. A Determination of the Optical Properties of Fluorite by Reflection in the Extreme Ultraviolet. RICHARD TOUSEY, *Harvard University.*—Specular reflecting powers at 45°, 65°, 75°, and 85° incidence have been measured for a polished fluorite surface, from 1026A to 1610A, by photographic photometry. The reciprocity law was used, and corrections for its failure were made in accordance with Harrison's work on fluorescent oils.[1] These correction exposures were made on each film with an inverse square law sensitometer. Drying in vacuum was found to affect the reciprocity failure. Hence the film was held in an evacuated chamber. The temperature was also controlled. The photographic error was reduced to about two percent. Reflecting powers of fluorite could not always be reproduced as closely as this, however, because of small changes in surface condition, though a standard cleaning procedure was followed. The index of refraction and the extinction coefficient have been computed from the reflecting power data for the one fluorite surface so far used. The dispersion is anomalous from roughly 1175A to 1100A. The extinction coefficient reaches a maximum at about 1120A. Thus an absorption band with center at about 1125A is indicated. The light from the grating was found to be unpolarized within experimental error, by calculation from the reflecting data where fluorite is transparent.

[1] G. R. Harrison, J.O.S.A. **20**, 313 (1930).

148. Magneto-Optical Rotation and Natural Dispersion in Gases. F. G. SLACK AND R. T. LAGEMAN, *Vanderbilt University.*—Formulae for the natural dispersion and for the magnetic rotation are tested together by use of recently determined experimental data for gases. Similar checks have been made by Evans and his co-workers for liquids.[1] Dispersion equations of the Ketteler-Helmholtz type, with a single ultraviolet absorption term, together with Becquerel's equation for the Verdet constant are found to fit the experimental data in the case of the gases acetylene, ethylene, and carbon dioxide. The computed wave-lengths of absorption bands lie within experimentally determined bands for these gases. For several other gases, methyl chloride, chloroform, oxygen, and nitrogen apparently more complicated formulae are required.

Evans, Phil. Mag. **18**, 386 (1934).

149. The Magnetostrictive Oscillation of Quartz Plates.* R. C. COLWELL AND L. R. HILL, *West Virginia University.*—Crystal quartz plates were vibrated by magnetostrictive rods at resonance frequencies below 100 kc. The modes of vibration were determined from sand figures and compared with those obtained when the plates were electrostatically driven. The frequency for a given mode of vibration was found to be the same whether the crystal was excited by an alternating electric field perpendicular to the electric axis or by a vibrating nickel rod. The mechanical response band for any mode of vibration was found to be much sharper than that of a brass Chladni plate.

* To be called for after paper No. 29.

150. Constant-Potential Technique and Equipment for Extremely High Voltages.* M. A. TUVE, L. R. HAFSTAD AND O. DAHL, *Department of Terrestrial Magnetism, Carnegie Institution of Washington.*—During the past five years a complete constant potential technique for nuclear physics studies utilizing electrostatic generators and cascade type high voltage tubes has been developed and critically tested in this laboratory on quantitative nuclear problems, with the ultimate objective of extending the technique to include the whole range of nuclear energies below cosmic rays. A year ago this experience was crystallized into the design of an equipment which can be relied upon to operate satisfactorily throughout a range of constant potentials well in excess of ten million volts, and which we hope ultimately may be realized and installed here. The equipment comprises a corona protected cascade tube, voltmeter resistor, and electrostatic generator enclosed in a large (60-foot diameter) spherical pressure tank filled with compressed air. Such tanks (for pressures up to 75 pounds per square inch) are in industrial use and are commercially available. For higher voltages, currents of many milliamperes, and maximum effectiveness, the Van de Graaff belt-type generator is supplanted by the earlier conception of a cascade of disk-type Holz generators. Electrons, as well as all types of ions, can be accelerated to extreme energies at will and under immediate and accurate control. Bombarding the targets in subterranean rooms beneath the pressure sphere generator permits the use of earth and water as gamma-ray and neutron shielding. Tests on details of design, including tubes, insulators, disk generators, voltage control, and other items, will be described.

* To be called for after paper No. 36.

151. Width of Neutron Resonance Levels.* H. A. BETHE, *Cornell University.*—In the Wigner-Breit theory, the powerful capture of neutrons by certain elements is ascribed to resonance. In Ag,** the resonance level lies near $E_0 = 16$ volts. An estimate of its width may be obtained from the ratio of the absorption coefficients of "resonance neutrons" and "temperature neutrons" in the same substance. According to Wigner-Breit, this ratio should be $K_{res} : K_{temp} = E_0^{\frac{1}{2}}(kT)^{\frac{1}{2}}\gamma^{-2}$. For Ag, $K_{temp} = 0.25$ per g/cm². K_{res} may be obtained from Fermi's experiments, taking account of the fact that the absorption of Ag resonance activity in Ag absorbers should not be exponential, the most active neutrons being absorbed first. The result is $K_{res} = 4.7$ per g/cm², giving $\gamma \approx 0.2$ volt. An alternative method for determining γ is from the absolute activities produced by temperature and resonance neutrons, whose ratio should be $A_{res}/A_{temp} = \pi N'_{res}(E_0 kT)^{\frac{1}{2}}/N_{temp}\gamma$, where N_{temp} is the number of temperature neutrons falling on the detector, and N'_{res}/E_0 the number of resonance neutrons per unit energy. Assuming diffusion equilibrium in the paraffin, we estimate $N'_{res}/N_{temp} = 1/30$. With an observed activity ratio $A_{res}/A_{temp} = 0.33$, we obtain again $\gamma = 0.2$, approximately. This tests also the laws of diffusion in paraffin. Observations of the absorption of the "resonance activity" in Ag by a Ag absorber of varying thickness, should give information about the "shape" of the resonance level.

* To be called for after paper No. 62.
** 2.3-minute period.

152. Search for Nuclear Cosmic-Ray Particles in the Stratosphere, Using Photographic Emulsions.* L. H. RUMBAUGH AND G. L. LOCHER, *Bartol Research Foundation of the Franklin Institute.*—Thirty-two specially prepared photographic plates (Imperial Process plates, treated with pinakryptol yellow, in an atmosphere of nitrogen) were placed in the gondola of the Explorer II (Nat'l Geog. Soc'y-Army Air Corps Flight) for the purpose of registering high energy nuclear particles. 17 of these plates were covered with materials representing 20 different elements. A part of these plates has been examined under a microscope for tracks of nuclear particles in the emulsions, with the following results: (1) from 8 to 20 low energy α-particle tracks per cm^3 (2 to 8 cm of air range) appear in all emulsions examined; (2) no α-particle tracks longer than 8 cm of air equivalent range, nor any high energy H-particle tracks have been observed in 60 cm^3 of emulsion. Probably all of the short α-tracks may be ascribed to radioactive contamination in the plates or their coverings. High energy α-particles of the kind reported by T. R. Wilkins and H. St. Helens[1] and protons must be too small in number to contribute appreciably to the total cosmic-ray ionization at the altitude reached by the balloon.

* To be called for after paper No. 73.
[1] Wilkins and St. Helens, Phys. Rev. **49**, 403 (1936).

153. Apparatus for the Measurement of Artificial Radioactivity.* S. N. VAN VOORHIS (National Research Fellow), *University of California.*—For more accurate determination of the decay curves of artificial radioactive substances, apparatus has been constructed consisting of a pressure ionization chamber of about one half-liter volume, filled with CO_2 to a pressure of three atmospheres, having a window of aluminum 0.1 mm thick. It is connected to an FP-54 pliotron, which is arranged to be used either with a high resistance for direct deflection, or with or without an extra condenser for rate-of-drift measurements. Tests with a radium sample have shown that the calibration has remained constant to within one percent over a period of four months, although the resistance has a temperature coefficient for which corrections must be made. The half-lives of the following substances, produced by deuteron bombardment of the target indicated, have been measured.

SUBSTANCE	TARGET	HALF-LIFE
Radio-sodium	Sodium fluoride	14.8 hours
Radio-chlorine	Lithium chloride	37.0 minutes
Radio-nitrogen	Soot Acheson graphite	10.0 minutes

These values should be good to about one percent or better. In each case the decay is accurately exponential over a range of intensity of one thousand or more.

* To be called for after paper No. 93.

154. Evidence for the Existence of Li^5.* A. KEITH BREWER, *Bureau of Chemistry and Soils, Washington, D. C.*—A mass spectrographic analysis of lithium thermions emitting from an impregnated platinum disk shows a distinct peak in the mass number 5 position. This peak is proportional to the Li^6 and Li^7 peaks, giving an abundance ratio close to Li^7/Li^5 = 20,000. The possibility of the peak being due to helium hydride is small since no peak was observed in the 4 position. Likewise no peak was found in the 10 position; it is highly improbable, therefore, that the peak could be due to doubly charged boron or beryllium.

* To be called for after paper No. 126.

155. Masses of Atoms between Neon and Argon.* C. J. BRASEFIELD AND E. POLLARD, *Yale University.*—Aston's[1] latest values for the masses of F^{19}, Ne^{20}, Al^{27}, Si^{28}, Si^{29} and A^{40}, and Bainbridge's values for Cl^{35} and Cl^{37} have been used, together with known data from alpha-particle induced transmutations involving these atoms, to derive masses of other atoms between neon and argon. A list of the isotopic masses thus determined—including Aston's 1927 value for A^{36}—follows:

Atom	Mass	Atom	Mass
$_{10}Ne^{20}$	19.9986 (A)	$_{15}P^{31}$	30.9844
$_{10}Ne^{22}$	21.9985	$_{16}S^{32}$	31.9812
$_{12}Mg^{24}$	23.9938	$_{16}S^{34}$	33.9799
$_{13}Al^{27}$	26.9909 (A)	$_{17}Cl^{35}$	34.9796 (B)
$_{14}Si^{28}$	27.9860 (A)	$_{18}A^{36}$	35.976 (a)
$_{14}Si^{29}$	28.9864 (A)	$_{17}Cl^{37}$	36.9777 (B)
$_{14}Si^{30}$	29.9845	$_{18}A^{38}$	37.9753
		$_{18}A^{40}$	39.9754

The extension of Oliphant's[2] curve permitted by this list shows indications of extra stability at each repetition of four mass units until A^{40} is reached, which is exceptional, indicating that the stability is due to alpha-particles and not to units of four irrespective of charge.

* To be called for after Paper No. 153.
[1] F. W. Aston, Nature **137**, 613 (1936).
[2] M. L. Oliphant, Nature **137**, 396 (1936).

156. Radiation from an Antenna Over a Plane Earth of Arbitrary Characteristics.* W. W. HANSEN AND J. G. BECKERLEY, *Stanford University.*—A rigorous and easily computed formula for the total radiation from an arbitrary current distribution above a plane "earth" of arbitrary characteristics is developed. The fields may also be found, though they are not needed to compute the energy radiated. As a by-product, two new expansions in cylindrical coordinates of $i(l)e^{ikr_{12}}/r_{12}$, where $i(l)$ is a vector, are found.

* To be called for after Paper No. 10.

157. Interference by Reflection from a Parallel Plate.* BERTRAND P. RAMSAY, *University of Kentucky.* (*Introduced by O. T. Koppius.*)—Calculations based on the usual assumption that parallel plate interferences by reflection are complementary to those observed by transmission indicate that reflection fringes have greater resolution and visibility than the corresponding transmission system, such as is employed in Fabry-Perot instruments. The desirable characteristics of the optical properties calculated in this way suggest the construction of an interferometer employing interference systems of this type. Several designs have been considered; and one of these has been used in the construction of an interferometer. This instrument is effective in producing fringes over variable path differences as great as ten centimeters. The central fringe is formed at the position of minimum deviation rather than at the position of normal emergence. The fringes, however, do not have the anticipated optical properties.

* To be called for after Paper No. 52.

158. Properties of Interference Systems Formed by Parallel Plates.* WALLACE E. ANDERSON, *University of Kentucky. (Introduced by O. T. Koppius.)*—The interference fringe pattern formed by reflection from a plane parallel plate is generally stated to be complementary to the fringe pattern transmitted through the parallel plate. This conclusion follows from the equations for the intensity of these patterns derived by using Stokes' relations between the reflection and refraction coefficients, or by using the energy principle. Careful analysis indicates that these relations cannot be applied whenever there is any absorption in the system. There is always a loss of intensity at the surfaces of a plate which is metallically coated. Experimental observations and photographs bear out the conclusion that the fringes by reflection from a parallel plate are not complementary to the fringes by transmission in any case observed. This fact has an important bearing on any interferometer designed to use parallel plate fringes by reflection.

* To be called for after Paper No. 157.

159. Energy Transmission by High Energy Electrons.* W. F. G. SWANN, *Bartol Research Foundation of the Franklin Institute.*—In considering the theory of energy transfer at close collisions between charged particles, one of which is of high energy, J. R. Oppenheimer has postulated the condition that in calculating the effect of the field of the high energy particle, one must omit from its appropriate Fourier analysis all of those harmonic terms which frequently lie above a certain critical value characteristic of the charged particle acted upon. Some time ago, the writer proposed a modification of the fundamental wave-mechanical equation which was designed so as to lead statistically to the classical equation of motion of an electron including the so-called radiation reaction terms. It is now shown that the Oppenheimer condition is a direct analytical consequence of the modified wave-mechanical equation referred to. The significant feature of the matter is that the terms which in Oppenheimer's postulate are simply omitted are, on the writer's theory, rendered automatically impotent by having associated with them large denominators which kill their effects.

* To be called for after Paper No. 152.

160. The Optical Sounder.* C. W. CHAMBERLAIN, *Michigan State College.*—The wetting method of measuring rainfall and the depth of a liquid in a container is found to be extremely inaccurate. This is especially true in the case of gasoline, naphtha and alcohol. A wetting film has been observed to rise 10 cm above the surface of a liquid. The optical sounder locates a liquid surface to an accuracy of $1.5(10)^{-7}$ cm. A method is described for instantly changing the optical system from a telescope, locating the liquid surface, to a microscope for reading the setting.

* To be called for after Paper No. 104.

161. Wetting Films.* C. W. CHAMBERLAIN AND K. L. WARREN, *Michigan State College.*—Certain liquids wet a vertical plate to a height much greater than can be accounted for by capillarity. Measurements made with the compound interferometer result in the following conclusions:

1. Wetting films are formed by liquids containing two or more components with different vapor tensions.
2. Liquids which produce no wetting films will produce such films when mixed if the component liquids have different vapor tensions.
3. Saturation and unsaturation of the hydrocarbons play no part in the production of wetting films.
4. The thickness of wetting films increases with rise of temperature, due to the increase of the true viscosity of the liquid mixture.
5. The small radius of curvature at the top of a wetting film results in a high rate of evaporation, producing a region of high surface tension, supplying the energy necessary to move the superficial layer upward. This movement drags with it some of the body of the liquid. The thickness of the upward moving layers depends on the true viscosity of the liquid mixture.
6. Wetting films have planes of cleavage whose distance apart are exact multiples of the Radius of Molecular Attraction.

* To be called for after Paper No. 160.

162. Geometry of a Focusing Crystal Spectrograph for Hard Radiation.* J. E. MACK, *University of Wisconsin.*—Let a crystal c be bent cylindrically so that the planes to be used for reflection are radial. Consider a section normal to the axis. All radiation incident from a source or slit S, reflected within c, is focused at points S' on the circle of radius OS about the crystal's center of curvature O such that $\angle OSS' = \theta$, the Bragg angle. The image is real if $SO > cO$. Except for alterations in the lattice constant d (and consequently in $\theta = \arcsin n\lambda/2d$) due to the bending, the focusing is geometrically perfect. All effective scattering points lie on the circular arc SOS'. Any number of crystals, bent to different radii, may be grouped about O along SOS' to increase the light gathering power. The geometric upper limit to the angular aperture is 2θ. The practical limit is considerably lower, depending upon the practical curvability of the crystals, the ratio of thickness of crystal to thickness of holder, and the necessity of a shield on the straight line SS'. The upper limit to the wave-lengths that can be studied is unusually great for a transmission spectrograph, for the opacity of the curved crystals depends primarily not upon extinction but upon ordinary scattering.

* To be called for after Paper No. 157.

163. A Search for Protons in the Primary Cosmic-Ray Beam.* C. G. MONTGOMERY, D. D. MONTGOMERY, W. E. RAMSEY AND W. F. G. SWANN, *Bartol Research Foundation of the Franklin Institute.*—It has been suggested that a large part of the cosmic-ray ionization at sea level is caused by high energy protons. Swann[1] has pointed out that the large specific ionization which occurs at the end of the range of a proton would be of sufficient magnitude and

frequency to be observable in an ionization chamber. Bursts of ionization occurring in a chamber 15.4 cm long and 6.7 cm in diameter, filled with nitrogen to a pressure of 15 atmospheres, have been measured. The effects of alpha-particles were eliminated by introducing a thin partition across the center of the chamber and observing only bursts of ionization occurring simultaneously in both halves. The effects of showers of rays were excluded by the use of sets of Geiger-Müller counters, of a type especially efficient for the detection of showers, placed under the chamber. On the basis of Bethe's theory for the energy loss of high speed protons, the number of spurts of ionization greater than 7.2×10^4 ion pairs in both halves of the vessel to be expected in 175 hours is 58. Twelve spurts of this size were observed, of which 10 were accompanied by a counter discharge. Similar observations of smaller spurts of ionization were also made. It must be concluded that protons produce an inappreciable fraction of the ionization at sea level unless their effectiveness is increased many-fold by the production of secondaries.

* To be called for after Paper No. 159.
[1] Swann, Phys. Rev. **49**, 478 (1936).

164. Experiments on Residual Neutrons.* H. H. GOLDSMITH AND F. RASETTI, *Columbia University*.—Further experiments have been performed on the determination of neutron energies by means of the absorption in boron.[1] Using 0.4 g/cm² Cd as filter it was found that 0.08 g/cm² B, which transmits 0.55 of the neutrons detected by Rh, will transmit 0.46 of the neutrons detected by In. Taking $E_{res}(\mathrm{Rh})=0.6$ ev, one obtains $E_{res}(\mathrm{In})=0.35$ ev. Preliminary results indicate that the residual neutrons detected by I and Br have energies of the same order of magnitude. The absorption of 0.6 ev neutrons in Gd and Sm was measured. Although about five times the half-value thickness for *C* neutrons was used less than 10 percent absorption was observed. A similar effect is exhibited by Cd.[2] This suggests that all cases of extremely large cross sections for *C* neutrons are due to the occurrence of resonance bands in the thermal region. For all of the neutron groups which have been studied it is found that as σ_c for the *C* neutrons increases E_{res} decreases as is expected on the Breit-Wigner theory.[3]

* To be called for after Paper No. 55.
[1] Abstract No. 55 of this meeting.
[2] L. Szilard, Nature **136**, 950 (1935).
[3] G. Breit and E. Wigner, Phys. Rev. **49**, 519 (1936).

AUTHOR INDEX TO ABSTRACTS OF THE WASHINGTON MEETING

Ahearn, A. J. and J. A. Becker—No. 102
Almy, G. M.—see Kinzer
—— **and R. B. Horsfall**—No. 109
Anderson, Wallace E.—No. 158
Ashworth, J. A. and J. C. Mouzon—No. 139

Bainbridge, Kenneth T.—see Jordan
—— **and Edward B. Jordan**—No. 123
Barnes, S. W.—see DuBridge
Barnes, T. G.—see Lindsay
Barr, E. S.—see Plyler
Bartlett, J. H., Jr. and J. J. Gibbons, Jr.—No. 42
Bayley, D. S., B. R. Curtis, E. R. Gaerttner and S. Goudsmit—No. 60
Beams, J. W.—see Snoddy
Bearden, J. A.—see Roseberry
Becker, J. A.—see Ahearn
Beckerley, J. G.—see Hansen
Bennett, Willard H.—see Darby
Benson, Albin and R. A. Sawyer—No. 44
Bethe, H. A.—Nos. 56, 151
Betz, Paul L. and S. Karrer—No. 6
Bleakney, Walker—see Hipple
—— see Sherr
—— see Smith, L. G.
Blewett, J. P.—see Jones
Bouckaert, L. and R. Smoluchowski—No. 82
Boyer, R. F. and C. Nusbaum—No. 127
Brasefield, C. J.—see Pollard
—— **and E. Pollard**—No. 155
Breit, G. and E. U. Condon—No. 35
Brewer, A. Keith—Nos. 39, 154
Brown, W. F.—No. 19
Buechner, W. W. and E. S. Lamar—No. 117

Carroll, Thomas—No. 142
Cartmel, W. B.—No. 145
Cashman, R. J. and N. C. Jamison—No. 94
Castleman, R. A., Jr.—No. 141
Chamberlain, C. W.—No. 160
—— **and K. L. Warren**—No. 161
Chambers, L. A.—No. 114
Christensen, C. J.—see Pearson
—— **and G. L. Pearson**—No. 26
Chiles, J. A., Jr.—No. 3
Coblentz, W. W. and R. Stair—No. 52
Collins, J. R. and C. Moran—No. 85
Colwell, R. C., A. W. Friend and N. I. Hall—No. 29
—— **and L. R. Hill**—No. 149
Condon, E. U.—see Breit
Cooksey, Donald and Ernest O. Lawrence—No. 33
Cortell, R.—see Roberts
Crane, H. R.—see Gaerttner
——, **E. R. Gaerttner and J. J. Turin**—No. 133
Curtis, B. R.—see Bayley

Dahl, O.—see Tuve
Darby, Paul F. and Willard H. Bennett—No. 116
Davey, Wheeler P.—No. 137
Devol, Lee—see Ruark
—— **and Arthur Ruark**—No. 92

Dieke, G. H.—No. 106
Dillinger, J. F.—No. 17
Driscoll, Raymond L.—No. 91
DuBridge, L. A.—see Hill
—— **and S. W. Barnes**—No. 30
Duffendack, O. S.—see Thomson
Durand, Milo A.—No. 20

Ellis, Cecil B.—No. 83
Evans, Robley D.—see Gingrich

Failla, G.—No. 93
Fay, Charles H.—No. 57
Feenberg, Eugene and Simon S. Share—No. 77
Fink, G. A.—see Rasetti
Fisk, J. B., P. M. Morse and L. I. Schiff—No. 58
Fox, M.—see Millman
Friend, A. W.—see Colwell

Gaerttner, E. R.—see Bayley
—— see Crane
——, **J. J. Turin and H. R. Crane**—No. 61
Gagge, A. P.—No. 46
Germer, L. H.—No. 135
Gibbons, J. J., Jr.—see Bartlett
Gingrich, Newell S. and Robley D. Evans—No. 140
Goldsmith, H. H.—see Rasetti
—— **and F. Rasetti**—No. 164
Goudsmit, S.—see Bayley
Gray, J. A. and A. G. Ward—No. 62
Green, J. B.—No. 37
—— see Maxwell
Grover, H. J.—No. 98
Guthrie, Albert N.—No. 45

Hafstad, L. R.—see Tuve
——, **N. P. Heydenburg and M. A. Tuve**—No. 36
Hahn, T. M. and Ben Ragland—No. 138
Hall, N. I.—see Colwell
Hansen, W. W. and J. G. Beckerley—No. 156
Hardy, J. D. and T. W. Oppel—No. 47
Hartman, Paul L.—see Smith, L. P.
Haworth, F. E.—No. 16
Henry, D. E.—see Rentschler
Heydenburg, N. P.—see Hafstad
—— see Tuve
Hill, A. G. and L. A. DuBridge—No. 95
Hill, L. R.—see Colwell
Hipple, J. A., Jr. and Walker Bleakney—No. 126
Hirsh, F. R., Jr.—No. 134
Horsfall, R. B.—see Almy
Howard, J. B. and E. Bright Wilson, Jr.—No. 112
Hubbard, J. C.—No. 27
Huffman, John—see Pegram
Hughes, A. L. and S. S. West—No. 97

Jahn, H. and E. Teller—No. 80
James, Hubert M.—No. 81
Jamison, N. C.—see Cashman
Jenkins, F. A. and Dean E. Wooldridge—No. 119
Jeppesen, C. R.—No. 48
Jones, E. J. and J. P. Blewett—No. 115
Jordan, Edward B.—see Bainbridge
—— **and Kenneth T. Bainbridge**—No. 124

Karrer, S.—see Betz
Kellogg, J. M. B., I. I. Rabi and J. R. Zacharias—No. 43
Kelly, Harry C.—No. 9
Kent, Norton A.—No. 70
King, Ronold—No. 28
Kinzer, G. D. and G. M. Almy—No. 108
Korff, S.—see Millikan
Kruger, P. Gerald—see Weissberg
—— **and S. G. Weissberg**—No. 73
Kusch, P. and F. W. Loomis—No. 107

Lageman, R. T.—see Slack
Lamar, E. S.—No. 8
—— see Buechner
Langmuir, Irving—see Taylor
Lawrence, Ernest O.—see Cooksey
Linder, E. G.—No. 1
Lindsay, R. B. and T. G. Barnes—No. 11
Livingood, J. J.—No. 89
Locher, Gordon L.—No. 63
—— see Rumbaugh
Loomis, F. W.—see Kusch
Luhr, Overton and Charles T. Male, Jr.—No. 5

Mack, J. E.—No. 162
Male, Charles T., Jr.—see Luhr
Malter, Louis—No. 103
Manley, J. H.—No. 40
Margenau, Henry—No. 76
Maxwell, H. N. and J. B. Green—No. 38
McMillan, Edwin—No. 86
Millikan, R. A., H. V. Neher and S. Korff—No. 66
Millman, S. and M. Fox—No. 41
Mitchell, Allan C. G., Edgar J. Murphy and Martin D. Whitaker—No. 59
Mitchell, D. P.—see Rasetti
Molby, F. A.—No. 146
Montgomery, C. G., D. D. Montgomery, W. E. Ramsey and W. F. G. Swann—No. 163
Montgomery, D. D.—see Montgomery, C. G.
Moran, C.—see Collins
Morgan, J. E.—No. 65
Morse, P. M.—see Fisk
Morton, G. A.—see Ramberg
—— **and E. G. Ramberg**—No. 23
Mouzon, J. C.—see Ashworth
Mulliken, Robert S.—No. 113
Murray, R. T. K.—No. 100
Murphy, Edgar J.—see Mitchell, A. C. G.
Myers, F. E.—see Roberts

Nathanson, J. B.—No. 143
Neher, H. V.—see Millikan
Nordheim, L. W.—see Peterson

Norgorden, Oscar—No. 22
Northrup, D. L.—see Van Atta, L. C.
Nusbaum, C.—see Boyer

O'Bryan, H. M.—No. 105
Oppel, T. W.—see Hardy

Patterson, A. L.—No. 128
Pearson, G. L.—see Christensen
—— **and C. J. Christensen**—No. 25
Pegram, G. B., H. C. Urey and John Huffman—No. 122
Peterson, E. and L. W. Nordheim—No. 74
Peterson, Max—see Welo
Pittman, M. A.—No. 49
Plyler, E. K. and E. S. Barr—No. 50
Pollard, E.—see Brasefield
—— **and C. J. Brasefield**—No. 90
Pool, M. L.—see Whitmer
Post, C. B.—No. 136
Purcell, E. M.—No. 84

Rabi, I. I.—see Kellogg
Ragland, Ben—see Hahn
Ramberg, E. G.—see Morton
—— **and G. A. Morton**—No. 24
Ramberg, Walter—see Tuckerman
Ramsey, Bertrand P.—No. 157
Ramsey, W. E.—see Montgomery, C. G.
Rank, D. H.—No. 110
Rasetti, F.—see Goldsmith
——, **G. A. Fink, H. H. Goldsmith and D. P. Mitchell**—No. 55
Rentschler, H. C. and D. E. Henry—No. 96
Rice, S. O.—No. 14
Roberts, A., T. Zandstra, R. Cortell and F. E. Myers—No. 87
Robertson, R. M.—No. 7
Rosin, Seymour—see Siegel
Rose, John L. and R. K. Stranathan—No. 68
Roseberry, H. H. and J. A. Bearden—No. 131
Rosselot, G. A.—No. 67
Ruark, Arthur—see Devol
Ruedy, J. E. and George Burr Sabine—No. 144
Rumbaugh, L. H.—No. 120
—— **and G. L. Locher**—No. 152

Sabine, George Burr—see Ruedy
Sawyer, R. A.—see Benson
Schiff, L. I.—see Fisk
Schneider, Edwin G.—No. 64
Share, Simon S.—see Feenberg
Sherr, Rubby and Walker Bleakney—No. 121
Shockley, W.—No. 79
Shrader, J. E.—No. 12
Siegel, Sidney and Seymour Rosin—No. 18
Slack, F. G. and R. T. Lageman—No. 148
Smith, Lincoln G. and Walker Bleakney—No. 125
Smith, Lloyd P. and Paul L. Hartman—No. 32
Smoluchowski, R.—see Bouckaert
Smyth, Harold T.—No. 69
Snoddy, L. B., E. J. Workman and J. W. Beams—No. 2
Southworth, G. C.—No. 54
Stair, R.—see Coblentz
Stibitz, G. R.—No. 15
Stranathan, R. K.—see Rose
Stuhlman, Otto, Jr.—No. 10
Swann, W. F. G.—No. 159
—— see Montgomery, C. G.

Taylor, John Bradshaw and Irving Langmuir—No. 101
Taylor, Lauriston S.—No. 4
Teller, E.—see Jahn
Thomson, K. B. and O. S. Duffendack—No. 111
Tonks, Lewi—No. 99
Tousey, Richard—No. 147
Tuckerman, L. B. and Walter Ramberg—No. 13
Turin, J. J.—see Crane
—— see Gaerttner
Turner, Louis A.—No. 75
Tuve, M. A.—see Hafstad
——, **L. R. Hafstad and O. Dahl**—No. 150
——, **N. P. Heydenburg and L. R. Hafstad**—No. 34

Urey, H. C.—see Pegram

Van Atta, C. M.—see Van Atta, L. C.
Van Atta, L. C., D. L. Northrup, C. M. Van Atta and R. J. Van de Graaff—No. 31
Van de Graaff, R. J.—see Van Atta, L. C.
Van Voorhis, S. N.—Nos. 88, 153

Ward, A. G.—see Gray
Warren, B. E.—No. 132
Warren, K. L.—see Chamberlain
Weber, Ernst—No. 104
Weissberg, S. G.—see Kruger
—— **and P. Gerald Kruger**—No. 72
Welo, Lars and Max Petersen—No. 21
West, S. S.—see Hughes
Whitaker, Martin D.—see Mitchell, A. C. G.
White, H. E.—No. 71
Whitmer, C. A. and M. L. Pool—No. 118
Williams, Dudley—No. 51
Wilson, E Bright, Jr.—see Howard
Wooldridge, Dean E.—see Jenkins
Workman, E. J.—see Snoddy

Young, Lloyd A.—No. 78

Zacharias, J. R.—see Kellogg
Zachariasen, W. H.—No. 130
Zandstra, T.—see Roberts
Ziegler, George E.—No. 129
Zworykin, V. K.—No. 53